université PARIS-SACLAY

NNT :2017SACLX100

Thèse de doctorat

Towards an improved description of spectroscopies for materials with localized electrons: Effective potentials and interactions

Thèse de doctorat de l'Université Paris-Saclay
préparée à l' École Polytechnique

n°572 : ondes et matières (EDOM)
Spécialité de doctorat: physique quantique

Thèse présentée et soutenue à Palaiseau, le 7/12/2017, par

Marilena Tzavala

Composition du Jury :

M. Stéphane Camiato Professeur, Université Pierre-et-Marie-Curie-Paris 6 (UMR 7641)	Président
M. John Rehr Professeur, University of Washington, Seattle, US	Rapporteur
Mme Pina Romaniello Chargée de recherche, Université Paul Sabatier (UMR 5152)	Rapporteur
M. Leonidas Tsetseris Professeur associé, National Technical University of Athens, Greece	Examinateur
M. Alberto Zobelli Maître de Conférences , Univérsité Paris-Sud (UMR 8520)	Examinateur
Mme Lucia Reining Directrice de recherche, Ecole Polytechnique (UMR 7642)	Directrice de thèse
Mme Claudia Rödl Chercheur, Friedrich-Schiller University of Jena, Germany	Invitée

Résumé

L'objectif de cette thèse est de développer des approximations pour décrire les effets à N-corps dans l'absorption et la photoémission des matériaux avec électrons localisés. Le traitement complet par la mécanique quantique de ce problème difficile repose sur la solution de l'équation de Schrödinger pour la fonction d'onde à N-corps, ce qui en pratique nécessite des approximations. Pour simplifier, la Théorie de le Fonctionnelle de la Densité (DFT) introduit le système de particules indépendantes de Kohn et Sham. Cependant, il s'avère difficile d' obtenir des propriétés autres que la densité et l'énergie totale. Dans cette thèse, nous travaillons avec des fonctions de Green. Le niveau de complexité de ce cadre, en principe exact, se situe entre la DFT et les méthodes des fonctions d'onde, et de nombreux problèmes restent à résoudre.

Quand on décrit l'excitation d'un électron localisé, certaines approximations introduisent une auto-interaction ou auto-écrantage. Ce problème est naturellement évité lorsque l'on utilise une interaction coulombienne généralisée (Chap.3). De plus, quand l'électron localisé a peu de recouvrement avec les autres électrons, on peut penser que leur interaction est classique. Dans ce cas, l'effet principal à N-corps est la réaction des autres électrons : ils écrantent l'excitation. Dans les approximations habituelles telles que le GW ou la "cumulant expansion", l'écrantage est traité seulement en réponse linéaire. Cependant, l'excitation d'un électron localisé devrait représenter une forte perturbation. Par conséquent, il se pourrait que les contributions non-linéaires à l'écrantage soient importantes. Comment peut-on vérifier quand cela est vrai? Et comment peut-on inclure des effets non-linéaires? D'autre part, même en réponse linéaire, on pourrait faire mieux que les approximations habituelles, parce que l'écrantage en réponse linéaire est souvent calculé dans l'approximation de la phase aléatoire (RPA). De combien peut-on améliorer les résultats, même en restant en réponse linéaire, si on va au-delà de RPA? Ces points seront adressés dans la thèse. En ce qui concerne l'écrantage, au Chap.5 on utilise un modèle zéro-dimensionel pour étudier d'un côté, les effets au-delà de RPA en réponse linéaire, et de l'autre côté, les effets au-delà de la réponse linéaire mais restant en RPA. Fait intéressant, on constate qu'on doit traiter les deux en même temps afin d'obtenir des améliorations significatives. On doit donc trouver des approximations pour aller au-delà de RPA qui sont suffisamment simples pour être utilisées même dans un régime non-linéaire. Dans cette thèse on développe des approximations basées sur la théorie des perturbations, et on en teste d' autres, déjà existantes, dans le modèle zéro-dimensionel.

L'écrantage est décrit par la fonction diélectrique. Cette fonction permet aussi de calculer des spectres d'absorption. Au Chap.6 on étudie la fonction diélectrique d'un solide modèle à l'aide des fonctions de Wannier localisées. Cela nous permet de mettre en évidence les annulations entre la self-énergie et les effets excitoniques dans le cadre des fonctions de Green et, à partir des résultats, de dériver un potentiel d' échange et corrélation de Kohn-Sham, et un noyau d'échange et corrélation pour la DFT dépendante du temps (TDDFT).

Le Chap.7 aborde la question de comment faire apparaître l'écrantage non linéaire explicitement dans la formulation ab initio. On propose une réponse possible, en utilisant la localisation de l'électron pour dériver une fonction de Green 'cumulant' au-delà de la réponse linéaire habituelle. On suggère deux niveaux d'approximations pour calculer les expressions en pratique, et on montre

quelques résultats préliminaires. Dans les deux cas, la TDDFT est utilisée pour décrire l'écrantage.

Etant donné qu'une combinaison de fonctions de Green et de TDDFT semble être une bonne stratégie pour simplifier le problème à N-corps, le Chap.8 conclut avec quelques idées supplémentaires.

Acknowledgments

I would like to thank my supervisor, Lucia Reining, for giving me the opportunity to conduct research in various directions, building upon the work of members of our group, and in the same time respecting my interests without limiting or patronizing my mind. I am grateful to Prof. John Rehr and Joshua Kash for their hospitality during my stay in Seattle and our scientific discussions which literally shaped my way of thinking. I would like to thank very much Claudia Rödl for her support and advices. Finally, I would like to thank the whole group of ETSF Palaiseau, my family and my friends for being always supportive and showing lots of understanding.

To my sister, Polina

Contents

Glossary

2PPE	2-photon photoemission 27
a.u.	atomic units: $(m_e = e = \hbar = \frac{1}{4\pi\epsilon_0} = 1)$ 15, 20
APS	appearance potential spectroscopy 28
ARPES	angular-resolved photoemission spectroscopy 27
BSE	Bethe-Salpeter equation 11–13, 44, 54, 55, 58, 102, 104, 118
DFT	density functional theory 10, 15, 23, 24, 26, 50, 51, 55, 56, 63, 89, 93, 104, 122, 126, 127, 136, 138
DMFT	dynamical mean-field theory 26
EELS	electron energy-loss spectroscopy 10, 11, 28, 36
EXAFS	extended x-ray absorption fine structure 28
GWA	GW approximation 11, 45–47, 50, 51, 55, 64, 89, 99, 104, 127
IPES	inverse photoemission spectroscopy 4, 27, 28, 32, 33
IXS	inelastic x-ray scattering 10, 11, 13, 28, 30, 54, 55, 90, 104, 137
KBE	Kadanoff-Baym equation 4–6, 11–13, 41, 42, 46–49, 52, 59–61, 76–78, 81, 88, 105–107, 126, 127, 137, 138, 156, 160
LDA	local density approximation 55
LRC	long-range contribution 12, 60, 64, 66, 69, 70, 72–75, 78–82, 87, 88, 153, 155, 159
MBPT	many-body perturbation theory 6, 11, 26, 31, 38, 40, 50, 56, 89, 105, 122, 137, 143–146
OEP	optimized effective potentials 95
OPM	one-point model 12, 50, 51, 58–62, 64, 66, 77, 88
PES	photoemission spectroscopy 4, 27, 28, 33
RDMFT	reduced density matrix functional theory 26
RPA	random-phase approximation 5, 6, 12, 45, 57–61, 63–81, 88, 138, 153–159
RTTDDFT	real-time time-dependent density functional theory 6, 122, 125, 138
SCF	self-consistent field 29, 30, 123
SSE	Sham-Schlüter equation 5, 56, 58, 89, 90, 95–97, 104

TDDFT	time-dependent density functional theory 5, 6, 12, 13, 48, 50–52, 54, 56–60, 64–67, 70, 72, 74, 78, 83, 86–90, 97, 99, 100, 102–104, 106, 122, 125–127, 133, 136–139, 147, 148, 156
XAFS	x-ray absorption fine structure 28
XANES	x-ray absorption near-edge spectroscopy 28
XAS	x-ray absorption spectroscopy 28
XPS	x-ray photoemission spectroscopy 25–27, 105, 113, 116, 122, 125

Introduction

Spectroscopies that probe materials with photons or charged particles are increasingly used to obtain information about their microscopic structure and processes on the atomic level. However, it is not easy to interpret experiments, and theory has an important role to play. This is a difficult task, because all particles in the system are interacting, and many-body effects do not allow one to draw simple conclusions. Therefore, on the theory side there is still a strong need for developments that will make calculations feasible for realistic systems, that lead to predictive results, and where results are presented in such a way that a clear analysis is possible.

The aim of this thesis is to develop approximations to describe many-body effects in photoemission, absorption and inelastic x-ray scattering IXS or electron energy-loss spectroscopy EELS involving localized electrons. With "localized electrons" we mean electrons which can to a certain extent be distinguished from the others, and to which one can ascribe a wavefunction that has its dominant amplitude in regions of space where the other electrons have little probability to be found. Several important cases fall into this class. On one side, core electrons are localized close to the nucleus and have often little overlap with other core electrons and with valence electrons. On the other side, d or f-electrons in transition-metal or rare-earth compounds are often quite distinguishable from the s or p-electrons in the same material. Nevertheless, their photoemission or absorption spectra display important many-body effects, such as lifetime broadening, satellites, or Rydberg series which are characteristic for bound electron-hole pairs, called excitons. Therefore, even for strongly localized electrons far from the others, the description of many-body effects is a tough problem.

Many-body effects are contained in the many-body wavefunctions of the ground and excited states of the electronic system, which are in principle obtained by solving the Schrödinger equation. In practice, however, except for very small systems, it is impossible to solve the Schrödinger equation, because the Hamiltonian contains the Coulomb interaction, which is a two-body interaction, and therefore the many-body wavefunction depends on every single electron in the system: the electrons are correlated. In order to solve the many-body problem, one has to find ways to deal with this correlation. Simplified approaches reduce the full problem to a system of single-particle equations, but they usually fail to capture the full correlation effects. Correlation is completely neglected in the Hartree-Fock approximation, where the wavefunction satisfies solely the requirement of antisymmetry, which leads to the Fock-exchange contribution that is added to the classical electrostatic potential. Density functional theory (DFT) in the Kohn-Sham formulation [1, 2] goes a step further in the description of correlation, and it can yield the exact density. On the other hand, quantum-chemistry methods, often referred to as post-Hartree-Fock methods (e.g. configuration interaction), calculate the many-body wavefunction by introducing correlation in an expansion which is in principle exact but relies on expensive calculations.

In this thesis we choose a different, in principle exact framework, namely Green's functions [3]. The Green's functions are intermediate in complexity between the density, which appears in DFT, and the full-wavefunction methods. They give direct access to many spectroscopic quantities: pho-

toemission experiments, for example, can be described by the spectral function of the one-body Green's function G, and the density-density response function χ or the inverse dielectric function ϵ^{-1} are derived from the two-body Green's function G_2. They allow one to describe absorption, inelastic x-ray scattering (IXS) or electron energy-loss spectra (EELS). Fig.1 displays these relations. The figure also shows schematically the complexity of the theory, with its various approximations

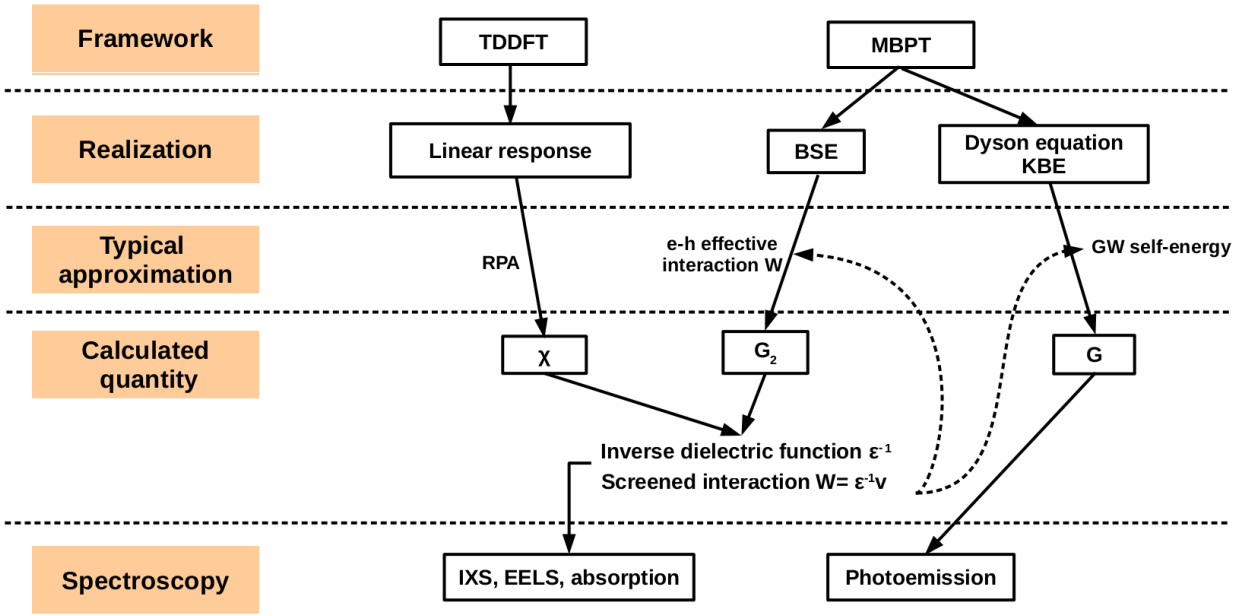

Fig. 0.1: Theoretical framework for the calculation of observables adopted in this thesis.

and links: Green's functions are calculated in the framework of many-body perturbation theory (MBPT), for example using the equation of motion of the one-body Green's function in the form of the Kadanoff-Baym equation (KBE) [4], or Hedin equations, which are derived from the KBE. Here, the central equation is the Dyson equation for the one-body Green's function, which is an integral equation describing the propagation of an electron in a momentum and frequency-dependent effective field, named self-energy. The self-energy contains all exchange-correlation effects. In Hedin's formulation it is expressed in terms of the screened interaction W [5]. On the other hand the KBE is a system of coupled functional differential equations whose solution reflects the exact correlation of the system. Similarly to the one-body Green's function, the two-particles Green's function is obtained by solving a Dyson-like equation called Bethe-Salpeter equation (BSE) [6]. This has a large computational cost, since it involves huge matrices. The inverse dielectric function obtained from the two-particle Green's function, which can be compared to experiment, screens the Coulomb interaction. On the other hand, the screened Coulomb interaction W is needed as input for the calculations of G and G_2. This feedback loop is expressed by the dashed arrows in the figure.

In any case, the exact treatment of correlation is impossible, and therefore the evaluation of screening relies on approximations, where the physics of the system (in our case localized electrons) needs to be taken into account. Standard approximations are Hedin's GW approximation (GWA) for the self-energy, which is expressed as a product of G and W, and a related approximation for the Bethe-Salpeter equation, where the direct interaction between the electron and the hole that is

left behind when the electron is excited is given by W. On a lower level, the two-body Green's function is obtained by completely neglecting the electron-hole interaction, or by allowing for the electron and the hole to interact only through the relaxation of the Hartree potential (random-phase approximation (RPA)) [7].

Another framework, which gives an in principle exact access to screening, is time-dependent density functional theory (TDDFT) [8]. It is computationally much more efficient than the solution of the BSE. Also in this case, the RPA is one of the possible approximations. However, this is often not sufficient, and the search for reliable effective potentials and interactions is still ongoing. This thesis also touches upon this point.

The objective of the thesis is to find approximations within this theoretical framework which are particularly suitable for localized electrons. For the removal or excitation of a localized electron one important point is to avoid self-interaction and self-screening errors. These errors appear often when different approximations are made to Hartree and exchange contributions. Common approximations for the self-energy, such as the GW approximation, suffer from self-screening. As I show in Chap.3, self-interaction and self-screening corrections are naturally included when one uses a generalized Coulomb interaction [9]. To go further, we suppose that the localized electron has little overlap with the others, such that their interaction is classical (there is no exchange). Then the main many-body effect is the reaction of the other electrons to the removal or excitation of the localized electron: this is screening of the hole or electron-hole pair by the other electrons. This can be related to the appearance of the screened interaction W in the formulation. However, in standard approximations such as GW or the cumulant expansion [10], screening appears only in the linear-response approximation. This might be a problem, since we can expect that the removal or excitation of a localized electron is a strong perturbation to the other electrons. Therefore, it could be that non-linear contributions to screening are important. How can we verify when this is true? And how can we include these effects? On the other hand, even in linear-response one could do better than standard approximations, where the linear-response screening is often calculated in the RPA. How much do things improve when one goes beyond the RPA but stays in linear-response? We address these points in this thesis.

Concerning the screening, we first use a very simple model, where all coordinates collapse to one single point. In this "one-point model" (OPM) [11, 12], the exact solution of the KBE is known, and we can test the quality of the solutions obtained within approximations. In Chap.5 we use the OPM to study, on one side, effects beyond the RPA within linear-response and, on the other side, effects beyond linear-response but staying within the RPA. Interestingly, we find that we have to treat both at the same time in order to find significant improvement. This means that we have to find promising ways to go beyond the RPA that are simple enough to allow us to go to the non-linear regime (this would be difficult for example using the BSE). Therefore we develop approximations based on perturbation theory, and we test some already existent ones (long-range contribution (LRC) [13] and bootstrap approximations [14, 15]) for calculating linear and non-linear screening within TDDFT.

Screening is expressed through the dielectric function, which gives us also directly absorption. This is another reason to explore it in detail. In order to be more realistic than the OPM, we study the dielectric function of a simple solid with one electron per lattice position using localized

Wannier functions. This allows us to highlight cancellations, in the framework of the BSE, between self-energy and excitonic effects. Such cancellations are for example observed in the IXS spectra of insulators. We use these results to derive, in the framework of TDDFT, a simple Kohn Sham exchange-correlation potential and its first derivative with respect to the density, the exchange-correlation kernel, which are self-interaction free. We will emphasize the analogy between the Kohn-Sham potential for extended systems with localized electrons and the atomic case. These points are the topic of Chap.6.

In Chap.7 we go back to the problem of non-linear screening and address the question: how can we make it appear explicitly in the full formulation of the KBE? We show how to do this, and how to use the approximation of a localized electron in order to derive a cumulant Green's function beyond the standard linear-response one [16]. We propose two levels of approximations to evaluate the result in practice, and show some preliminary results. In both cases, TDDFT is used to describe screening.

Since a combination of Green's functions and TDDFT seems to be a good strategy to simplify the many-body problem, Chap.8 contains some more considerations about possible combinations.

1

Introduction to the many-body problem

Most of us have seen birds in the sky that fly in a flock (fig.1.1). The following questions might have come to our minds: Why do birds fly in flocks? Why can flocks of birds have different shapes? Why do birds prefer flying in a V-formation? One reason for birds flying in flocks is to save energy. One explanation is that the ratio of mass per surface for a single bird, is larger than the ratio of mass per surface for a flock of birds, and atmospheric forces compensate easily gravitational forces. Moreover, the ratio of surface to volume for a single bird, is much larger than the ratio of surface to volume for a flock of birds. Smaller surface has smaller resistance in aerodynamics. Making a formation, a flock of birds can decrease further the resistance. For example ibis choose to fly in a V-formation. Forming a V ibis can profit from the airflows that they create with their wings and save energy [17]. Other mechanisms such as the dynamics, the emission of heat, or the visual contact needed in their orientation can also contribute to the configuration of the birds in a flock and give rise to different shapes.

Fig. 1.1: Flocks of birds in a V-formation (`http://www.huffingtonpost.com/2014/01/21/birds-v-formation_n_4638708.html`).

A system of birds is interacting and changing its shape in order to minimize its energy. This is an example of interaction between the elements of a system giving rise to phenomena that we observe. We are able to understand the mechanisms behind the observation, because we can analyze the interaction of each bird with the rest of the birds in the flock. In a similar way we can look for the explanation of the morphology and the color of matter. The explanation is again found in the interaction between the elements of the system or particles. But contrary to the few tenths of birds in a flock, for a cm^3 of matter we have to deal with a huge number of particles (around 10^{23}), which adopt an energetically favorable configuration. Given the fact that each particle will interact with

every other particle in the system, we can only imagine that it is extremely complicated to analyze the effects of interaction in such systems. Besides, the mechanisms of the interaction can also vary for systems with different kinds of particles. The difficulty to analyze and predict the effects of the interaction between particles in matter is called the many-body problem in physics.

In this chapter we will give the quantum-mechanical description of a system of electrons. It is given by the Schrödinger equation. Then we will discuss the electronic correlation which is the main complication of the many-body problem. Simplified approaches to the problem of electronic correlation are given by the Hartree and Hartree-Fock approximations. At the end of the chapter, DFT is presented as a theory that goes beyond those approximations.

1.1 The Schrödinger equation for electrons

All the objects that we use in our everyday life are made of materials. In order to be able to understand their properties and to optimize them or to produce new materials, we need to elucidate the mechanisms which govern their behavior. Matter is a system of particles which are the building blocks and are arranged in some configuration in space. It can be the molecules in a molecular solid, or the atoms in a bulk solid. The smaller the dimensions we are looking at, the bigger becomes the number of objects we will have to treat. From a microscopic point of view, as elementary particles, for the scope of this thesis, we think of the electrons which are bound to nuclei. The number of electrons per cm^3 is of the order of the Avogadro number, which is 10^{23}.

For the scope of the thesis we are interested in the properties that have to do with the interaction of matter with light. These can be optical properties, like the color of materials, or magnetic properties, which can be measured for example from the interaction of x-rays with localized electrons. The light-matter interaction is mediated by electrons rather than by nuclei. For this reason we treat the nuclei as classical positive charges that contribute to the external field of the electronic system. With this assumption we are ready to start looking at mechanisms that arise from the interaction between the electrons in the system.

Electrons are negatively charged particles that interact through the *Coulomb interaction*,

$$v(\mathbf{r}_i - \mathbf{r}_j) = \frac{1}{|\mathbf{r}_i - \mathbf{r}_j|}. \tag{1.1}$$

Here and in the rest of the thesis atomic units (a.u.: $m_e = e = \hbar = \frac{1}{4\pi\epsilon_0} = 1$) will be used. $\mathbf{r}_i$, $\mathbf{r}_j$ are vectors in the three-dimensional space. Each electron in a position $\mathbf{r}_i$ will interact with the other electrons in the system at positions $\mathbf{r}_j$. Here and in the following we neglect relativistic effects. The Coulomb interaction is a two-body interaction, and it is spin-independent.

The Hamiltonian for the electronic system is given by

$$\hat{H}(\mathbf{r}_1, \mathbf{r}_2, ..., \mathbf{r}_N) = \sum_i^N \hat{h}(\mathbf{r}_i) + \frac{1}{2}\sum_{i,j\neq i}^N \frac{1}{|\mathbf{r}_i - \mathbf{r}_j|}. \tag{1.2}$$

The sum over the i and j indices runs over the N electrons in the system. An electron cannot interact with itself and therefore $i \neq j$ in the summation. The fact that in many approximations, which we will encounter later, the term $i = j$ is not properly excluded is called the *self-interaction* problem. The Hamiltonian consists of the Coulomb interaction and one-body operators. The single-particle Hamiltonian

$$\hat{h}(\mathbf{r}_i) = \hat{T}(\mathbf{r}_i) + \hat{V}(\mathbf{r}_i), \tag{1.3}$$

consists of the one-body operators $\hat{T}$ of the kinetic energy and the external potential $\hat{V}$, which stems for example from the nuclei.

The main complication of the many-electron system is that every possible pair of electrons is interacting through the Coulomb interaction. This causes correlation between the electrons. Therefore the origin of the problem of correlation is the large number of electrons and the fact that the Coulomb interaction is a two-body interaction. Taking into account the correlation of the electronic system in the evaluation of properties of the system is important. A first indication comes from the singular behavior of the Coulomb interaction for $\mathbf{r}_i = \mathbf{r}_j$, which makes it impossible to place two electrons at the same position in space because such a process requires an infinite amount of energy.

1.2 The problem of electronic correlation

In quantum mechanics the problem posed by correlation is equivalent to the problem of solving the *Schrödinger equation* for the electronic wavefunction for a system with N electrons,

$$\hat{H}\Psi_\lambda(x_1, x_2, ..., x_N) = E_\lambda^{tot}\Psi_\lambda(x_1, x_2, ..., x_N), \tag{1.4}$$

where $x_i = (\mathbf{r}_i, \sigma_i), i = 1, 2, ..., N$ stand for the space and spin degrees of freedom. The eigenvalues E_λ^{tot} correspond to the total energies of the many-electron states λ. The corresponding wavefunctions Ψ_λ give the probability amplitude with which the system of particles can be found in the many-body state λ. The lowest energy eigenvalue and the corresponding eigenvector are the ground-state of the electronic system.

Electrons are fermions. Following the *Pauli principle*, two fermions cannot occupy the same single-particle state. This is translated into the requirement for the electronic wavefunction to be antisymmetric under the exchange of two particles. The electronic wavefunction can be written as a linear combination of any N-particle basis wavefunctions $\tilde{\Psi}_p$,

$$\Psi_\lambda(x_1, x_2, ..., x_N) = \sum_p C_\lambda^p \tilde{\Psi}_p(x_1, x_2, ..., x_N), \tag{1.5}$$

where p is labeling the set of single-particle states that are occupied in the N-particle basis state. C_λ^p are the expansion coefficients. If one writes eq.1.4 using eq.1.5, the Schrödinger equation for the wavefunction becomes an equation for the coefficients C_λ^p. Then it remains to choose the set of basis wavefunctions $\tilde{\Psi}_p$. If the basis functions $\tilde{\Psi}_p$ are antisymmetric, the wavefunction $\tilde{\Psi}_p$ will be antisymmetric too. Hence we require that

$$\tilde{\Psi}_p(x_1, x_2, ..., x_i, ..., x_j, ..., x_N) = -\tilde{\Psi}_p(x_1, x_2, ..., x_j, ..., x_i, ..., x_N) \tag{1.6}$$

for all i and j. Such an example of basis wavefunctions introduced by Dirac [18] is the basis of Slater determinants $\tilde{\Psi}_p^S$,

$$\tilde{\Psi}_p^S(x_1, x_2, ..., x_N) = \frac{1}{\sqrt{N!}} \begin{vmatrix} \phi_1(x_1) & \phi_1(x_2) & ... & \phi_1(x_N) \\ \phi_2(x_1) & \phi_2(x_2) & ... & \phi_2(x_N) \\ \vdots & \ddots & \ddots & \vdots \\ \vdots & \ddots & \ddots & \vdots \\ \phi_N(x_1) & \phi_N(x_2) & ... & \phi_N(x_N) \end{vmatrix}. \tag{1.7}$$

In a *Slater determinant* all possible configurations of N electrons in the single particle states are spanned, satisfying the demand of antisymmetry. The Slater determinants are constructed from a basis of single-particle states $\phi_i(x)$ giving the probability amplitude that an electron at a position $\mathbf{r}$ occupies the single-particle state i. The single-particle states are not eigenstates of the electrons in the interacting system. Note that the dimension of the single-particle basis is bigger than the number of electrons. For further reading one can look at [19],[20].

Even though the calculation of the many-body wavefunction using the expansion in a basis (eq.1.5) includes in principle all correlation of the electronic system, in practice it is extremely complicated to obtain such a solution for extended systems. The reason is the big number of electrons. For a system with only two electrons we need to solve the Schrödinger equation for wavefunctions which depend on eight coordinates (6 spatial and two spin degrees of freedom). We can imagine that for systems with a larger number of particles, the problem of solving eq.1.4 gets arbitrarily complicated. For this reason we will first take a look at the simplest approximations, namely the mean field due to the Hartree and the Hartree-Fock approximation. Then we look at approaches to treat the problem of correlation, that go beyond those approximations.

1.2.1 The variational principle

Since it is impossible to exactly solve the electronic problem for systems with a large number of particles, one can start from an ansatz for the wavefunction and extract a set of single-particle equations. The solution of the single-particle equations will be a single-particle basis for the construction of the electronic wavefunction of the ground-state. Such equations are usually easier to solve due to the fact that the coupling between electrons is simplified.

The total energy of the ground-state of the electronic system is given by the expectation value of the many-body Hamiltonian in the ground-state, integrating over all degrees of freedom of all particles,

$$E^{tot} = \langle \Psi | \hat{H} | \Psi \rangle = \prod_i^N \int dx_i \Psi^\star(x_1, x_2, ...) H(x_1, x_2, ...) \Psi(x_1, x_2, ...). \tag{1.8}$$

One can apply the *variational principle* [21] and minimize the total energy

$$\frac{\partial}{\partial u}(\langle \Psi | \hat{H} | \Psi \rangle - \sum_i \lambda_i (\langle i | i \rangle - 1)) = 0. \tag{1.9}$$

In the most general case the single-particle basis used for the expansion of the ground-state in many-particle basis functions (e.g. Slater determinants) is fixed and variations are taken with respect to the expansion coefficients $u = C^p$ (eq.1.5). Instead approximations such as Hartree and

Hartree-Fock fix the coefficients and vary with respect to the single-particle basis functions $u = \phi_i$. In the variational principle one constrains the search to a single-particle basis which is orthonormal, introducing the numbers λ_i as Lagrange multipliers. The outcome is a system of N coupled single-particle equations with λ_i being the single-particle eigenvalues. From the calculation of the single-particle basis one can construct the exact many-body wavefunction. However solving such a system is cumbersome, since the coupling between the single-particle equations is complex. Usual approximations such as the Hartree and the Hartree-Fock approximations are based on the decoupling of the single-particle equations.

1.2.2 The Hartree approximation

Electrons are fermions and according to the Pauli principle the many-body wavefunction must be antisymmetric under the exchange of coordinates between two fermions. However, to start with, we limit ourselves to a single product of single-particle wavefunctions , which does not satisfy the requirement of antisymmetry. Neglecting in this way the fermionic nature of the electrons gives the Hartree ansatz for the ground-state wavefunction eq.1.5

$$\Psi(x_1, x_2, ..., x_N) = \prod_{i=1}^{N} \phi_i(x_i). \tag{1.10}$$

The single-particle states involve an expansion in the spin states, $\phi_i(x) = \sum_s \psi_{is}(\mathbf{r})\chi_s(\sigma)$, where the labels $i = (i, s)$ stand for the pair of orbital and spin states. Spin states $\sigma = (\uparrow, \downarrow)$ can be either spin-up or spin-down. In many cases a spin state is assigned to an orbital state. This approximation is known as the *unrestricted Hartree-Fock* approximation (UHF), where the spin breaks the spatial symmetry of the Hamiltonian. We can plug the Hartree ansatz into the Schrödinger equation 1.4 to obtain

$$\sum_{i=1}^{N} h_{ii} + \frac{1}{2}\sum_{i,j\neq i}^{N} v_{iijj} = E^{tot}. \tag{1.11}$$

The general matrix element of the Coulomb interaction in a single-particle basis is given by

$$v_{ijkl} = \delta_{\sigma_i\sigma_j}\delta_{\sigma_k\sigma_l} \int d\mathbf{r}_1 \int d\mathbf{r}_2 \frac{\psi^{\star}_{i\sigma_i}(\mathbf{r}_1)\psi_{j\sigma_j}(\mathbf{r}_1)\psi_{k\sigma_k}(\mathbf{r}_2)\psi^{\star}_{l\sigma_l}(\mathbf{r}_2)}{|\mathbf{r_1} - \mathbf{r_2}|}. \tag{1.12}$$

We now apply the minimization principle (eq.1.9) to the Schrödinger equation 1.11 to obtain a set of single-particle equations

$$\left(h(\mathbf{r}) + \int d\mathbf{r}' \frac{\sum_{(i,\sigma_i)\neq(a,\sigma_a)}^{N} \psi^{\star}_{i\sigma_i}(\mathbf{r}')\psi_{i\sigma_i}(\mathbf{r}')}{|\mathbf{r} - \mathbf{r}'|}\right)\phi_a(x) = \lambda_a\phi_a(x), \tag{1.13}$$

known as the *Hartree equations* [22], named after Hartree who had the idea to obtain a single-particle potential for atoms by adding the interaction with the static charge destribution from the electrons in the system, to the central-force field of the nucleus. The sum of states in eq.1.13 excludes the self-interaction contribution $i = a$. Instead, if it is included, each electron interacts via the Coulomb interaction with the density $\rho(\mathbf{r})$ of all electrons given by

$$\rho(\mathbf{r}) = \sum_{(i,\sigma_i)}^{N} \psi^{\star}_{i\sigma_i}(\mathbf{r})\psi_{i\sigma_i}(\mathbf{r}). \tag{1.14}$$

The sum in the density extends over the first N occupied states. The interaction with the density constitutes the classical or Hartree potential,

$$V^H(\mathbf{r}) = \int d\mathbf{r}' \frac{\rho(\mathbf{r}')}{|\mathbf{r} - \mathbf{r}'|}, \tag{1.15}$$

which, as we have seen, is derived violating the Pauli principle and introducing the self-interaction problem. Even though the original Hartree equations have been derived with the self-interaction correction [23], they are usually written using the Hartree potential which puts back the self-interaction. This potential can be treated as an external potential and is an explicit functional of the density calculated self-consistently from the single-particle equations. Even though it suffers from self-interaction, it gives the electrostatics, which is a major contribution in the electronic system. In later chapters we will discuss its importance for systems with localized electrons.

1.2.3 The Hartree-Fock approximation

Now taking into account the fact that electrons are fermions one may ask for the many-body wavefunction of the ground-state configuration to be given by a single Slater determinant $\Psi^S(x_1, x_2, ..., x_N)$ (eq.1.7) [24] and obtain the total energy of the ground-state from the Schrödinger equation as

$$\langle \Psi^S | \hat{H} | \Psi^S \rangle = E^{tot}. \tag{1.16}$$

Then we apply again the minimization principle eq.1.9 to obtain the single-particle equations

$$\Big(h(\mathbf{r}) + V^H(\mathbf{r}) \Big) \psi_{a\sigma_a}(\mathbf{r}) - \int dx' \frac{\sum_{j\sigma_j} \psi^\star_{j\sigma_j}(\mathbf{r}')\psi_{j\sigma_j}(\mathbf{r})\delta_{\sigma_a\sigma_j}}{|\mathbf{r} - \mathbf{r}'|} \psi_{a\sigma_a}(\mathbf{r}') = \lambda_a \psi_{a\sigma_a}(\mathbf{r}). \tag{1.17}$$

Those are known as the *Hartree-Fock equations* [25], where the density matrix $\rho_{\sigma_a}(\mathbf{r}, \mathbf{r}')$ of σ_a spin states appears, defined as

$$\rho_{\sigma_a}(\mathbf{r}, \mathbf{r}') = \sum_j^{N_{\sigma_a}} \psi^\star_{j\sigma_a}(\mathbf{r}')\psi_{j\sigma_a}(\mathbf{r}). \tag{1.18}$$

Here the sum over N_{σ_a} occupied states with spin σ_a appears, where spin σ_a can be either spin up or spin down. The total number of electrons is equal to the sum of electrons with spin-up and spin-down $N = N_\downarrow + N_\uparrow$. In the Hartree-Fock equations the Hartree potential from electrons with spin σ_a is corrected for self-interaction by the Coulomb interaction with the density matrix of the electrons with the same spin. This means that in the Hartree-Fock equations an electron sees the field from the electrons with opposite spin as a classical potential which can be added to the nuclear potential. Therefore the Hartree-Fock equations are spin-dependent. This can be seen clearly in the one-level model for two electrons, where the effect of the interaction in the ground-state is a classical potential from the electron of opposite spin. In eq.1.17 the interaction with the density matrix gives the exchange term or Fock correction accounting for the Pauli exclusion principle and automatically removing the self-interaction problem in the classical potential. The notion of exchange has been introduced by Dirac[26]. Still the Hartree-Fock equations lack the description of correlation since the real electronic wavefunction cannot be a single Slater determinant but would rather be written as a linear combination of Slater determinants reflecting the electronic correlation, as explained above.

When the single-particle orbital $\psi_{a\sigma_a}(\mathbf{r})$ is very localized and shows little overlap with any other orbital $j \neq a$, the approximation

$$\psi_{a\sigma_a}(\mathbf{r})\psi^{\star}_{j\sigma_a}(\mathbf{r}) = 0 \quad j \neq a \tag{1.19}$$

may be used in eq.1.17 and the Hartree-Fock equations reduce to the original Hartree equations (eq.1.13). Therefore an electron which does not overlap with others can only interact through the Hartree potential via the density corrected for self-interaction. Electronic states that show this property are deep core states and valence d or f electrons. They will be the main topic of discussion of the later chapters of this thesis.

1.3 Post-Hartree-Fock methods

In Hartree-Fock the wavefunction is given as a single Slater determinant. A single Slater determinant is able to capture the exchange contribution from the Coulomb interaction and it starts from a single-particle basis with dimensionality equal to the number of particles in the system. This introduces a huge simplification since one does not have to find the coefficients in eq.1.5. The exact treatment of correlation given in eq.1.5 requires an expansion in all N-particles basis wavefunctions. For example in a basis of Slater determinants this would mean an expansion in the wavefunctions of every possible configuration including a basis of single-particle states much bigger than the number of particles in the system. This is usually done in *configuration-interaction* (CI) methods, where a basis of N-particle wavefunctions is constructed from a single-particle basis (e.g. of atomic orbitals), and then the expansion coefficients giving the interacting state are determined.

Let us illustrate the effects of correlation in a system with two particles [27]. The H_2 molecule in the ground-state has two atoms at a distance of 1.4 a.u. and each atom contributes one electron to the system. We can construct the Hartree-Fock wavefunction from the $1s$ states of a basis with atomic-like wavefunctions accounting also for some effects of the interaction in the Hartree-Fock sense. The case where the $1s_1$ and $1s_2$ wavefunctions have the same radial part and different spin is in the sense of the *restricted Hartree-Fock* method (RHF) which does not allow the system to break symmetry. In an unrestricted Hartree-Fock (UHF) calculation the system is allowed to break symmetry in order to lower its energy. Then the $1s_1$ and $1s_2$ states get a different radial part, for spin-up and spin-down respectively. In tab.1.1 we give for an UHF calculation the atomic-like single-particle states for the $1s$ and $2s$ states, which have spherical symmetry [28]. For a RHF calculation the bonding and antibonding molecular orbitals are given by the symmetric and antisymmetric combinations of the single-particle states, one located at position $r = 0$ and one at position $r = 1.4$ a.u., along the z axis,

$$\psi^{+}_{1s}(r) = \frac{1}{\sqrt{2}}(\psi_{1s}(r) + \psi_{1s}(r - 1.4)) \tag{1.20}$$

$$\psi^{-}_{1s}(r) = \frac{1}{\sqrt{2}}(\psi_{1s}(r) - \psi_{1s}(r - 1.4)). \tag{1.21}$$

In principle the system has cylindric symmetry, and we should keep the angle around the axis in the calculations, on top of the z-direction. In the following we will treat the molecule as a one-dimensional model for the sake of a simple illustration, and ignore the angular coordinate. Then r stands for a coordinate along the axis. For an RHF calculation the radial part of the molecular wavefunction is the same for a spin up or a spin down state. In tab.1.2 we also list the bonding and antibonding molecular orbitals for the UHF case, made of the $1s_1, 1s_2, 2s_1$ and $2s_2$ states. The basis of molecular orbitals is not normalized due to the fact that there is finite overlap between the atomic wavefunctions of the two electrons. Moreover in the UHF case the molecular orbitals for the states with opposite spin $(1s_1, 1s_2)$ are not orthogonal due to the fact that the atomic wavefunctions for these states are not orthogonal. Therefore the basis of molecular orbitals, whose states are shown in tab.1.2, is not orthonormal. In general this can cause problems, but it is fine for now, since the scope of this section is merely to illustrate the effect of correlation.

$1s_1(r) =$	$\sqrt{\frac{0.965^3}{\pi}}e^{-0.965\|r\|}$
$2s_1(r) =$	$\sqrt{\frac{1.16^5}{3\pi}}\|r\|e^{-1.16\|r\|}$
$1s_2(r) =$	$\sqrt{\frac{1.43^3}{\pi}}e^{-1.43\|r\|}$
$2s_2(r) =$	$\sqrt{\frac{1.78^5}{3\pi}}\|r\|e^{-1.78\|r\|}$

Tab. 1.1: Atomic orbitals. $1s_1$ stands for ψ_{1s_1}.

$1s_1^{\pm}(r) =$	$\frac{1}{\sqrt{2}}(1s_1(r) \pm 1s_1(r-1.4))$
$1s_2^{\pm}(r) =$	$\frac{1}{\sqrt{2}}(1s_2(r) \pm 1s_2(r-1.4))$
$2s_1^{\pm}(r) =$	$\frac{1}{\sqrt{2}}(2s_1(r) \pm 2s_1(r-1.4))$
$2s_2^{\pm}(r) =$	$\frac{1}{\sqrt{2}}(2s_2(r) \pm 2s_2(r-1.4))$

Tab. 1.2: Molecular-orbital basis. $1s_{\pm}^1$ stands for $\psi_{1s}^{\pm}$.

Then the molecular wavefunction, which is a two-particle wavefunction, is taken as a linear combination of the molecular orbitals made of $1s$ spin states. For a RHF calculation it is given as

$$\Psi^{HF\pm}(x_1, x_2) = \frac{1}{2}(\psi_{1s}^{\pm}(r_1)\psi_{1s}^{\pm}(r_2) + \psi_{1s}^{\pm}(r_2)\psi_{1s}^{\pm}(r_1))(\uparrow\downarrow - \downarrow\uparrow). \tag{1.22}$$

We take the symmetric linear combination of spatial wavefunctions since the spin wavefunction will be antisymmetric in the ground-state and the full wavefunction, hence, fulfills the Pauli principle. For an UHF calculation the radial part of the two-particle wavefunction is given in tab.1.3, where the radial part of the molecular orbitals is different for the spin-up and down states. In order to include also correlation effects one needs to construct molecular orbitals from higher atomic

$1s_1^+, 1s_2^+(r_1, r_2) =$	$\frac{1}{2}(1s_1^+(r_2)1s_2^+(r_1) + 1s_1^+(r_1)1s_2^+(r_2))$
$1s_1^-, 1s_2^+(r_1, r_2) =$	$\frac{1}{2}(1s_1^-(r_2)1s_2^+(r_1) + 1s_1^-(r_1)1s_2^+(r_2))$
$2s_1^+, 2s_2^+(r_1, r_2) =$	$\frac{1}{2}(2s_1^+(r_2)2s_2^+(r_1) + 2s_1^+(r_1)2s_2^+(r_2))$

Tab. 1.3: Molecular basis wavefunctions. $1s_1^+, 1s_2^+(r_1, r_2)$ stands for the radial part, which is also equal to the UHF wavefunctions $\Psi_{1s}^{UHF++}(r_1, r_2)$.

states like $2s$ and $2p$ orbitals. For the H_2 molecule the $1s$, $2s$ and $2p$ orbitals are sufficient to obtain the major effects of correlation along the axis which connects the two atoms [28]. Then the molecular wavefunction can be approximated by the linear combination

$$\Psi^{CI}(r_1, r_2) = c_1 1s_1^+, 1s_2^+(r_1, r_2) + c_3 1s_1^-, 1s_2^+(r_1, r_2) + c_2 2s_1^+, 2s_2^+(r_1, r_2), \tag{1.23}$$

where the molecular states that appear are the ones that contribute to the ground-state and are given in tab.1.3. The constants take the values $c_1 = 0.2946, c_2 = 0.0302, c_3 = -0.1654$ [28].

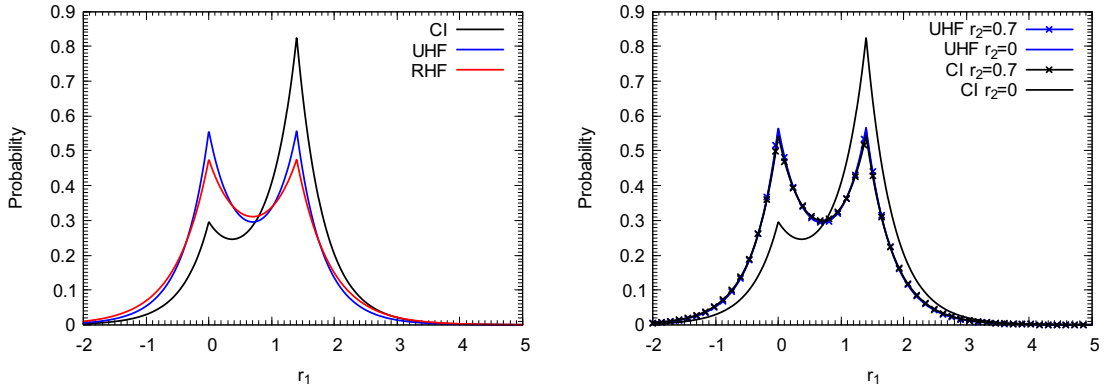

(a) Fixed electron at $r_2 = 0$ *(b)* Comparison between $r_2 = 0$ and $r_2 = 0.7$

Fig. 1.2: Probability to find one electron at position r_1 when an electron is fixed at position r_2. Comparison between the correlated and the uncorrelated (Hartree-Fock) wavefunctions.

In fig.1.2 we fix the position of one electron at the position of one nucleus $r_2 = 0$ and we plot the probability $|\Psi(r_1, r_2)|^2$ to find the second electron along the axis connecting the two atoms. We compare for the RHF (eq.1.22), the UHF (tab.1.3) and the CI result in [28]. The correlation is properly accounted for only in the CI. In fig.1.2a we see that the probability given by both the UHF and RHF is symmetric and the electron can be found with equal probabilities at positions $r_1 = 0$ and $r_1 = 1.4$. Both cases show that the effect of the Pauli principle is that the two charges do not see each other and that only the electrostatic effect from a Hartree potential affects the amplitude of the wavefunction. However one expects that the effect of the Coulomb interaction between the two electrons, which is repulsive, will lower the probability for the two charges to be found at the same position. And indeed this is what happens for the CI wavefunction. The electron moves towards the second atom $r_1 = 1.4$ and can be found with higher probability there

than at $r_1 = 0$. This illustrates the effect of the correlation coming from the Coulomb repulsion between the two electrons. In a last step we see what happens when we move the first electron from $r_2 = 0$ to $r_2 = 0.7$, i.e. in the middle of the line connecting the two atoms (1.2b). In this case, the displacement of the electron does not affect the UHF wavefunction. From the CI wavefunction the electron will be found with equal probability at each nuclei position.

1.4 Exchange and correlation within DFT

As we have discussed in the previous sections, in the Hartree approximation a simplified description of the electronic system has been achieved through a set of single-particle equations accounting for the interaction of electrons via the Hartree potential, which is a functional of the density. This description reproduces only certain aspects of the many-body wavefunction as it violates the Pauli principle. On the other hand the Hartree-Fock equations satisfy the Pauli principle, but they introduce a non-local exchange part which makes their solution more complicated. May the description of correlation achieved by the two schemes not be satisfactory, but it provides ideas for further improvement. First, thinking of the fact that the Hartree potential is a pure functional of the density, whereas in the Hartree-Fock equations the density matrix appears, one might want to try to find pure functionals of the density that improve the description of exchange and correlation compared to the Hartree potential. In a similar sense one may also look for a fictitious system given by a simplified set of one-particle equations in order to obtain an improved description of correlation. The two concepts of finding potentials which are functionals of the density and introducing an auxiliary system with simplified equations have settled the framework of DFT as a theory which targets the improved ab initio description of correlation.

Hohenberg and Kohn [1] stated that for a system of interacting electrons there is a one-to-one correspondence between an external potential $V(x)$ and the ground-state density $\rho(x)$ up to an arbitrary additive constant. They also stated that the total energy of the ground-state of the system is a unique functional of the density. Using the fact that the total energy of the ground-state becomes minimal for the exact density, Kohn and Sham [2] applied the variational principle and derived a set of single-particle equations known as the *Kohn-Sham equations*,

$$\big(h(\mathbf{r}) + V^H(\mathbf{r}) + V^{xc}(x)\big)\phi_i^{KS}(x) = E_i^{KS}\phi_i^{KS}(x). \tag{1.24}$$

Here $V^{xc}(x)$ is the exchange-correlation potential. The sum of external, Hartree (V^H) and exchange-correlation (V^{xc}) potentials is often referred to as Kohn-Sham potential. Writing the the exchange-correlation contribution to the total energy as a functional of the density $E^{xc}[\rho(x)]$, the exchange-correlation potential is defined as

$$V^{xc}(x) = \frac{\delta E^{xc}(x)}{\delta\rho(x)}. \tag{1.25}$$

As we can see, exchange and correlation effects appear in the potential of an auxiliary system of independent particles. In real systems the difficulty is to find the exact energy functional of the density and extract the Kohn-Sham potential. Numerous approximations to it have been developed such as local density (LDA), generalized gradient (GGA) and Perdew-Burke-Ernzerhof (PBE) approximations or hybrid functionals [29], but usually they are reliable only for certain

classes of systems. In the Kohn-Sham equations correlation effects beyond Hartree-Fock are taken into account through the exchange-correlation potential. But still constructing from the N lowest Kohn-Sham orbitals the many-body wavefunction in the form of a single Slater determinant is not equal to the ground-state wavefunction of the interacting system. The only common property between the Kohn-Sham and the interacting system is the ground-state density. Therefore, properties of the interacting system can only be evaluated from the Kohn-Sham system under the condition that they can be written as pure functionals of the ground-state density. Unfortunately, the density functionals for most observables are not known. An example for a quantity where good approximations have been developed is, as we have already discussed, the total energy of the ground-state of the interacting system. For further reading about DFT one can look at [29], [30].

Summary

In the Schrödinger equation for electrons the Coulomb interaction correlates the electrons in a way that makes the equations too difficult to be solved exactly. Simplifications of the problem include the reduction of the Schrödinger equation to a system of single-particle equations and the replacement of the interaction by a simplified potential which depends only on the density or density matrix. These simplifications are the standard Hartree and Hartree-Fock approximations, which succeed to reproduce only certain aspects of the electronic system and fail to capture the full correlation effects. In a similar sense, using a set of single-particle equations for an auxiliary system of independent particles (Kohn-Sham) in an effective potential, DFT goes a step further in the description of correlation being able to give the exact density. DFT however requires all properties of the system to be given as functionals of the density in order to be calculated. Moreover, the exact Kohn-Sham potential is not known. In this thesis we will derive an approximate Kohn-Sham potential for systems with localized electrons, where the self-interaction correction is of major importance.

2

Observables in spectroscopy from measurements and theory

We are interested in spectroscopic measurements of properties of materials which are based on the interaction of matter with light. The essential tools for a spectroscopic measurement are the periodic table of elements (fig.2.1) and the electromagnetic spectrum of radiation (fig.2.2). Each element in the periodic table consists of a nucleus and a certain number of electrons. Contrary to a system of independent particles, where each electron occupies a well-defined energy level, in an interacting system, energy levels are attributed to the whole many-body system and they rearrange in a way that reflects the configuration of electrons in the atom, molecule, liquid or solid.

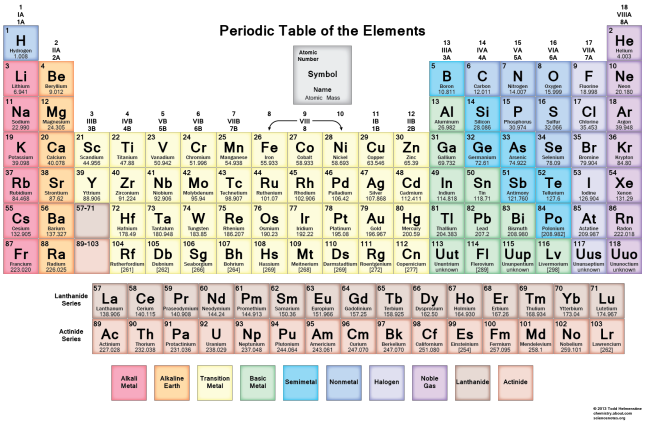

Fig. 2.1: Periodic table of elements. [31]

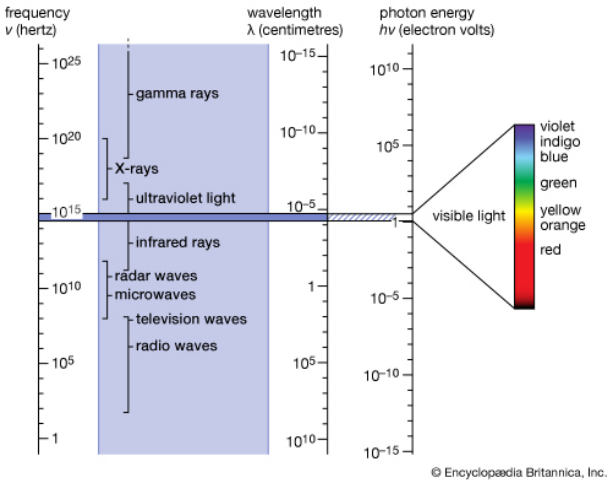

Fig. 2.2: Electromagnetic spectrum of radiation [32].

Using electromagnetic radiation we can probe the properties of a material with light. As response to this perturbation, the sample can emit electrons or photons, or nothing at all. In order to respond, the system must be able to absorb a photon, obeying energy conservation and transition probabilities. In this sense the spectroscopic measurement indicates the probability that electrons respond to each photon energy of the electromagnetic spectrum.

From a practical point of view the experimental setup consists of a light source, the sample and a spectrometer or an electron detector. We give as an example a sketch of x-ray photoemission spectroscopy (XPS) in fig.2.3. We will discuss XPS in more detail later in this chapter.

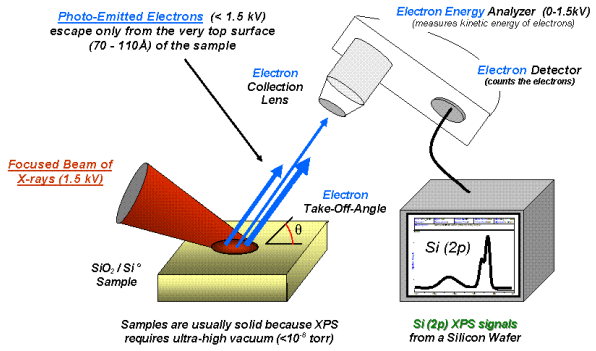

Fig. 2.3: Experimental setup for XPS. An x-ray beam impinges on a sample and electrons are emitted. Their kinetic energy is analyzed in a detector. [33]

From a theoretical point of view the spectroscopic measurement corresponds to the probability that an operation will leave the ground-state of the system unaffected. Given an observable $\hat{O}$ the expectation value with the ground-state wavefunction of a system with N-particles $|N0\rangle$ is defined as

$$\langle O(t)\rangle = \langle N0|\hat{O}(t)|N0\rangle \tag{2.1}$$
$$= \prod_i^N \int dx_i |\Psi(x_1, x_2, ...)|^2 O(x_1, x_2, ..., t).$$

The observables can be given by static operators $\hat{O}$ such as the position ($\mathbf{r}$) or the momentum ($-i\nabla_{\mathbf{r}}$) operator, or dynamical operators measuring for example the probability that a system makes a transition between two states in the time interval t. Dynamical operators are closely related to the spectroscopic measurement through Green's functions.

As we have shown in chap.1 the calculation of expectation values from the many-body wavefunction is cumbersome. There are at least two ways to overcome this difficulty. One is to become system specific and treat only systems that are well described within approximations that simplify the calculation of the wavefunction or allow for a direct calculation of the expectation value. This is the case for example if we neglect some of the correlation of the wavefunction within the Hartree and Hartree-Fock approximations. The second possibility is to map the full many-body system to simplified auxiliary systems that reproduce only some quantities of the exact system ($o(t)$) and the expectation values need to be evaluated as functionals of those quantities $\langle O\rangle[o(t)]$. Such an example is the Kohn-Sham system of DFT, or going a step further, the density matrices from reduced density-martix functional theory (RDMFT) [34] or the one-body Green's function from dynamical mean-field theory (DMFT) [35] or many-body perturbation theory (MBPT) [36].

In this chapter dealing with the interaction of matter with radiation we will divide the different spectroscopies into three categories: processes that involve the absorption of photons and emission of photons, processes where electrons are added and processes where electrons are ejected from the system. We will introduce the theory underlying these processes and improvements on the description of correlation. Then we will present the observables that describe the spectroscopic processes. We will explain the information that they contain, the difficulties for their calculation and standard approximations for their evaluation. For the scope of this chapter we refer to zero-temperature measurements in equilibrium. A detailed explanation of the formalism going beyond zero temperature and equilibrium within MBPT will be the subject of the following chapter.

2.1 Spectroscopies

One major category of spectroscopies uses photon sources in order to probe excited states of matter. The measurements give observables which correspond to the physical processes that take place in the experiment. The photon plays the role of an external field

$$\mathbf{A}(\mathbf{r},t) = \int_{\infty}^{+\infty} d\omega \mathbf{A}(\omega) e^{i\mathbf{qr}} e^{i\omega t} \tag{2.2}$$

propagating with momentum $\mathbf{q}$ and frequency ω. This frequency gives the energy to be exchanged with electrons. For negligible photon momentum $\mathbf{q}$

$$e^{i\mathbf{qr}} \approx 1 + i\mathbf{qr} \tag{2.3}$$

one obtains the *dipole approximation*, which gives the dipole selection rules for vanishing momentum transfer, filtering transitions. For the scope of this thesis we will remain in the dipole approximation, where energy transfer happens only through the photon-frequency. Of course this is sometimes a crude approximation, but it allows us to treat light in terms of a frequency-dependent external potential.

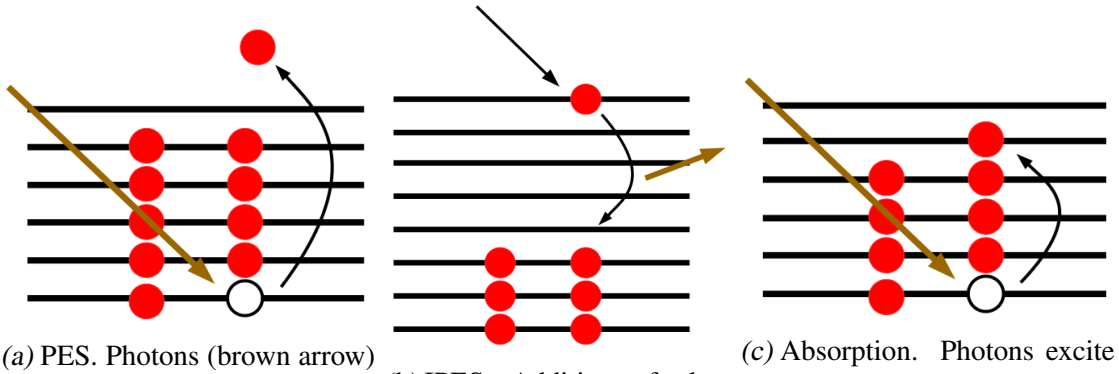

(a) PES. Photons (brown arrow) remove electrons from the sample.

(b) IPES. Addition of electrons followed by the emission of photons.

(c) Absorption. Photons excite electrons.

Fig. 2.4: Schematic illustration of PES, IPES and absorption in an independent-particle picture.

In photoemission spectroscopy (PES) the photon removes electrons from the sample (fig.2.4a). With this process one can measure the so-called "binding energy" of electrons in the ground-state of the interacting system or to be precise, the energy difference between the ground-state of the N-electron system and an excited state of the $(N-1)-$electron system. One can use UV photons for the emission of electrons close to the Fermi level, or x-rays for the emission of valence or core electrons (XPS). From angular-resolved photoemission spectroscopy (ARPES) one can also obtain information about the energy dispersion with the momentum of the photoelectron $E(\mathbf{k})$, which can be linked to the crystal momentum in the periodic system and which can hence be used to probe the electronic structure of the interacting system. The photoemission of excited states can also be measured by $2-$photon photoemission (2PPE), where an electron first is excited and then emitted from this excited state.

The energy to add an electron to one of the unoccupied states of the electronic system, which is a process complementary to photoemission, is given by inverse photoemission spectroscopy (IPES) (fig.2.4b). In this spectroscopy the material is bombarded with electrons that occupy high-energy conduction states. Radiation is emitted due to the decay of electrons in low-energy conduction states.

The energies for the transition between the ground and excited states of the N-electron system are obtained from absorption or inelastic x-ray scattering (IXS). In IXS an x-ray photon is absorbed by a low-energy electron, which gets excited in a conduction state leaving a hole behind. Then an electron from a lower state can be deexcited and recombine with the hole emitting a photon of lower energy. The difference between the incoming and outgoing photons is equal to the energy of the excitation being created in the process.

For core electrons excitation energies can be measured with x-ray absorption spectroscopy (XAS) where a high-energy x-ray photon is used to excite an electron from a low-lying core state to an unoccupied state of the system. The XAS can be divided into x-ray absorption near-edge spectroscopy (XANES), which probes the edge of the x-ray absorption spectrum for transitions in unoccupied states close to the Fermi level and Extended x-ray absorption fine structure (EXAFS) which probes the high-energy part of the x-ray absorption spectrum, where an excited photoelectron can be scattered by neighboring atoms. Therefore the EXAFS spectrum can be used to obtain information about the structural environment of an atom. Both XANES and EXAFS can be unified under x-ray absorption fine structure (XAFS).

Another category of spectroscopies are the electron-beam spectroscopies, where a high-energy electron beam is used to induce inelastic scattering events in matter that lead to excited states. In appearance potential spectroscopy (APS) the emitted radiation and the energy of the outgoing electron beam are indicative of the relaxation events that take place in the material. In electron energy loss spectroscopy (EELS) the energy loss of the electron beam gives information about inner transitions and scattering events that have taken place during the transmission of the beam through the sample.

2.1.1 Koopmans' theorem

The energy for the photoemission of an electron from a state i can be approximated by *Koopmans' theorem* [37] as the difference between the total energy of a system with N-particle and the total energy of a system with $N-1$ particles with an electron missing from the single-particle state i,

$$E_{PES} = E_N - E_{N-1,i}. \tag{2.4}$$

Eq.2.4 is in principle exact, but Koopmans' theorem is a simplification of the fact that after the photoemission the system has $N-1$ electrons in an excited many-body state i (fig.2.4a). In a similar way the inverse photoemission of an electron in a state f (fig.2.4b) is given by Koopmans' theorem as the difference between the total energies of a system with N particles and the total energy of a system with $N+1$ particles with an electron added to the single-particle state f,

$$E_{IPES} = E_N - E_{N+1,f}. \tag{2.5}$$

Note that in the photoemission and inverse photoemission processes the number of electrons in the sample is not conserved.

Using Koopmans' theorem the photon-absorption process (fig.2.4c) can be treated as the combination of an inverse-photoemission and a photoemission process, where an electron has been removed from the level i of a system and an electron has been added to the level f. In the photoabsorption process the number of electrons is conserved. The energy for the transition of the electron from the state i to the state f is approximately given by the difference between the system of $N+1$ particles with an additional electron in a state f and the system with $N-1$ particles with an electron missing from a state i,

$$\Delta E = E_{N+1,f} - E_{N-1,i}. \tag{2.6}$$

Treating spectroscopies using Koopmans' theorem we neglect two important effects both stemming from correlation. The first is the relaxation of the wavefunction of the system in the absence/presence of an electron. The second is that in this description of the absorption one has separately $N+1$ or $N-1$ electrons saying that the interaction between the electron and the hole is missing. Koopmans' theorem becomes exact in Hartree-Fock and in the frozen-orbital approximation, because Hartree-Fock contains no correlation.

2.1.2 The self-consistent field approach

As we have mentioned above, even remaining in a one-electron picture the single-particle wavefunctions should be corrected in order to account for the presence/absence of an electron in the system. Roothaan [38, 39] and Bagus [40] developed the self-consistent field (SCF) approach which allowed the self-consistent calculation of the single-particle wavefunctions ϕ_i of the system with $N-1$ or $N+1$ particles based on the minimization of the total energy of a Hartree-Fock Hamiltonian for the ionized system. Such a calculation involves the solution of the Hartree-Fock single-particle equations,

$$H_i\phi_i = (h_i + V_i^{HF})\phi_i \tag{2.7}$$

$$H_i^j\phi_i^j = (h_i^j + V_i^{HFj})\phi_i^j. \tag{2.8}$$

V_i^{HF} in eq.2.7 is the single-particle Hartree-Fock potential for the electron in the state i of the system with N-particles in its ground-state configuration, whereas j refers to the state which is empty or occupied in the ionized system and V_i^{HFj} is the single-particle Hartree-Fock potential for the electron in the state i of the ionized system with $N-1$ or $N+1$ particles in the ground-state configuration. In both cases the Hartree-Fock equations are solved self-consistently in the sense that the single-particle basis states minimize the total energy of the ground-state configuration.

Using Koopmans' theorem (eq.2.4) the ionization potential for removing an electron from a state j is given by eq.2.7 as the single-particle Hartree-Fock energy of the state j (ϵ_j^{HF}) evaluated from the matrix elements of the Coulomb interaction taken with a basis which is not relaxed for the absence of the j^{th} electron. Using eq.2.8 we obtain a correction to Koopmans' theorem given by V^p

$$V^p = \sum_{i\neq j}(V_i^{HFj} - V_i^{HF}), \tag{2.9}$$

adding the polarization contribution from the relaxation of the Hartree-Fock orbitals in the ionized system. In 1969 Hedin and Johansson [41] introduced the ΔSCF approach (eq.2.9) for the photoemission of core states, which is based on the difference between two SCF calculations, one for the ground-state (eq.2.7) and one for the ionized state (eq.2.8). From a ΔSCF calculation, Koopmans' theorem gets corrected as

$$E = \epsilon_j^{HF} + \frac{1}{2}V^p, \tag{2.10}$$

where V^p is the polarization correction, given by eq.2.9, that is due to the removal of the electron j from the system with N particles.

In the Hartree-Fock approximation polarization corrections are obtained only from the Hartree and exchange part of the potential. The Kohn-Sham potential is a way to account for polarization corrections including more correlation effects. Therefore ΔSCF calculations are often done within Kohn-Sham.

The SCF and ΔSCF methods have been successfully applied to the photoemission of core electrons, because core states are decoupled from the rest of the states to a good level of approximation. The decoupling of the core levels is a key approximation for spectroscopies that we will describe later in more detail.

2.2 What has to be calculated for spectroscopy?

The measurable quantity for the various spectroscopies is the cross-section $\sigma(\omega)$ defined as the section (area) crossed by the number of photons that correspond to the absorbed energy. Its unit is m^2. The cross-section is usually measured in experiments but can be calculated as well following Hedin [42] and using *Fermi's golden rule*

$$J(\omega) = \sum_s f_s \delta(\omega - \omega_s) \tag{2.11}$$

for the probability of the system in its ground-state to absorb a photon with frequency ω. s labels excited states, f_s is the transition probability. It equals $f_s = |\langle N_s|\hat{D}|N\rangle|^2$, where N_s is an excited state of the N-body system and $\hat{D}$ the dipole operator, which can be written as $\sum_{ij} \Delta_{ij} c_i^\dagger c_j$ in second quantization. Spectra such as IXS are directly proportional to this quantity. In photoemission we are interested in an excited state, where an electron is in an unbound state far from the sample, and $J(\omega)$ is the *photocurrent*. In the *sudden approximation* this can be expressed as

$$|N, s\rangle = |N-1\rangle|k\rangle \approx c_k^\dagger |N-1, s\rangle, \tag{2.12}$$

i.e. the photoelectron with momentum k is decoupled from the system. Then the photocurrent is proportional to

$$J(\omega, k) = \sum_s \sum_{ij} \Delta_{ij} |\langle N-1, s|c_k c_i^\dagger c_j|N\rangle|^2 \delta((E_N - E_{N-1,s} - \epsilon_k) - \omega). \tag{2.13}$$

In eq.2.13 the photocurrent is proportional to the probability amplitude that the system with N particles makes a transition to an excited state s with $N-1$ electrons and a photoelectron k with

energy ϵ_k. In the sudden approximation effects from the interaction of the photoelectron with the hole left behind, and of the propagation of the photoelectron inside the material and through the surface are neglected [43].

2.3 The tools of theoretical spectroscopy

In this section we focus on the calculation of the cross-sections for different spectroscopies from Green's functions. We will start with an introduction to Green's function theory and discuss the information given by those quantities. Green's functions are calculated from MBPT and this will be the subject of the next chapter. In MBPT a perturbing potential can be applied in order to probe equilibrium and non-equilibrium properties stemming from the interaction between the particles in the system. The equation of motion of the Green's function provides an alternative approach to the many-body problem which is exact. The perturbative treatment of the external potential implies that the equilibrium limit can always be taken at the end, so that ground-state properties of the electronic system can be extracted in a way which is equivalent to the knowledge of the many-body wavefunction [44]. In the following discussion we will give expressions that are valid in equilibrium and at zero temperature. Our illustrations will refer to systems with independent particles.

2.3.1 The one-particle Green's function

Let us first introduce the field operators in the *Heisenberg picture* under the effect of a static hamiltonian $\hat{H}$

$$\hat{\Psi}^\dagger(x,t) = e^{i\hat{H}t}\sum_k a_k^\dagger \phi_k^\star(x) e^{-i\hat{H}t} \tag{2.14}$$

for the creation of particles and

$$\hat{\Psi}(x,t) = e^{i\hat{H}t}\sum_k a_k \phi_k(x) e^{-i\hat{H}t} \tag{2.15}$$

for the annihilation of particles. The operators $a_k^\dagger$ and a_k are creation and annihilation operators satisfying the *fermionic algebra* of anticommutators

$$[a_i, a_j^\dagger]_+ = \delta_{ij} \tag{2.16}$$

$$[a_i, a_j]_+ = 0 \tag{2.17}$$

$$[a_i^\dagger, a_j^\dagger]_+ = 0. \tag{2.18}$$

Similar relations are satisfied also by the anticommutators of the field operators. The field operators $\hat{\Psi}(x,t)$ are used to pass between Hilbert spaces with different particle numbers that altogether constitute the Fock space. The density operator is expressed in terms of the field operators as

$$\hat{\rho}(x,t) = \hat{\Psi}^\dagger(x,t)\hat{\Psi}(x,t). \tag{2.19}$$

The equilibrium one-particle Green's function is defined as the expectation value of the time-ordered product of two field operators, one for the creation and one for the annihilation of a particle,

taken in the many-body ground-state of the system with N particles,

$$G(x_1,t_1,x_2,t_2) = -i\langle N0|\hat{T}\{\hat{\Psi}(x_1,t_1)\hat{\Psi}^\dagger(x_2,t_2)\}|N0\rangle. \tag{2.20}$$

Here, $\hat{T}\{\}$ is the *time-ordering operator* giving the time-ordered product of the field operators as

$$\hat{T}\{\hat{\Psi}(x_1,t_1)\hat{\Psi}^\dagger(x_2,t_2)\} = \hat{\Psi}(x_1,t_1)\hat{\Psi}^\dagger(x_2,t_2)\theta(t_1-t_2) - \hat{\Psi}^\dagger(x_2,t_2)\hat{\Psi}(x_1,t_1)\theta(t_2-t_1). \tag{2.21}$$

The one-particle Green's function describes the propagation of a particle between two points in space and time. The one-particle Green's function of the interacting electrons is given with respect to the one of the non-interacting system G^0 from the equation,

$$G(12) = G^0(12) + G^0(1\bar{3})\Sigma(\bar{3}\bar{4})G(\bar{4}2). \tag{2.22}$$

Here we use number notation as abbreviation for the pair of space-spin and time coordinates $1 \to (r_1,\sigma_1,t_1)$. Coordinates with a bar are integrated over, i.e. $f(\bar{1})g(\bar{1}) \equiv \int d1 f(1)g(1)$. Eq.2.22 is the Dyson equation for the one-particle Green's function of the interacting system. It contains Σ, the electronic *self-energy*, as an effective dynamical and non-local field for the propagation of the electron which accounts for all effects of the interaction. A detailed derivation of the Dyson equation and the self-energy going beyond the equilibrium limit will be given in the following chapter. In the equilibrium limit the Green's function does not depend explicitly on two times, but only on a single time difference $\tau = t_1 - t_2$. It can be written in terms of its two time-ordered components as

$$G(x_1,x_2,\tau) = G^>(x_1,x_2,\tau)\theta(\tau) + G^<(x_1,x_2,\tau)\theta(-\tau). \tag{2.23}$$

The first time-ordered component is the electron propagator, G^e, which contains the *greater Green's function* ($G^>$) and describes the propagation of an electron to later times from t_2 to t_1. It corresponds to an IPES experiment. The second component is the hole propagator, G^h, which contains the *lesser Green's function* ($G^<$) and describes the propagation of a hole from t_1 to t_2. This component corresponds to a photoemission experiment. We can also define the *retarded* and *advanced* Green's functions

$$G^R(x_1,x_2,\tau) = \theta(\tau)(G^>(x_1,x_2,\tau) + G^<(x_1,x_2,\tau)) \tag{2.24}$$

$$G^A(x_1,x_2,\tau) = -\theta(-\tau)(G^>(x_1,x_2,\tau) + G^<(x_1,x_2,\tau)). \tag{2.25}$$

2.3.2 IPES from the one-particle Green's function

For the evaluation of the greater and lesser Green's function we insert a full set of many-body states of the Hilbert space between the two field operators in eq.2.20. The greater Green's function is then given by

$$G^>(x_1,x_2,\tau) = -i\sum_s e^{i(E_N - E^s_{N+1})\tau} f_s(x_1) f_s^\star(x_2) \tag{2.26}$$

with

$$f_s(x) = \langle N0|\hat{\Psi}(x)|N+1,s\rangle \tag{2.27}$$

the probability amplitude that when an electron is added to the ground-state of the N-particle system at a point x, the system will be in the eigenstate $|N+1,s\rangle$. $\epsilon_s = E^s_{N+1} - E_N$ is the energy

difference between the ground-state and the state s of the interacting system with $N+1$ particles. The functions f_s are also called Dyson orbitals [45] and include the effect of the self-energy on the many-body states. For a system without interaction they reduce to the single-particle orbitals. In frequency space the electron propagator is given by

$$G^e(x_1, x_2, \omega) = \lim_{\delta \to 0} \sum_s \frac{f_s(x_1) f_s^\star(x_2)}{\omega - \epsilon_s + i\delta}. \tag{2.28}$$

The energies ϵ_s are real and δ is an infinitesimal, positive frequency so that the integral of the Fourier transform converges. The imaginary part of the electron-Green's function

$$-\frac{\Im G^e(x_1, x_2, \omega)}{\pi} = A^e(x_1, x_2, \omega) = \sum_s f_s^\star(x_2) f_s(x_1) \delta(\omega - \epsilon_s), \tag{2.29}$$

is the spectral function for the electron-propagator. The spectral function yields the spectrum as a superposition of δ peaks. The electron-propagator is then given by integrating the *spectral function* $A^e(x_1, x_2, \omega)$ along a chosen path C

$$G^e(x_1, x_2, \omega) = \int_C d\omega' \frac{A^e(x_1, x_2, \omega')}{\omega - \omega'}. \tag{2.30}$$

In the spectrum obtained from the Green's function each peak is weighted with the Dyson orbitals.

2.3.3 PES from the one-particle Green's function

The lesser Green's function is given by

$$G^<(x_1, x_2, \tau) = i \sum_s e^{-i(E_N - E^s_{N-1})\tau} f_s^\star(x_2) f_s(x_1) \tag{2.31}$$

with

$$f_s(x) = \langle N-1, s | \hat{\Psi}(x) | N0 \rangle \tag{2.32}$$

the Dyson orbitals giving the probability amplitude that when an electron is removed from the ground-state of the N-particle system at a point x, the system will be in the eigenstate $|N-1, s\rangle$. $\epsilon_s = E_N - E^s_{N-1}$ is the energy difference between the state s of the interacting system with $N-1$ particles and the ground-state. In practice for both PES and IPES it is difficult to calculate the Dyson orbitals f_s, since it is equivalent to solving the Schrödinger equation for the interacting $N-1$, $N+1$ and N-particle systems. In frequency domain the expression of the hole-propagator becomes

$$G^h(x_1, x_2, \omega) = \lim_{\delta \to 0} \sum_s \frac{f_s^\star(x_2) f_s(x_1)}{\omega - \epsilon_s - i\delta} \tag{2.33}$$

The imaginary part of the hole-Green's function gives

$$\frac{\Im G^h(x_1, x_2, \omega)}{\pi} = A^h(x_1, x_2, \omega) = \sum_s f_s^\star(x_2) f_s(x_1) \delta(\omega - \epsilon_s), \tag{2.34}$$

which is called the spectral function for the hole-propagator. The hole-propagator is given by the integration of the *spectral function* $A^h(x_1, x_2, \omega')$ along a chosen path C as

$$G^h(x_1, x_2, \omega) = \int_C d\omega' \frac{A^h(x_1, x_2, \omega')}{\omega - \omega'}. \tag{2.35}$$

As we can see by comparing eq.2.29 and eq.2.34 to eq.2.13, the Green's function gives direct access to direct and inverse photoemission spectra.

2.3.4 The spectrum from the diagonal approximation for the self-energy

At zero temperature the Dyson equation for the Green's function in frequency domain and in a basis of single-particle orbitals becomes

$$G_{ij}(\omega) = G^0_{ij}(\omega) + \sum_{kl} G^0_{ik}(\omega)\Sigma_{kl}(\omega)G_{lj}(\omega). \tag{2.36}$$

The diagonal part of the matrix of the one-particle Green's function is given by the Dyson equation as

$$G^{-1}_{ii}(\omega) = G^{0-1}_{ii}(\omega) - \Sigma_{ii}(\omega) = \omega - \epsilon^0_i - \Sigma_{ii}(\omega), \tag{2.37}$$

where ϵ^0_i are the energy eigenvalues of the non-interacting system and where we have chosen the basis such that G^0 is diagonal. In general the diagonal elements of the inverse of a matrix differ from the inverse of a diagonal element,

$$G^{-1}_{ii}(\omega) \neq \frac{1}{G_{ii}(\omega)}. \tag{2.38}$$

The reason for this is that the off-diagonal matrix elements contribute to the inversion process. Only under the approximation of neglecting the contributions from the off-diagonal matrix elements, we can write

$$G_{ii}(\omega) = \frac{1}{\omega - \epsilon^0_i - \Sigma_{ii}(\omega)}. \tag{2.39}$$

Then making use of the *Kramers-Kronig* relations

$$\Re G_{ii}(\omega) = \frac{1}{\pi} PV\left(\int_{-\infty}^{+\infty} d\omega' \frac{\Im G_{ii}(\omega')}{\omega' - \omega}\right), \tag{2.40}$$

where PV indicates the principal value, and of the *Dirac identity*

$$\lim_{\delta\to 0^+} \frac{1}{\omega - \omega' + i\delta} = PV\left(\frac{1}{\omega - \omega'}\right) - i\pi\delta(\omega - \omega'), \tag{2.41}$$

the Green's function can be written entirely in terms of its imaginary part as

$$G_{ii}(\omega) = \frac{1}{\pi} \lim_{\delta\to 0^+} \int_{-\infty}^{+\infty} d\omega' \frac{\Im G_{ii}(\omega')}{\omega - \omega' + i\delta}. \tag{2.42}$$

From eq.2.42 one can extract the *spectral function* given by the imaginary part of the Green's function as

$$A_{ii}(\omega) = \frac{1}{\pi}|\Im G_{ii}(\omega)|. \tag{2.43}$$

The imaginary part of the Green's function is then written in terms of the real and imaginary parts of the self-energy as

$$\Im G_{ii}(\omega) = \frac{\Im\Sigma_{ii}(\omega)}{(\omega - \epsilon^0_i - \Re\Sigma_{ii}(\omega))^2 + (\Im\Sigma_{ii}(\omega))^2}, \tag{2.44}$$

where ϵ^0_i is the single-particle energy for the state i in the non-interacting system. This equation relates the spectral functions of eq.2.29,2.34 to the self-energy [46].

2.4 Spectroscopies from the "blue electron" theory

Since mid 60s spectroscopies for systems with localized electrons have become a major interest for theoretical spectroscopy [47]. The main reason for this is that intuitively one can consider an electron which is very localized to behave as an independent particle, or at least, one can imagine the localized electron as a distinguishable particle separated from the rest of the electrons by a large energy difference and small spatial overlap. The *"blue electron"* theory was proposed by Lars Hedin [48], setting the theoretical framework for the photoemission of a localized state. The "blue electron" is a distinguishable particle, which interacts with the rest of the particles only classically since there is no exchange between the "blue electron" and the rest of the electrons in the system. In this sense one can talk about a single particle in an effective medium, which has the effect of a classical potential acting on the "blue electron" [49].

In photoemission the "blue electron" is actually a "blue hole", and it refers to the approximation of the excited state of the system with $N-1$ electrons $|N-1,s\rangle$. The potential from the "blue hole" is often called core-hole potential. Different schemes have been proposed for the evaluation of $|N-1,s\rangle$. The "blue electron" theory provides a well-stated physical framework of approximations for the treatment of systems with localized states and has been extensively adopted and successfully applied over the past decades. In this thesis, we will also often make use of the idea that our localized electron or hole is distinguishable from the others.

2.5 Absorption spectra

We will now proceed to the calculation of the photocurrent (eq.2.13) for the photon-absorption process, where the system makes a transition to an excited final state with the same number of particles (fig.2.4c). The function that describes such processes is the density-density response dunction. The response function in the *linear-response approximation* is given by

$$\chi(x_1,t_1,x_2,t_2) = \lim_{U\to 0}\frac{\delta\rho(x_1,t_1)}{\delta U(x_2,t_2)}, \tag{2.45}$$

the variations of the density with respect to an applied potential U, taken for small values of the applied potential. The response is a causal function giving the variations of the density at later times than the times when the external potential is applied, $t_1 > t_2$. The density-density response function is a correlation function

$$\chi(x_1,t_1,x_2,t_2) = -i\langle\hat{\rho}(x_1,t_1)\hat{\rho}(x_2,t_2)\rangle_c \tag{2.46}$$

$$= -i\theta(t_1-t_2)[\langle N,0|\hat{\rho}(x_1,t_1)\sum_s |N,s\rangle\langle N,s|\hat{\rho}(x_2,t_2)|N,0\rangle$$

$$-\langle N,0|\hat{\rho}(x_1,t_1)|N,0\rangle\langle N,0|\hat{\rho}(x_2,t_2)|N,0\rangle], \tag{2.47}$$

where we have inserted a complete set of N-particle states in the two contributions to the correlator. In eq.2.46 the linear response function is given by the correlator $\langle\rangle_c$ of the density taken at two

different times, one is the time t_2 when the external potential is applied to the system and the other is the time t_1 when the measurement of the induced density is taken. In eq.2.47 the correlator is evaluated as the probability density of finding the system in its ground-state having passed through all possible excited states s of the N-particles system obtained from single-electron-hole excitations. The density-density correlator accounts only for single-electron-hole excitations since the density operator is a one-body operator. In equilibrium one can fix the time of the applied potential t_2 and measure the induced density at different times t_1. This is equivalent to considering the linear response function to depend only on time differences instead of two times. Therefore also its Fourier transform will depend only on a single frequency. In finite systems, the linear response function in frequency domain from eq.2.47 yields directly the absorption cross-section [50],

$$\sigma(\omega) \propto \Im \sum_{ij} \chi_{ij}(\omega). \tag{2.48}$$

In eq.2.48 the sum of the matrix elements of the density-density correlation function eq.2.47 in frequency domain is used, which stands for the average over all possible transitions between the ground-state and excited states of the system with N particles. The difference with respect to the photocurrent given in eq.2.13 is that here the flux of incident photons is not transformed to a current of ejected electrons, but to electronic excitations. The imaginary part of the response function also gives the losses taking place for example in inelastic x-ray scattering.

Also the inverse dielectric function, which is related to the response function, is often calculated. The *inverse dielectric function* is defined as

$$\epsilon^{-1}(x_1, t_1; x_2, t_2) = \frac{\delta V^{tot}(x_1, t_1)}{\delta U(x_2, t_2)}, \tag{2.49}$$

the variation of the total classical potential (applied + Hartree potential) with respect to the applied potential. The induced Hartree potential in the linear-response approximation is given by the equation

$$\delta V^H(x, t) = \int dx' v(x, x') \delta\rho^1(x', t), \tag{2.50}$$

where $\delta\rho^1(x', t)$ is the induced density in the linear-response approximation. Then the inverse dielectric function is related to the response function by the equation

$$\epsilon^{-1}(x_1, t_1, x_2, t_2) = v(x_1, x_2)\delta(t_1 - t_2) + \int dx' v(x_1, x')\chi(x', t_1, x_2, t_2). \tag{2.51}$$

The imaginary part of the inverse dielectric function is measured in electron energy-loss (EELS) experiments.

2.6 The independent-particle response function

The simplest approximation for absorption is obtained considering the independent propagation of the excited electron and the hole in the independent-particle response function,

$$\chi^{0>}(x_1, x_2, \tau)\theta(\tau) = -i\theta(\tau)G^{>}(x_1, x_2, \tau)G^{<}(x_2, x_1, -\tau). \tag{2.52}$$

This is a product of an electron and a hole propagating forward in time $\tau > 0$. This is called the resonant part of the independent-particle response function contrary to the propagation of the electron and the hole backwards in time $\tau < 0$, which gives the antiresonant part. Using eq.2.26,2.31 in time domain the response function of independent particles is written as

$$\chi^{0>}(x_1, x_2, \tau) = -i \sum_{is} f_i(x_2) f_s^\star(x_2) f_i^\star(x_1) f_s(x_1) e^{-i(\epsilon_s - \epsilon_i)\tau}. \tag{2.53}$$

$\epsilon_s = E^s_{N+1} - E_N$ is the energy for the addition of an electron, while $\epsilon_i = E_N - E^i_{N-1}$ is the energy for the removal of an electron. The product of the Dyson orbitals,

$$f^{2p}_{si}(x_2) = f_i(x_2) f_s^\star(x_2) \tag{2.54}$$

can be interpreted as electron-hole pair states. In frequency domain the resonant part of the response function takes the expression

$$\chi^0(x_1, x_2, \omega) = \sum_{is} \frac{(f_i(x_2) f_s^\star(x_2))(f_i^\star(x_1) f_s(x_1))}{\omega - (\epsilon_s - \epsilon_i) + i\delta}. \tag{2.55}$$

This gives the propagation of an electron-hole pair, as a process which requires energy $\epsilon_s - \epsilon_i$, treating the creation of a hole and the addition of an electron as independent processes. The independent-particle response function lacks the electron-hole interaction. Ways to introduce such corrections will be discussed in following chapters.

Summary

In spectroscopy we measure the events that take place when radiation interacts with matter. These events are the addition or removal of electrons in the photon-ionization of the sample and the excitation of electrons in the photon-absorption processes. A theoretical description of the measurements is provided by Green's function theory, which gives the probability of the propagation or the excitation of electrons. The single-particle propagators take a simple form for the case of non-interacting systems, while the two-particles propagator is simplified when the contributions from the electron and hole propagators are treated independently in the formation of the excitation. Taking into account the contribution of the Coulomb interaction introduces all the complication of the many-body problem into the description of the spectroscopic measurement, making it as cumbersome as solving the Schrödinger equation. Therefore the description of spectroscopic measurements for the case of an interacting system can be only carried out within approximations which will be the subject of discussion in the following chapters of this thesis.

3

Green's function theory

In chap.2 we linked the equilibrium one and two-particles Green's function to measurements in spectroscopies. The propagators reflect the complexity of the interacting system which makes their evaluation not easier than the evaluation of the many-electron wavefunction. For this reason a lot of effort has been put over the part decades into the development of approximations that can capture the main physics of correlation.

In chap.2 we discussed the information given by the Green's functions but we said nothing about their evaluation, which is the main challenge in theoretical spectroscopy. In this chapter we will present some of the main techniques for the evaluation of the one particle Green's function, which are the equation of motion and Hedin equations. We will discuss common approximations to those equations, their deficiencies and ways to fix them.

3.1 Non-equilibrium Green's function

As we briefly mentioned in chap.2 we can use MBPT in order to evaluate Green's functions. One possibility to derive the equations is to use a fictitious external potential U to drive the electronic system out-of-equilibrium, and let it evolve under the effects of the interaction. Moreover, in spectroscopies one really applies an external potential to the system, for example a photon field (eq.2.2). In sec.2.3.1 we introduced the basics of the second quantization formalism applied to Green's functions theory. However we limited ourselves to the equilibrium formulation of the theory. The derivation of the formal theory of Green's functions for interacting systems given in this chapter involves the formulation of the theory out-of-equilibrium.

3.1.1 Expectation values out-of-equilibrium

For the scope of this thesis we will use the Heisenberg picture for the definition of the Green's function as has been done in sec.2.3.1. However for completeness we will introduce the distinction between the possible representations of an operator. Given an operator $O(t)$ in the *Schrödinger picture* can only show its explicit time dependence

$$\hat{O}(t) = \int dx \hat{\Psi}^\dagger(x) o(x,t) \hat{\Psi}(x). \tag{3.1}$$

The field operators are written in the Schrödinger picture as

$$\hat{\Psi}(x) = \sum_i a_i \phi_i(x) \tag{3.2}$$

$$\hat{\Psi}^{\dagger}(x) = \sum_i a_i^{\dagger}\phi_i^{\star}(x) \tag{3.3}$$

Where ϕ_i is a basis of single-particle orbitals that can be chosen arbitrarily. The field operators in the Schrödinger representation cannot evolve an eigenstate in time, and therefore they cannot describe the propagation of particles, which is a dynamical process even when the system is in equilibrium or the self-energy is static. Therefore it is convenient to evaluate expectation values using the Heisenberg representation. Eq.2.14, 2.15 show the transformation of the field operators from the Schrödinger to the Heisenberg picture in equilibrium. In non-equilibrium the Hamiltonian is time dependent and the Heisenberg representation of the field operators (eq.2.14, 2.15) becomes

$$\hat{\Psi}(x,t) = e^{i\int_{-T_0}^{t} d\tau \hat{H}(\tau)} \sum_i a_i\phi_i(x) e^{-i\int_{-T_0}^{t} d\tau \hat{H}(\tau)} \tag{3.4}$$

$$\hat{\Psi}^{\dagger}(x,t) = e^{i\int_{-T_0}^{t} d\tau \hat{H}(\tau)} \sum_i a_i^{\dagger}\phi_i^{\star}(x) e^{-i\int_{-T_0}^{t} d\tau \hat{H}(\tau)}. \tag{3.5}$$

At time $-T_0$ the Schrödinger and the Heisenberg pictures coincide. In non-equilibrium both the field operators and the many-body states evolve under the effects of the interaction and the applied potential. Therefore one evaluates the expectation values of the field operators in the Heisenberg picture, accounting also for the fact that the interacting ground-state is no longer a stationary state of the hamiltonian. All the time-dependent effects are taken into account in the Hamiltonian through the operator

$$\hat{S}(\tau) = \int dx \hat{\Psi}^{\dagger}(x,\tau) U(x,\tau) \hat{\Psi}(x,\tau), \tag{3.6}$$

written in the Heisenberg picture. Eq.3.6 includes the time-dependent density operator $\hat{\rho}(x,\tau) = \hat{\Psi}^{\dagger}(x,\tau)\hat{\Psi}(x,\tau)$. The operator $\hat{S}$ accounts for all the effects of the applied potential $U(x,t)$. In this thesis we adopt the definitions of Hedin and and Lunqvist [44] and Strinati [51] which are inspired by the approach introduced in 1951 by *Gell-Mann and Low* [52] for the evaluation of the interacting many-body state. We will adopt the adiabatic assumption saying that we switch on the applied potential at time $t = -T_0$ and we let the ground-state evolve adiabatically up to time t_0 under the effects of the applied potential. This time will appear only as a parameter and can be chosen arbitrarily. We also make the assumption that we switch off the applied potential adiabatically at time $t = T_0$. The interacting many-body state at time t_0 after switching on the interaction is

$$\langle N0, t_0| = \langle N0| e^{-i\int_{-T_0}^{t_0} d\tau \hat{S}(\tau)}. \tag{3.7}$$

$\langle N0|$ is the interacting many-body state in equilibrium at time $-T_0$. After switching off the interaction the interacting many-body state becomes

$$\langle N0, T_0| = \langle N0, t_0| e^{-i\int_{t_0}^{T_0} d\tau \hat{S}(\tau)} = \langle N0| e^{-i\int_{-T_0}^{T_0} d\tau \hat{S}(\tau)}. \tag{3.8}$$

The last expression shows the effect of the applied potential on the ground-state of the system. The non-equilibrium contribution comes from the fact that the many-body state at time T_0 can be different from the many-body state at time $-T_0$, showing memory effects from the applied potential. T_0 can be taken as ∞. Expectation values are evaluated between the interacting ground-state at time $-T_0 = -\infty$ and the interacting ground-state at time $T_0 = +\infty$,

$$\langle \hat{O}(t) \rangle = \frac{\langle N0| e^{-i\int_{-\infty}^{+\infty} d\tau \hat{S}(\tau)} \hat{O}^H(t) |N0\rangle}{\langle N0| e^{-i\int_{-\infty}^{+\infty} d\tau \hat{S}(\tau)} |N0\rangle}. \tag{3.9}$$

with $\hat{O}^H(t)$ the Heisenberg representation of the operator $\hat{O}(t)$. Taking the limit of the applied potential to be equal to zero, the ground-states at times $-\infty$ and $+\infty$ coincide. Originally the operator $\hat{S}$ had been introduced in the interaction representation evolving the many-body state adiabatically under the effects of the interaction switched on and off at different times. However it can be applied as well to the non-equilibrium Green's function theory evolving the interacting ground-state under the effects of an applied potential. The one-particle Green's function under the effects of the applied potential is defined as the expectation value

$$G(12) = -i\frac{\langle N0|\hat{T}\{e^{-i\int_{-\infty}^{+\infty}d\tau\hat{S}(\tau)}\hat{\Psi}(1)\hat{\Psi}^\dagger(2)\}|N0\rangle}{\langle N0|\hat{T}\{e^{-i\int_{-\infty}^{+\infty}d\tau\hat{S}(\tau)}\}|N0\rangle}. \tag{3.10}$$

In a similar way we can also define the two-particles Green's function from the expectation value,

$$G^{2p}(1323) = (-i)^2\frac{\langle N0|\hat{T}\{e^{-i\int_{-\infty}^{+\infty}dt\hat{S}(t)}\hat{\Psi}(1)\hat{\Psi}(3)\hat{\Psi}^\dagger(3)\hat{\Psi}^\dagger(2)\}|N0\rangle}{\langle N0|\hat{T}\{e^{-i\int_{-\infty}^{+\infty}dt\hat{S}(t)}\}|N0\rangle}. \tag{3.11}$$

There is a series of equations allowing for the evaluation of higher order Green's function with respect to the previous orders. Those can be obtained from the derivative of the Green's function with respect to the applied potential. Taking the derivative of the one-particle Green's function with respect to the applied potential we obtain the following relation

$$\begin{aligned}\frac{\delta G(12)}{\delta U(3)} = (-i)^2\Bigg[&\frac{\langle N0|\hat{T}\{e^{-i\int_{-\infty}^{+\infty}d\tau\hat{S}(\tau)}\hat{\rho}(3)\Psi\hat{(1)}\hat{\Psi}^\dagger(2)\}|N0\rangle}{\langle N0|\hat{T}\{e^{-i\int_{-\infty}^{+\infty}d\tau\hat{S}(\tau)}\}|N0\rangle}\\ &-\frac{\langle N0|\hat{T}\{e^{-i\int_{-\infty}^{+\infty}d\tau\hat{S}(\tau)}\Psi\hat{(1)}\hat{\Psi}^\dagger(2)\}|N0\rangle}{\langle N0|\hat{T}\{e^{-i\int_{-\infty}^{+\infty}d\tau\hat{S}(\tau)}\}|N0\rangle}\frac{\langle N0|\hat{T}\{e^{-i\int_{-\infty}^{+\infty}d\tau\hat{S}(\tau)}\hat{\rho}(3)\}|N0\rangle}{\langle N0|\hat{T}\{e^{-i\int_{-\infty}^{+\infty}d\tau\hat{S}(\tau)}\}|N0\rangle}\Bigg].\end{aligned} \tag{3.12}$$

We see that from the derivative of the Green's function with respect to the applied potential, higher order correlation functions appear with an explicit dependence on the density operator. Therefore one can relate the two-particles Green's function to the functional derivative of the one-particle Green's function as

$$G^{2p}(13^+23) = G(12)G(33^+) - \frac{\delta G(12)}{\delta U(3)}. \tag{3.13}$$

The last equation is usually refered as the *Schwinger-Dyson* equation [53, 54] and plays a role of key importance in MBPT.

3.1.2 The equation of motion for the one-particle Green's function

In this section we will give the basic steps for the derivation of the equation of motion for the one particle Green's function. We start from the Hamiltonian of the many-electron system (eq.1.2) written in the Heisenberg picture

$$\begin{aligned}\hat{H}(t) = &\int dx_1\hat{\Psi}^\dagger(x_1,t)h(x_1)\hat{\Psi}(x_1,t) + \int dx_1\hat{\Psi}^\dagger(x_1,t)U(x_1,t)\hat{\Psi}(x_1,t)\\ &+\frac{1}{2}\int dx_1\int dx_2\hat{\Psi}^\dagger(x_1,t)\hat{\Psi}^\dagger(x_2,t)v(x_1,x_2)\hat{\Psi}(x_2,t)\hat{\Psi}(x_1,t).\end{aligned} \tag{3.14}$$

The *time-dependent Schrödinger equation* for the field operator reads

$$[\hat{\Psi}(x_1,t_1),\hat{H}(t_1)] = i\frac{\partial}{\partial t_1}\hat{\Psi}(x_1,t_1). \tag{3.15}$$

After evaluating the commutators between the Hamiltonian and the field operator from eq.2.16-2.19), we obtain the equation of motion for the field operator

$$i\frac{\partial}{\partial t_1}\hat{\Psi}(x_1,t_1) = [h(x_1) + U(x_1,t_1) + \int dx_2 v(x_1,x_2)\hat{\Psi}^\dagger(x_2,t_1)\hat{\Psi}(x_2,t_1)]\hat{\Psi}(x_1,t_1). \quad (3.16)$$

This relation can be used to calculate the time-derivative of the one-body Green's function. Taking into account the time ordered products that appear in its definition (eq.3.10) and using

$$\frac{\partial\theta(t_1-t_2)}{\partial t_1} = \delta(t_1-t_2) \quad (3.17)$$

we arrive at the final expression for the equation of motion for the one-particle Green's function,

$$[i\frac{\partial}{\partial t_1} - h(x_1) - U(1)]G(12) + i\int d3v(1,3)G^{2p}(13^{++}23^{+}) = \delta(12). \quad (3.18)$$

Here, the Coulomb interaction is written as $v(1,3) = \delta(t_1-t_3)v(\mathbf{r_1}-\mathbf{r_3})$. It appears in the equation of motion for the Green's function together with the two-particles Green's function. Amongst the time arguments appear also augmented times $t^+ = t+\epsilon$, in order to specify the ordering of the field operators at equal times. At the end the limit $\epsilon \to 0$ has to be taken. Following the same process one may also derive the equation of motion for the field operator for the creation of a particle $\hat{\Psi}^\dagger$ and derive the equation of motion for the one-particle Green's function for the motion over times t_2. Finally one may substitute the two-particles Green's function from the Schwinger-Dyson eq.3.13 and write the equation of motion for the one-particle Green's function as

$$[i\frac{\partial}{\partial t_1} - h(x_1) - U(1)]G(12) + i\int d3v(1,3)G(33^{+})G(12) - i\int d3v(1,3)\frac{\delta G(12)}{\delta U(3^{+})} = \delta(12). \quad (3.19)$$

Using the equation of motion for the Green's function of the non-interacting system G_0, $[i\frac{\partial}{\partial t_1} - h(x_1) - U(1)]G_0(12) = \delta(12)$, eq.3.19 is written as

$$G(12) = G_0(12) - iG_0(1\bar{1})v(\bar{1},\bar{3})G(\bar{3}\bar{3}^{+})G(\bar{1}2) + iG_0(1\bar{1})v(\bar{1},\bar{3})\frac{\delta G(\bar{1}2)}{\delta U(\bar{3}^{+})}. \quad (3.20)$$

Eq.3.20 is the equation of motion of the one-particle Green's function written in a closed form as an integro-differential equation. It also known as the Kadanoff-Baym Equation (KBE) [55]. The interaction with the two-particles Green's function has been replaced with the interaction with the density, which makes the classical potential (Hartree potential eq.1.15), together with the derivative of the Green's function with respect to the applied potential, which adds all the exchange and correlation effects, going beyond the classical potential. Eq.3.20 can also take the form of a Dyson equation (eq.2.22) where the self-energy is given by

$$\Sigma(13) = -i\delta(13)v(1,\bar{4})G(\bar{4}\bar{4}^{+}) + iv(1,\bar{4})\frac{\delta G(1\bar{2})}{\delta U(\bar{4}^{+})}G^{-1}(\bar{2}3). \quad (3.21)$$

The self-energy stands for the effective potential accounting for the interaction with the density through the Hartree potential and all exchange and correlation effects given by the functional derivative of the Green's function with respect to the applied potential. The second term can be summarized in a non-local potential, namely a mass term

$$M(13) = iv(1,\bar{4})\frac{\delta G(1\bar{2})}{\delta U(4^{+})}G^{-1}(\bar{2}3). \quad (3.22)$$

The *mass operator* accounts for all the effects contributing to the electron propagator that go beyond a system with independent particles in a Hartree potential. The equation of motion for the Green's function may be summarized as

$$[i\frac{\partial}{\partial t_1} - h(x_1) - U(1)]G(12) - \int d3\Sigma(13)G(32) = \delta(12). \tag{3.23}$$

Eq.3.20 can give in principle the exact solution for the propagation of an electron in the interacting many-electrons system. Only once its solution has been obtained, the limit of zero perturbing potential may be applied. However this solution is difficult to be obtained in an exact way because eq.3.20 is a differential equation with respect to the applied potential, and an integral equation with respect to space, spin and time. Therefore the problem is analogous to the one of solving a system of coupled differential equations for matrices that have infinite dimensions. In the following sections we will introduce alternative approaches to the solution of the KBE that provide better starting points for approximations. We have already given a clue towards this direction by introducing the exact self-energy in eq.3.21 and transforming the KBE into a Dyson equation for the one-particle Green's function. Of course then the problem reduces to the one of evaluating the exact self-energy. In following sections we will also discuss approximations where the equation of motion for the one-particle Green's function can be exactly solved.

3.2 Hedin's approach to the many-body problem for electrons

Lars Hedin [5] in 1965 introduced an alternative approach to the equation of motion for the one-particle Green's function replacing the derivative term in eq.3.20 with a set of five quantities which form a closed set of integral equations whose self-consistent solution is in principle exact. The quantities that he introduced have a clear physical interpretation which can be seen also in Feynman diagrams. This approach doesn't provide a simplification to the solution of the equation of motion for the one-particle Green's function, but it provides a better starting point for approximations. In this section we will introduce Hedin equations and discuss common approximations to their exact form.

3.2.1 Hedin equations

We can see in eq.3.20 that the Hartree potential is a local potential, similar to the applied potential. The only effect of the interaction is that it is an explicit functional of the density that has to be calculated self-consistently. However it shows no quantum effects and therefore can be obtained from the classical treatment of electrons as charges. For this reason Hedin introduced the idea of grouping the Hartree with the applied potential into a *"total classical" potential*,

$$V^{tot}(1) = U(1) - i\int d3v(1,3)G(33^+). \tag{3.24}$$

Variations of the applied potential induce variations of the density appearing in the total potential, which gives a classical contribution from the variation of the charge in the system. The variation of the total potential with respect to the applied potential is given by the inverse dielectric function in eq.2.49 as

$$\epsilon^{-1}(12) = \frac{\delta V^{tot}(1)}{\delta U(2)}. \tag{3.25}$$

Then the classically *screened interaction* is defined with respect to the bare Coulomb interaction from the inverse dielectric function as

$$W(12) = \int d3\epsilon^{-1}(23)v(1,3). \tag{3.26}$$

The *response function* is defined as the variation of the density with respect to the applied potential, consistent with eq.2.45,

$$\chi(12) = -i\frac{\delta G(11^+)}{\delta U(2)}. \tag{3.27}$$

Combining eq.3.24 and eq.3.27 the inverse dielectric function can also be written in terms of the Coulomb interaction and the response function as

$$\epsilon^{-1}(12) = \delta(12) + v(1,\bar{3})\chi(\bar{3}2). \tag{3.28}$$

The screened Coulomb interaction (eq.3.26) is given in terms of the response function as,

$$W(12) = v(1,2) + v(2,4)\chi(\bar{4}\bar{3})v(\bar{3},1). \tag{3.29}$$

One can also define a different response, namely the *irreducible polarizability* which is given by the variation of the density with respect to the "total classical" potential,

$$P(12) = -i\frac{\delta G(11^+)}{\delta V^{tot}(2)}. \tag{3.30}$$

Then the inverse dielectric function is given in terms of the screened interaction and the irreducible polarizability as

$$\epsilon^{-1}(12) = \delta(12) + \int d3W(13)P(32). \tag{3.31}$$

The screened interaction then takes the expression

$$W(12) = v(1,2) + W(1\bar{3})P(\bar{4}\bar{3})v(\bar{4},2). \tag{3.32}$$

This is a Dyson equation for the screened interaction given in terms of the irreducible polarizability. The irreducible polarizability is a response to a potential, which partially accounts for the interaction, since it includes a part standing for the interaction with the induced density. The idea behind the use of the irreducible polarizability instead of the response to the bare potential corresponds to a transformation of variables between the non-interacting system and the bare Coulomb interaction to the classical system and the screened interaction. We will discuss this observation in more detail in the following chapters.

At this point we will apply this transformation to the mass operator (eq.3.22) in the self-energy: we apply the chain rule with respect to the total potential to obtain

$$M(12) = iW(1,\bar{4})\frac{\delta G(1\bar{3})}{\delta V^{tot}(\bar{4})}G^{-1}(\bar{3}2). \tag{3.33}$$

Using

$$\frac{\delta G(13)}{\delta V^{tot}(4)} = -G(1\bar{1})\frac{\delta G^{-1}(\bar{1}\bar{3})}{\delta V^{tot}(\bar{4})}G(\bar{3}3) \tag{3.34}$$

we can define the *vertex function* as

$$\Gamma(\bar{3}2:\bar{4}) = -\frac{\delta G^{-1}(\bar{3}2)}{\delta V^{tot}(\bar{4})}, \tag{3.35}$$

and finally the mass operator takes the form

$$M(12) = iW(1\bar{4})G(1\bar{3})\Gamma(\bar{3}2:\bar{4}). \tag{3.36}$$

In this expression there is no longer a derivative explicitly appearing in the mass operator, but it is substituted with the screened interaction and the vertex function. The vertex function stands for all exchange and correlation effects that go beyond the classical screening. Choosing to screen with the exact self-energy is equivalent to a modified $\tilde{W}$

$$\tilde{W}(1\bar{3}2) = W(1\bar{4})\Gamma(\bar{3}2:\bar{4}), \tag{3.37}$$

which makes eq.3.36 free of vertex corrections. Eq.3.34 gives the irreducible polarizability in terms of the vertex function. Eq.3.35 can give the vertex function in terms of the irreducible polarizability. The two equations are equivalent to the Bethe Salpeter equation (BSE), which will be derived and discussed in the following chapter.

The Dyson equation for the Green's function, the equation for the mass operator (eq.3.36), the Dyson equation for the screened interaction (eq.3.32), the equation for the irreducible polarizability (from eq.3.34) and the equation for the $\Gamma-$ function (eq.3.35) form a closed set of five equations known as *Hedin equations*, whose self-consistent solution is equivalent to the exact solution of the many-body problem.

$$G(12) = G_0(12) + G_0(1\bar{3})V^{tot}(\bar{3})G(\bar{3}2) + G_0(1\bar{3})M(\bar{3}\bar{4})G(\bar{4}2) \tag{3.38}$$
$$M(12) = iG(1\bar{3})W(1\bar{4})\Gamma(\bar{3}2:\bar{4}) \tag{3.39}$$
$$W(14) = v(1,4) + v(4,\bar{3})P(\bar{3}\bar{2})W(1\bar{2}) \tag{3.40}$$
$$P(13) = -iG(1\bar{5})G(\bar{6}1)\Gamma(\bar{5}\bar{6}:3) \tag{3.41}$$
$$\Gamma(12:3) = \delta(13)\delta(23) + i\frac{\delta M(12)}{\delta G(\bar{5}\bar{6})}P(\bar{5}\bar{6}:3) \tag{3.42}$$

In App.A one can find the Hedin equations written in a discrete basis of single-particle wavefunctions.

The screening from the "total classical" potential is intuitive for systems with localized electrons. We can consider, for example core electrons, which are localized states that do not overlap with other states in space. Such particles do basically interact with the density of the rest of the electrons with a Hartree potential. We can therefore imagine that when we add, remove or excite an electron inducing locally some charge to the system, the major contribution to the screening of such a charge will come from the variation of the "total classical" potential with respect to the perturbation and for this kind of physical systems the vertex corrections in eq.3.36 will be small.

3.2.2 Approximations of the vertex function Γ

Neglecting vertex corrections from the vertex function Γ,

$$\Gamma(12:3) = \delta(13)\delta(23) \tag{3.43}$$

is equivalent to the irreducible polarizability been given by an independent-particle like response function

$$P(13) = -iG(13)G(31). \tag{3.44}$$

The last gives the independent propagation of two particles (an electron and a hole) in the system with many electrons, each particle in an effective field given by the self-energy. Then the screened interaction satisfies the Dyson equation

$$W(14) = v(1,4) - i\int d23 v(4,3)G(32)G(23)W(12) \tag{3.45}$$

This is known as the RPA and was firstly introduced by Bohm and Pines in [56] for the electron gas. Then the self-energy in the GWA is given by

$$\Sigma(12) = -i\delta(12)\int d3 v(1,3)G(33^+) + iG(12)W(12). \tag{3.46}$$

In the GWA the correlation effects are approximated screening the Fock term with the independent particles polarizability. In this approximation the electron propagates independently from the hole. Therefore the effect of the interaction between the electron and the hole is absent from this description. In many cases the G^0W^0 approximation is used, where G^0 is the Green's function of a system with independent particles, it can be taken as the non-interacting Green's function or as the Green's function of the Kohn-Sham system. In these cases the polarization is approximated as $P(13) = -iG^0(13)G^0(31)$. Going beyond the GWA means to include vertex corrections. One systematic way to do this is to look at the expansion of the vertex function in orders of the screened interaction W. A nice review on the GWA has been written by Aryasetiawan and Gunnarsson in 1998 [57].

3.3 Hedin's equations from a four-point interaction

In the equation of motion for the Green's function eq.3.18 the two-particles Green's function appears. One can use the commutation relations between the field operators that are coupled to the Coulomb interaction $\Psi(1)\Psi(3) = -\Psi(3)\Psi(1)$ [9] together with the fact that the Green's functions are time-ordered and rewrite the two-particles Green's function as

$$G^{2p}(13^+23) = \frac{1}{2}(G^{2p}(13^+23) - G^{2p}(33^+21)) = \frac{1}{2}(\delta(1\bar{4})\delta(3\bar{5}) - \delta(3\bar{4})\delta(1\bar{5}))G^{2p}(\bar{4}3^+2\bar{5}). \tag{3.47}$$

The prefactor of the last equation together with the Coulomb interaction allows us to define a four-point interaction

$$v_0(1453) = \frac{1}{2}(\delta(14)\delta(35) - \delta(34)\delta(15))v(13). \tag{3.48}$$

The four-point interaction is a local in time, but non-local in space interaction. It has been introduced by Hugenholtz in [58]. The four-point interaction has the symmetry $v_0(1453) = v_0(3541)$ and $v_0(1453) = -v_0(1543)$. Its matrix elements are

$$v_{0ijkl}(1453) = \delta(t_1 - t_3)\delta(t_1 - t_4)\delta(t_1 - t_5)\frac{1}{2}\Delta v_{ijkl}. \tag{3.49}$$

The matrix elements of the four-point interaction are written as differences between the direct and the exchange matrix elements of the Coulomb interaction,

$$\Delta v_{ijkl} = v_{ijkl} - v_{ikjl}. \tag{3.50}$$

The matrix elements appearing in eq.3.50 taken with an orbitals' basis are defined as

$$v_{ijkl} = \int d\mathbf{r}_1 \int d\mathbf{r}_2 \frac{\phi_i^\star(\mathbf{r}_1)\phi_j(\mathbf{r}_1)\phi_k(\mathbf{r}_2)\phi_l^\star(\mathbf{r}_2)}{|\mathbf{r}_1 - \mathbf{r}_2|}. \tag{3.51}$$

Using the four-point interaction the equation of motion for the Green's function becomes

$$[i\frac{\partial}{\partial t_1} - h(x_1) - U(1)]G(12) + iv_0(1\bar{4}\bar{5}\bar{3})G^{2p}(\bar{4}\bar{3}^+2\bar{5}) = \delta(12). \tag{3.52}$$

We can rewrite eq.3.13 for a non-local in space, but local in time applied potential. This makes use of the fact that the Coulomb interaction is local in time. Therefore we can write

$$\delta(t_1 - t_3)G^{2p}(33^+21) = \delta(t_1 - t_3)(G(32)G(13^+) - \frac{\delta G(32)}{\delta U(3^+1)}). \tag{3.53}$$

The KBE becomes

$$G(12) = G_0(12) - iG_0(1\bar{1})v_0(\bar{1}\bar{4}\bar{5}\bar{3})G(\bar{3}\bar{5})G(\bar{1}2) + iG_0(1\bar{1})v_0(\bar{1}\bar{4}\bar{5}\bar{3})\frac{\delta G(\bar{4}2)}{\delta U(\bar{3}\bar{5})}, \tag{3.54}$$

where G_0 contains the space-non-local potential U. Introducing the four-point interaction automatically accounts for the cancellation between the direct and the exchange terms in the Hartree-Fock equations. This shows that also in the correlation part of the self-energy the self-interaction correction needs to be taken into account. In the original formulation of the KBE the self-interaction correction is given by the exchange and correlation part of the self-energy separately. This is the reason why making approximations in the correlation part in the original KBE eq.3.20 introduces self-interaction errors. In the Hedin equations the self-interaction correction in the correlation is given by the vertex function Γ. Therefore approximations of the vertex function may introduce a self-interaction error. For example the GWA suffers from a self-interaction error in the correlation, also called self-screening error [59, 60]. It is important to note that eq.3.54 has been formulated using a non-local in space applied potential.

One may introduce the definition of a total non-local potential

$$V^{tot\ nl}(12) = U(12) - iv_0(12\bar{5}\bar{3})G(\bar{3}\bar{5}), \tag{3.55}$$

where the non-local in space but local in time applied potential $U(12)$ is summed with half of the Hartree-Fock self-energy. The other half is in the correlation part. Using the total non local potential and the four-point interactions the Hedin equations are generalized as

$$G(12) = G_0(12) + G_0(1\bar{3})V^{tot\ nl}(\bar{3}\bar{4})G(\bar{4}2) + G_0(1\bar{3})M(\bar{3}\bar{4})G(\bar{4}2) \tag{3.56}$$

$$M(12) = iW(1\bar{1}\bar{4}\bar{5})G(\bar{1}\bar{3})\Gamma(\bar{3}2\bar{5}\bar{4}) \tag{3.57}$$
$$W(1245) = v_0(1245) + W(124\bar{3}\bar{4})P(\bar{3}\bar{4}\bar{5}\bar{6})v_0(\bar{5}\bar{6}45) \tag{3.58}$$
$$P(3456) = -iG(3\bar{3})G(\bar{4}4)\Gamma(\bar{3}\bar{4}\bar{5}\bar{6}) \tag{3.59}$$
$$\Gamma(1234) = \delta(13)\delta(24) + i\frac{\delta M(12)}{\delta G(\bar{5}\bar{6})}P(\bar{5}\bar{6}34). \tag{3.60}$$

The Hedin equations with the four-point interaction can straightforwardly be written in a discrete basis of single-particle wavefunctions. In this scheme the four-point interaction is screened with the total non-local potential having a portion of exchange. This makes the equations qualitatively different from the original scheme of Hedin. The difference with the original set of equation with the bare Coulomb interaction is that here W, P and Γ are four-point matrices and the respective equations are equations for four-point matrices. This increases the difficulty of their solution. On the other hand they are better starting point for approximations, since they don't suffer from the self-interaction error. This can be immediately verified from the GWA with the difference that W in this scheme is a four-point matrix. A correction of the GWA along these lines has been presented by Aryasetiawan, Sakuma and Karlsson in 2012 [61].

3.4 Solutions from approximations on the one-particle Green's function

We introduced both the KBE (eq.3.20) and the Hedin equations in a continuous space and time representation. These are matrix equations for continuous functions of at least four arguments if we neglect the spin degrees of freedom. The coupling between the arguments make the exact solution of the equations impossible without approximations. One way to reduce the dimensionality of the basis and also obtain a better starting point for approximations is to write the Hedin equations in a discrete basis of single particle wavefunctions. The choice of the basis is closely related to the level of approximation that we want to introduce. The Hedin equations in a basis can be found in App.A. The complication that comes from the coupling in times is usually treated going to frequency domain. In the limit of equilibrium all functions of two times can be written as functions of time differences leading to a single argument. This simplifies the Dyson equation for the Green's function to depend on a single frequency argument which can be treated as a parameter. Moreover considering a self-energy which is instantaneous in times, meaning that its time dependence is limited to a $\delta-$function, it is given only by a number in frequency space. The simplification of the space and the time arguments usually play an important role for the numerical solution of the equations. On the other hand numerical solutions are usually obtained from iteration schemes of the Hedin equations and within approximations for the vertex function Γ. For the scope of this thesis we will introduce models and approximations for analytically solvable cases that make it possible to get an exact solution.

3.4.1 Linearization of the KBE

Eq.3.20 is an integro-differential equation. Its complication doesn't come only from the coupling of matrices, but it is also due to the fact that the Hartree potential depends on the exact density, which gives rise to a non-linear contribution. One way to remove the non-linearity is to expand the

density in orders of the applied potential and keep only up to the linear order,

$$-iG(33^+) = -iG(33^+)|_{U=0} + \chi(3\bar{4})|_{U=0}U(\bar{4}). \tag{3.61}$$

Then the screened interaction becomes

$$W(35) = \epsilon^{-1}(3\bar{3})v(\bar{3}5) = (\delta(3\bar{3}) + v(3\bar{4})\chi(\bar{3}\bar{4})|_{U=0})v(\bar{3}5), \tag{3.62}$$

which is also independent of the density. The last equation gives the screened interaction in the linear-response approximation. In the linear-response approximation the "total classical" potential becomes

$$\begin{aligned} V^{tot}(1) &= U(1) + \int d3v(13)(-iG(33^+)|_{U=0} + \chi(3\bar{4})|_{U=0}U(\bar{4})) \\ &= \epsilon^{-1}(1\bar{4})U(\bar{4}1) - iv(1\bar{3})G(\bar{3}\bar{3}^+)|_{U=0}. \end{aligned} \tag{3.63}$$

The external potential is renormalized with the inverse dielectric function which we will refer to as $\tilde{U}$, while in the Hartree potential only the equilibrium density remains. Then we can substitute the non-interacting Green's function $\tilde{G_0}$, which is a functional of the renormalized applied potential and note as $V^H|_{U=0}$ the Hartree potential in equilibrium. Applying the chain rule with the renormalized potential in the differential term of the eq.3.20 we can rewrite the KBE as

$$G(12) = \tilde{G_0}(12) + \tilde{G_0}(1\bar{3})V_0^H(\bar{3})G(\bar{3}2) + i\tilde{G_0}(1\bar{3})W(\bar{3}\bar{5})\frac{\delta G(\bar{3}2)}{\delta\tilde{U}(\bar{5})}. \tag{3.64}$$

This is one way to get rid of the non-linearity. The renormalized potential $\tilde{U}$ is equivalent to the "total classical" potential in the equilibrium limit. This suggests that the linear-response approximation is equivalent to applying the equilibrium limit to the "total classical" potential before solving the KBE. It also suggests that introducing the screened interaction W corresponds to the transformation of the KBE from the applied potential to the "total classical" potential.

In a following chapter we will generalize this transformation beyond the linear-response approximation, and present an alternative idea for the linearization of the KBE using TDDFT.

3.4.2 The cumulant solution

Starting from the KBE in the linear-response approximation one can write it in the basis of the non-interacting system. Making the assumption that each state of the basis remains decoupled from the rest of the states, one obtains the *linearized KBE* for each state as

$$G_i(t_1,t_2) = \tilde{G_{0i}}(t_1,t_2) + \tilde{G_{0i}}(t_1,\bar{t}_3)V_{0i}^H(\bar{t}_3)G_i(\bar{t}_3,t_2) + i\tilde{G_{0i}}(t_1,\bar{t}_3)W_i(\bar{t}_3,\bar{t}_5)\frac{\delta G_i(\bar{t}_3,t_2)}{\delta\tilde{U}_i(\bar{t}_5)}. \tag{3.65}$$

In the last equation quantities are coupled only through their time arguments. This approximation is equivalent to neglecting the overlap between a single particle state and the rest of the states in the matrix elements of the Coulomb interaction and moreover neglecting the Coulomb interaction between different states. Here we forget the photoelectron and only talk about the core-hole. The argument is: "The neglect of the overlap is justified for core-electrons, which are localized far away from the other electrons". One can further simplify the coupling in times by neglecting the

coupling between electron and hole contributions to G_i. This argument completes the decoupling approximation for the removal of an electron from the interacting system and results in the equation

$$G_i^h(t_1,t_2) = \tilde{G_{0i}}^h(t_1,t_2) + \theta(t_2-t_1)\int_{t_1}^{t_2} dt_3 \tilde{G_{0i}}^<(t_1,t_3)V_{0i}^H G_i^<(t_3,t_2) + i\theta(t_2-t_1)\int_{t_1}^{t_2} dt_3 \int dt_5 \tilde{G_{0i}^<}(t_1,t_3)W_i(t_3,t_5)\frac{\delta G_i^<(t_3,t_2)}{\delta \tilde{U}_i(t_5)}. \quad (3.66)$$

One may write the equivalent equation for $G_i^e(t_1,t_2)$ to describe the inverse photoemission of an electron in the decoupling approximation. The solution of the eq.3.66 is given by

$$G_i^h(t_1,t_2) = \tilde{G_{0i}^h}(t_1,t_2)e^{i\tilde{V}_{0i}^H(t_2-t_1)}e^{C(t_1,t_2)} \quad (3.67)$$

All the exchange and correlation effects are given by the second exponent $C(t_1,t_2)$ known as the *cumulant* [62], which is found in terms of the screened interaction in the linear-response approximation [63]

$$C(t_1,t_2) = -i\int_{t_1}^{t_2} d\tau \int_{\tau}^{t_2} d\tau' W_i(\tau',\tau). \quad (3.68)$$

3.4.3 The exact solution for one electron

It is instructive to solve the equation of motion for the Green's function for a model system with only one electron. The solution is given in detail in App.B. Starting from the simplest case which is to consider only two states, a valence and a conduction state one can solve the KBE evaluating all orders of an expansion in the Coulomb interaction. For this purpose it is convenient to use the four point interaction (eq.3.48). The self-energy of the two level model is equal to the lowest order of the expansion, which neglecting the spin polarization, is given by Hartee-Fock. This shows that the Hartree-Fock self-energy is the exact self-energy for a system with two levels and one electron. Correlation beyond Hartree-Fock arises including more unoccupied states in the basis and it becomes more complicated increasing the number of particles. Hartree-Fock introduces the self-interaction correction to the self-energy of the electron. We see that for the removal of the electron there is no contribution from the interaction. This happens because there is no other particle for the electron to interact with. On the other hand we see that for the addition of a second electron in the empty level we need an energy equal to the effect of the Hartree-Fock field from the electron which is already in the system. The reason why there is no correlation (that is screening the interaction) is that screening of the electron can only come from a second electron in the system pairing with the hole, and in the same sense screening of the hole can only come from a second empty level pairing with the electron.

In the general case of one electron with many empty states, we see that the one electron is non-interacting due to the self-interaction cancellation which doesn't allow for the electron to interact with itself and due to the self-screening cancellation which doesn't allow the electron to screen itself. It needs to have a second electron in the system to pair with the empty levels and screen the electron. On the other hand we see that for the addition of a second electron in the system the lowest order of the self-energy is the Hartree-Fock from the electron, while screening appears due to the fact that there are more empty levels in the system to pair with the electron.

Nelson, Bokes, Rinke and Godby in 2007 [59] and Fernandez in 2009 [64] discussed the fact that self-screening is a problem that appears in approximations such as the GWA, while it can be shown that from the exactly solvable system with one electron it shouldn't appear in the interacting system. They suggested that it is important to develop approximations in both MBPT and in DFT, which are free from the self-interaction and self-screening problems. In 2009 Romaniello, Guyot and Reining [60] discussed the self-interaction and self-screening cancellations in the Hubbard atom and suggested that it can be applied to create self-interaction free potentials in TDDFT. This will be the topic of discussion of a following chapter where we will present an extension to a system with localized electrons.

3.4.4 The one-point model

A system, which is even simpler than the one electron problem is the One Point Model (OPM) [65, 66, 11]. In this model all degrees of freedom collapse into a single point of the $0-$dimensional space. Then matrices are transformed to scalar quantities as $U \rightarrow iz$, the Green's function $G \rightarrow -iy$ and $G^0 \rightarrow -iy_0$ and the Coulomb interaction $v \rightarrow iv$. Functionals are transformed to functions and therefore the variable of eq.3.20 is the applied potential z or $y_0(z)$. The Coulomb interaction appears as a parameter. In the OPM the equation of motion for the Green's function (eq.3.20) becomes

$$y(z) = y_0(z) - y_0(z)vy^2(z) + \lambda y_0(z)v\frac{dy(z)}{dz}. \tag{3.69}$$

In the last equation the non-linearity appears in the classical term where the exact density enters. In the OPM one cannot distinguish the density from the Green's function. v can be interpreted either as the bare Coulomb interaction or as the four-point interaction given in eq.3.48. The second is always zero in the original OPM showing that this model is in fact a one electron model. Therefore in order to study approximations we will use the bare Coulomb interaction. Moreover, in front of the exchange and correlation term a prefactor λ is introduced. Since the exchange contribution comes from the lowest order approximation (no vertex-correction) to the self-energy, introducing λ we can simulate cases where the exchange term cancels only partially the classical term. This is the case where one has more than one electron localized in different regions of space, which leads to reduced exchange. The OPM neglects the dependence in time but allows one to treat the full correlation since it makes it possible to solve a differential equation for the Green's function.

Having a model with scalar quantities for the Green's function has certain advantages. The exact solution has been evaluated by A.Berger et al. [12]. For the case of $\lambda = 1$ it is the non-interacting solution $y = y_0$ while for the case of $\lambda = \frac{1}{2}$ it is a Hartree-Fock Green's function $y_{\frac{1}{2}} = \frac{2y_0}{2+vy_0^{02}}$, where the self-energy is built with the non-interacting density-matrix. Even though omitting the degrees of freedom of the matrix quantities remove most of the physics of the equation of motion of the Green's function, it is astonishing how much intuition about real systems one gains from the solution on one point. The case of $\lambda = 1$ can be related to the one electron case and therefore it is physical that one obtains the physical solution to be equal to the non-interacting solution. On the other hand the case of $\lambda = \frac{1}{2}$ can be seen as a case where the exchange is smaller than the Hartree contribution and relies on a non-interacting density. Moreover, there is no polarization contribution, which is typical of systems with localized states.

Using the model, one may apply approximations to the exchange and correlation part of the self-energy and check the quality of the solution. The first approximation is the linear-response approximation where one assumes that the density is taken in the linear-response approximation. Then one needs to solve eq.3.65 in the OPM

$$y(z) = y_0^0 + y_0^0 \tilde{z} y(\tilde{z}) + \lambda y_0^0 w \frac{dy(\tilde{z})}{d\tilde{z}}. \tag{3.70}$$

In the last equation $\tilde{z}$ accounts for the applied potential summed with the classical potential in the linear-response approximation, while y_0^0 is the Green's function of the static and non-interacting system. w is the screened interaction which in the linear-response approximation is scalar. Lani, Romaniello and Reining in [11] have solved this equation to obtain the solution

$$y(\tilde{z}) = \sqrt{\frac{\pi}{-2w\lambda}} e^{-\frac{\tilde{z}^2}{2\lambda w}} (erf(\frac{\tilde{z}}{\sqrt{-2\lambda w}}) + 1). \tag{3.71}$$

This is the equivalent to the cumulant solution (eq.3.67) in the OPM. It satisfies the non-interacting solution in the limit $w \to 0$. It will be the subject of chap.5 to examine approximations that go beyond the linear-response approximation in the OPM.

Summary

In this chapter we introduced the equation of motion for the Green's function and the Hedin equations. Common approximations such as the GWA in this approach suffer from the self-screening problem. From the one electron model one can understand that it is important to take into account the self-interaction correction also in the correlation part of the self-energy since it gives the most interesting physics. For this reason the equation of motion for the Green's function and the Hedin equations are rewritten with a four-point interaction which accounts for the self-interaction correction in all levels of approximations. This is a better starting point for approximations. We also discussed the solution of the equation of motion in the linear-response approximation and in the decoupling approximation. We introduced the OPM which is a model that allows for the exact treatment of correlation. In the following chapters we will propose the derivation of a self-interaction free potential of DFT for systems with localized electrons. We will use the OPM to explore trends for TDDFT. We will finally try to go beyond the linear-response approximation in the cumulant solution, and in the last chapter, we will model vertex corrections.

4

Response functions

In chap.2 we introduced the response function, which yields the absorption properties of the many-electron system via the creation of electron-hole pairs. The response function describes such processes because it is given by the density-density correlation function. The density-density correlation function in the equilibrium limit gives the linear-response approximation where only processes that involve the creation of a single electron-hole pair are taken into account, i.e. processes described by a single pair of field operators $\Psi^\dagger\Psi$. For the absorption the linear response is a good approximation in cases where the system is weakly perturbed. In equilibrium, treating the propagation of the electron independent from the propagation of the hole, we obtained the independent-particle polarizability.

As we have seen in chap.3 the photoemission process measures the binding energy of an electron. It can be described either from the solution of the Hedin equations for the one-body Green's function, obtained within approximations, or from the solution of the KBE. There a generalized response function again appears both in the correlation part of the self-energy, by means of the vertex function Γ or of the functional derivative of the Green's function with respect to the total potential, and in the screening of the interaction. Iterating the equations to infinite order makes all higher order correlation functions appear in the equations. This means that the correlation part of the self-energy includes all possible multi-particle excitations and not only the electron-hole pairs. Taking the equilibrium limit of the response function before solving the equations introduces a huge simplification since we neglect from the solution the effects of higher order correlation functions and we only account for correlation from electron-hole pairs. Therefore for an exact description of correlation only once the equations are solved, the applied potential can be taken to zero giving the equilibrium solution of the equations.

Going beyond the independent particles picture, in the first section of this chapter, we will present a way to account also for excitonic properties coming from the interaction between the electron and the hole. In the following section we will introduce TDDFT as the alternative theory to obtain the density response function in a way which is in principle exact. We will finally discuss ways to develop approximations for TDDFT and present some that have already been developed.

4.1 The equation of motion for the two-particles correlation function

In this section we generalize the definitions of the non-equilibrium Green's functions eq.3.10,3.11 to an applied potential which is non-local in space and time. The general two-particles correlation

function is defined from the variation of the Green's function with respect to such a generalized non-local in space-time potential U, which adds a contribution [55], [9]

$$\hat{S}(\tau_1, \tau_2) = \int dx_1 x_2 \hat{\Psi}^\dagger(x_1, \tau_1) U(x_1, \tau_1, x_2, \tau_2) \hat{\Psi}(x_2, \tau_2), \tag{4.1}$$

to the hamiltonian. The two-particles correlation function can be written as

$$L(1234) = \frac{\delta G(12)}{\delta U(34)} = G^{2p}(1234) - G(12)G(43). \tag{4.2}$$

This is a generalization of the Schwinger-Dyson equation to a non-local in space and time applied potential. The two-particles correlation function gives the propagation of two particles between four points in the configuration space. It is the probability amplitude to find the system in its ground-state after two single-particle processes have occured. Those involve processes that conserve the number of particles (creation of electron-hole pairs), but also processes that do not conserve the number of particles in the system where 2 electrons or 2 holes have been created in the system, passing respectively through excited states of the $N+2$ and $N-2$-particles system. Therefore the two-particles correlation function accounts also for the effects of double ionizations created by the applied potential.

Using the derivative of the inverse as in eq.3.34

$$\frac{\delta G(12)}{\delta U(34)} = -G(1\bar{1}) \frac{\delta G^{-1}(\bar{1}\bar{2})}{\delta U(34)} G(\bar{2}2) \tag{4.3}$$

and introducing the self-energy from eq.2.22 for the inverse Green's function, we obtain

$$L(1234) = G(13)G(42) + G(1\bar{1})G(\bar{2}2) \frac{\delta \Sigma(\bar{1}\bar{2})}{\delta U(34)}. \tag{4.4}$$

This is the equation of motion for the two-particles correlation function. The correlated motion of two particles in a system with many electrons is given by the independent propagation of two particles $G(13)G(42)$ corrected for the interaction between the two particles through the second term that appears in eq.4.4. Using a chain rule we can rewrite the second term of eq.4.4 as

$$\frac{\delta \Sigma(\bar{1}\bar{2})}{\delta U(34)} = \frac{\delta \Sigma(\bar{1}\bar{2})}{\delta G(\bar{3}\bar{4})} L(\bar{3}\bar{4}34), \tag{4.5}$$

where the four-point kernel K stands for the interaction between the electron and the hole

$$K(1234) = \frac{\delta \Sigma(12)}{\delta G(34)}. \tag{4.6}$$

For example when the self-energy is given by the Hartree potential,

$$\Sigma^H(12) = -i\delta(12) v(1, \bar{3}) G(\bar{3}\bar{3}^+) \tag{4.7}$$

the effective interaction is given by

$$K^H(1234) = -i\delta(12)\delta(34) v(1, 3), \tag{4.8}$$

the bare Coulomb interaction, which is the classical interaction between charged particles. Therefore the bare Coulomb interaction gives the interaction between an electron and a hole in the classical system. In any other case, the Coulomb interaction will be dressed with the exchange and correlation effects from the self-energy.

We summarize the Dyson equation for the two particles correlation function

$$L(1234) = G(13)G(42) + G(1\bar{1})G(\bar{2}2)K(\bar{1}\bar{2}\bar{3}\bar{4})L(\bar{3}\bar{4}34). \tag{4.9}$$

Eq.4.9 is known as the Bethe-Salpeter Equation (BSE) after Bethe and Salpeter who were the first to discuss it in 1951 [6]. The BSE is complicated to solve since it is an equation for matrices with four points in configuration space. However, often one is interested to obtain the density-density response function instead of the two particles correlation function. This response function is a two-point matrix defined from the two particles correlation function as

$$\chi(12) = -iL(11^{+}22). \tag{4.10}$$

The response measures variations of the density with respect to the local part of the applied potential instead of variations of the one-body Green's function with respect to the full non-local potential. It contains the correlation from the creation of an electron-hole pair passing through excited states of the N-particle system, but doesn't describe the propagation of two particles or two holes. The equation of motion for the response function is then given by eq.4.9 as

$$-iL(11^{+}33) = -iG(13)G(31) - iG(1\bar{1})G(\bar{2}2)K(\bar{1}\bar{2}\bar{3}\bar{4})L(\bar{3}\bar{4}33). \tag{4.11}$$

We see that the BSE for the response function cannot be written in a closed form because it also includes the three-point correlation function $L(\bar{3}\bar{4}33)$. This happens due to the fact that the self-energy, which is a non-local in space and time effective field, is known as a functional of the Green's function but not of the density. For this reason we had to introduce the chain-rule with respect to the Green's function. In the following section we will use Time-Dependent Density Functional Theory (TDDFT) to skip this problem and get the equation of motion directly for the response function [67].

Now we will illustrate with the example of NiO the effect of the electron-hole interaction on the absorption. NiO is an oxide with quite localized valence states. In fig.4.1 we show a calculation by Matteo Gatti [68] of the IXS spectrum of NiO. In a Kohn-Sham spectrum of independent particles, there is a low-energy peak at 2 eV broadened over a few eV. The position of the peak corresponds to the magnitude of the band gap in the Kohn-Sham band structure. The peak is broadened meaning that there is dispersion of the transition energies, coming from dispersion of the conduction and valence bands.

The GW calculation corresponds mainly to a screened exchange correction with respect to the classical system. The transition energies are shifted to higher values, around 7 eV, which indicates the opening of the band gap. Still the spectrum is broadened around the position of the peak, meaning that the valence and conduction bands are dispersive. This happens because the GW approximation has been performed perturbatively, without recalculating the density, such that it results mainly in a scissor shift of the transition energies.

In a last step the BSE is solved. This accounts for the effect of the interaction between the electron and the hole. Now the peak of the spectrum is shifted to lower energies, close to the Kohn-Sham result. This shows a cancellation between the potential from the interaction in the GW approximation and the correction when we take into account the electron-hole interaction. The peak now is

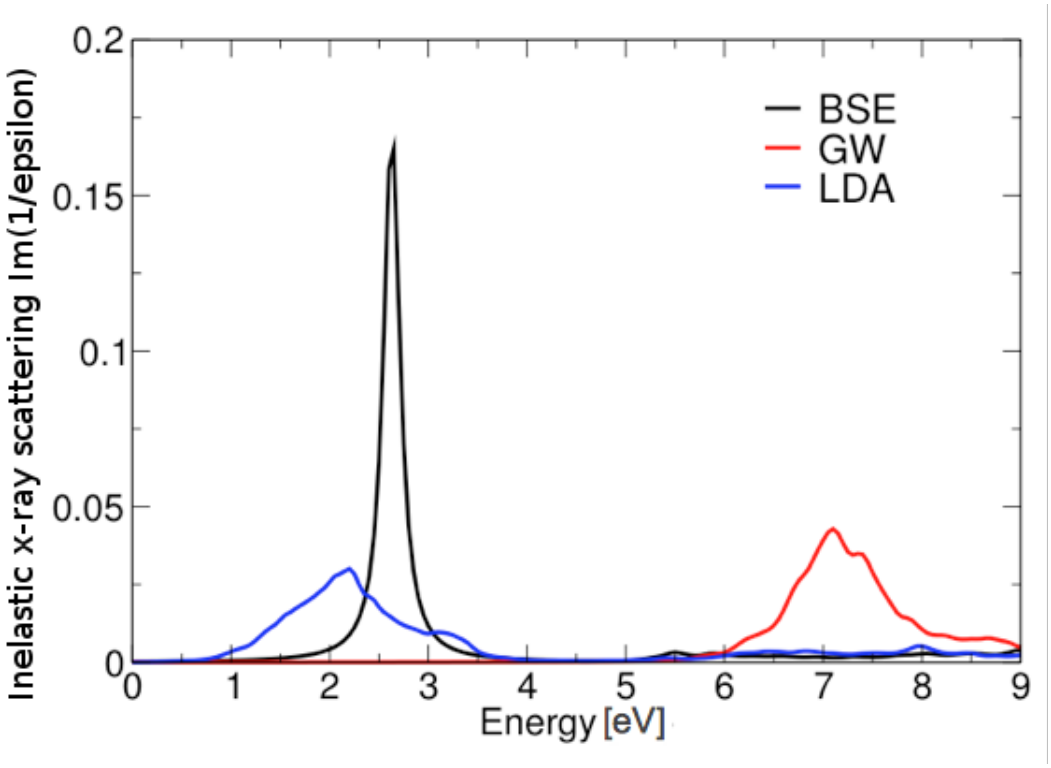

Fig. 4.1: IXS spectrum of NiO as a result of three calculations: DFT-Kohn-Sham in the LDA, which corresponds to an independent-particle response function in the Kohn-Sham system (blue curve); GW calculation, which corresponds to an independent-particle response function with particles that are dressed by the GWA (red curve); BSE calculation, which corresponds to a system with an attractive interaction between the electron and the hole.

sharp because the attractive interaction between electron and hole localizes the electron-hole pair. It is however intriguing how close the final result is energetically to the one of the independent Kohn-Sham electrons.

4.2 The T-matrix equation and the two-particles Green's function

Starting from eq.4.9 one can multiply and integrate with K and introduce the *scattering matrix* T [55],[51] defined as

$$T(12\bar{1}\bar{2})G(\bar{1}3)G(4\bar{1}) = K(12\bar{1}\bar{2})L(\bar{1}\bar{2}34). \tag{4.12}$$

The scattering matrix T stands for all the scattering events that happen due to the interaction between two particles. Then eq.4.9 can be rewritten as

$$T(1234) = K(1234) + K(12\bar{3}\bar{4})G(\bar{3}\bar{5})G(\bar{6}\bar{4})T(\bar{5}\bar{6}34). \tag{4.13}$$

The last equation gives the T-matrix in terms of the two-particles Kernel and the interacting one-body propagators. The two-particles Green's function can also be written with respect to the T-matrix as

$$G_2(1234) = G(13)G(42) - G(12)G(43) - G(1\bar{1})G(\bar{2}2)T(\bar{1}\bar{2}\bar{3}\bar{4})G(\bar{3}3)G(4\bar{4}). \tag{4.14}$$

The last equation shows that the equation of motion for the T-matrix is equivalent to the equation of motion for the two-particles Green's function.

4.3 The response function from TDDFT

We have already mentioned that the response function cannot be given self-consistently as a two points function, but needs to be obtained as a part of the two-particles correlation function unless the self-energy is known as an explicit functional of the density. Of course the self-energy is a complicated quantity which we don't know how to calculate exactly. For this reason it is convenient to use Time-Dependent Density Functional Theory (TDDFT), which is the extension of DFT to time-dependent systems. TDDFT states that given the initial state, there is a one to one correspondence between the time dependent density and the time dependent potential, apart from an additive time dependent constant [8]. TDDFT can be combined with MBPT, in order to eliminate the non-local exchange and correlation part of the self-energy. In TDDFT the role of the self-energy is played by a local and time-dependent Kohn Sham potential for a system of independent particles. An overview of possibilities to combine MBPT and TDDFT can be found in [69]. For the scope of this thesis we will focus on ways to design the Kohn-Sham system so that we obtain quantities of the interacting system. The quantity that one may obtain from TDDFT is the density-response function of the interacting system. It gives the absorption spectrum or the screening of the Coulomb interaction in MBPT. Moreover knowing the Kohn-Sham potential one can obtain also its variation from the derivative with respect to the time dependent density. In this section we will first present the Sham-Schlüter Equation (SSE) from which one can derive Kohn-Sham potentials. Then we will present schemes to evaluate directly the derivative of the Kohn-Sham potential with respect to the density, which is the fundamental quantity that enters the evaluation of the response function.

4.3.1 TDDFT from the Sham-Schlüter Equation (SSE)

The time dependent density is equal to the local part of the Green's function

$$\rho(1) = -iG(11^+). \tag{4.15}$$

We require the time dependent density of the real system to be equal to the time dependent density of the Kohn-Sham system. This results in the following condition linking the Kohn-Sham potential and the self-energy

$$\int d34 G(13)\Sigma(34)G(41) = \int d3 G^{KS}(13)G^{KS}(31)V^{KS}(3), \tag{4.16}$$

where G^{KS} stands for the Green's function of the Kohn-Sham system. Eq.4.16 is known as the Sham-Schlüter Equation (SSE), named after Sham and Schlüter who introduced this equation [70], [71].

4.3.2 TDDFT from response functions

In the framework of TDDFT one has an equation equivalent to eq.4.9, but where one has to replace the effective interaction K from the self-energy with the one derived from the Kohn-Sham potential

K^{KS} as

$$K^{KS}(12) = \frac{\delta V^{KS}(1)}{\delta \rho(2)}. \tag{4.17}$$

Moreover, the Green's function G have to be replaced by Kohn-Sham Green's functions G^{KS}. This transforms the equation of motion of the response function (eq.4.11) into

$$\chi(12) = \chi^0(12) + \chi^0(1\bar{1})K^{KS}(\bar{1}\bar{2})\chi(\bar{2}2), \tag{4.18}$$

where we have shortened the notation of the independent-particle response function as $\chi^0(12) = -iG^{KS}(12)G^{KS}(21)$. The response given by the TDDFT eq.4.18 is in principle exact. Moreover this equation is written in a closed two-points form contrary to eq.4.11. The quality of the response function calculated this way depends on the quality of the Kohn-Sham potential and its effective interaction K^{KS}.

The Kohn-Sham potential includes also the contribution from the classical potential. The derivative of the classical potential with respect to the density is the bare Coulomb interaction. Instead, the effective interaction from the exchange and correlation part of the Kohn-Sham potential is

$$f^{xc}(12) = \frac{\delta V^{xc}(1)}{\delta \rho(2)}. \tag{4.19}$$

Separating the classical potential from the exchange and correlation part eq.4.18 becomes

$$\chi(12) = \chi^0(12) + \chi^0(1\bar{1})(v(\bar{1}\bar{2}) + f^{xc}(\bar{1}\bar{2}))\chi(\bar{2}2). \tag{4.20}$$

On the RPA, the response function given with respect to the independent-particle response function is obtained by setting f^{xc} to zero:

$$\chi^{RPA}(12) = \chi^0(12) + \chi^0(1\bar{1})v(\bar{1}\bar{2})\chi^{RPA}(\bar{2}2). \tag{4.21}$$

At this point we note that there is a lot of freedom in the definition of the RPA. The only constraint is that the response function is obtained from an independent particles response function via a Dyson equation involving only the bare Coulomb interaction. Combining eq.4.21 and eq.4.20 one may eliminate the Coulomb interaction and obtain the equation

$$\chi(12) = \chi^{RPA}(12) + \chi^{RPA}(1\bar{1})f^{xc}(\bar{1}\bar{2})\chi(\bar{2}2). \tag{4.22}$$

One can invert eq.4.22 and obtain a relation which gives the exact f^{xc} with respect to the RPA

$$f^{xc}(12) = \chi^{-1RPA}(12) - \chi^{-1}(12). \tag{4.23}$$

The f^{xc} given by the last equation is exact only when the exact χ is used. This is in general not known, so one has to use approximations for χ. In the following section we will give such approximations based on iterative schemes. Usually the physical meaning of such approximations can be understood in terms of perturbation theory. Before we close this section let us note that eq.4.23 is not the only equation defining the exact f^{xc}. One may for example rewrite it with respect to the irreducible polarizability as

$$f^{xc}(12) = \chi^{0-1}(12) - P^{-1}(12). \tag{4.24}$$

The last equation is still exact. Here f^{xc} is defined from the independent-particle response function from the Kohn-Sham Green's function, but one could introduce a different f^{xc} defined as

$$f^{xc'}(12) = \chi^{0'-1}(12) - P^{-1}(12), \tag{4.25}$$

with a $\chi^{0'}$ being the independent-particle response function from the Green's function of another system, for example the Green's function of the non-interacting or the classical system. The $f^{xc'}$ is in principle exact but different from f^{xc}, because the two kernels satisfy a different Dyson equation.

4.3.3 Approximations for TDDFT

The simplest approximation to f^{xc} is obtained when one uses eq.4.25 with $\chi^{0'}$ defined as $\chi^{0'} = -iGG$. Then often improvements with respect to the RPA are obtained by setting

$$f^{xc'}(12) = -\alpha v(12), \tag{4.26}$$

which is equal to the Coulomb interaction rescaled by a number α that is related to static screening [13]. Using this kernel, eq.4.20 becomes

$$\chi(12) = \chi^{0'}(12) + \chi^{0'}(1\bar{1})(1-\alpha)v(\bar{1}\bar{2})\chi(\bar{2}2). \tag{4.27}$$

The next simple approximation is the bootstrap approximation. In its scalar version, the f^{xc} in [14] is approximated as

$$f^{xcBO} = \frac{\epsilon^{-1}(\omega=0)v}{\epsilon^{RPA}(\omega=0)-1}. \tag{4.28}$$

Eq.4.28 has to be solved together with eq.4.20 (with $\chi^{0'}$) self-consistently. If the inverse RPA dielectric function is used instead of ϵ^{-1} in eq.4.28 one obtains the RPA bootstrap approximation [15],

$$f^{xcRBO}(12) = \frac{1}{\epsilon^{RPA}\chi^{RPA}}. \tag{4.29}$$

This kernel does not lead to a self-consistency requirement.

Summary

In this section we introduced ways to go beyond the independent particles approximation for the response function. We started with the BSE whose solution is cumbersome because it involves high-dimensional matrices. TDDFT on the other hand leads to simplified equations, but the quality of the results depends on the level of approximation for the Kohn-Sham potential or the effective interaction. One may look for such approximations using the Sham-Schlüter equation (SSE) to derive Kohn-Sham potentials or interactions for TDDFT. We closed the chapter giving two examples, the long-range and the bootstrap approximations for TDDFT. In following chapters we will check the efficiency of these kernels using the OPM and we will use the SSE to derive a Kohn-Sham potential and its kernel.

5

Insights for non-linear screening from the one-point model

In this chapter we explore the question how to obtain expressions for the Green's function that go beyond the standard GW approximation. To this end, we study the functional differential equation (eq.3.20) of Kadannof and Baym (KBE). Solving the KBE is a very complicated task. It is a matrix equation for the Green's function, which is a high-dimensional matrix, since it is a two point matrix, where each point represents a space, time and spin index. Moreover, since space and time are continuous, it is an integral equation. It is a non-linear equation due to the self-consistent density, which appears in the classical potential. Finally, it is also a first order differential equation. Altogether the KBE is a system of first order integrodifferential equations. Despite the complicated form of the KBE, the variable of the equation of motion of the Green's function is the external potential, which is introduced as the perturbation. Therefore the essential physics of the differential equation is given from the response of the Green's function to the variations of the perturbing potential. In order to make the equation tractable, one has to make drastic simplifications. If one disregards all space, spin and time indices, one obtains the scalar KBE eq.3.69 which has been exactly solved [12].

This model, called OPM, which we introduced in Chap.3, has been used to enumerate the Feynman diagrams of the exact self-energy [65, 66]. It has also been used to study Hedin equations [72]. Following the idea of Hedin (Chap.3) to screen the Coulomb interaction with the "total classical" potential given by eq.3.24, Lani, Romaniello and Reining in [11] have written the KBE with respect to the Green's function of the classical system, introducing the screened interaction w in the KBE (eq.3.70). They have treated the density appearing in the classical potential in the linear-response approximation, linearizing the equation. Then they used the OPM to solve the equation for the two cases $\lambda = 1$ and $\lambda = \frac{1}{2}$, where λ is a prefactor that scales the strength of the exchange.

In this chapter we will use the OPM to study different approximations for screening. The structure of this chapter is complicated and we try to give an overview in fig.5.1. We will start from the equation of motion for the Green's function with the screened interaction (eq.5.1). One way to go is to study approximations for screening in the linear-response approximation. Another way to go is to introduce non-linear screening. This can be done in the RPA as a first step, and beyond the RPA within TDDFT. At this point one should be careful to choose the variable of the equation. The non-linearities of the equation, can be replaced with non-linear transformations. We will discuss how non-linear transformations reflect the multiplicity of the solutions and have an effect on the approximations used in screening. In all cases the problem of multiple solutions will arise once we obtain a general solution of a differential equation. It is useful for the reader at any stage of reading to refer to fig.5.1 for a pictorial illustration of the logic behind the discussions. Moreover,

throughout the chapter, one may find the most important conclusions highlighted with italics.

$$y(z) = y_0(z) + y_0(z)vy^2(z) + \lambda y_0(z)w(z)\frac{dy(z)}{dV^{tot}}. \tag{5.1}$$

In this chapter, using the OPM, we will discuss different levels of approximations for the screened interaction in the linear-response approximation. We will look for the reason of the deficiencies of the linear-response approximation of the KBE by exploring non-linear effects appearing in the exact screening. Then we will look for improvement towards non-linear effects emerging from TDDFT. We will also refer to the problems of the choice of the variable and of multiple solutions of the differential equation.

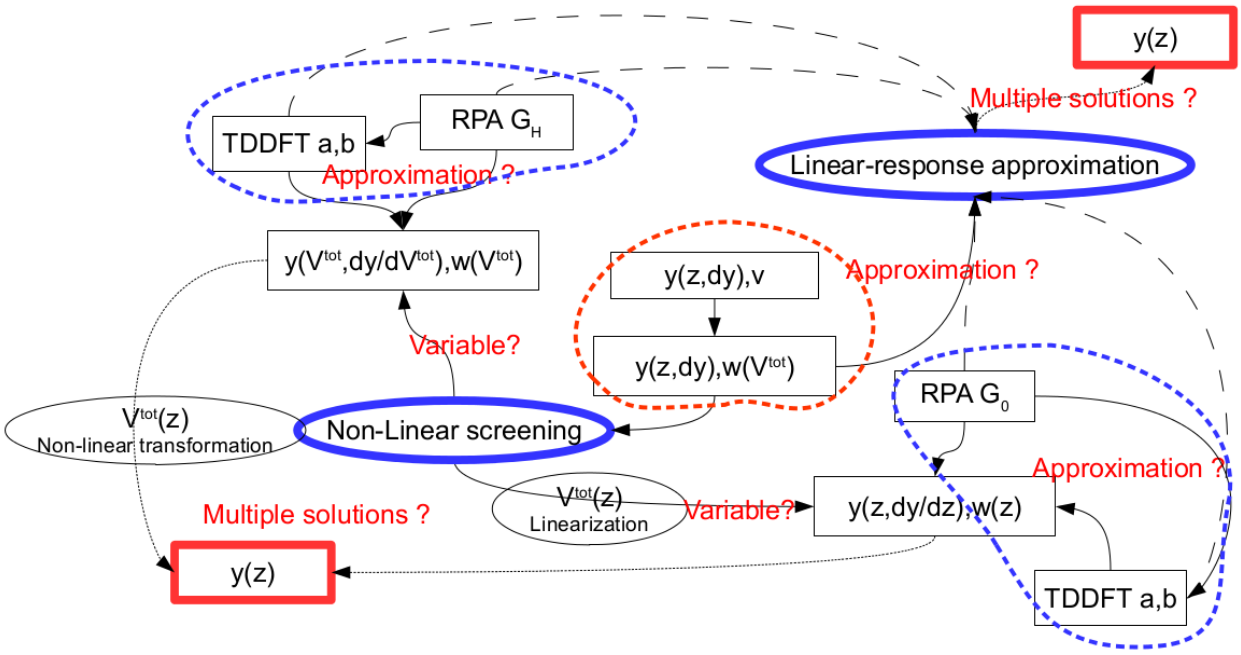

Fig. 5.1: Looking for solutions within approximations for screening: the structure of this chapter.

5.1 The interaction variable in the KBE

The KBE (eq.3.69) is a first order differential equation, which we will solve on different levels of approximations for the screened interaction. Such approximations are the linear-response approximation (eq.3.70) and beyond. In both cases one can choose to screen the Coulomb interaction from the RPA and beyond the RPA in TDDFT (see Chap.4). Screening within TDDFT is equivalent to including vertex corrections in many-body perturbation theory. Standard approximations that we will use in the framework of the OPM are the LRC (eq.4.26) and the bootstrap (eq.4.28) approximations. For the solution of the equation within different approximations it is important to choose the variable, which simplifies the process. This means that one from one side should try to have in an equation as few parameters as possible and from the other side one might need to make

transformations. In this section we will discuss the choice of the variable and present different ways to transform the KBE based on the RPA starting point.

In order to underly the importance of the choice of variable, we will make a link to the problem of multiple solutions, which is inherent to differential equations. In its simplest form, solving a first order differential equation (e.g. $\frac{dy(z)}{dz} = ay(z)$), one obtains the solution ($y(z) = Ce^{az}$) with the freedom of choice of the constant of the integration (C), which immediately gives a family of solutions. The traditional way to face the problem of multiple solutions is to apply boundary or initial conditions which reflects the fact that we fix the solution for some value of the variable ($y(z_0) = y_0$). However, this requires that there exist values of the variable (z_0) where we know the exact solution (y_0). In eq.3.69 the interaction appears as a parameter and not as a variable, meaning that we need to solve such an equation for $y(z)$ and then evaluate it parametrically with respect to the Coulomb interaction. On the other hand there are no values of the applied potential for which we know the exact solution for the interacting propagator, which makes it impossible to detect the physical solutions. The only thing that we know for the interacting propagator is that it must be equal to the non-interacting one for vanishing interaction. Therefore the idea is to group the applied potential with the Coulomb interaction. This yields an interaction variable for which we can then take the non-interacting value, where we know that the physical solution for interacting Green's function must be equal to the non-interacting Green's function. In the following discussions we will define such interaction variables and present possible ways to transform them.

Before we write the KBE using an interaction variable, we need to work on the choice of the variable. For this purpose let us rewrite the KBE in the OPM. The usual way to introduce screening in the spirit of Hedin (Chap.3) is to screen the Coulomb interaction with the "total classical" potential $V^{tot}(z) = z - vy(z)$

$$y = y_0^0 + y_0^0 V^{tot} y + \lambda y_0^0 v \frac{dy}{dV^{tot}} \frac{dV^{tot}}{dz}. \tag{5.2}$$

The "total classical" potential also contains the non-linear contribution, originally coming from the density. Then we can introduce the screened interaction $w = \epsilon^{-1} v$, where $\epsilon^{-1} = 1 - v\frac{dy}{dz}$

$$y = y_0^0 + y_0^0 V^{tot} y + \lambda y_0^0 w \frac{dy}{dV^{tot}}. \tag{5.3}$$

Eq.5.1 is exact. At this point we can introduce approximations in $w \approx \epsilon^{-1}_{approx} v$ and solve the equation. At this stage we can see that both z and V^{tot} appear in the equation and one needs to make a choice for the variable.

In cases where the approximation of $w(z)$ is an explicit expression of the external potential z, then it is convenient to solve the equation keeping the external potential as the variable instead of transforming w to a function of V^{tot}. For this purpose, we make a second chain rule with respect to the external potential z

$$v\epsilon^{-1}_{approx}(z)\frac{dy}{dV^{tot}} = v\epsilon^{-1}_{approx}(z)\frac{dy}{dz}\frac{dz}{dV^{tot}} = v\frac{\epsilon^{-1}_{approx}(z)}{\epsilon^{-1}_{exact}(z)}\frac{dy}{dz}, \tag{5.4}$$

where $\frac{1}{\epsilon^{-1}_{exact}(z)} = \frac{dz}{dV^{tot}(z)}$ is the exact dielectric function. We rewrite eq.5.1 as

$$y(z) = y_0^0 + y_0^0 V^{tot}(z) y + \lambda y_0^0 v \frac{\epsilon^{-1}_{approx}(z)}{\epsilon^{-1}_{exact}(z)} \frac{dy(z)}{dz}. \tag{5.5}$$

In this equation we have introduced screening within an approximation, but have kept the external potential as the variable. The expression of $\epsilon^{-1}_{exact}(z)$ relies on the choice of the "total classical" potential.

On the other hand, in cases where the approximation for $w(V^{tot})$ is an explicit expression of the "total classical" potential, one may solve eq.5.1, as a linear differential equation, whose solution is given as a function of the "total classical" potential,

$$y(V^{tot}) = y_0^0 + y_0^0 V^{tot} y + \lambda y_0^0 w(V^{tot}) \frac{dy(V^{tot})}{dV^{tot}}. \tag{5.6}$$

Then using the expression of the "total classical" potential, one may obtain the solution $y(z)$ as a function of the external potential. Therefore, both in the case of a functional of the external potential $w(z)$ and of a functional of the "total classical" potential $w(V^{tot})$, the transformation between the external and the "total classical" potentials needs to be applied. For this transformation to be exact, the density in the "total classical" potential is equal to the exact solution, which we cannot know unless we have solved the equation. Moreover, even the self-consistent evaluation of the density is not always possible, especially when one introduces approximations for the screening, where the differential equation becomes highly non-linear. Therefore, one can base the solution of the differential equation on choices of the transformation between the external and the "total classical" potential.

In the most general case, where the density is obtained self-consistently from the solution y, the equation for the classical propagator x, where $iG^H \to x$ in the OPM, is given by

$$x(y_0) = y_0 - y_0 v y(y_0) x(y_0). \tag{5.7}$$

The transformation between the potentials $z \to V^{tot}$ is equivalent to the transformation between the propagators $y_0 \to x$. Eq.5.7 is a highly non-linear transformation. This means that the inverse transformation $y_0(x)$ is not single-valued given a value of x. Therefore starting from an external potential z in a certain range of values Z_1, which we consider to be the physical range, we obtain a range X_1 for x and the solution $y(X_1)$. Due to the fact that the transformation $x \to z$ is non-linear the domain X_1 corresponds to a much larger domain $\{Z_i\}$. This automatically gives $y(\{Z_i\})$, and the domain of validity of the solution exceeds the physical domain. Then one needs to constrain the domain of validity of the solution to the physical range Z_1 and keep $y(Z_1)$. We will illustrate this with an example later in this section.

The fact that a non-linear transformation gives rise to multiple solutions has recently been discussed by Tarantino, Romaniello, Berger and Reining [73] in the problem of perturbative expansions of self-energy functionals for the Hubbard atom. It is possible to write the self-energy as a functional of the non-interacting or of the interacting Green's function using perturbation theory. One may pass from a functional of G_0 to a functional of G inverting the transformation $G[G_0] \to G_0[G]$. This is a non-linear equation, giving rise to multiple functionals of G (fig.5.2). One then needs to constrain the domain of each functional to the physical domain.

5.1.1 The choice of the "total classical" potential

Since a self-consistent calculation of the density is not always possible, we will choose the expression of the "total classical" potential based on the exact solutions of eq.3.69 for the cases of $\lambda = 1$

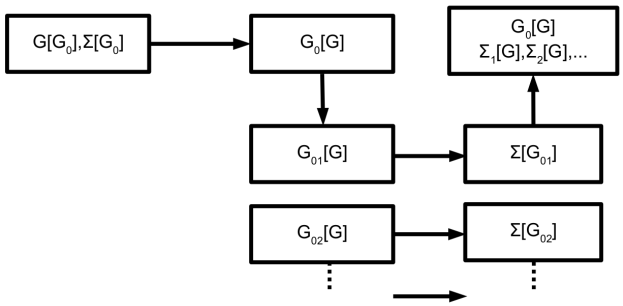

Fig. 5.2: While the self-energy is a unique functional of G_0, it gives multiple functionals of $\Sigma[G[G_0]]$.

and $\lambda = \frac{1}{2}$. The case of $\lambda = 1$ reflects the case where there is an exact cancellation between the classical and exchange terms and the exact solution is equal to the non-interacting solution. In this case the density is equal to the non-interacting solution. On the other hand the choice of $\lambda = \frac{1}{2}$ reflects the case where there is a partial cancellation between the classical and exchange terms. The exact solution of eq.3.69 for the case of $\lambda = \frac{1}{2}$ can be written as a Dyson equation for $y_{\frac{1}{2}}$

$$y_{\frac{1}{2}}(v, y_0) = y_0 - \frac{1}{2} y_0 v y_0 y_{\frac{1}{2}}. \tag{5.8}$$

Eq.5.8 has the form of a particle propagating in an effective potential, that is linear in the Coulomb interaction and that depends only on the density of the non-interacting system. This form of the potential can be encountered also in the fully indexed equation for a localized level interacting in the non-overlapping approximation, where there is no exchange, and in the decoupling approximation, where the interacting density remains equal to the density of the non-interacting system. In this case the classical potential depends only on the non-interacting solution, but not on the exact solution $\rho = y_0 \neq y_{\frac{1}{2}}$. This fact reflects the partial cancellation between the direct and exchange terms in eq.3.69 written with the non-interacting density if there is no correlation in the system. Therefore, in both cases of $\lambda = 1$ and $\lambda = \frac{1}{2}$ from the exact solution one can motivate to choose the classical potential based on the non-interacting density

$$V^{tot} = z - v y_0(z). \tag{5.9}$$

This is an approximate transformation between the "total classical" potential and the external potential that we will apply on eq.5.5 and 5.6. We stress again that here, in the "total classical" potential we have used the non-interacting density, which is equal to the exact density for the case of $\lambda = 1$. In the realistic case, where we don't know the exact solution, it would be reasonable to take the density from DFT.

5.1.2 Approximations for the screened interaction from the RPA with the non-interacting propagator

In order to introduce a screened interaction which depends explicitly on the external potential, we need to keep the external potential as the variable of the equation. Moreover in order to be able to distinguish the physical solutions with the non-interacting limit it is convenient to introduce an interaction variable, as explained in the beginning. In this case we rewrite eq.3.69 using the "total classical" potential from eq.5.9 and the interaction variable $o(z) = v y_0^2(z)$, which is also dimensionless.

Let us briefly discuss the case where we first renormalize the resulting equation with the non-interacting propagator $\tilde{y} = y_0^{-1}(z)y(z)$ as

$$\tilde{y}(z) = 1 - vy_0^2\tilde{y}(z) + \lambda v\frac{d\tilde{y}(z)}{dz} + \lambda v\tilde{y}(z)y_0^2. \tag{5.10}$$

For the choice of $\lambda = 1$ there is an exact cancellation between the classical and exchange terms, while the derivative adds the correlation. Accounting for the cancellation before introducing screening gives an equation which is always satisfied by the non-interacting solution $\tilde{y} = 1$. Therefore once the self-interaction correction is taken into account in the lowest order of perturbation theory the solution is always equal to the physical solution of the model system independently or not screening is introduced in the correlation term.

Having made this observation, we now start from the screened eq.5.3 and from eq.5.4, where the approximate prefactor $\frac{\epsilon^{-1}_{approx}}{\epsilon^{-1}_{exact}}$ appears. Again, we renormalize with the non-interacting propagator. This leads to a screened exchange, which cancels partially the classical potential. Such a case reflects calculations in real systems under approximations (e.q.GWA), where the self-interaction correction is not complete. Now, we introduce the interaction variable $o = vy_0^2$ to get the final form of the equation

$$\tilde{y}(o) = 1 - o\tilde{y} + \frac{\lambda\tilde{w}(o)}{1-o}\frac{d\tilde{y}(o)}{do}2o + \frac{\lambda\tilde{w}(o)}{1-o}\tilde{y}(o), \tag{5.11}$$

where $\tilde{w} = y_0^2 w(z)$ is the screened interaction renormalized with the non-interacting propagator. $\frac{1}{\epsilon^{-1}_{exact}} = 1 - o$ is the inverse dielectric function corresponding to the "total classical" potential of eq.5.9.

The inverse dielectric function screening the interaction ϵ^{-1}_{approx} needs also to be written in terms of this interaction variable. For screening within the RPA from the non-interacting Green's function $\chi^{RPA} = y_0^2(1 - v\chi^{RPA})$, the inverse dielectric function can be written in terms of o as

$$\epsilon^{-1}_{RPA}(o) = \frac{1}{1+o}. \tag{5.12}$$

In order to go beyond the RPA, we will use TDDFT (see Chap.4). This is done within standard approximations for the exchange-correlation kernel f^{xc} such as the LRC (eq.4.26) and bootstrap approximations (eq.4.29), which read in the OPM

$$f^{xcLRC}y_0^2 = ao \text{ for the LRC,} \tag{5.13}$$

$$f^{xcBO}y_0^2 = b \text{ for the bootstrap.} \tag{5.14}$$

In the OPM in the LRC a is a parameter scaling the Coulomb interaction, which stands for the inverse dielectric function. In the bootstrap approximation b is a parameter scaling the inverse of the independent-particle response function as $\frac{\epsilon^{-1}}{y_0^2}$, so it again stands for the inverse dielectric function. Within these approximations, the inverse dielectric functions $\epsilon^{-1} = 1 + v\chi$ become

$$\epsilon_a^{-1}(o) = \frac{1-ao}{1+(1-a)o}, \tag{5.15}$$

$$\epsilon_b^{-1}(o) = \frac{1-b}{1-b+o}. \tag{5.16}$$

For the model we can also determine the exact f^{xc}. This can be calculated with respect to the RPA as introduced in eq.4.23. For TDDFT usually in the RPA the independent-particle response function is chosen to be the one of the Kohn-Sham system. Here, we choose for the RPA the independent-particle response function from the propagator of the non-interacting system. The renormalized $y_0^2 f^{xc}$ reads

$$y_0^2 f^{xc} = 1 - \frac{y_0^2}{\chi(z)} + v y_0^2. \tag{5.17}$$

$\chi = \frac{dy}{dz}$ is evaluated from the derivative of the exact solutions. We have

$$\frac{\chi}{y_0^2} = 1, \tag{5.18}$$

for the case of $\lambda = 1$ and

$$\frac{\chi}{y_0^2} = \frac{2(2-o)}{(2+o)^2}, \tag{5.19}$$

for the case of $\lambda = \frac{1}{2}$ as a function of the interaction variable o. With this, eq.5.17 gives the exact f^{xc}. Using approximations for the f^{xc} one may also solve with respect to $\chi(z)$ to obtain the response within a given approximation.

5.1.3 Approximations from the screened interaction from the RPA with the classical propagator

In order to introduce a screened interaction $w(V^{tot})$, which depends explicitly on the "total classical" potential it is convenient to rewrite eq.5.6 with respect to the classical propagator $iG^H \to x$. Doing this we obtain a system of two equations

$$y(x) = x + \lambda w(x) x^3 \frac{dy(x)}{dx} \tag{5.20}$$

$$w(x) = v(1 - w(x) x^2 \frac{dy(x)}{dx}) \tag{5.21}$$

for the Green's function $y(x)$ and the screened interaction $w(x)$, with an explicit dependence on the Coulomb interaction and the classical propagator.

Starting from eq.5.20 we can renormalize the propagator of the interacting system with respect to the classical propagator $\bar{y} = \frac{y}{x}$ and introduce the interaction variable $u = vx^2$. For the choice of the "total classical" potential of eq.5.9 the transformation between o and u reads

$$u = \frac{o}{(1+o)^2}. \tag{5.22}$$

The inverse transformation has two branches,

$$o^{\pm}(u) = \frac{-(2u-1) \pm \sqrt{-4u+1}}{2u}. \tag{5.23}$$

In fig.5.3 we show the two branches of the transformation $o^{\pm}(u(o))$ as a function of o given in eq.5.23 and eq.5.22. A similar discussion for a non-linear transformation, giving rise to multiple

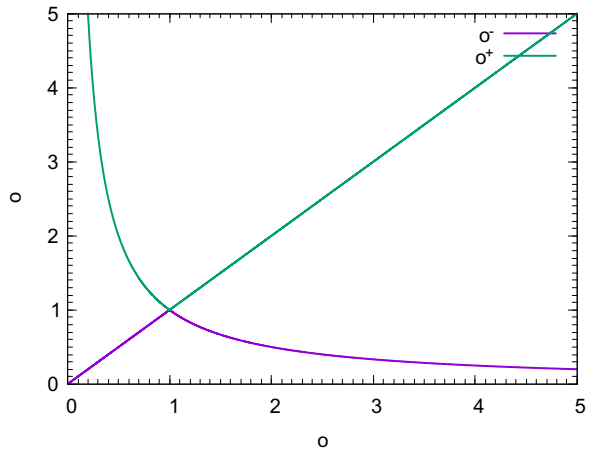

Fig. 5.3: Transformation of eq.5.23

self-energy functions can be found in [74]. For small values of u (or o) the branch with the " $-$ " sign is the physical branch since it satisfies the non-interacting limit for vanishing $o^- = 0$. For larger values of u (or o), the branch with the " $+$ " should be used. Now we also renormalize the screened interaction as $\bar{w} = wx^2$. Finally, by introducing the interaction variable u of the classical system, eq.5.20 becomes

$$\bar{y}(u) = 1 + \lambda\bar{w}(u)(\frac{d\bar{y}(u)}{du}2u + \bar{y}(u)). \tag{5.24}$$

We can use this equation as a starting point to study the screening from the RPA with the Green's function of the classical system $\chi^{RPA} = x^2(1 - v\chi^{RPA})$. The inverse dielectric function in the RPA can be written as a function of u as

$$\epsilon^{-1}_{RPA}(u) = \frac{1}{1+u}. \tag{5.25}$$

Beyond the RPA, the LRC (eq.4.26) and bootstrap approximations (eq.4.29) to TDDFT read in the OPM (see also eq.5.13 and 5.14)

$$f^{xcLRC}x^2 = au \text{ for the LRC,} \tag{5.26}$$
$$f^{xcBO}x^2 = b \text{ for the bootstrap.} \tag{5.27}$$

Therefore with $\epsilon^{-1} = 1 + v\chi$ the inverse dielectric functions become

$$\epsilon^{-1}_a(u) = \frac{1-au}{1+(1-a)u}, \tag{5.28}$$
$$\epsilon^{-1}_b(u) = \frac{(1-b)}{1-b+u}. \tag{5.29}$$

In the LRC the parameter a scales now the variable u, while b in the bootstrap approximation is a number, which corresponds to screening the independent-particle response function of the classical system with the inverse dielectric function as $\frac{\epsilon^{-1}}{x^2}$. For the model we can also determine the exact f^{xc}. Starting from the definition of the f^{xc} with eq.4.23 and choosing for the RPA

the independent-particle response function from the Green's function of the classical system, the renormalized $F^{xc} = x^2 f^{xc}$ reads

$$F^{xc}(o) = 1 - \frac{x^2}{\chi(z)} + vx^2. \tag{5.30}$$

$\chi = \frac{dy}{dz}$ is evaluated from the derivative of the exact solutions for the cases of $\lambda = 1$ and $\lambda = \frac{1}{2}$ (eq.5.19,5.18). The exact exchange-correlation kernel is evaluated from the exact χ and is a function of the interaction variable $o = vy_0^2$.

Since the transformation 5.23 has two branches, it gives also two different functions $F^{xc\pm}(u)$. Since each function leads in principle to a different solution, this is one case where the problem of multiple solutions shows up. However, in this case of the transformation to u, we will focus on the quality of the solution from the branch of the transformation which is valid for small interaction, and we will study the problem of multiple solutions in a later section with a transformation to a different interaction variable, which also contains the screened interaction.

5.2 Solutions in the linear-response approximation

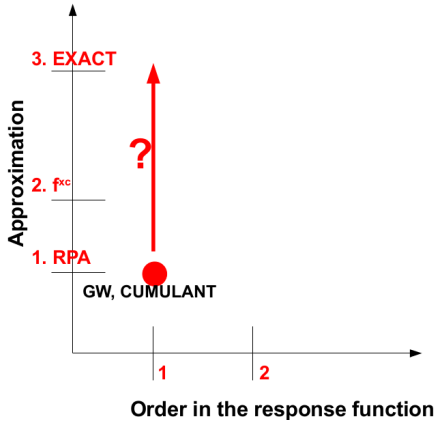

Fig. 5.4: The topic of section 5.2: steps to improve screening in the linear-response approximation.

In the linear-response approximation the screened interaction within approximations (eq.5.12, 5.15, 5.16,5.25,5.28,5.29) is taken in equilibrium, where it is given by merely a number $w_0 = w(z = 0)$ and then eq.5.1 is solved. This is what the GW and the cumulant approximations use. One may look for an improvement of the solution, trying to improve the screened interaction starting from the RPA towards the exact one, within TDDFT. This is the topic of the discussion that follows in this section. This way to go is indicated schematically in fig.5.4.

5.2.1 Solutions from screening in the RPA

In fig.5.5 and 5.6 we plot respectively the solutions of eq.5.1 from the screened interaction in the RPA with the non-interacting Green's function and of eq.5.20 from the screened interaction in the RPA with the Green's function of the classical system, taken in the linear-response approximation.

We compare with the GW approximation with a self-consistent G and a $w(z=0) = v(1-v\chi(z=0))$ with χ evaluated from the exact solutions for each case of $\lambda = 1$ and $\lambda = \frac{1}{2}$. In all cases we see that the solutions satisfy the exact solution in the non-interacting limit.

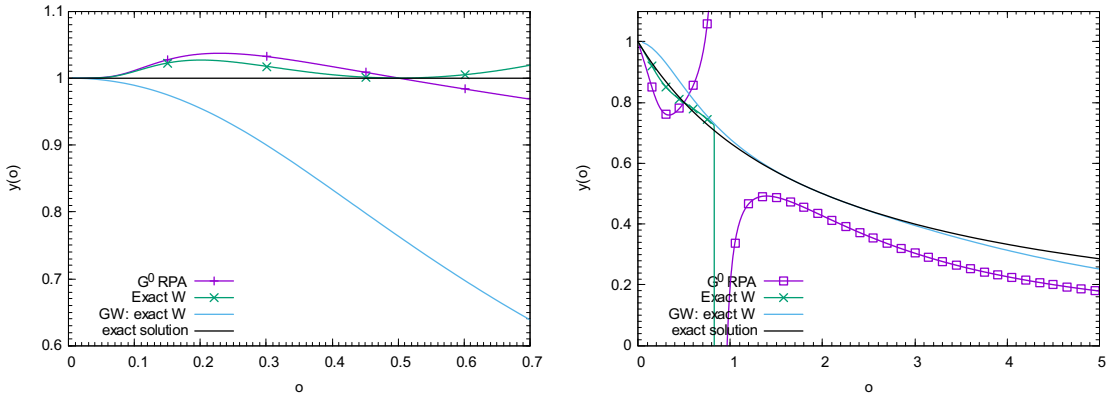

(a) $\lambda = 1$ *(b)* $\lambda = \frac{1}{2}$

Fig. 5.5: Solutions in the linear-response approximation from the RPA $\chi_{RPA} = \frac{y_0^2}{1+vy_0^2}$. Comparison with the solution from the exact W and the GW solution using the exact W.

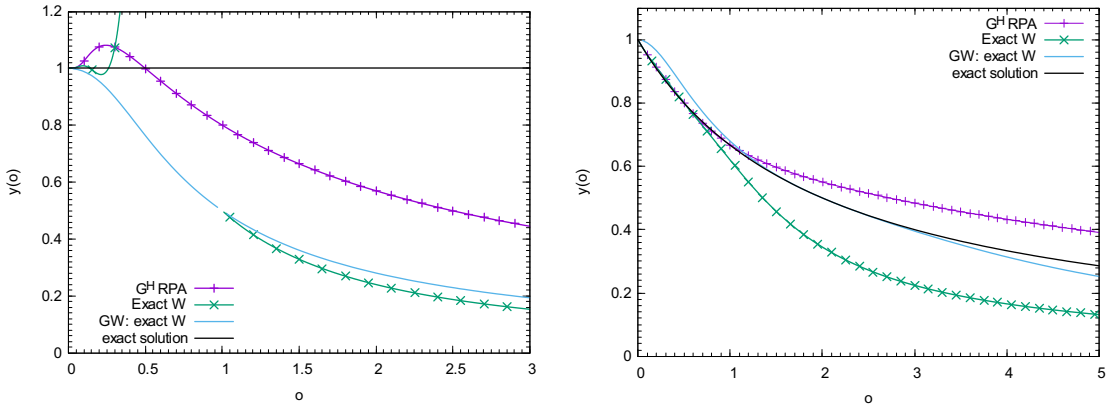

(a) $\lambda = 1$ *(b)* $\lambda = \frac{1}{2}$

Fig. 5.6: Solutions in the linear-response approximation from the RPA $\chi_{RPA} = \frac{x^2}{1+vx^2}$. Comparison with the solution from the exact W and the GW solution using the exact W and the exact solution.

For the case of $\lambda = 1$, for the RPA with the non-interacting propagator (fig.5.5a) all solutions except from the GW one soon diverge to infinity. Therefore we plot a window of values of $o \in [0, 0.7]$. For small values of o the solutions show a behavior which is qualitatively the same as the GW one. For values of $o > 0.1$ the GW solution becomes worse, while the rest of the solutions oscillate around the exact solution. For the RPA with the propagator of the classical system fig.5.6a shows that even though all solutions start soon to deviate from the exact solution, for the RPA solution the deviation is smaller than for the exact w and the GW solutions.

For the case of $\lambda = \frac{1}{2}$ and the RPA with the non-interacting propagator fig.5.5b shows again that all solutions except from the GW deviate for $o > 0.7$ to infinity. Therefore again it is useless to

look at the solutions for $o > 0.7$. The solution from the exact w shows improvement with respect to the RPA. For the RPA with the propagator of the classical system in fig.5.6b we see that all solutions except from the GW are very good for $o < 1$. For values of $o \approx 2$ the GW shows the best behavior being close to the exact solution. *Overall, the way to calculate screening in linear response and the RPA has a dramatic influence on the solution. The GW solution is good for the case of $\lambda = \frac{1}{2}$ in a broad range of values of the interaction variable.*

5.2.2 Solutions from screening beyond the RPA

In fig.5.7 and 5.8 we complement the plots given in fig.5.5 and 5.6, by improving the screened interaction beyond the RPA using the LRC and the bootstrap approximations. The exchange-correlation kernels are determined by the choice of the parameters a and b.

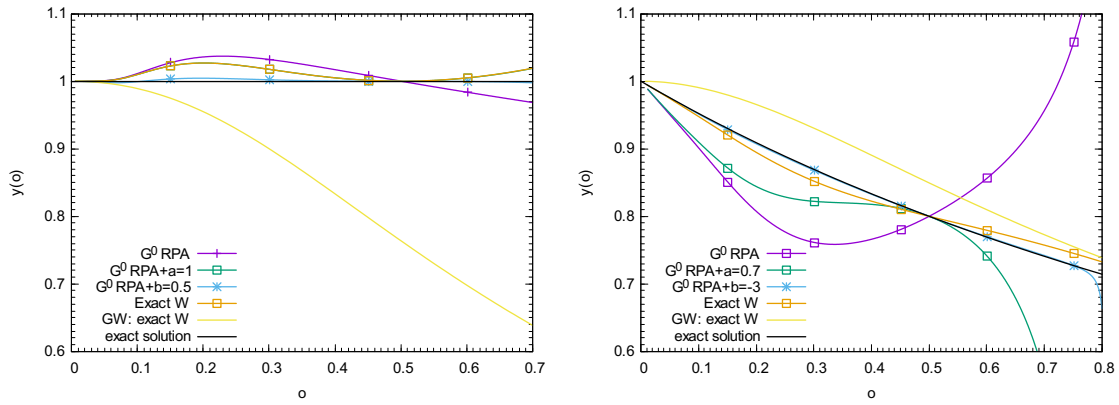

(a) $\lambda = 1$ *(b)* $\lambda = \frac{1}{2}$

Fig. 5.7: Solutions in the linear-response approximation from the RPA $\chi_{RPA} = \frac{y_0^2}{1+vy_0^2}$ and beyond the RPA in the LRC and bootstrap approximations. Comparison with the solution from the exact W and the GW solution using the exact W, and with the exact solution.

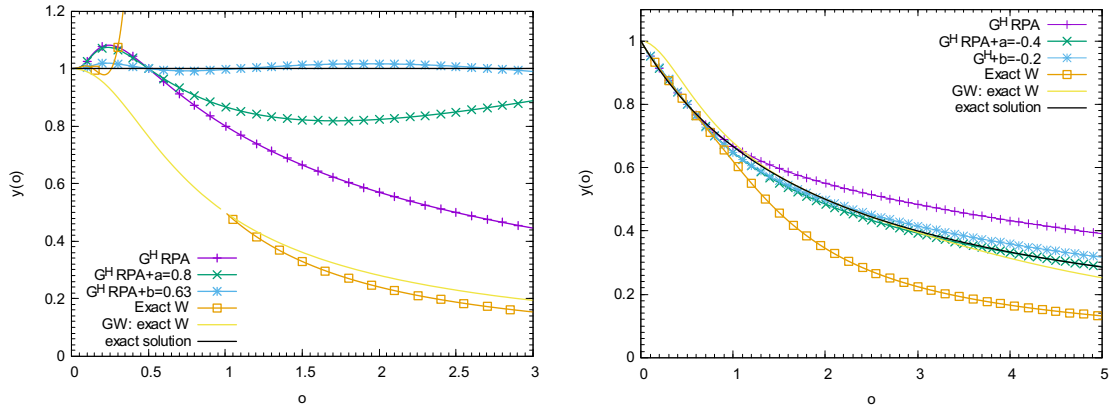

(a) $\lambda = 1$ *(b)* $\lambda = \frac{1}{2}$

Fig. 5.8: Solutions in the linear-response approximation from the RPA $\chi_{RPA} = \frac{x^2}{1+vx^2}$ and beyond the RPA in the LRC and bootstrap approximations. Comparison with the solution from the exact W and the GW solution using the exact W, and with the exact solution.

In this section, we choose the parameters such that the solution is as good as possible. For the case of $\lambda = 1$ we see that for the RPA with the non-interacting Green's function (fig.5.7a) the LRC for $a = 1$ coincides with the exact screening and improves upon the RPA showing smaller deviation from the exact solution. Indeed, for $a = 1$ the LRC contains the exact cancellation of Hartree and exchange effects to the screening. The bootstrap approximation for $b = 0.5$ remains close to the exact solution. For the RPA with the Green's function of the classical system (fig.5.8a) we see that the deviations of the TDDFT solutions are smaller that the exact W and the GW solutions. The LRC for $a = 0.8$ improves upon the RPA, while the bootstrap approximation for $b = 0.63$ remains close to the exact solution even though it shows an oscillatory behavior.

For the case of $\lambda = \frac{1}{2}$ and the RPA with the non-interacting Green's function (fig.5.7b) we see again that the LRC for $a = 0.7$ improves upon the RPA, while the bootstrap approximation for $b = -3$ shows the optimum behavior. For the RPA with the Green's function of the classical system (fig.5.8b) we see that for values of $o > 1$ the bootstrap approximation for $b = -0.2$ improves upon the RPA and the LRC for $a = -0.4$ improves upon the bootstrap.

From the *linear-response approximation* we can draw the following conclusions. *The RPA with the classical Green's function indeed seems more appropriate to describe the case of $\lambda = \frac{1}{2}$, while the RPA with the non-interacting Green's function seems more appropriate to describe the case of $\lambda = 1$. The exact screening in the linear-response approximation doesn't improve much the solution. On the other hand, in most of the cases the parameters a and b of TDDFT can be tuned and improve over the RPA. In the linear-response approximation we need a lot of tuning for the screening to improve the quality of the solution, but without the improvement to be systematic for all the values of the interaction variables. Drawbacks of the linear response solutions are oscillations and divergences that show up.* In the following sections we will try to justify the deficiencies of the linear-response approximation and look for ways to improve it systematically.

5.3 Non-linear effects on screening

In this section we will compare the screening within different approximations. We will make the comparison between the linear-response approximation and non-linear screening, either exact, or in the RPA and the TDDFT approximations, and try to explain which are the the non-linear features that screening within TDDFT needs to reproduce. In eq.4.23 the inverse response function indicates the non-linear effects of the exchange-correlation kernel beyond the RPA. Comparing the inverse response function for different approximations for the f^{xc} and the RPA is a measure of their performance.

5.3.1 Screening in the RPA

Let us first discuss attempts to improve the screening in the RPA beyond the linear-response approximation (direction shown by the arrow in fig.5.9). In fig.5.10b and 5.11 we plot χ^{-1} taken respectively in the RPA with the non-interacting propagator and with the classical propagator,

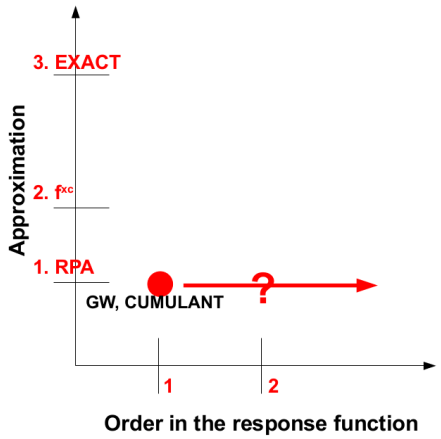

Fig. 5.9: Steps to improve screening beyond the linear-response approximation.

renormalized with the non-interacting Green's function y_0. We display χ^{-1} in the linear-response approximation and beyond, as a function of o. In the linear-response approximation w or χ is in equilibrium and the interaction variable $vy_0^0y_0^0$ appears as a parameter. We compare to non-linear screening in the RPA, which a function of o.

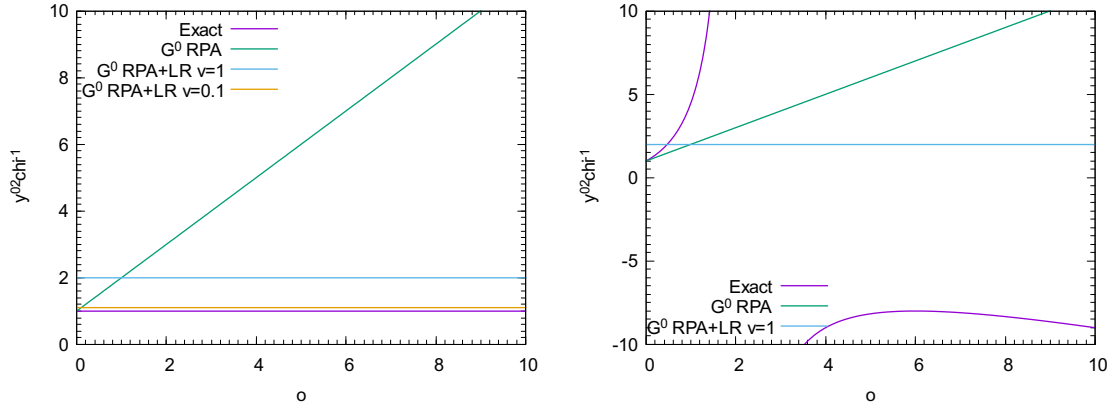

(a) $\lambda = 1$ *(b)* $\lambda = \frac{1}{2}$

Fig. 5.10: Screening $y_0^2\chi^{-1}(o)$ from the RPA with G^0 (i.e. y_0) as a function of the interaction variable. Comparison between the linear-response approximation (LR) and non-linear screening in the RPA.

For the case of the RPA with the non-interacting propagator G^0 (i.e. y_0) and the choice of $\lambda = 1$ (fig.5.10a) we see that the non-linear RPA coincides to the exact screening (eq.5.18) only in the non-interacting limit. In the linear-response approximation, the RPA in the non-interacting limit is equal to the exact screening in the whole range of the interaction variable. Therefore non-linear effects do not emerge for the screening in the case of $\lambda = 1$. In fig.5.10b we see that for the case of $\lambda = \frac{1}{2}$ the exact screening is non-linear and the RPA in the linear-response approximation can only intersect it, whereas beyond the linear-response approximation it is tangent to the exact screening in the non-interacting limit.

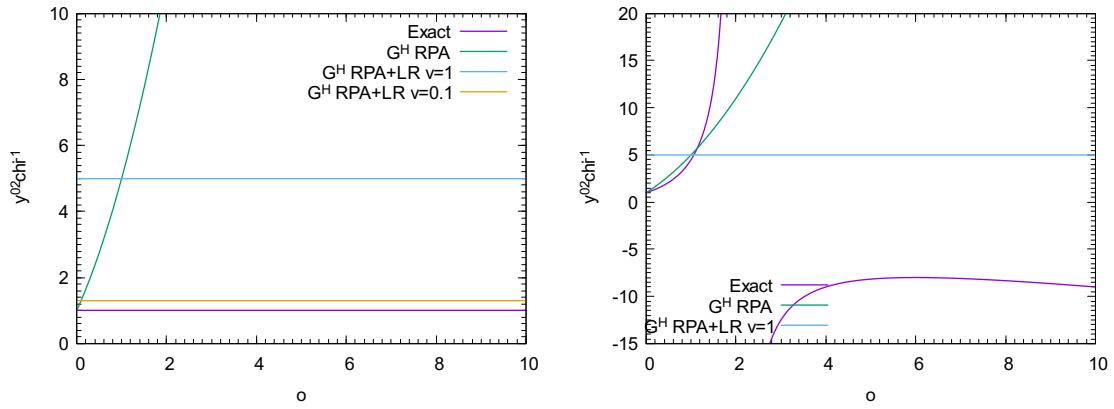

(a) $\lambda = 1$ *(b)* $\lambda = \frac{1}{2}$

Fig. 5.11: Screening $y_0^2\chi^{-1}(o)$ from the RPA with G^H (i.e. x) as a function of the interaction variable. Comparison between the linear-response approximation (LR) and non-linear screening in the RPA.

For the case of $\lambda = 1$ and for the RPA with the classical propagator (fig.5.11a) we see that the non-linear RPA coincides with the exact screening only for vanishing interaction. Again the RPA in the linear-response approximation for vanishing interaction is exact. The parabolic screening given by the RPA seems to capture some of the curvature of the exact screening for the case of $\lambda = \frac{1}{2}$ (fig.5.11b).

5.3.2 Screening beyond the RPA

The last step that we discuss is trying to improve the non-linear screening beyond the RPA and the linear-response approximation (fig.5.12). In fig.5.13b and 5.14 we plot $y_0^2\chi^{-1}$ in the linear-

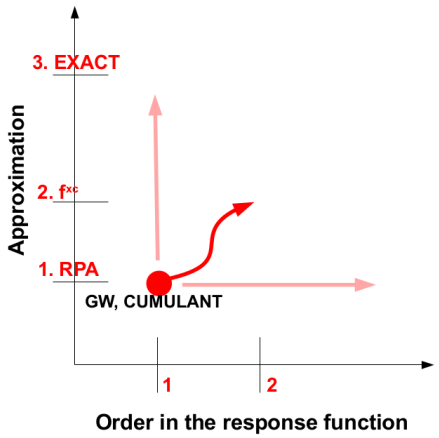

Fig. 5.12: Improving screening beyond the linear-response approximation and the RPA.

response approximation and beyond, correcting also the RPA from TDDFT LRC and bootstrap approximations. We compare between the RPA and the TDDFT approximations in the linear-response approximation and for non-linear screening.

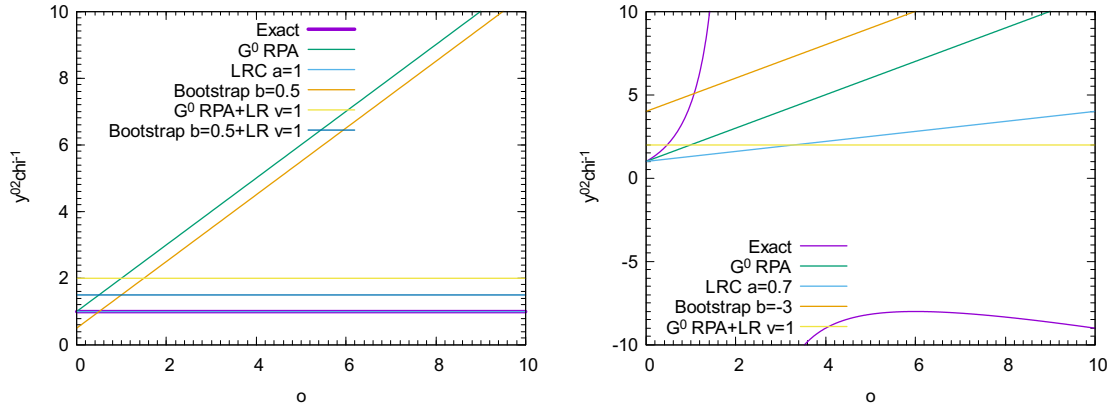

(a) $\lambda = 1$ *(b)* $\lambda = \frac{1}{2}$

Fig. 5.13: Screening $y_0^2\chi^{-1}(o)$ from the RPA with G^0 as a function of the interaction variable and screening within the LRC and bootstrap approximations. Comparison between the linear-response approximation and non-linear screening.

For the case of the RPA with the non-interacting propagator G^0 and the choice of $\lambda = 1$ (fig.5.13a) we see that the LRC with $a = 1$ gives the exact screening as in fig.5.7a. Other approximations coincide with the exact screening only for vanishing interaction. In fig.5.13b we see that for the case of $\lambda = \frac{1}{2}$ the exact screening is non-linear, which cannot be captured by the linear-response approximation (numbers) and the linear behavior given by the LRC and the bootstrap approximations. We note that the bootstrap approximation shifts the RPA, while the LRC rotates it around the origin.

For the case of $\lambda = 1$ the RPA with the classical Green's function (fig.5.14a) satisfies the exact solution only in the non-interacting limit. Parabolic screening given by the LRC and bootstrap approximations, which seems to capture some of the curvature of the exact screening for the case

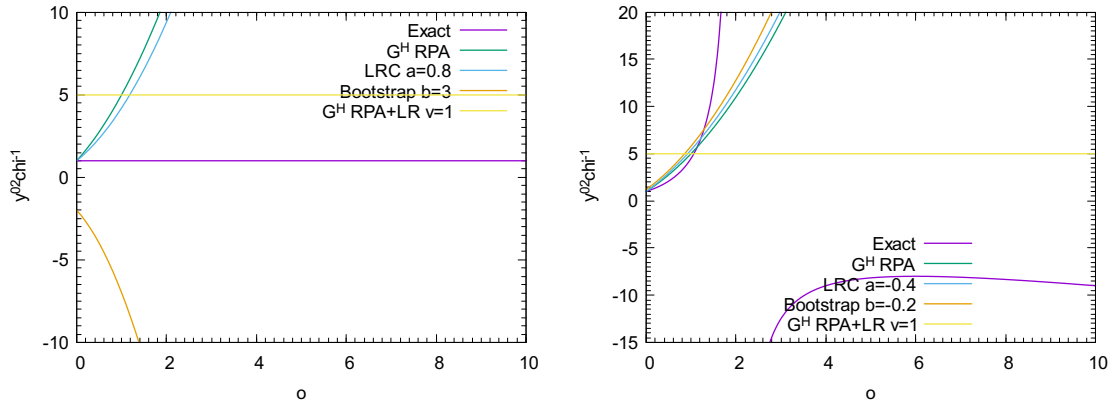

(a) $\lambda = 1$ *(b)* $\lambda = \frac{1}{2}$

Fig. 5.14: Screening $y_0^2\chi^{-1}(o)$ from the RPA with G^H as a function of the interaction variable and screening within the LRC and bootstrap approximations. Comparison between the linear-response approximation and non-linear screening.

of $\lambda = \frac{1}{2}$ (fig.5.14b), requires tuning to values of a and b different from the values found in the linear-response approximation. *Non-linear screening in the RPA with the classical propagator and in TDDFT emerges in the case of* $\lambda = \frac{1}{2}$.

5.3.3 Non-linear screening from perturbation theory in the interaction variable

Up to now, we have tuned the unknown parameters a and b of the LRC and bootstrap kernels. Using eq.5.17 and 5.30 one may profit from the exact screening given by

$$\frac{y_0^2}{\chi} = 1, \tag{5.31}$$

for the case of $\lambda = 1$ and by

$$\frac{y_0^2}{\chi} = \frac{(2+o)^2}{2(2-o)}, \tag{5.32}$$

for the case of $\lambda = \frac{1}{2}$ and derive the expression of the exact f^{xc} or F^{xc} in these cases. Then simple approximations to those can be obtained from expansions in the interaction variables.

For the case of $\lambda = 1$ we obtain

$$f^{xc} y_0^2 = o. \tag{5.33}$$

This justifies the fact that the choice of $a = 1$ in the LRC approximation, where f^{xc} corrects the RPA with the non-interacting Green's function, gives the exact screening. For the case of $\lambda = 1$ the exact F^{xc} is given by

$$F^{xc} = 1 - \frac{x^2}{y_0^2} + vx^2. \tag{5.34}$$

In order to expand this in terms of the interaction variable u we apply the transformation 5.23. This transformation gives an F^{xc} with two branches from which we distinguish the branch that is exact in the non-interacting limit, which is the one with the " $-$ " sign,

$$F^{xc}(u) = \frac{1}{2} + 2u - \frac{\sqrt{1-4u}}{2}. \tag{5.35}$$

For the moment we will only work with this branch, which is exact for small values of the interaction variable. The expansion in orders of u gives

$$F^{xc}(u) \approx 3u. \tag{5.36}$$

This corresponds to correcting the RPA with the Green's function of the classical system in the LRC approximation choosing $a = 3$.

For the case of $\lambda = \frac{1}{2}$ the f^{xc} is given by

$$f^{xc} y_0^2 = 1 - \frac{1}{2}\frac{(2+o)^2}{2-o} + o. \tag{5.37}$$

The lowest order of the expansion in o gives

$$f^{xc} y_0^2 \approx -\frac{o}{2}. \tag{5.38}$$

This corresponds to the choice of $a = -\frac{1}{2}$ for the LRC approximation, which corrects the RPA with the Green's function of the non-interacting system. The physical branch of $F^{xc}(u)$ is given by

$$F^{xc}(u) = 1 - \frac{(2 + o^-(u))^2}{2(1 + o^-(u))^2(2 - o^-(u))} + u. \tag{5.39}$$

The last can be rewritten as

$$\begin{aligned} F^{xc}(u) &= 1 - u\frac{(2 + o^-(u))^2}{2o^-(u)(2 - o^-(u))} + u = 1 - u\frac{4 + 3o^{-2}(u)}{4o^-(u) - 2o^{-2}(u)} \\ &= 1 - u(-\frac{3}{2} + \frac{1}{o^-(u)} + \frac{4}{2 - o^-(u)}) \\ &= 1 + u\frac{3}{2} + \frac{1}{2}(2u - 1 - \sqrt{1 - 4u}) - 4u\frac{8u - 1 - \sqrt{1 - 4u}}{32u - 6}. \end{aligned} \tag{5.40}$$

The lowest order of the expansion of $F^{xc}(u)$ in u are given by

$$F^{xc}(u) \approx 1 + \frac{3u}{2} - 1 + 2u + \frac{4u}{3} \approx 2u + \frac{3u}{2} + \frac{4u}{3}, \tag{5.41}$$

which corresponds to the choice of $a = 2 + \frac{3}{2} + \frac{4}{3}$ for the LRC approximation, which corrects the RPA with the Green's function of the classical system.

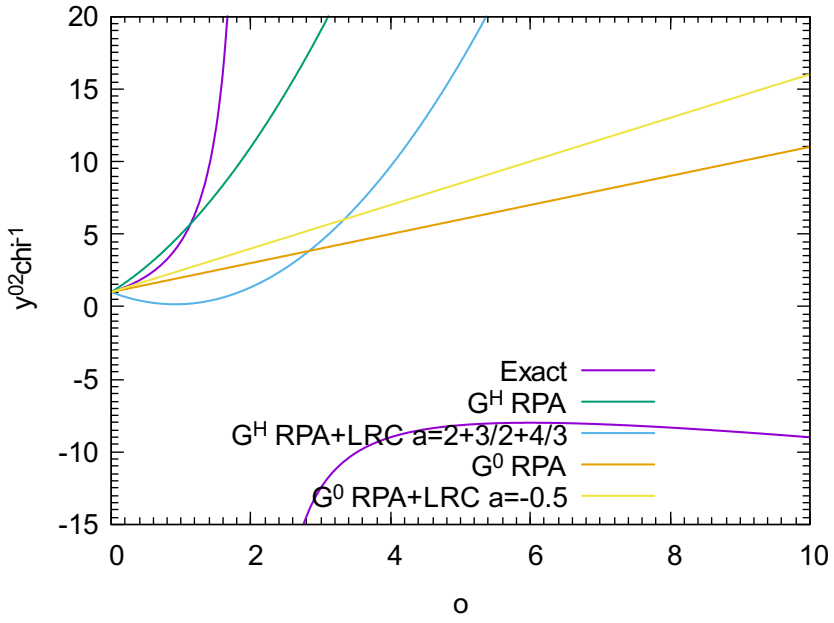

Fig. 5.15: Screening $y_0^2\chi^{-1}$ from expansions in o and u for the case of $\lambda = \frac{1}{2}$. Comparison with the RPA and the exact screening.

For the case of $\lambda = 1$ the choice of $a = 1$ gives the exact screening, which can also be taken in the linear-response approximation. Other choices cannot improve the quality of the solution. Therefore it is meaningful to look for improvements from perturbation theory only for the case of $\lambda = \frac{1}{2}$. In fig.5.15 we plot for the case of $\lambda = \frac{1}{2}$ the response function $y_0\chi^{-1}$ obtained with the

λ	RPA	Expansion	a
1	G^0	o	1
1	G^H	u	3
$\frac{1}{2}$	G^0	o	$-\frac{1}{2}$
$\frac{1}{2}$	G^H	u	$2+\frac{3}{2}+\frac{4}{3}$

Tab. 5.1: The values of a and b found from expansions (eq.5.33, 5.36, 5.38, 5.41).

values of a from perturbative expansions in o and in u. We find that the correction with respect to the RPA with the non-interacting Green's function can only give a linear curve, which in the best case is tangent to the exact one at $o = 0$ ($a = -0.5$). On the other hand corrections with respect to the RPA with the Green's function of the classical system give parabolic screening, which obtained from an expansion in u, merely shifts the parabola and passes from $o = 0$ ($a = 2 + \frac{3}{2} + \frac{4}{3}$). *As we can see, it is extremely difficult to model non-linear screening using simple corrections to the RPA. This is a problem, since in real systems it will certainly be impossible to introduce more complex expressions. The hope is that even quite poor approximations to non-linear screening, when used in the KBE might lead to reasonable Green's functions. This will be explored in the next section.*

5.4 Solutions from non-linear screening in the RPA

In this section we solve eq.5.11 and 5.24 with non-linear screening calculated in the RPA with the non-interacting propagator and with the propagator of the classical system, respectively. We use the RPA as a starting point to specify the particular solution which satisfies the non-interacting limit and deviates less from the exact solution.

5.4.1 Solutions from the RPA with the non-interacting propagator

The general solution of eq.5.11 is given by the expression

$$\tilde{y}(o) = \frac{M(c)}{M(o)}(\tilde{y}(c) + \frac{1}{D(c)}) - \frac{1}{D(o)} - \frac{1}{M(o)} \int_c^o d\tau M(\tau) \frac{D'(\tau)}{D(\tau)^2} \tag{5.42}$$

with $M(o)$ and $D(\tau)$ functions that depend on the choice of the screening. For screening in the RPA with the non-interacting Green's function (eq.5.12) $M(o)$ and $D(o)$ are given by

$$M(o) = e^{\frac{o^2}{4\lambda} + \frac{1}{2\lambda o} + \frac{o}{2\lambda}} \tag{5.43}$$

and

$$D(o) = -(1+o) + \frac{\lambda o}{1-o^2} o^{\frac{1}{2} - \frac{1}{2\lambda}}. \tag{5.44}$$

Here, λ appears as a parameter. The fact that we solve a differential equation is another source of multiple solutions. Eq.5.42 corresponds to a family of solutions, from which we need to extract the physical ones. Particular solutions are taken by fixing the value of the solution to $\tilde{y}(c)$ at a point c. Here one needs to choose the point c, and $\tilde{y}(c)$ should be in principle the value of the exact solution at that point. In the OPM we can profit from the fact that we know the exact solution for the cases of $\lambda = 1$ and $\lambda = \frac{1}{2}$. In general this will not be the case. One might then try to fix particular solutions to approximate solutions obtained from perturbative expansions in low orders in the interaction. We have not explored this possibility here, but always used the exact solution $\tilde{y}(c)$.

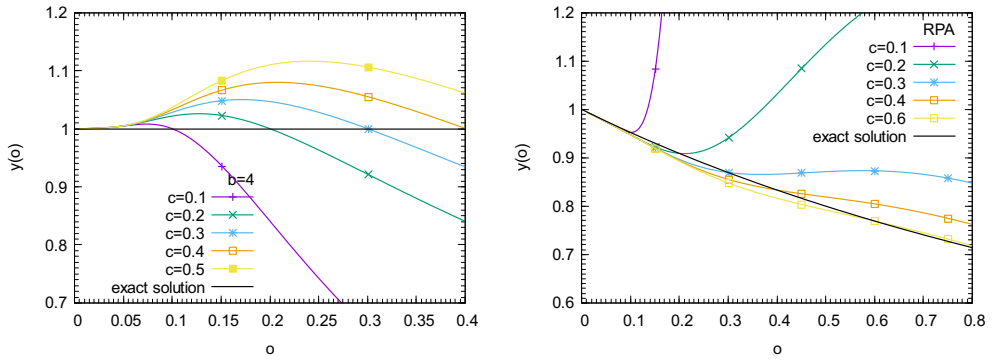

(a) $\lambda = 1$ *(b)* $\lambda = \frac{1}{2}$

Fig. 5.16: Solutions to the KBE using non-linear screening in the RPA with the non-interacting Green's function, for different values of c.

In fig.5.16a we plot the Green's function obtained using non-linear RPA screening and fixing the solution to the exact solution at different values of c for the case of $\lambda = 1$ for the values of $o \in [0, 0.7]$. We show this window because for higher values the solution diverges. All solutions satisfy the non-interacting limit, but fixing the solution at higher values deviations from the exact solution are larger. For this reason we choose the value of $c = 0.2$ to be used in sec.5.5.

In fig.5.16b we plot the solution for the case of $\lambda = \frac{1}{2}$. We show a window $o \in [0, 0.8]$, because for higher values the solutions diverge. The solution fixed to the exact solution for larger values seems to remain closer to the exact solution for an extended range of o.

5.4.2 Solutions from the RPA with the propagator of the classical system

For screening in the RPA with the Green's function of the classical system, the general solution of eq.5.24 has the form of eq.5.42 with the functions D and M given by

$$M(u) = u^{\frac{1}{2}-\frac{1}{2\lambda}} e^{\frac{1}{2\lambda u}} \tag{5.45}$$

$$D(u) = -1 + \frac{\lambda u}{1+u}. \tag{5.46}$$

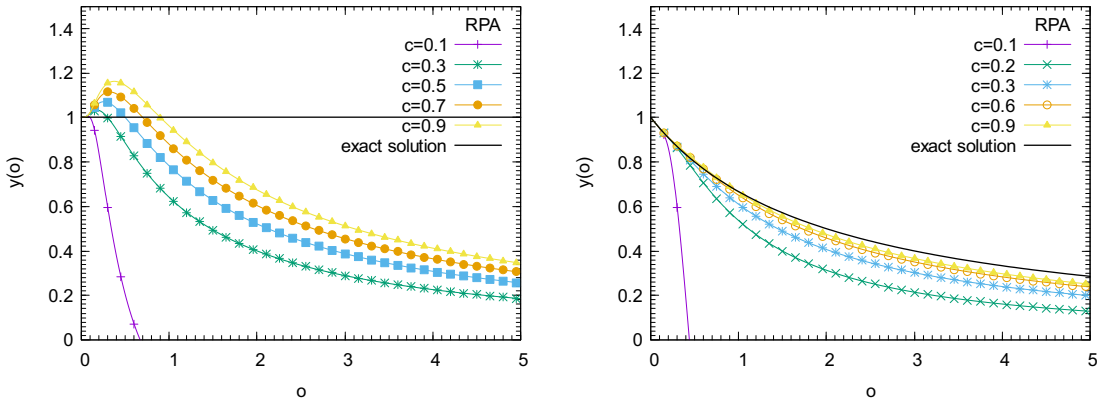

(a) $\lambda = 1$ *(b)* $\lambda = \frac{1}{2}$

Fig. 5.17: Solutions to the KBE using non-linear screening from the RPA with the propagator of the classical system, fixed to the exact solution at different values of c.

For the case of $\lambda = 1$ in fig.5.17a we plot the solution of the KBE obtained using the RPA with the Green's function of the classical system by fixing the solution to the exact solution at different values of c. Varying c doesn't improve the quality of the solution as an oscillatory behavior always shows up.

In fig.5.17b we fix the solution to the exact solution at different values of c for the *case of* $\lambda = \frac{1}{2}$. *This solution satisfies the non-interacting limit and the deviation with respect to the exact solution is small and becomes smaller the larger is the value of* c *that we choose. This is one case where the RPA performs well, and we can improve the quality of the solution without modifying the approximation, but by merely fixing the solution to the exact solution for larger values of the interaction variable.*

5.5 Solutions from non-linear screening beyond the RPA

In this section we solve eq.5.11 and 5.24 with non-linear screening beyond the RPA within the TDDFT LRC and bootstrap approximations, choosing appropriately the parameters a and b.

5.5.1 Solutions from screening beyond the RPA with the non-interacting propagator

The general solution of eq.5.11 given by eq.5.42 is evaluated from tab.5.2 for the three choices of $\tilde{w}$, correcting the RPA with the non-interacting Green's function (eq.5.12) with the LRC (eq.5.15) and the bootstrap approximations (eq.5.16). λ appears as a parameter.

In fig.5.18 we plot the solutions obtained by correcting the RPA with the non-interacting Green's function with the bootstrap approximation for the cases of $\lambda = 1$ and $\lambda = \frac{1}{2}$. We have fixed the values for c from the RPA solutions in sec.5.4. In fig.5.18a we plot the particular solutions in the

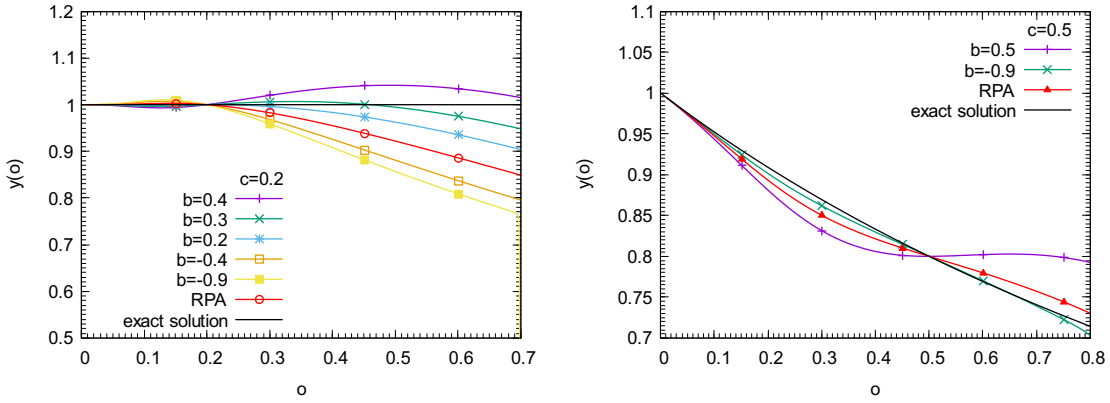

(a) $\lambda = 1$ and $c = 0.2$. *(b)* $\lambda = \frac{1}{2}$ and $c = 0.5$.

Fig. 5.18: Solutions of eq.5.11 correcting the RPA with the non-interacting Green's function with the bootstrap approximation varying b.

bootstrap approximation fixed to the exact solution for the case of $\lambda = 1$ at $c = 0.2$ for values of $b \in [-0.9, 0.5]$ and in the window $o \in [0 : 0.7]$. We see that the choice of $b = 0.3$ seems to deviate less from the exact solution, which is different from the choice of $b = 0.5$ that we had made for the linear-response approximation. In fig.5.18b we plot the solutions in the bootstrap approximation fixed at $c = 0.5$ to the exact solution for the case of $\lambda = \frac{1}{2}$ for different choices of $b \in [-0.9, 0.5]$. All solutions satisfy the non-interacting limit. We see that for the negative values of b in our range the solutions remain closer to the exact solution.

For the solution in the bootstrap approximation we have used the RPA to fix the solution and then varied b, since for the choice of $b = 0$ the bootstrap approximation gives the RPA. This is not the case for the LRC, since it doesn't take the value $a = 0$. In this case we need to fix the solution for an arbitrary choice of a. We do this for the case of $\lambda = 1$ in fig.5.19a and for the case of $\lambda = \frac{1}{2}$ in fig.5.19b. For the case of $\lambda = 1$ we used $a = 1.1$ since for $a = 1$ we recover the exact solution independent of the choice of c. For the case of $\lambda = \frac{1}{2}$ we used $a = 1$. We see that in all cases the solutions satisfy the exact solution in the non-interacting limit. From both figures we choose $c = 0.5$ since the solution remains close enough to the exact solution and in a large enough interval.

a	b	M(o)	D(o)
a	0	$o^{\frac{1}{2}-\frac{1}{2\lambda}}(1-ao)^{\frac{1}{2\lambda a}(a-\frac{1}{a})}e^{\frac{o}{2\lambda}(1-\frac{1}{a})+\frac{1}{2\lambda o}}$	$-1-o+\lambda o\frac{1-ao}{(1-o)(1+(1-a)o)}$
0	b	$e^{\frac{1}{2\lambda o}+\frac{o}{2\lambda}+\frac{o^2}{4\lambda(1-b)}}o^{\frac{1}{2}-\frac{1}{2\lambda(1-b)}}$	$-1-o+\frac{\lambda o(1-b)}{(1-o)(1-b+o)}$

Tab. 5.2: The solution of eq.5.11 for the RPA with the non-interacting Green's function for different choices of screening.

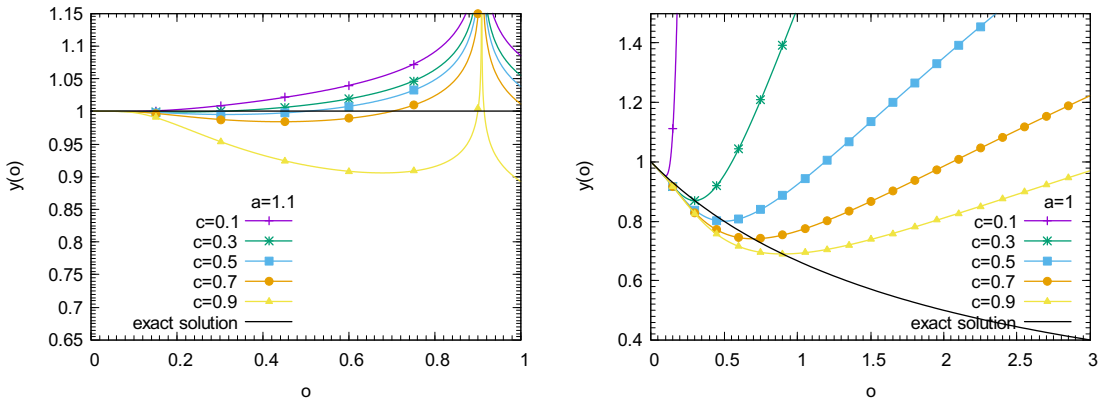

(a) $\lambda = 1$. *(b)* $\lambda = \frac{1}{2}$.

Fig. 5.19: Solutions from the LRC varying c, while $a = 1$ is fixed.

In fig.5.20a we plot the solution for the LRC varying a. We see that for $a = 1$ we obtain the exact solution, because it cancels exactly the Coulomb interaction in the RPA and gives the non-interacting solution. For the case of $\lambda = \frac{1}{2}$ in fig.5.20b we see that the choice of negative values for a improves the quality of the solution but it still deviates from the exact solution. This suggests that using the RPA with the non-interacting Green's function as a starting point is an appropriate choice in order to study the case of $\lambda = 1$. Different choices of a and b give merely shifts or change the slope of the plots in fig.5.14b and cannot reproduce the curvature of the exact screening.

5.5.2 Solutions obtained from non-linear screening beyond the RPA with the classical propagator

Finally, for the case of screening in the RPA with the classical propagator the general solution of eq.5.24 is given by eq.5.42 with the functions D and M given in tab.5.3.

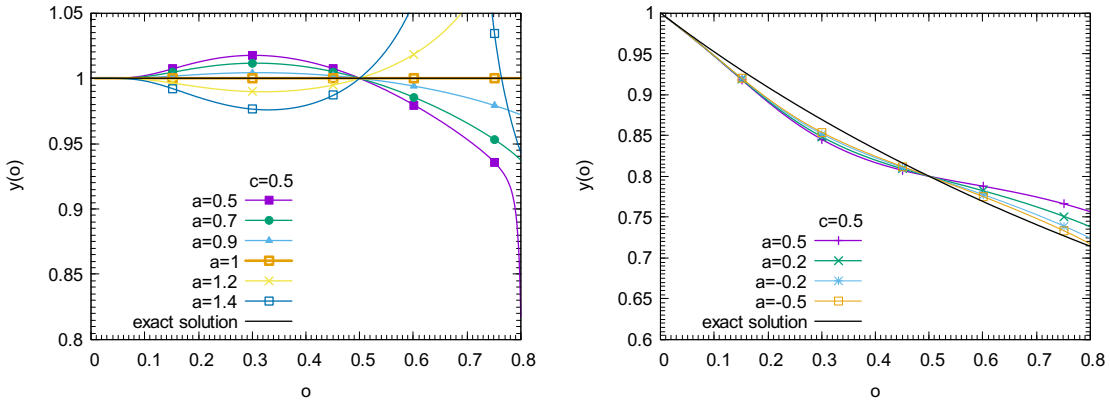

(a) $\lambda = 1$. *(b)* $\lambda = \frac{1}{2}$.

Fig. 5.20: Solutions from the LRC varying a, while $c = 0.5$ is fixed.

a	b	M(u)	D(u)
a	0	$u^{\frac{1}{2}-\frac{1}{2\lambda}}(1-au)^{\frac{1}{2\lambda}}e^{\frac{1}{2\lambda u}}$	$-1+\frac{\lambda u(1-au)}{1+(1-a)u}$
0	b	$u^{\frac{1}{2}-\frac{1}{2\lambda(1-b)}}e^{\frac{1}{2\lambda u}}$	$-1+\frac{\lambda u(1-b)}{1-b+u}$

Tab. 5.3: The solution of eq.5.24 for the RPA with the non-interacting propagator for different choices of screening.

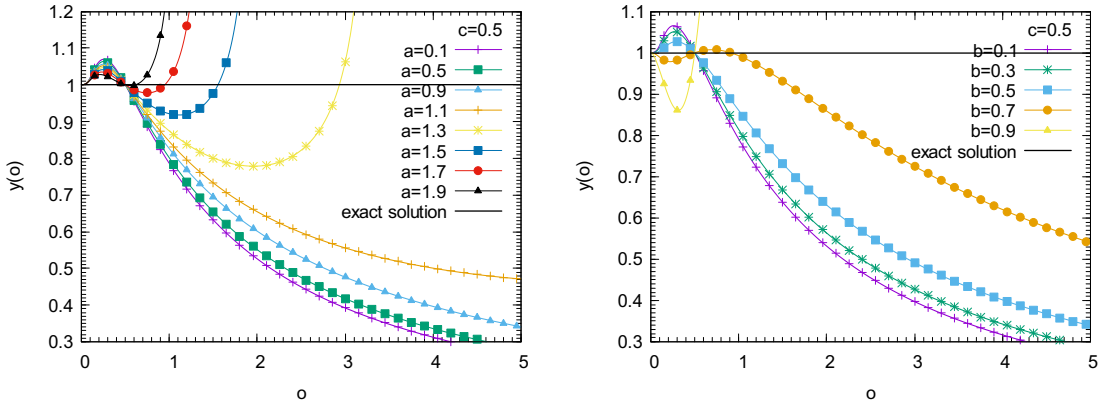

(a) Varying a. *(b)* Varying b.

Fig. 5.21: For the case of $\lambda = 1$ solutions from the LRC and the bootstrap approximation upon the RPA fixed at $c = 0.5$.

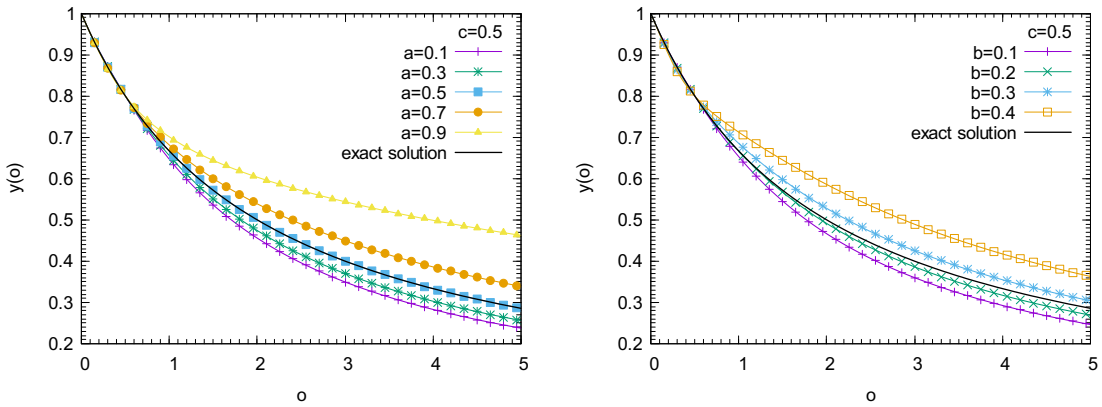

(a) Varying a. *(b)* Varying b.

Fig. 5.22: For the case of $\lambda = \frac{1}{2}$ the solution from the LRC and the bootstrap approximation upon the RPA fixed at $c = 0.5$.

In fig.5.21 and 5.22 we plot the solutions of the KBE obtained using the RPA screening with the classical Green's function corrected with the bootstrap and LRC approximations for the cases of $\lambda = 1$ and $\lambda = \frac{1}{2}$. The values for c are chosen from the RPA solutions. For the case of $\lambda = 1$ in fig.5.21a we take the solution fixed to the exact solution at $c = 0.5$ and vary the value of the

parameter a. We cannot find an argument to choose a value of a that improves the quality of the solution due to the oscillatory behavior around the exact solution. In fig.5.21b we vary the value of b and we see that the choice of $b = 0.7$ seems to improve the quality of the solution.

For the case of $\lambda = \frac{1}{2}$ *in fig.5.22a* we plot the LRC approximation varying a. Increasing the value of a the deviation from the exact solution increases. *The choice of* $a = 0.5$ *seems to be the most appropriate.* In fig.5.22b we plot the bootstrap approximation varying b. All solutions satisfy the non-interacting limit and the deviation from the exact solution increases with increasing value of b. *The choice of* $b = 0.2$ *seems appropriate.*

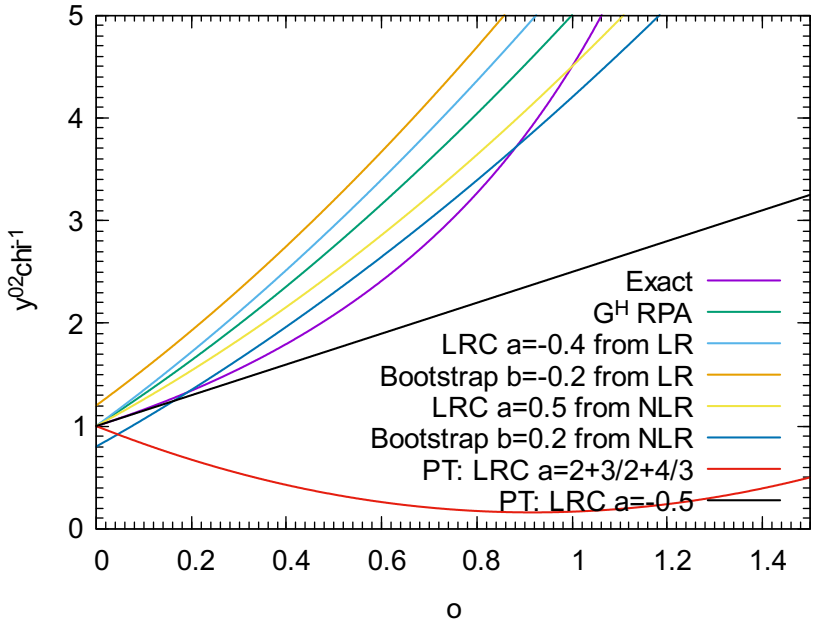

Fig. 5.23: Screening from $y_0^{-1}\chi$ as a function of o. Comparison between non-linear screening for the choices of a and b as were found in the linear-response approximation and those estimated from fig.5.21a,5.21b.

In fig.5.23 we compare the screening with values for a and b obtained from fitting in the linear-response approximation (LR), fitting beyond the linear-response approximation (NLR) and from perturbation theory. Compared to the linear-response approximation ($a = -0.4$ and $b = -0.2$), the choices of $a = 0.5$ and $b = 0.2$ improve screening making it closer to the exact screening for small values of o. On the other hand perturbation theory (PT) fails to improve the screening obtained from fitting. The fact that the values of of a and b fitted beyond the linear-response approximation improve the screening in fig.5.23 is a nice illustration of the fact that the solution of the differential equation at a given value of o depends on the screening at all values of o.

5.6 Transformation to the screened interaction variable

The transformation 5.22 in sec.5.1 has raised the problem of multiple solutions and domains. Here, we explore this problem further, by introducing the screened interaction in the transformation. This will not be useful for practical purposes, but it is interesting, because the GW approximation can be seen as stemming from a functional of the interacting Green's function and the screened interaction.

In analogy to eq.5.11 and 5.24, where we introduced the interaction variables $o = vy_0^2$ and $u = vx^2$, we can also write the system of the two equations (eq.5.20, eq.5.21) using an interaction variable where the screened interaction appears $Q(w, x) = wx^2$. Similar to the case of u this is a non-linear transformation, made of the propagator of the classical system and the screened interaction. In this non-linear transformation we will focus on the multiplicity of the functionals of the interaction variable. Similar to u we have to renormalize $\tilde{y}(x, v) = \frac{y(x,v)}{x}$. The non-interacting limit corresponds to values of $Q = 0$ and the equilibrium limit to values $Q_0 = w_0 x_0^2$, with $x_0 = x(z = 0)$. In App.C we introduce exchange and correlation effects through TDDFT and we show the derivation of a differential equation $\tilde{y}(Q, F^{xc}(Q))$ (eq.C.17) or equivalently of a set of two complementary equations $\tilde{y}(Q, P)$(eq.C.6) and $P(Q, F^{xc}(x; v))$ (eq.C.13). TDDFT is introduced with F^{xc}. In order to be able to obtain a differential equation in terms of Q, we need to write $F^{xc}(Q)$ as a pure function of Q. We can derive the transformation $Q(o)$ using the "total classical" potential of eq.5.9. A complement of this chapter can be found in App.E.

5.6.1 Derivation of the transformation from the non-interacting density

In this section we will derive the transformation between the interaction variable o and Q. For this purpose we need not only the classical potential as a function of o, but also the screened interaction. We obtain both from the "total classical" potential of eq.5.9 as

$$\frac{x}{y_0} = \frac{1}{1+o}, \tag{5.47}$$

$$\frac{w}{v} = 1 - o. \tag{5.48}$$

Then $Q(o) = wx^2$ is given by

$$Q(o) = o\frac{1-o}{(1+o)^2}. \tag{5.49}$$

This is a non-linear transformation given by a quadratic equation. There is not '1-1' correspondence between o and Q, since a value of Q corresponds in two values of o. For example $Q = 0$ corresponds to $o = 0$ and $o = 1$, where $o = 0$ is the non-interacting value, while $o = 1$ is the value where the screened interaction vanishes and the solution intersects the classical propagator. Inverting the transformation we obtain two functions of Q,

$$o^{\pm}(Q) = \frac{1}{2}\frac{(1 \pm \sqrt{1-8Q})^2}{4Q + 1 \pm \sqrt{1-8Q}}. \tag{5.50}$$

We need to constrain the domain of definition for o^+ and o^- so that they give the exact solution and therefore specify the physical transformation. First of all o is a real variable. Therefore the

square root in eq.5.50 is real for $Q \leq \frac{1}{8}$. The value of $Q = \frac{1}{8}$ corresponds to $o = \frac{1}{3}$ and is the point where the physical transformation changes branch. In order to find the physical domain we expand the square root around $Q = 0$ and then we take the non-interacting limit $Q \to 0$

$$\lim_{Q\to 0} o^+(Q) = \lim_{Q\to 0} \frac{(1-2Q-4Q^2)^2}{1-4Q^2} = 1, \tag{5.51}$$

$$\lim_{Q\to 0} o^-(Q) = \lim_{Q\to 0} 2Q\frac{(1+2Q)^2}{1+Q} = 0. \tag{5.52}$$

The branch $o^+(Q)$ for vanishing Q takes the value $o^+(Q=0) = 1$, which belongs to the domain $o \in [\frac{1}{3}, +\infty]$ that does not contain the non-interacting value. The branch $o^-(Q=0) = 0$ belongs to the domain $o \in [0, \frac{1}{3}]$ which is the physical domain since it contains the non-interacting value. In fig.5.24a I show $o^+(o)$ and $o^-(o)$. The result shows that the physical transformation, where $o^\pm(o) = o$ is given by o^- for vanishing interaction, while it changes branch at $o = \frac{1}{3}$ and for higher values of o, $o^+(Q)$ is physical. In fig.5.24b we plot $Q(o)$ and we identify that for $Q \in [0, \frac{1}{8}]$ both o^+ and o^- take values, while for $Q \in [-\infty, 0]$ only o^+ takes values. We summarize the domain of validity of each transformation as

$$o(Q) = \begin{cases} o^-(Q) & o < \frac{1}{3} \quad 0 < Q < \frac{1}{8} \\ o^+(Q) & o > \frac{1}{3} \quad Q < \frac{1}{8} \end{cases} . \tag{5.53}$$

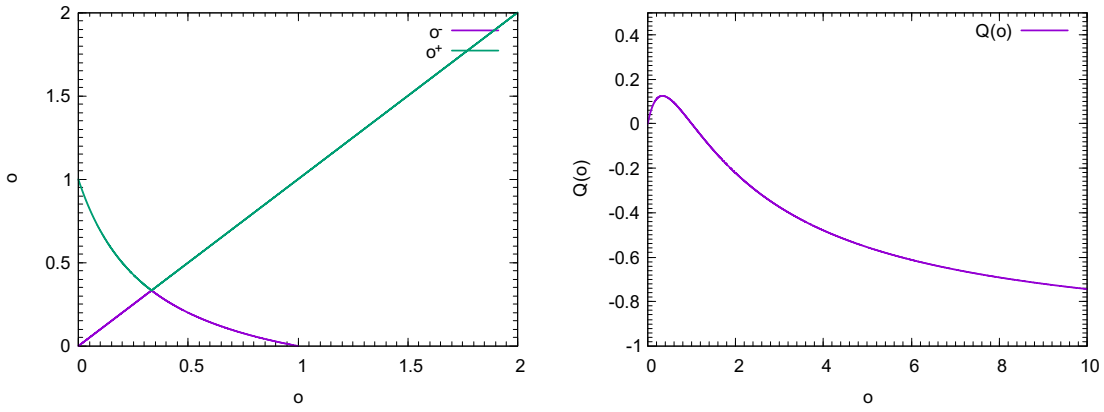

(a) $o^\pm(o)$ (eq.5.50). *(b)* $Q(o)$ (eq.5.49) as a function of o.

Fig. 5.24: The transformation $o(Q)$.

5.6.2 Application of the transformation $o(Q)$ to the exact solution for the case of $\lambda = 1$

We start from the transformation of eq.5.50. There we set the new variable

$$t^\pm = 1 \pm \sqrt{1-8Q}. \tag{5.54}$$

and obtain that

$$o^\pm = \frac{t^\pm}{4-t^\pm}. \tag{5.55}$$

The exact solution for the case of $\lambda = 1$ becomes

$$\tilde{y}(o) = 1 + o = -\frac{4}{t-4}, \tag{5.56}$$

where t has two branches. For $Q = 0$, $t^- = 0$, while $t^+ = 2$. For $t^- = 0$ the solution becomes $\tilde{y}(t^- = 0) = 1$. Therefore the branch with the "-" sign satisfies the non-interacting limit and gives the physical solution in the domain $o \in [0, \frac{1}{3}]$. The branch with the "+" sign will give the physical solution in the domain $o \in [\frac{1}{3}, +\infty]$. Using eq.5.54 we write the solution as a function of Q

$$\tilde{y}(Q) = \begin{cases} \tilde{y}^-(Q) = -\frac{4}{-3-\sqrt{1-8Q}} & o < \frac{1}{3} \quad 0 < Q < \frac{1}{8} \\ \tilde{y}^+(Q) = -\frac{4}{-3+\sqrt{1-8Q}} & o > \frac{1}{3} \quad Q < \frac{1}{8} \end{cases}, \tag{5.57}$$

which has two branches in analogy to eq.5.53.

In fig.5.25 we plot the exact solution $\tilde{y}^{\pm}(o)$ as a function of the interaction variable o. There $\tilde{y}^-$ gives the exact solution for $o < \frac{1}{3}$, while $\tilde{y}^+$ gives the exact solution for $o > \frac{1}{3}$. This means that if we stick to a transformation, the solution will not be equal to the exact solution for $o > \frac{1}{3}$. In other words the solution that satisfies the non-interacting limit might not be the physical solution in the whole range of values of the domain of its definition. Therefore one needs to restrict the domain of the definition for each solution and look for ways to find its complementary solutions.

5.6.3 $F^{xc}(Q)$ for the case of $\lambda = 1$

For the case of $\lambda = 1$ the effective interaction $f^{xc} = v$ is equal to the bare Coulomb interaction when evaluated from y_0 the exact solution. F^{xc} is given by eq.5.30 and from the exact solution for the case of $\lambda = 1$ as

$$F^{xc}(o) = 1 - \frac{1-o}{(1+o)^2}. \tag{5.58}$$

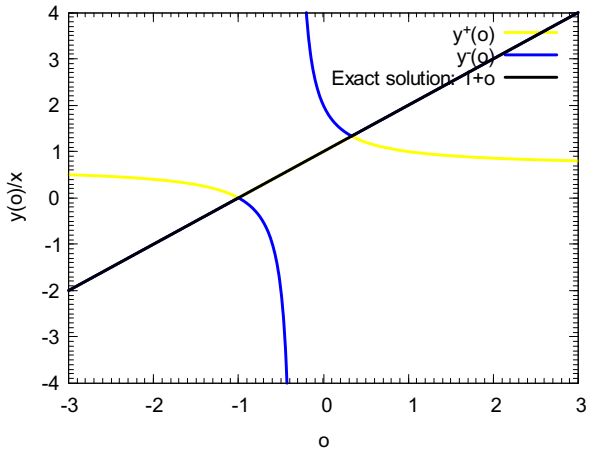

Fig. 5.25: The exact solution $\tilde{y}(o) = 1 + o$ for the case of $\lambda = 1$ and the two branches $\tilde{y}^{\pm}(o)$ from eq.5.57.

Applying the transformation given by eq.5.50, we obtain

$$F^{xc}(Q) = \begin{cases} F^{xc-}(Q) = 1 - \frac{(4Q+1-\sqrt{1-8Q})^2}{4(1-\sqrt{1-8Q})^2} + \frac{4Q+1-\sqrt{1-8Q}}{8} & o < \frac{1}{3} \quad 0 < Q < \frac{1}{8} \\ F^{xc+}(Q) = 1 - \frac{(4Q+1+\sqrt{1-8Q})^2}{4(1+\sqrt{1-8Q})^2} + \frac{4Q+1+\sqrt{1-8Q}}{8} & o > \frac{1}{3} \quad Q < \frac{1}{8} \end{cases}, \tag{5.59}$$

which again has two branches. In fig.5.26 we plot $F^{xc}(o)$ as a function of o. There F^{xc-} gives the exact F^{xc} (eq.5.58) for $o < \frac{1}{3}$, while F^{xc+} gives the exact F^{xc} for $o > \frac{1}{3}$. Since in TDDFT the solution that we obtain depends on the choice we make for the F^{xc} in the screening, the exact solution will be given by the branch of F^{xc}, which is exact in each domain. This also means that fitting each branch of F^{xc} with a function, each function alone will not be able to reproduce the exact solution in the whole domain of its definition. Therefore, in order to build approximations for TDDFT, one needs to combine different functions and restrict the domain of definition for each one of them.

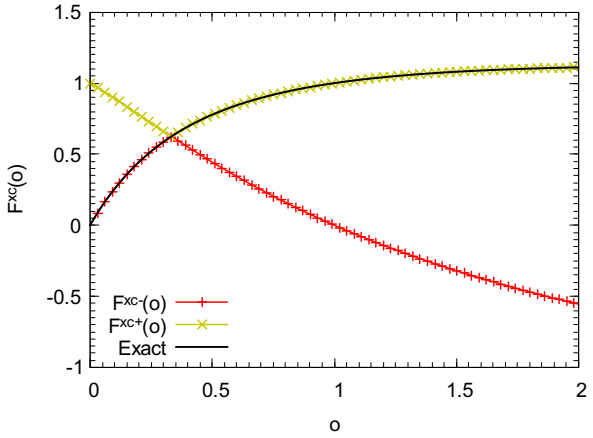

Fig. 5.26: Comparison between the exact $F^{xc}(o)$ (eq.5.58) and $F^{xc\pm}(o)$ (eq.5.59).

Instead of fitting F^{xc} with a function, one may look for ways to expand F^{xc}. Here we will first look at an expansion for small values of Q, where both branches take values. We expand F^{xc-} for small Q. We first expand the square root $\sqrt{1-8Q} \approx 1 - 4Q - 8Q^2$ up to the second order in Q. We substitute to the expression of the $F^{xc-}[Q]$ (eq.5.59) and get the lowest order, which is the linear order as

$$F^{xc-}(Q) = 3Q. \tag{5.60}$$

Similarly the lowest order of the expansion of $F^{xc+}(Q)$ for small Q is given by a number

$$F^{xc+}(Q) = 1. \tag{5.61}$$

From eq.5.53 it is also interesting to look at the expansion around the point where F^{xc} changes branch, $Q = \frac{1}{8} - \epsilon$, where ϵ is an infinitesimal positive quantity, but we leave this as an outlook.

In fig.5.27 we plot the real and imaginary parts of $F^{xc-}(Q)$ (eq.5.59) for $0 < Q < \frac{1}{8}$ (eq.5.53) and $F^{xc+}(Q)$ (eq.5.59) for $Q < \frac{1}{8}$ (eq.5.53). In fig.5.27a $F^{xc-}(Q)$ shows a linear behavior for small values of Q, which we fit with $F^{xc}(Q) \approx 3Q$, which corresponds to the lowest order of the

expansion given in eq.5.60. In fig.5.27b $F^{xc+}(Q)$ for small values of Q shows a behavior which is constant and close to 1 which agrees with the lowest order of the expansion given by eq.5.61. In App.E we discuss the F^{xc} as a function of y_0^{-1}.

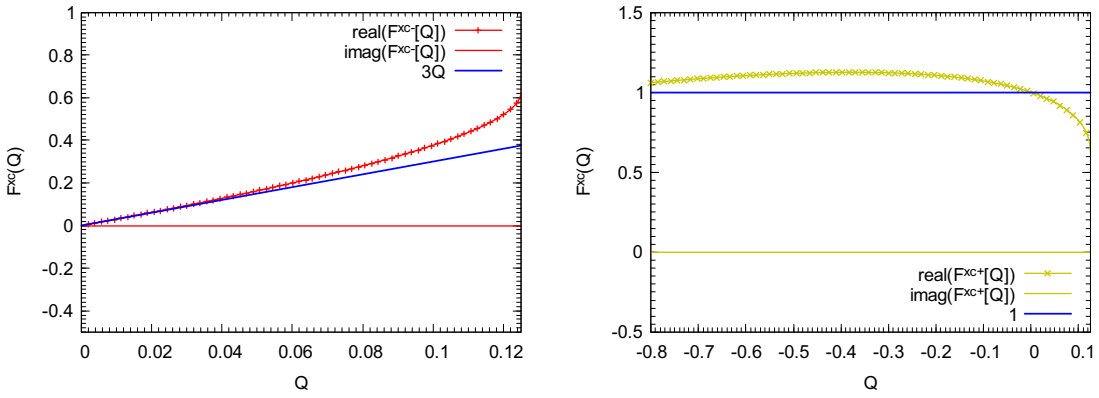

(a) $F^{xc-}(Q)$ for $Q \in [0, \frac{1}{8}]$. *(b)* $F^{xc+}(Q)$ for $Q < \frac{1}{8}$.

Fig. 5.27: $F^{xc\pm}(Q)$ from eq.5.59 (real and imaginary parts) and fitting from the expansion in small Q.

Summarizing, we find that applying the transformation $o^{\pm}(Q)$ on F^{xc}, we obtain two branches F^{xc+} and F^{xc-}. We restrict the domain of definition for each branch, for F^{xc-} being $o \in [0, \frac{1}{3}]$ and for F^{xc+} being $[\frac{1}{3}, +\infty]$. One may approximate each branch with a function of Q either from perturbation theory, or from fitting in a larger range of values. Here, for the case of $\lambda = 1$ we find that for small values of Q the LRC for $a = 3$ gives the F^{xc-} branch, while the bootstrap approximation for $b = 1$ gives the F^{xc+} branch. This is an example, where in TDDFT a different functional should be used for each interval of the domain of definition of the solution. In App.D we discuss the solutions from the LRC and the bootstrap approximations with the parameters suggested in this section, but we find that our approximations always give the solution which is physical in the non-interacting limit. How to find the solution which is physical for large values of the interaction variable remains an open question. Similar considerations hold for the case of $\lambda = \frac{1}{2}$. Our observations can be put in analogy with the observations in [73] for the Green's function and self-energy of the Hubbard atom. This is interesting, since it indicates that the general structure of the interacting problem lead to some fundamental issues that still wait for a solution.

Summary

In this section using the OPM, we studied the performance of solutions obtained within various approximations for the screened interaction. On one hand, in the linear-response approximation we found that one can improve the solution screening beyond the RPA in the LRC and bootstrap approximations. This requires tuning the parameters a and b that appear in these approximations, and their choice cannot be made in a systematic way. For the RPA we studied two different starting points, the RPA from the independent-particle response function with the non-interacting Green's function and the RPA from the independent-particle response function with the classical Green's function. The second case requires a non-linear transformation, which gives rise to multiple functionals and therefore multiple solutions. In the OPM we argued that for a model of independent particles screening is given merely by a number, while for a strongly interacting model screening is non-linear. We find that for independent particles the RPA with the Green's function of the non-interacting system and the LRC gives the exact screening both in the linear-response approximation and beyond. On the other hand, the RPA with the Green's function of the classical system beyond the linear-response approximation is promising for the strongly interacting model, since it has a parabolic behavior which partially reflects the non-linear effects of the exact screening. Again one needs to tune the parameters a and b in order to see improvement when adding an exchange-correlation kernel within TDDFT. Perturbation theory can only partially explain the choice of the parameters. We also explored the case of a non-linear transformation giving rise to two different expressions for the effective interaction, one valid in the non-interacting limit and one valid for stronger values of the interaction. Altogether, it seems to be worthwhile to search for ways to treat non-linear screening in the KBE. We will pursue this further in Chap.7.

6

Time-dependent effective theory for systems with localized electrons

Soon after the Kohn-Sham system of independent particles in DFT has been formulated, it was understood that a local exchange potential needs to correct for self-interaction. In a Kohn-Sham potential, which is local, like the classical potential, the self-interaction correction needs to be included explicitly. In the Hartree-Fock approximation, instead, the self-interaction correction appears as an intrinsic property. This makes the non-local Fock operator a good starting point to derive Kohn-Sham potentials accounting for self-interaction. One major difficulty to include the self-interaction correction in local DFT potentials is that it leads to a different treatment for each state, giving rise to local state-dependent potentials. Slater in 1951 [24] had rewritten the Fock term weighted with the ratio of the density-matrix with respect to the density, in order to obtain a local potential $F(x)$ which, when applied to an occupied orbital $\phi_j(x)$, yields approximately the same effect as the non-local Fock operator. It reads

$$F(x)\phi_j(x) = -\int dx_1 \frac{\rho(x,x_1)}{\rho(x)} \frac{\phi_j(x)\rho(x_1,x)}{|x_1-x|}\phi_j(x_1). \tag{6.1}$$

In the one-electron case this gives the exact cancellation of the Hartree term. Slater mentioned that local potentials with exchange taken as a mean field can overcome the difficulty of having state-dependent potentials. In 1953 Sharp and Horton [75] corrected the Slater potential to give the ground-state of systems correctly and named it optimized effective potential (OEP). In 1980 Perdew and Zunger [76] introduced the self-interaction correction (SIC) to DFT based on the one-electron self-interaction cancellation in Hartree-Fock. These functionals are state dependent. Based on the Slater-method Görling et al. in 2002 [77], [78] derived orbital and state-dependent exact-exchange (EXX) potentials and kernels for DFT and TDDFT.

The usual way to extract local exchange and correlation potentials is using the Schrödinger equation. An alternative way to derive Kohn-Sham potentials corrected for the self-interaction error makes use of the Sham-Schlüter equation (SSE) and has been applied by Bruneval in 2009 [79]. Using the SSE the authors derived a screened time-dependent EXX potential and its effective interaction kernel f^{xc} for TDDFT. In many-body perturbation theory (MBPT), the self-interaction can appear in the exchange part of the self-energy, and it can also appear in the correlation part. This has been discussed for the one-electron case in 2009 by Romaniello et al. [60]. The effect of the self-screening error in the GWA has been discussed by Aryasetiawan et al. in 2012 [61]. Usually the Kohn-Sham calculation is used as a starting point for a GW calculation. It has been shown by Nelson, Bokes, Rinke and Godby [59], that for the hydrogen atom it is important to take into account the self-interaction cancellation in the Kohn-Sham potential.

In this chapter we will try to elucidate some aspects of the physics of the many-electron system with localized electrons starting from the physics of one electron. We will introduce a generalized one-electron model for a solid with localized electrons assuming one electron per lattice position and using wavefunctions that are localized and supposed to be almost atomic-like, namely Wannier functions. We will start from a Hartree-Fock model for the self-energy and add screening with the inverse dielectric constant ϵ^{-1}. Based on the self-interaction cancellation we will derive an adiabatic Kohn-Sham potential for TDDFT using two different ways, the Schrödinger equation and the Sham-Schlüter equation (SSE) for localized electrons. At the end using perturbation theory on a two-level model we compare the excitation energies from TDDFT to the exact energies from the screened Hartree-Fock model. We will show that our self-interaction-corrected Kohn-Sham potential succeeds to predict cancellations between the self-energy and the electron-hole interaction observed in the IXS spectra of solids with localized electrons (fig.4.1).

6.1 Wannier functions

This chapter is based on ideas of my master thesis, but the derivations have been done in a different and more rigorous way. In the following we suppose to have a solid with only one localized electron per unit cell. We can write the Bloch wavefunctions using Wannier functions $w_v(\mathbf{r}-\mathbf{R})$ as

$$\phi_{v\mathbf{k}}(\mathbf{r}) = \frac{1}{\sqrt{N_{lat}}} \sum_{\mathbf{R}} e^{i\mathbf{k}\mathbf{R}} w_v(\mathbf{r}-\mathbf{R}). \tag{6.2}$$

Here, N_{lat} is the number of lattice positions in the solid. $\mathbf{R}$ is a Bravais-lattice vector written in the basis of primitive lattice vectors $\{\mathbf{a}_i\}$. The summation over the lattice vectors runs over all the lattice positions in the solid, which we won't write explicitly. The reciprocal vectors $\mathbf{k}$ lie in the first Brillouin Zone. Wannier functions can be made very localized, almost atomic-like wavefunctions, and their spatial extension is often limited to $|\mathbf{r}-\mathbf{R}| \leq r_c$, with r_c the radius of the unit cell. In the case of very localized core electrons we may specify the radius of localization r_l to be even smaller than r_c.

Let us now summarize the basic properties of Wannier functions. The completeness of the basis of Bloch wavefunctions can be written in terms of Wannier functions as

$$\sum_{\mathbf{R}n} w_n(\mathbf{r}-\mathbf{R}) w_n^\star(\mathbf{r}'-\mathbf{R}) = \delta(\mathbf{r}-\mathbf{r}'), \tag{6.3}$$

showing that Wannier functions form a complete basis of the Bravais lattice. The last relation is equivalent also to the completeness of the atomic basis functions $w_n(\mathbf{r})$ in the region of a unit cell ($|\mathbf{r}| \leq r_c$). The density-matrix contains the sum over all $\mathbf{k}-$points in the first Brillouin zone. It is written in terms of Wannier functions as

$$\rho(\mathbf{r},\mathbf{r}') = \sum_{\mathbf{k}}^{BZ} \phi_{v\mathbf{k}}(\mathbf{r}) \phi_{v\mathbf{k}}^\star(\mathbf{r}') = \sum_{\mathbf{R}} w_v(\mathbf{r}-\mathbf{R}) w_v^\star(\mathbf{r}'-\mathbf{R}), \tag{6.4}$$

where we used that $\sum_{\mathbf{k}}^{BZ} e^{i\mathbf{k}(\mathbf{R}_1-\mathbf{R}_2)} = N_{lat}\delta_{\mathbf{R}_1\mathbf{R}_2}$ and that we have only one occupied band. We disregard spin, which means that we consider only electrons with one spin direction. For localized

electrons the summation of Bloch wavefunctions over the $\mathbf{k}-$points in the first Brillouin Zone equals the summation of Wannier functions over the lattice vectors. This is equivalent to summing over all the atomic density-matrices in the solid. One can obtain the density from the diagonal part of the density-matrix which can be easily seen to be periodic, since translations over the Bravais lattice are absorbed by the summation over the lattice vectors. Under the assumption of electrons localized in the region of a unit cell, the overlap between two Wannier functions localized on different lattice positions is zero. This is expressed with the following relation

$$w_i(\mathbf{r}-\mathbf{R}_i)w_j(\mathbf{r}-\mathbf{R}_j) = \delta_{\mathbf{R}_i\mathbf{R}_j} w_i(\mathbf{r}-\mathbf{R}_i)w_j(\mathbf{r}-\mathbf{R}_i), \tag{6.5}$$

where i, j are indices of the Wannier functions.

6.2 The Kohn-Sham potential of a solid with localized electrons

In order to model a solid with localized electrons we will use one electron per lattice position and no magnetism. We denote the occupied level v in the ground-state of the system. We use a Hartree-Fock single-particle hamiltonian , where the Fock operator is a spatially non-local operator $F(\mathbf{r},\mathbf{r}') = -\frac{1}{2}v(\mathbf{r}-\mathbf{r}')\rho(\mathbf{r},\mathbf{r}')$. The factor of $\frac{1}{2}$ stands for the spin-dependent exchange of the Hartree-Fock equations. In following section we will screen the Fock term with the inverse dielectric constant ϵ^{-1}. The Hartree-Fock single-particle Hamiltonian can be written as

$$\hat{H}(\mathbf{r},\mathbf{r}') = \hat{h}(\mathbf{r}) + \hat{V}^H(\mathbf{r}) + \hat{F}(\mathbf{r},\mathbf{r}'). \tag{6.6}$$

Since it describes the electrons in a periodic solid, the Hamiltonian acts on a Bloch wavefunction to give the Schrödinger equation

$$\begin{aligned} &\int d\mathbf{r}'\hat{H}(\mathbf{r},\mathbf{r}')\phi_{v\mathbf{k}}(\mathbf{r}') = E_v(\mathbf{k})\phi_{v\mathbf{k}}(\mathbf{r}) \\ &\Rightarrow \hat{h}(\mathbf{r})\phi_{v\mathbf{k}}(\mathbf{r}) + \int d\mathbf{r}'\frac{\rho(\mathbf{r}')}{|\mathbf{r}-\mathbf{r}'|}\phi_{v\mathbf{k}}(\mathbf{r}) - \int d\mathbf{r}'\frac{\rho(\mathbf{r},\mathbf{r}')}{|\mathbf{r}-\mathbf{r}'|}\phi_{v\mathbf{k}}(\mathbf{r}') = E_v(\mathbf{k})\phi_{v\mathbf{k}}(\mathbf{r}). \end{aligned} \tag{6.7}$$

Here, we have written the Schrödinger equation for a valence state. This equation displays the self-interaction correction appears between the Hartree and exchange terms of the Hartree-Fock model.

6.2.1 Derivation from the Hamiltonian equation

We now insert Wannier functions into equation 6.7 using eq.6.4 together with eq.6.5. The Hartree term becomes

$$\int d\mathbf{r}'\frac{\rho(\mathbf{r}')}{|\mathbf{r}-\mathbf{r}'|}\phi_{v\mathbf{k}}(\mathbf{r}) = \frac{\sum_{\mathbf{R}}^{N_{lat}}}{\sqrt{N_{lat}}}\int d\mathbf{r}'\frac{\rho(\mathbf{r}')}{|\mathbf{r}-\mathbf{r}'|}e^{i\mathbf{k}\mathbf{R}}w_v(\mathbf{r}-\mathbf{R}), \tag{6.8}$$

while the exchange term is given by

$$-\int d\mathbf{r}'\frac{\rho(\mathbf{r},\mathbf{r}')}{|\mathbf{r}-\mathbf{r}'|}\phi_{v\mathbf{k}}(\mathbf{r}') = -\frac{\sum_{\mathbf{R}}^{N_{lat}}}{\sqrt{N_{lat}}}\int d\mathbf{r}'\frac{|w_v(\mathbf{r}'-\mathbf{R})|^2}{|\mathbf{r}-\mathbf{r}'|}e^{i\mathbf{k}\mathbf{R}}w_v(\mathbf{r}-\mathbf{R}). \tag{6.9}$$

In the Hartree term appears the interaction with the density, which is running over all the lattice positions. The exchange term cancels the on-site (for the site $\mathbf{R}$) contribution. The Schrödinger equation becomes

$$\sum_{\mathbf{R}} e^{i\mathbf{kR}}\left[h(\mathbf{r})+\int d\mathbf{r}'\frac{\sum_{\mathbf{R}_1\neq\mathbf{R}}|w_v(\mathbf{r}'-\mathbf{R}_1)|^2}{|\mathbf{r}-\mathbf{r}'|}\right]w_v(\mathbf{r}-\mathbf{R})=\sum_{\mathbf{R}} e^{i\mathbf{kR}}E_v(\mathbf{k})w_v(\mathbf{r}-\mathbf{R}). \quad (6.10)$$

Now we suppose that the energy eigenvalue shows no dispersion in $\mathbf{k}$, which is reasonable for localized electrons. This allows us to integrate over the $\mathbf{k}-$points with a plane wave, $\sum_{\mathbf{k}} e^{-i\mathbf{kR}_0}$,

$$\left[h(\mathbf{r})+\int d\mathbf{r}'\frac{\sum_{\mathbf{R}_1\neq\mathbf{R}_0}|w_v(\mathbf{r}'-\mathbf{R}_1)|^2}{|\mathbf{r}-\mathbf{r}'|}\right]w_v(\mathbf{r}-\mathbf{R}_0)=E_v w_v(\mathbf{r}-\mathbf{R}_0). \quad (6.11)$$

Introducing reduced coordinates $\tilde{\mathbf{r}}=\mathbf{r}-\mathbf{R}_0$ and shifting $\mathbf{r}''=\mathbf{r}'-\mathbf{R}_0$ we obtain

$$\left[h(\mathbf{r})+\int d\mathbf{r}''\frac{\sum_{\mathbf{R}_1\neq\mathbf{R}_0}|w_v(\mathbf{r}''+\mathbf{R}_0-\mathbf{R}_1)|^2}{|\tilde{\mathbf{r}}-\mathbf{r}''|}\right]w_v(\tilde{\mathbf{r}})=E_v w_v(\tilde{\mathbf{r}}). \quad (6.12)$$

We replace $\mathbf{R}_1-\mathbf{R}_0=\mathbf{R}$ and we obtain the Schrödinger equation for the Wannier function

$$\left[h(\mathbf{r})+\int d\mathbf{r}''\frac{\sum_{\mathbf{R}\neq 0}|w_v(\mathbf{r}''-\mathbf{R})|^2}{|\tilde{\mathbf{r}}-\mathbf{r}''|}\right]w_v(\tilde{\mathbf{r}})=E_v w_v(\tilde{\mathbf{r}}), \quad (6.13)$$

where the fact that an electron interacts with the density of electrons in the solid outside its unit cell is given by a local potential.

In order to find the Kohn-Sham potential, we need to write the Schrödinger equation for the valence electron with a local and periodic potential. The potential that appears in eq.6.13 is local, but not periodic, and it acts on a Wannier function, but not on the electronic wavefunction. We start from eq.6.10 inserting a complete set of Wannier functions (eq.6.3)

$$\sum_{\mathbf{R}} e^{i\mathbf{kR}}\left[h(\mathbf{r})+\int d\mathbf{r}''\int d\mathbf{r}'\frac{\sum_{\mathbf{R}_1\neq\mathbf{R}}|w_v(\mathbf{r}'-\mathbf{R}_1)|^2}{|\mathbf{r}''-\mathbf{r}'|}\sum_{n\mathbf{R}_2} w_n(\mathbf{r}''-\mathbf{R}_2)w_n^{\star}(\mathbf{r}-\mathbf{R}_2)\right]w_v(\mathbf{r}-\mathbf{R})$$
$$=\sum_{\mathbf{R}} e^{i\mathbf{kR}}E_v w_v(\mathbf{r}-\mathbf{R}). \quad (6.14)$$

Then we apply the overlap condition given in eq.6.5 to obtain

$$\sum_{\mathbf{R}} e^{i\mathbf{kR}}\left[h(\mathbf{r})+\int d\mathbf{r}''\int d\mathbf{r}'\frac{\sum_{\mathbf{R}_1\neq\mathbf{R}}|w_v(\mathbf{r}'-\mathbf{R}_1)|^2}{|\mathbf{r}''-\mathbf{r}'|}\sum_{n} w_n(\mathbf{r}''-\mathbf{R})w_n^{\star}(\mathbf{r}-\mathbf{R})\right]w_v(\mathbf{r}-\mathbf{R})$$
$$=\sum_{\mathbf{R}} e^{i\mathbf{kR}}E_v w_v(\mathbf{r}-\mathbf{R}). \quad (6.15)$$

We set $\mathbf{r}''-\mathbf{R}=\mathbf{x}$,

$$\sum_{\mathbf{R}} e^{i\mathbf{kR}}\left[h(\mathbf{r})+\int d\mathbf{x}\int d\mathbf{r}'\frac{\sum_{\mathbf{R}_1\neq\mathbf{R}}|w_v(\mathbf{r}'-\mathbf{R}_1)|^2}{|\mathbf{x}+\mathbf{R}-\mathbf{r}'|}\sum_{n} w_n(\mathbf{x})w_n^{\star}(\mathbf{r}-\mathbf{R})\right]w_v(\mathbf{r}-\mathbf{R})$$

$$= \sum_{\mathbf{R}} e^{i\mathbf{k}\mathbf{R}} E_v w_v(\mathbf{r}-\mathbf{R}). \tag{6.16}$$

We set $\mathbf{R}-\mathbf{r}' = -\mathbf{x}'$,

$$\sum_{\mathbf{R}} e^{i\mathbf{k}\mathbf{R}} \left[h(\mathbf{r}) + \int d\mathbf{x} \int d\mathbf{x}' \frac{\sum_{\mathbf{R}_1 \neq \mathbf{R}} |w_v(\mathbf{x}'+\mathbf{R}-\mathbf{R}_1)|^2}{|\mathbf{x}-\mathbf{x}'|} \sum_n w_n(\mathbf{x}) w_n^\star(\mathbf{r}-\mathbf{R}) \right] w_v(\mathbf{r}-\mathbf{R})$$
$$= \sum_{\mathbf{R}} e^{i\mathbf{k}\mathbf{R}} E_v w_v(\mathbf{r}-\mathbf{R}). \tag{6.17}$$

We set $\mathbf{R}_1 - \mathbf{R} = \mathbf{R}'$,

$$\sum_{\mathbf{R}} e^{i\mathbf{k}\mathbf{R}} \left[h(\mathbf{r}) + \int d\mathbf{x} \int d\mathbf{x}' \frac{\sum_{\mathbf{R}' \neq 0} |w_v(\mathbf{x}'-\mathbf{R}')|^2}{|\mathbf{x}-\mathbf{x}'|} \sum_n w_n(\mathbf{x}) w_n^\star(\mathbf{r}-\mathbf{R}) \right] w_v(\mathbf{r}-\mathbf{R})$$
$$= \sum_{\mathbf{R}} e^{i\mathbf{k}\mathbf{R}} E_v w_v(\mathbf{r}-\mathbf{R}). \tag{6.18}$$

In this equation one can no longer distinguish the electronic wavefunction. The potential term of this equation is independent of the lattice vector. One can replace $w_n^\star(\mathbf{r}-\mathbf{R})$ with $\sum_{\mathbf{R}_2} w_n^\star(\mathbf{r}-\mathbf{R}_2)$ under the condition that eq.6.5 holds. Then eq.6.18 can be written in the following way

$$\sum_{\mathbf{R}} e^{i\mathbf{k}\mathbf{R}} \left[h(\mathbf{r}) + \int d\mathbf{x} \int d\mathbf{x}' \frac{\sum_{\mathbf{R}' \neq 0} |w_v(\mathbf{x}'-\mathbf{R}')|^2}{|\mathbf{x}-\mathbf{x}'|} \sum_n w_n(\mathbf{x}) \sum_{\mathbf{R}_2} w_n^\star(\mathbf{r}-\mathbf{R}_2) \right] w_v(\mathbf{r}-\mathbf{R})$$
$$= \sum_{\mathbf{R}} e^{i\mathbf{k}\mathbf{R}} E_v w_v(\mathbf{r}-\mathbf{R}), \tag{6.19}$$

where the Bloch wavefunction appears. The potential acting on the electronic wavefunction is a local and periodic Hartree-plus-exchange potential, which can be used as a Kohn-Sham potential for DFT as $V^{KS} = V^{ext} + V^{HXC}$, and is given by

$$V^{HXC}(\mathbf{r}) = \int d\mathbf{x} \int d\mathbf{x}' \frac{\sum_{\mathbf{R}' \neq 0} |w_v(\mathbf{x}'-\mathbf{R}')|^2}{|\mathbf{x}-\mathbf{x}'|} \sum_n w_n(\mathbf{x}) \sum_{\mathbf{R}_2} w_n^\star(\mathbf{r}-\mathbf{R}_2). \tag{6.20}$$

The fact that it is periodic can be seen due to the fact that it is invariant under translations over the lattice vector. Potential 6.20 is a superposition of atomic-like potentials for each of the electrons in the system. The sum

$$P^w(\mathbf{x},\mathbf{r}) = \sum_n w_n(\mathbf{x}) \sum_{\mathbf{R}_2} w_n^\star(\mathbf{r}-\mathbf{R}_2), \tag{6.21}$$

is a projector operator, which when acting on an electron localized in some lattice position $\mathbf{R}$ projects the atomic-like potential for this electron. The potential is atomic-like in the sense that its short-range part is canceled standing for self-interaction cancellation, while the long-range part reflects the interaction with the density of the other electrons in the system. Therefore many-body effects appear only through a classical potential, which is similar to an external potential. Potential 6.20, when applied to the electronic wavefunction gives eq.6.13.

The appearance of the projector operator (eq.6.21) in eq.6.20 complicates the derivation of the exchange-correlation kernel f^{xc} from this potential. We may decompose the Kohn-Sham potential of eq.6.20 in two terms

$$V^{KS}(\mathbf{r}) = V^{ext}(\mathbf{r}) + V^{H}(\mathbf{r}) + V^{X}(\mathbf{r}), \tag{6.22}$$

where V^H is the classical term, and $V^X(\mathbf{r})$ is the exchange, given by

$$V^{H}(\mathbf{r}) = \int d\mathbf{x} \int d\mathbf{x}' \frac{\rho(\mathbf{x}')}{|\mathbf{x}-\mathbf{x}'|} \sum_n w_n(\mathbf{x}) \sum_{\mathbf{R}_2} w_n^\star(\mathbf{r}-\mathbf{R}_2) \tag{6.23}$$

$$= \int d\mathbf{x} \int d\mathbf{x}' \frac{\rho(\mathbf{x}')}{|\mathbf{x}-\mathbf{x}'|} \sum_{n\mathbf{R}_2} w_n(\mathbf{x}-\mathbf{R}_2) w_n^\star(\mathbf{r}-\mathbf{R}_2) \tag{6.24}$$

$$= \int d\mathbf{x}' \frac{\rho(\mathbf{x}')}{|\mathbf{r}-\mathbf{x}'|} \tag{6.25}$$

$$V^{X}(\mathbf{r}) = -\int d\mathbf{x} \int d\mathbf{x}' \frac{|w_v(\mathbf{x}')|^2}{|\mathbf{x}-\mathbf{x}'|} \sum_n w_n(\mathbf{x}) \sum_{\mathbf{R}_2} w_n^\star(\mathbf{r}-\mathbf{R}_2). \tag{6.26}$$

The Hartree potential (eq.6.25) is periodic, depends explicitly on the density and has both long and short-range parts. The projector operator in this case can be removed duw to the fact that the density is periodic. On the other hand the projector appears in the exchange term (eq.6.26). The exchange term contains the interaction between two points on the same atom at position $\mathbf{R} = 0$. This is imposed from the product of the two Wannier functions $w_v(\mathbf{x}')w_n(\mathbf{x})$, which is different from zero only when both Wannier orbitals are taken at position $\mathbf{R} = 0$. The fact that the points $\mathbf{x}$ and $\mathbf{x}'$ are close to the same lattice position, may be expressed with the condition that $|\mathbf{x}-\mathbf{x}'| < r_l$, which is true only when the Wannier functions are maximally localized, meaning that they are localized over a radius $r_l < 2r_c$ to ensure that the short-range interaction appears only between points in the same unit cell. In this case we can substitute the Coulomb interaction with

$$v^{sr}(\mathbf{x}-\mathbf{x}') = \frac{\theta(r_l - |\mathbf{x}-\mathbf{x}'|)}{|\mathbf{x}-\mathbf{x}'|} \tag{6.27}$$

and introduce the density to the exchange potential $\frac{1}{2}\rho(\mathbf{x}') = \sum_{\mathbf{R}} |w_v(\mathbf{x}'-\mathbf{R})|^2$, where the terms $\mathbf{R} \neq 0$ will not interact,

$$V^{X}(\mathbf{r}) = -\int d\mathbf{x} \int d\mathbf{x}' \rho(\mathbf{x}') v^{sr}(\mathbf{x}-\mathbf{x}') \sum_n w_n(\mathbf{x}) \sum_{\mathbf{R}_2} w_n^\star(\mathbf{r}-\mathbf{R}_2). \tag{6.28}$$

We substitute with $\mathbf{x} = \mathbf{r}' - \mathbf{R}_2$ and $\mathbf{x}' = \mathbf{r}'' - \mathbf{R}_2$ to obtain

$$V^{X}(\mathbf{r}) = -\int d\mathbf{r}' \int d\mathbf{r}'' \sum_{\mathbf{R}_2} \rho(\mathbf{r}''-\mathbf{R}_2) v^{sr}(\mathbf{r}'-\mathbf{r}'') \sum_n w_n(\mathbf{r}'-\mathbf{R}_2) w_n^\star(\mathbf{r}-\mathbf{R}_2). \tag{6.29}$$

Due to the fact that the density is periodic the exchange potential becomes

$$V^{X}(\mathbf{r}) = -\int d\mathbf{r}' \int d\mathbf{r}'' \rho(\mathbf{r}'') v^{sr}(\mathbf{r}'-\mathbf{r}'') \sum_{n\mathbf{R}_2} w_n(\mathbf{r}'-\mathbf{R}_2) w_n^\star(\mathbf{r}-\mathbf{R}_2). \tag{6.30}$$

We use the completeness relation for the basis of Wannier functions to obtain

$$V^X(\mathbf{r}) = -\int d\mathbf{r}''\rho(\mathbf{r}'')v^{sr}(\mathbf{r}-\mathbf{r}''). \tag{6.31}$$

This is a local potential accounting only for the short-range interaction of an electron at position $\mathbf{r}$. The exchange potential given in eq.6.31 is an explicit functional of the density. This is useful in order to derive the f^{xc}.

Instead, allowing for the Wannier function to be localized in the whole region of the unit cell r_c, would require to define the short-range interaction depending explicitly on the range of each Wannier function

$$v^{sr'}(\mathbf{x},\mathbf{x}') = \frac{\theta(r_c-|\mathbf{x}|)\theta(r_c-|\mathbf{x}'|)}{|\mathbf{x}-\mathbf{x}'|}, \tag{6.32}$$

which is a short-range interaction, depending explicitly on two points and not on their distance. This won't make it possible to get rid of the projector operator and arrive at the simple expression of eq.6.31, whose f^{xc} is straightforward.

In eq.6.20 for $|\mathbf{x}'| < r_c$ the Hartree and exchange contributions cancel. The Kohn-Sham potential gives the interaction with a density for $|\mathbf{x}'| > r_c$ and can be written as

$$V^{HXC}(\mathbf{r}) = \int d\mathbf{x}\int d\mathbf{x}'\frac{\rho(\mathbf{x}')\theta(|\mathbf{x}'|-r_c)}{|\mathbf{x}-\mathbf{x}'|}\sum_n w_n(\mathbf{x})\sum_{\mathbf{R}_2} w_n^\star(\mathbf{r}-\mathbf{R}_2). \tag{6.33}$$

In the limiting case of only one electron, the Kohn-Sham potential is zero, since there is no other electron in the solid to interact with.

6.2.2 Derivation from the Sham-Schlüter equation

It is also interesting to derive the Kohn-Sham potential from a general relation between the former and the self-energy, since this is done for example in the context of "optimized effective potentials (OEP)" [80]. To this end, we write the Sham-Schlüter equation (SSE) (eq.4.16) between the Green's function of the Kohn-Sham system (G^{KS}) and the Green's function of the Hartree-Fock self-energy G^{SE}

$$G^{KS}(1\bar{3})V^X(\bar{3})G^{SE}(\bar{3}1) = G^{KS}(1\bar{3})F(\bar{3}\bar{4})G^{SE}(\bar{4}1). \tag{6.34}$$

Both the local exchange potential V^X and the Fock operator F are static. With bar we note the quantities which are integrated. In equilibrium, we obtain the equation

$$\begin{aligned} &G^{KS}(\mathbf{r}_1,\bar{\mathbf{r}}_3,t_1-\bar{t}_3)V^X(\bar{\mathbf{r}}_3)G^{SE}(\bar{\mathbf{r}}_3,\mathbf{r}_1,\bar{t}_3-t_1) \\ &\qquad = G^{KS}(\mathbf{r}_1,\bar{\mathbf{r}}_3,t_1-\bar{t}_3)F(\bar{\mathbf{r}}_3,\bar{\mathbf{r}}_4)G^{SE}(\bar{\mathbf{r}}_4,\mathbf{r}_1,\bar{t}_3-t_1). \end{aligned} \tag{6.35}$$

For $t_1 > \bar{t}_3$ the last equation contains a hole G^{SE} coupled to an electron G^{KS} and vice versa for $t_1 < \bar{t}_3$. The electron and the hole propagator grouped together give a generalized independent-particle response function

$$\chi^{SSE}(\mathbf{r}_1,\mathbf{r}_3,\mathbf{r}_4,\mathbf{r}_1,t_1-t_3) = G^{KS}(\mathbf{r}_1,\mathbf{r}_3,t_1-t_3)G^{SE}(\mathbf{r}_4,\mathbf{r}_1,t_3-t_1). \tag{6.36}$$

With the integration $\int d\bar{t}_3$, the SSE becomes

$$\int d\mathbf{r}_3 \chi^{SSE}(\mathbf{r}_1,\mathbf{r}_3,\mathbf{r}_3,\mathbf{r}_1,\omega=0)V^X(\bar{\mathbf{r}}_3) = \int d\mathbf{r}_3 \int d\mathbf{r}_4 \chi^{SSE}(\mathbf{r}_1,\mathbf{r}_3,\mathbf{r}_4,\mathbf{r}_1,\omega=0)F(\bar{\mathbf{r}}_3\bar{\mathbf{r}}_4). \tag{6.37}$$

χ^{SSE} has a resonant and an antiresonant part. Here we write explicitly only the resonant part, but it is understood that the anti-resonant part has to be added. The static generalized independent-particle response function for a system with a gap, written in terms of Wannier functions , is given by

$$\chi^{SSE}(\mathbf{r}_1,\mathbf{r}_3,\mathbf{r}_4,\mathbf{r}_1,\omega=0) = \sum_{s\mathbf{k}}\sum_{\mathbf{k}'} \frac{\phi^{KS}_{s\mathbf{k}'}(\mathbf{r}_1)\phi^{KS\star}_{s\mathbf{k}'}(\mathbf{r}_3)\phi_{v\mathbf{k}}(\mathbf{r}_4)\phi^{\star}_{v\mathbf{k}}(\mathbf{r}_1)}{E^{SE}_v(\mathbf{k}) - E^{KS}_s(\mathbf{k}')}, \tag{6.38}$$

where $\phi^{KS}_{s\mathbf{k}'}$ are the Hartree-Fock wavefunctions of the Kohn-Sham system, while $\phi_{v\mathbf{k}}$ are the Hartree-Fock wavefunctions of the model system. s stands for the conduction states of the Kohn-Sham system, while there is only one valence state v in the model system. The difference for the antiresonant part is that in that case the valence will be of the Kohn-Sham system, while the conduction will be for the model system. In the most general case, where there is more than one conduction state in the system, the wavefunction for the conduction states of the Kohn-Sham system will be an expansion over Wannier functions

$$\phi^{KS}_{s\mathbf{k}'}(\mathbf{r}_1) = \sum_{\mathbf{R}} e^{i\mathbf{k}\mathbf{R}} \sum_n c_{sn} w^{KS}_n(\mathbf{r}_1 - \mathbf{R}), \tag{6.39}$$

where c_{sn} are the coefficients mixing the basis states n for the conduction state s. The size of the basis and the choice of the basis states are major source of complication for the use of Wannier functions [81]. In the "extreme tight-binging" case $c_{sn} = 1$ for all states in the system. Here we will assume only one conduction state and also that there is no dispersion of the energy eigenvalues for the conduction and valence bands. Then we can write

$$\chi^{SSE}(\mathbf{r}_1,\mathbf{r}_3,\mathbf{r}_4,\mathbf{r}_1,\omega=0) = \frac{1}{N^2_{lat}} \sum_{\mathbf{k}}^{BZ}\sum_{\mathbf{k}'}^{BZ}\sum_{\mathbf{R}_1}\sum_s e^{i\mathbf{k}'\mathbf{R}_1} w_s(\mathbf{r}_1-\mathbf{R}_1) \sum_{\mathbf{R}_3} e^{-i\mathbf{k}'\mathbf{R}_3} w^{\star}_s(\mathbf{r}_3-\mathbf{R}_3)$$
$$\sum_{\mathbf{R}_4} e^{i\mathbf{k}\mathbf{R}_4} w_v(\mathbf{r}_4-\mathbf{R}_4) \sum_{\mathbf{R}_2} e^{-i\mathbf{k}\mathbf{R}_2} w^{\star}_v(\mathbf{r}_1-\mathbf{R}_2) \frac{1}{E^{SE}_v - E^{KS}_s}. \tag{6.40}$$

We carry out the summation over the $\mathbf{k}-$points $\sum_{\mathbf{k}'}^{BZ} e^{i\mathbf{k}'(\mathbf{R}_1-\mathbf{R}_3)} = N_{lat}\delta_{\mathbf{R}_1\mathbf{R}_3}$ and obtain

$$\chi^{SSE}(\mathbf{r}_1,\mathbf{r}_3,\mathbf{r}_4,\mathbf{r}_1,\omega=0) = \sum_{\mathbf{R}_1}\sum_s w_s(\mathbf{r}_1-\mathbf{R}_1) w^{\star}_s(\mathbf{r}_3-\mathbf{R}_1) \frac{\sum_{\mathbf{R}_2} w_v(\mathbf{r}_4-\mathbf{R}_2) w^{\star}_v(\mathbf{r}_1-\mathbf{R}_2)}{E^{SE}_v - E^{KS}_s}. \tag{6.41}$$

We also apply the overlap condition (eq.6.5) between Wannier functions in position $\mathbf{r}_1$ and obtain

$$\chi^{SSE}(\mathbf{r}_1,\mathbf{r}_3,\mathbf{r}_4,\mathbf{r}_1,\omega=0) = \sum_{\mathbf{R}_1}\sum_s w_s(\mathbf{r}_1-\mathbf{R}_1) w^{\star}_s(\mathbf{r}_3-\mathbf{R}_1) \frac{w_v(\mathbf{r}_4-\mathbf{R}_1) w^{\star}_v(\mathbf{r}_1-\mathbf{R}_1)}{E^{SE}_v - E^{KS}_s}. \tag{6.42}$$

We write the Fock term (eq.6.6) of the SSE applying the overlap condition between the Wannier functions of the density matrix and χ^{SSE} with the arguments $\mathbf{r}_3$ and $\mathbf{r}_4$ to obtain

$$\chi^{SSE}F = -\sum_{\mathbf{R}}\sum_s w_s(\mathbf{r}_1-\mathbf{R}) w^{\star}_s(\bar{\mathbf{r}}_3-\mathbf{R}) \frac{w_v(\bar{\mathbf{r}}_4-\mathbf{R}) w^{\star}_v(\mathbf{r}_1-\mathbf{R})}{E^{SE}_v - E^{KS}_s} \frac{w_v(\bar{\mathbf{r}}_3-\mathbf{R}) w^{\star}_v(\bar{\mathbf{r}}_4-\mathbf{R})}{|\bar{\mathbf{r}}_3-\bar{\mathbf{r}}_4|}. \tag{6.43}$$

We can group the Wannier function with argument $\mathbf{r}_4$ and the non-local Fock term is replaced with a local potential. Substituting this to the SSE, it becomes

$$\chi^{SSE}(V^X + F) = \sum_{\mathbf{R}} \sum_{s} w_s(\mathbf{r}_1 - \mathbf{R}) w_s^\star(\bar{\mathbf{r}}_3 - \mathbf{R})$$
$$\frac{w_v^\star(\mathbf{r}_1 - \mathbf{R}) w_v(\bar{\mathbf{r}}_3 - \mathbf{R})}{E_v^{SE} - E_s^{KS}} (V^X(\bar{\mathbf{r}}_3) + \frac{|w_v(\bar{\mathbf{r}}_4 - \mathbf{R})|^2}{|\bar{\mathbf{r}}_3 - \bar{\mathbf{r}}_4|}) = 0. \tag{6.44}$$

We then introduce a complete set of Wannier functions in front of the Fock term to obtain

$$\chi^{SSE}(V^X - F) = \sum_{\mathbf{R}} \sum_{s} w_s(\mathbf{r}_1 - \mathbf{R}) w_s^\star(\bar{\mathbf{r}}_3 - \mathbf{R}) \frac{w_v^\star(\mathbf{r}_1 - \mathbf{R}) w_v(\bar{\mathbf{r}}_3 - \mathbf{R})}{E_v^{SE} - E_s^{KS}}$$
$$(V^X(\bar{\mathbf{r}}_3) + \sum_{n\mathbf{R}'} w_n^\star(\bar{\mathbf{r}}_3 - \mathbf{R}') w_n(\bar{\mathbf{r}}_3' - \mathbf{R}') \frac{|w_v(\bar{\mathbf{r}}_4 - \mathbf{R})|^2}{|\bar{\mathbf{r}}_3' - \bar{\mathbf{r}}_4|}) = 0. \tag{6.45}$$

Because of the overlap condition between the Wannier functions in $\mathbf{r}_3$ we can replace the Fock term with

$$- \sum_{n\mathbf{R}'} w_n^\star(\bar{\mathbf{r}}_3 - \mathbf{R}') w_n(\bar{\mathbf{r}}_3' - \mathbf{R}') \frac{|w_v(\bar{\mathbf{r}}_4 - \mathbf{R}')|^2}{|\bar{\mathbf{r}}_3' - \bar{\mathbf{r}}_4|} \tag{6.46}$$

so that it does no longer depend on $\mathbf{R}$, and factorize with χ^{SSE} to obtain

$$\chi^{SSE}(V^X - F) = \chi^{SSE}(\mathbf{r}_1, \bar{\mathbf{r}}_3, \omega)(V^X(\bar{\mathbf{r}}_3) + \sum_{n\mathbf{R}'} w_n^\star(\bar{\mathbf{r}}_3 - \mathbf{R}') w_n(\bar{\mathbf{r}}_3') \frac{|w_v(\bar{\mathbf{r}}_4)|^2}{|\bar{\mathbf{r}}_3' - \bar{\mathbf{r}}_4|}) = 0. \tag{6.47}$$

Inverting the independent particles response function, the last equation gives the local exchange as

$$V^X(\mathbf{r}_3) = - \sum_{n\mathbf{R}_3'} w_n^\star(\mathbf{r}_3 - \mathbf{R}_3') w_n(\bar{\mathbf{r}}_3') \frac{|w_v(\bar{\mathbf{r}}_4)|^2}{|\bar{\mathbf{r}}_3' - \bar{\mathbf{r}}_4|}, \tag{6.48}$$

where the projector operator of eq.6.21 appears. The last is equal to the local exchange we derived in eq.6.26 from the Schrödinger equation.

6.2.3 f^{xc} for localized electrons

The f^{xc}, which can be used in absorption from TDDFT, is taken from the derivative of the exchange-correlation potential with respect to the density. If we evaluate it from eq.6.33, we will also need to evaluate the derivative of the projector operator with respect to the density, which is cumbersome. Therefore, in the approximation of maximally localized Wannier functions, the Hartree plus exchange-correlation kernel f^{HXC} will take two contributions, from the derivative of the Hartree and exchange potentials of eq.6.25,6.31

$$f^{HXC}(\mathbf{r}, \mathbf{r}_1) = \frac{\delta V^{HXC}(\mathbf{r})}{\delta \rho(\mathbf{r}_1)} = f^H(\mathbf{r}, \mathbf{r}_1) + f^{xc}(\mathbf{r}, \mathbf{r}_1), \tag{6.49}$$

where f^H gives the derivative of the Hartree potential with respect to the density

$$f^H(\mathbf{r}, \mathbf{r}_1) = \frac{\delta V^H(\mathbf{r})}{\delta \rho(\mathbf{r}_1)} = \int d\mathbf{x}' \frac{\delta(\mathbf{x}' - \mathbf{r}_1)}{|\mathbf{r} - \mathbf{x}'|} = \frac{1}{|\mathbf{r} - \mathbf{r}_1|}. \tag{6.50}$$

This is equal to the bare Coulomb interaction. This is both short and long-range. f^{xc} gives the derivative of the exchange potential with respect to the density

$$f^{xc}(\mathbf{r},\mathbf{r}_1)=\frac{\delta V^X(\mathbf{r})}{\delta\rho(\mathbf{r}_1)}=-\int d\mathbf{r}''\frac{\delta\rho(\mathbf{r}'')}{\delta\rho(\mathbf{r}_1)}v^{sr}(\mathbf{r}-\mathbf{r}'')=-v^{sr}(\mathbf{r}-\mathbf{r}_1), \tag{6.51}$$

which is equal to the short-range part of the Coulomb interaction. f^{xc} cancels the short-range part of the Coulomb interaction. Therefore the total f^{xc} is long-range.

6.2.4 Screening the exchange

Hartree-Fock is a very rough approximation. The most important contribution that is neglected with respect to the true self-energy is screening. We can easily derive the Kohn-Sham potential for the case of a Fock potential screened with the inverse dielectric constant. The Hartree-plus-exchange-correlation potential is the sum of a Hartree and a screened exchange terms,

$$V^{HXC}(\mathbf{r})=V^H(\mathbf{r})+\epsilon^{-1}V^X(\mathbf{r}), \tag{6.52}$$

where $V^H(\mathbf{r})$ is given in eq.6.25, while $V^X(\mathbf{r})$ is given in eq.6.31. The contribution of the screened Fock term is to add a short-range part on the potential allowing for the screened interaction between two points on the same lattice position. This term allows for the short-range interaction between an electron and a hole or between two dipoles localized on the same unit cell. Since screening is a simple constant here, it also introduces some self-interaction which is not physical in the model. However, in the most general case self-interaction cancellation can be taken into account in all orders of correlation in the screening, using a four-point interaction (eq.3.57), and therefore the screened exchange will be free of self-interaction. Introducing screening in the exchange instead of the f^{HXC} of eq.6.49, we obtain

$$f^{HXC}(\mathbf{r},\mathbf{r}_1)=f^H(\mathbf{r},\mathbf{r}_1)+\epsilon^{-1}f^{xc}(\mathbf{r},\mathbf{r}_1). \tag{6.53}$$

The contribution of screening is the fact that the short-range Coulomb interaction in the kernel f^{HXC} is not completely canceled.

6.3 Application to a two-level model

In order to check the performance of the Kohn-Sham potential and its kernel given by eq.6.52 and 6.53 we will use a two-level model. We assume that the basis of Wannier functions has only two states, one valence v and one conduction state c. The two-particles wavefunctions for an independent electron-hole pair are taken as the product of two single-particle Bloch states,

$$\phi_{cv\mathbf{k}\mathbf{k}'}(\mathbf{r}_1,\mathbf{r}_2)=\phi^\star_{c\mathbf{k}}(\mathbf{r}_1)\phi_{v\mathbf{k}'}(\mathbf{r}_2). \tag{6.54}$$

The two particles wavefunction in a basis of Wannier functions is given by

$$w_{cv}(\mathbf{r}_1,\mathbf{r}_2)=w^\star_c(\mathbf{r}_1)w_v(\mathbf{r}_2), \tag{6.55}$$

since we are interested in local electron-hole pairs given by an electron and a hole localized on the same lattice position

$$\phi_{cv\mathbf{k}\mathbf{k}'}(\mathbf{r}_1) = \frac{1}{N_{lat}} \sum_{\mathbf{R}} e^{i(\mathbf{k}-\mathbf{k}')\mathbf{R}} w_c^\star(\mathbf{r}_1 - \mathbf{R}) w_v(\mathbf{r}_1 - \mathbf{R}). \tag{6.56}$$

Taking $\mathbf{R} = 0$ the last expression gives a localized excitation which is not allowed to propagate in the solid outside the unit cell. Its wavefunction is independent of the $\mathbf{k}-$points. Note for comparison that in the atomic case there is only one $\mathbf{k}-$point, namely $\mathbf{k} = 0$.

In this application our starting point is the eigenvalues and eigenvectors of the Kohn-Sham system. As we show in App.B the exact self-energy for a model with one electron of one kind of spin and two levels is the Hartree-Fock self-energy. The effect of the solid is merely to screen the exchange. This can be also seen as the effect of a self-energy in the GWA where a screened exchange appears. Therefore for the scope of this application we will use a static HSF (Hartree-Screened Fock) self-energy,

$$\Sigma^{HSF}(\mathbf{r}_1, \mathbf{r}_2) = \delta(\mathbf{r}_1 - \mathbf{r}_2) V^H(\mathbf{r}_1) + \epsilon^{-1} F(\mathbf{r}_1, \mathbf{r}_2). \tag{6.57}$$

We will evaluate the non-local Fock correction to the Kohn-Sham eigenvalues using standard perturbation theory. In the same way we will evaluate the transition energies from both the HSF and TDDFT kernels. It was the subject of my master thesis to study the cancellations between the HSF self-energy and its kernel in the transition energies of a two-level model. Here, the purpose is to compare the transition energies from the TDDFT kernel to the transition energies obtained from the HSF model for the self-energy end get an estimation for its performance.

6.3.1 Corrections to the Kohn-Sham eigenvalues

We start from the transition energies of an independent electron-hole pair. Then the transition energy $\omega_{cv} = E_c - E_v$, is the difference between single-particle energy eigenvalues. The equation of motion for the Green's function in a basis of Bloch orbitals can be written as

$$\sum_{l\mathbf{k}} [\delta_{il}\delta_{\mathbf{k}'\mathbf{k}}(-\omega + E_{i\mathbf{k}}) + \Delta_{il\mathbf{k}'\mathbf{k}}] G_{lj\mathbf{k}\mathbf{k}''}(\omega) = -\delta_{ij\mathbf{k}'\mathbf{k}''}, \tag{6.58}$$

where $E_{i\mathbf{k}}$ are the single-particle Kohn-Sham eigenvalues. We now consider that we are in the case of an insulating solid with flat bands, since dispersion can only come from the overlap between neighbors. Therefore we take the Kohn-Sham eigenvalues as independent of the $\mathbf{k}-$points. Δ is a non-local operator giving the correction to the Kohn-Sham eigenvalues and eigenfunctions due to the Screened Fock operator,

$$\Delta(\mathbf{r}_1, \mathbf{r}_2) = \epsilon^{-1}(F(\mathbf{r}_1, \mathbf{r}_2) - V^X(\mathbf{r}_1)\delta(\mathbf{r}_1 - \mathbf{r}_2)). \tag{6.59}$$

The Green's function and the matrix elements of $\Delta_{il\mathbf{k}'\mathbf{k}} = \delta_{\mathbf{k}\mathbf{k}'}\Delta_{il}$ are diagonal in $\mathbf{k}-$space. They are determined by the matrix elements of the Coulomb interaction taken with Wannier functions. Therefore the correction with respect to Kohn-Sham is given by the matrix

$$\Delta_{\mathbf{k}\mathbf{k}'} = \delta_{\mathbf{k}\mathbf{k}'}\epsilon^{-1} \begin{pmatrix} -v_{cvcv} + v_{ccvv} & -v_{cvvv} + v_{cvvv} = 0 \\ -v_{vvcv} + v_{vcvv} = 0 & -v_{vvvv} + v_{vvvv} = 0 \end{pmatrix}. \tag{6.60}$$

As we can see in eq.6.60, for the valence states the screened exchange of the Kohn-Sham potential cancels exactly the screened Fock term of the self-energy. The same holds for the off-diagonal matrix elements due to the symmetry of the Coulomb interaction, meaning that the eigenstates of the Kohn-Sham system and those of the model system are the same. This is not the case for the matrix elements taken with conduction states which constitute the only contribution. The cancellation between the matrix elements with the valence states is physical, since there should be no self-interaction for an electron in the unit cell. Moreover, there should be no self-energy correction to the Kohn-Sham result for the removal of an electron in the highest occupied state.

6.3.2 Corrections to the transition energies

In order to study neutral excitations, we use the linear response Dyson-like screening equation (the equation of motion for the response function) in the four-point representation of the Bethe-Salpeter equation [27]. This means that we start from the usual independent-particle response function from the non-interacting system (G_0)

$$\chi^0(12) = -iG_0(12)G_0(21^+), \tag{6.61}$$

and define a four-point independent-particle response function as $\chi^0(1234) = -iG(14)G(23)$. This using a basis of Bloch wavefunctions, becomes

$$\chi^0_{ijkl,\mathbf{k}_i\mathbf{k}_j\mathbf{k}_k\mathbf{k}_l}(\omega) = \frac{[n_i - n_j]\delta_{lj}\delta_{ki}\delta_{\mathbf{k}_l\mathbf{k}_j}\delta_{\mathbf{k}_k\mathbf{k}_i}}{(-\omega + \omega_{ij,\mathbf{k}_i\mathbf{k}_j} - i\delta)}, \tag{6.62}$$

where

$$\omega_{ij,\mathbf{k}_i\mathbf{k}_j} = E_{i\mathbf{k}_i} - E_{j\mathbf{k}_j} \tag{6.63}$$

are the transition energies evaluated from single-particle energy differences and n_i are occupation numbers. The equation of motion for the response function can be written in the following form in frequency space

$$\begin{aligned}&\sum_{st,\mathbf{k}_s\mathbf{k}_t}\left[\delta_{is,\mathbf{k}_i\mathbf{k}_s}\delta_{tj,\mathbf{k}_t\mathbf{k}_j}(-\omega - \omega_{ji,\mathbf{k}_j\mathbf{k}_i}) + [n_i - n_j](-h^{2p}_{i\mathbf{k}_i j\mathbf{k}_j s\mathbf{k}_s t\mathbf{k}_t})\right]\chi_{s\mathbf{k}_s t\mathbf{k}_t k\mathbf{k}_k l\mathbf{k}_l}(\omega)\\ &= [n_i - n_j]\delta_{lj,\mathbf{k}_l\mathbf{k}_j}\delta_{ki,\mathbf{k}_k\mathbf{k}_i}.\end{aligned} \tag{6.64}$$

Here, h^{2p} is the effective interaction from the Hartree-screened Fock (HSF) model or from TDDFT, which plays the role of an interaction contribution to a two-particles hamiltonian. In our model i, j is a pair of conduction ($c, n_c = 0$) and valence states ($v, n_v = 1$), since only this choice gives $n_i - n_j \neq 0$. For simplicity we choose $\mathbf{q} = \mathbf{k}_v - \mathbf{k}_c \approx 0$, which describes optics; The case of $\mathbf{q} \neq 0$ would work in strict analogy. In the same sense we allow for $\mathbf{k}_s = \mathbf{k}_t$, while the pair (s, t) runs over all the possible combinations between valence and conduction states. Combinations of the form $s = t$ give zero matrix elements of the response function. Therefore the basis of two particles states can be taken to be two-dimensional consisting of states that involve combinations of occupied and unoccupied states. This means that the two-particles hamiltonian which contributes in the response is given by a two-dimensional square matrix written in the basis of two particles states. Therefore we obtain two equations, one for the resonant and one for the antiresonant part of the response given respectively by

$$\sum_{st,\mathbf{k}''}\left[\delta_{sv}\delta_{\mathbf{k}\mathbf{k}''}\delta_{tc}(-\omega - \omega_{cv\mathbf{k}}) - h^{2p}_{vc\mathbf{k}st\mathbf{k}''}\right]\chi_{st\mathbf{k}''vc\mathbf{k}'}(\omega) = \delta_{\mathbf{k}\mathbf{k}'} \tag{6.65}$$

and

$$\sum_{st,\mathbf{k}''}\left[\delta_{cs}\delta_{tv}\delta_{\mathbf{k}\mathbf{k}''}(-\omega-\omega_{vc,\mathbf{k}})+h^{2p}_{cv\mathbf{k}st\mathbf{k}''}\right]\chi_{st\mathbf{k}''cv\mathbf{k}'}(\omega)=-\delta_{\mathbf{k}\mathbf{k}'}. \tag{6.66}$$

6.3.3 The matrix elements of the Coulomb interaction

For the evaluation of the matrix elements of the two-particles hamiltonian we need to evaluate the matrix elements of the Coulomb interaction in the basis of Bloch functions. We start from the matrix elements taken with an electron-hole pair, with crystalline momentum $\mathbf{k}$ and another electron-hole pair, with different crystalline momentum $\mathbf{k}'$. These matrix elements are given by

$$v_{cv\mathbf{k}cv\mathbf{k}'}=\int d\mathbf{r}_1\int d\mathbf{r}_2 w_c^\star(\mathbf{r}_1)w_v(\mathbf{r}_1)\frac{\sum_{\mathbf{R}}v(\mathbf{r}_1-\mathbf{r}_2+\mathbf{R})}{N_{at}}w_c(\mathbf{r}_2)w_v^\star(\mathbf{r}_2). \tag{6.67}$$

The matrix elements of eq.6.67 do not depend on $\mathbf{k}-$points. The transition of an electron, in position $\mathbf{r}_1$, from a valence to a conduction state (electron-hole pair creation), in a lattice position, is coupled via the Coulomb interaction with the transition of another electron, in position $\mathbf{r}_2$, from a valence to a conduction state in another lattice position. This interaction is averaged over all the possible lattice positions. This is an interaction of the type dipole-dipole that makes a dipole-like potential. It is like a dipole hopping from one atom to the next and is equivalent to a strongly-bound exciton propagation over the crystal.

The second contribution to the matrix elements of the Coulomb interaction is given by the interaction between an electron with crystalline momentum $\mathbf{k}$ and a hole with different crystalline momentum $\mathbf{k}'$ as

$$v_{cc\mathbf{k}vv\mathbf{k}'}=\frac{\int d\mathbf{r}_1\int d\mathbf{r}_2}{N_{at}}\sum_{\mathbf{R}}e^{-i(\mathbf{k}-\mathbf{k}')\mathbf{R}}|w_c(\mathbf{r}_1)|^2v(\mathbf{r}_1-\mathbf{r}_2+\mathbf{R})|w_v(\mathbf{r}_2)|^2. \tag{6.68}$$

The interaction between an electron and a hole takes both short and long-range contributions $v=v^{sr}+v^{lr}$. We first treat the short-range contribution, knowing that v^{lr} will also give a contribution. In the short-range contribution, when the electron and the hole are in the same or in neighboring unit cells at a small distance from each other the dominant contribution to the Coulomb interaction comes from the $\mathbf{R}=0$ term. This is the picture of an electron charge and a hole charge being bound to each other at a small distance. In this case the strong Coulomb attraction dominates the screening from the rest of the electrons and one may talk about a strongly bound exciton. This was the assumption that we had used in my master thesis in order to obtain matrix elements that are $\mathbf{k}-$independent. This assumption is equivalent to neglecting the long-range part of the Coulomb interaction. The matrix elements of the short-range part of the Coulomb interaction are given by

$$v_{cc\mathbf{k}vv\mathbf{k}'}=\frac{\int d\mathbf{r}_1\int d\mathbf{r}_2}{N_{at}}|w_c(\mathbf{r}_1)|^2v^{sr}(\mathbf{r}_1-\mathbf{r}_2)|w_v(\mathbf{r}_2)|^2=\frac{1}{N_{at}}v_{ccvv}. \tag{6.69}$$

The matrix elements of v^{sr} are $\mathbf{k}-$independent reflecting the fact that we are in a solid made of atomic-like electrons. One may say that we can equally obtain the same result by assuming that $\mathbf{k}=\mathbf{k}'$, however this is equivalent to assuming only one $\mathbf{k}-$point which is equal to the atomic case, meaning that we are no longer in a solid. The matrix elements of the form $v_{c\mathbf{k}c\mathbf{k}'v\mathbf{k}v\mathbf{k}'}$ take a similar expression which is valid under the same assumption of short-range Coulomb interaction and a strongly bound exciton. The approximation of a localized and strongly-bound exciton refers also to the two-particles wavefunction (eq.6.56) taken for $\mathbf{R}=0$, which is $\mathbf{k}-$independent.

6.3.4 The matrix elements of the kernel from the HSF model and TDDFT

In order to compare TDDFT and BSE results, we also have to calculate the matrix elements of the HSF kernel,

$$K^{HSF}(\mathbf{r}_1\mathbf{r}_2\mathbf{r}_3\mathbf{r}_4) = (\delta(\mathbf{r}_1-\mathbf{r}_2)\delta(\mathbf{r}_3-\mathbf{r}_4) - \epsilon^{-1}\delta(\mathbf{r}_1-\mathbf{r}_3)\delta(\mathbf{r}_4-\mathbf{r}_2))\frac{1}{|\mathbf{r}_1-\mathbf{r}_4|}, \tag{6.70}$$

which leads to the set of equations for the resonant and antiresonant parts respectively

$$\sum_{st,\mathbf{k}''}\left[\delta_{cs}\delta_{tv}\delta_{\mathbf{k}''\mathbf{k}}(-\omega-\omega_{vc\mathbf{k}}-i\delta) + v_{cv\mathbf{k}st\mathbf{k}''} - \epsilon^{-1}v_{c\mathbf{k}s\mathbf{k}''v\mathbf{k}t\mathbf{k}''}\right]\chi_{st\mathbf{k}''cv\mathbf{k}'}(\omega) = -\delta_{\mathbf{k}\mathbf{k}'} \tag{6.71}$$

and

$$\sum_{st,\mathbf{k}''}\left[\delta_{vs}\delta_{tc}\delta_{\mathbf{k}''\mathbf{k}}(-\omega-\omega_{vc\mathbf{k}}-i\delta) - v_{vc\mathbf{k}st\mathbf{k}''} + \epsilon^{-1}v_{v\mathbf{k}s\mathbf{k}''c\mathbf{k}t\mathbf{k}''}\right]\chi_{st\mathbf{k}''cv\mathbf{k}'}(\omega) = \delta_{\mathbf{k}\mathbf{k}'}. \tag{6.72}$$

Here, $\omega_{vc\mathbf{k}}$ are transition energies between HSF states. The matrix elements from the classical part of the interaction are taken from eq.6.67, they have both short and long-range contributions and they are $\mathbf{k}-$independent. Under the assumption that the exchange part of the interaction is only short-range, the matrix elements elements of the Coulomb interaction (eq.6.69) are also $\mathbf{k}-$independent. With this assumption we are aware of the fact that we neglect the long-range part of the exchange contribution to the kernel. Once the Coulomb matrix elements are $\mathbf{k}-$independent we can sum over $\mathbf{k}$ and $\mathbf{k}'$ and the corrections to the two-particles transition energies are given by the matrix elements

$$N_{lat}K^{HSF} = \begin{pmatrix} \sum_{\mathbf{R}} v_{cvcv}(\mathbf{R}) - \epsilon^{-1}v_{ccvv} & \sum_{\mathbf{R}} v_{cvvc}(\mathbf{R}) - \epsilon^{-1}v_{cvvc} \\ \sum_{\mathbf{R}} v_{vccv}(\mathbf{R}) - \epsilon^{-1}v_{vccv} & \sum_{\mathbf{R}} v_{vcvc}(\mathbf{R}) - \epsilon^{-1}v_{vvcc} \end{pmatrix}. \tag{6.73}$$

In a similar way we evaluate the matrix elements of the f^{xc} given by eq.6.53 as

$$\sum_{\mathbf{k}} f^{xc}_{cv\mathbf{k}cv\mathbf{k}'} = \sum_{\mathbf{R}} v_{cvcv}(\mathbf{R}) - \epsilon^{-1}v_{cvcv}. \tag{6.74}$$

The matrix elements of the TDDFT kernel are $\mathbf{k}-$independent. Similar to the HSF model the Kohn-Sham transition energies will take corrections given by the matrix elements

$$f^{xc} = \begin{pmatrix} \sum_{\mathbf{R}} v_{cvcv}(\mathbf{R}) - \epsilon^{-1}v_{cvcv} & \sum_{\mathbf{R}} v_{cvvc}(\mathbf{R}) - \epsilon^{-1}v_{cvvc} \\ \sum_{\mathbf{R}} v_{vccv}(\mathbf{R}) - \epsilon^{-1}v_{vccv} & \sum_{\mathbf{R}} v_{vcvc}(\mathbf{R}) - \epsilon^{-1}v_{vcvc} \end{pmatrix}. \tag{6.75}$$

As we can see, the two matrices eq.6.73 and 6.75 only differ by their diagonal elements. This means that indeed, we can replace the more complicated Bethe-Salpeter equation based on HSF by our TDDFT potential and kernel.

6.4 Two-particle transition energies from perturbation theory

The Kohn-Sham transition energies in first order perturbation theory take corrections only from the diagonal matrix elements of the f^{xc} and give the transition energies E^{KS} within TDDFT as

$$E^{KS} = \begin{pmatrix} E^{KS}_{cv} + \sum_{\mathbf{R}} v_{cvcv}(\mathbf{R}) - \epsilon^{-1} v_{cvcv} & 0 \\ 0 & E^{KS}_{vc} - (\sum_{\mathbf{R}} v_{vcvc}(\mathbf{R}) - \epsilon^{-1} v_{vcvc}) \end{pmatrix}. \tag{6.76}$$

The corresponding electron-hole wavefunctions are given by the vector $\vec{w}^{HSF} = (w_1^{HSF} w_2^{HSF})$, where the new transition states w_1^{HSF} and w_2^{HSF} mix the transition states of the Kohn-Sham system $\vec{w}^{KS} = (w_{cv}, w_{vc})$ through the off-diagonal elements of f^{xc}

$$\vec{w}^{HSF} = \vec{w}^{KS} \begin{pmatrix} 1 & a \\ a^\star & 1 \end{pmatrix}, \tag{6.77}$$

where

$$a = \frac{\sum_{\mathbf{R}} v_{cvvc}(\mathbf{R}) - \epsilon^{-1} v_{cvvc}}{E^{KS}_{cv} - E^{KS}_{vc}}, \tag{6.78}$$

$a^\star$ is the complex conjugate of a.

Since the Fock corrections given in Δ (eq.6.60) have zero off-diagonal elements, the single-particle Kohn-Sham basis gets no perturbative correction. Instead, the Δ_{cc} elements will contribute corrections to the transition energies. From those the screened exchange of the Kohn-Sham potential will cancel the screened Fock part of the kernel to give the transition energies as

$$\begin{aligned} E^{HSF} &= \begin{pmatrix} E^{KS}_{cv} + \Delta_{cc} + K^{HSF}_{cvcv} & 0 \\ 0 & E^{KS}_{vc} - \Delta_{cc} - K^{HSF}_{vcvc} \end{pmatrix} \\ &= \begin{pmatrix} E^{KS}_{cv} - \epsilon^{-1} v_{cvcv} + \sum_{\mathbf{R}} v_{cvcv}(\mathbf{R}) & 0 \\ 0 & E^{KS}_{vc} + \epsilon^{-1} v_{vcvc} - \sum_{\mathbf{R}} v_{vcvc}(\mathbf{R}) \end{pmatrix}. \end{aligned} \tag{6.79}$$

For the HSF case the electron-hole wavefunctions will take corrections from the off-diagonal matrix elements of the HSF kernel,

$$\vec{\phi}^{QP} = \vec{\phi}^{KS} \begin{pmatrix} 1 & b \\ b^\star & 1 \end{pmatrix}, \tag{6.80}$$

where

$$b = \frac{\sum_{\mathbf{R}} v_{cvvc}(\mathbf{R}) - \epsilon^{-1} v_{cvvc}}{E^{KS}_{cv} - E^{KS}_{vc} + 2\Delta_{cc}}, \tag{6.81}$$

and $b^\star$ is the complex conjugate of b. As we can see the transition energies given by the HSF kernel in eq.6.79 are identical to those given by TDDFT in eq.6.76. The two-particles eigenvectors differ in the fact that in b (eq.6.81) the screened-Fock correction needs to be taken into account in the transition energies that appear in the denominator. This, however, is a correction of higher order.

In the IXS spectrum of NiO (fig.4.1) we have noticed the cancellation between GWA and the BSE. Our model HSF hamiltonian explains this observation as a cancellation happening between the screened-Fock kernel and the screened exchange potential of DFT. Moreover the final transition energies are given by a screened dipole-like potential canceling the short-range part of a long-range dipole-like potential. Therefore for the choice of $\epsilon^{-1} = 1$ the cancellation of the short-range part is exact and the final contribution is merely given by the long-range part of a dipole-like potential, which we expect to be small for cases where the electron and the hole are strongly bound in a distance smaller than the radius of the unit cell. This remaining long-range potential may explain the small shift in the final position of the spectrum in fig.4.1 with respect to the Kohn-Sham independent-particles spectrum. Larger values of the dielectric constant will give short-range contributions which we expect to give a final position of the spectra being shifted to higher energies than the Kohn-Sham independent-particles spectra.

To sum up, the present discussion suggests that the derivation of an exchange potential with the self-interaction correction as it appears in the one-electron model gives correctly cancellations between the non-local self-energy and the electron-hole interaction taken into account in the BSE. The result is promising to give IXS spectra within TDDFT. For photoemission spectra, it suggests that this is the way to include cancellations in the response for systems with localized electrons in order to screen the interaction which enters the self-energy, and also to have a simplified way to calculate x-ray absorption spectra.

Summary

In this chapter, using the self-interaction cancellation for the one-electron case and maximally localized Wannier functions, we derived a Kohn-Sham potential for localized electrons. This potential gives correctly the self-interaction correction to the atomic potential of each electron in the solid. We verified the result using two different ways, the derivation from the Schrödinger equation and the Sham-Schlüter equation (SSE). Using perturbation theory we evaluated the correction to the transition energies of an electron-hole pair from TDDFT and we found that it reproduces the cancellation between the Fock part of the effective interaction and the screened exchange of DFT. This explains the cancellation between the GWA and the BSE observed in the IXS spectrum of NiO(fig.4.1) and makes our self-interaction-derived potential promising for application in real materials with localized electrons.

7

Non-linear screening for localized electrons

In XPS of core-levels one measures the energy required to extract a localized electron from the many-electrons system. The removal of the core electron can be seen as the addition of a core-hole charge in the system. The energy for the removal of a core electron involves the screening of the core-hole charge from the rest of the particles in the system. The basic mechanism of screening is the collective oscillations of valence electrons called plasmons. There can also be interband transitions and excitons. These phenomena are in general coupled. Models used to describe such mechanisms often distinguish between two subsets of states based on spatial and energy separation: a high binding-energy regime where core-electrons are localized in the sense that they cannot exchange position with other electrons, and a low binding-energy regime where valence electrons are considered as delocalized in a sense that they can exchange positions with each other, but they cannot exchange position with the core electrons. In this sense the density-response from the valence electrons can be seen as contributing only to an external potential for the core electrons.

Approaches to evaluate the propagation of an electron that is decoupled from the rest of the valence states (within the decoupling approximation) include the application of model hamiltonians on scattering theory [20], which is an approach based on traditional time-dependent perturbation theory, or the solution of the KBE within approximations, which is a later approach related to MBPT. Following the second approach, the solution of the KBE is obtained within the cumulant approximation, where screening is usually taken in the linear-response approximation. Nozieres and Dominicis were the first to solve for the cumulant accounting for screening from single-particle transitions [82], while Langreth introduced also the plasmon contribution [83]. The hole-plasmon coupling for core-electron photoemission has been originally studied by Hedin and Lundqvist [84, 85] using model hamiltonians and was found to give rise to multiple plasmon satellites in photoemission spectra. The cumulant approach has not only been applied to core electrons, but also to metals for the photoemission of valence electrons again in the decoupling approximation, taking into account recoil effects from the scattering from the Fermi sea [86]. For valence-electron photoemission the cumulant expansion with a cumulant linear in the screened Coulomb interaction has shown non-trivial behavior, reproducing for example the multiple plasmon satellites of the spectral function of metals [87]. For valence electrons in semiconductors the cumulant with screening in the linear-response approximation described in a single plasmon pole model was found to show astonishing agreement with the photoemission experiment for Si [10].

On overall, the photoemission of an electron of relatively high binding energy is well described within the linear-response approximation. However in the photoemission of a core-electron, the potential from the core-hole might be strong enough to introduce non linear effects in the screening. Non-linear effects might affect the spectra constituting mechanism for the decay of single-particle or plasmon excitations into additional satellite structures in insulating and semiconducting materi-

als. The model study in Chap.5 shows that taking into account non-linear screening might indeed improve the description of the Green's function substantially.

In this chapter we will address the following questions: Is the photoemission of a core level a strong perturbation to the many-electron system ? In cases where this is true, how do non-linear screening effects show up in the KBE? How could we include them in a fully ab initio framework? In order to address these questions we will extend the cumulant solution to account also for non-linear screening. Then in order to answer our question we will introduce two different approaches to evaluate the response to the core-hole charge. The first is based on the solution of the equation of motion of the linear response function using TDDFT for zero and finite core-hole charge. The second is a real-time TDDFT approach, which involves the solution of the Schrödinger equation within TDDFT for fractional core-hole occupation. In both cases we will evaluate the non-linear effects from the variation of the linear-response approximation with respect to the core-hole occupation.

7.1 Transformation of the KBE to the time-dependent density

To start, we write the equation of motion for the Green's function with respect to the Green's function of the classical system and in a basis of single-particle states. The Dyson equation for the matrix elements of the Green's function of the classical system taken with a single basis element c standing for a core state is

$$G^H_{cc}(t_1,t_2) = G^0_{cc}(t_1,t_2) + \sum_{ijkl} G^0_{ci}(t_1,\bar{t}_3) v_{ijkl} n_{kl}(\bar{t}_3) G^H_{jc}(\bar{t}_3,t_2), \tag{7.1}$$

where n_{kl} are the matrix elements of the exact density. Now we apply the decoupling approximation on the matrix elements of the Green's function of the non-interacting system $G^0_{cj} = \delta_{cj} G^0_{cc}$. We also apply the non-overlapping approximation, saying that the core level is so localized that it shows zero overlap with the rest of the levels in the system. This gives $v_{cdkl} = \delta_{cd} v_{cckl}$. Eq.7.1 becomes

$$G^H_{cc}(t_1,t_2) = G^0_{cc}(t_1,t_2) + \sum_{kl} G^0_{cc}(t_1,\bar{t}_3) v_{cckl} n_{kl}(\bar{t}_3) G^H_{cc}(\bar{t}_3,t_2). \tag{7.2}$$

The non-overlapping approximation for core states applied to the matrix elements of the Coulomb interaction leads to a decoupling of the matrix elements of the Green's function of the classical system. We also make the approximation that only the lesser parts of the Green's function of the non-interacting system with the level c have non-zero matrix elements, meaning that there is always a hole propagating to the core-level c in the non-interacting system. This gives that $G^{H>}_{cc} = 0$ and therefore there is always a hole propagating to the core-level c also in the classical system $G^H_{cc}(t_1,t_2) = G^{H<}_{cc}(t_1,t_2)\theta(t_2-t_1)$. This finally gives the Dyson equation for the Green's function of the classical system,

$$G^{H<}_{cc}(t_1,t_2) = G^{0<}_{cc}(t_1,t_2) + \int_{t_1}^{t_2} dt_3 \sum_{kl} G^{0<}_{cc}(t_1,t_3) v_{cckl} n_{kl}(t_3) G^{H<}_{cc}(t_3,t_2), \tag{7.3}$$

where we used that

$$\int dt_3 \theta(t_3-t_1)\theta(t_2-t_3) = \theta(t_2-t_1)\int_{t_1}^{t_2} dt_3. \tag{7.4}$$

Since $G^{0-1} = i\frac{\partial}{\partial t} - \hat{h}$, the solution of eq.7.3 is

$$G^{H<}_{cc}(t_1, t_2) = G^{0<}_{cc}(t_1, t_2)C(t_2)e^{-i\sum_{kl} v_{cckl}\int_{t_1}^{t_2} d\tau n_{kl}(\tau)}, \tag{7.5}$$

where $C(t_2)$ is a function which still needs to be specified. Since for $v \to 0$ we must obtain the non-interacting solution, we set $C(t_2) = 1$. The Green's function of the classical system is a pure functional of the density $G^H[n]$, whereas the Coulomb interaction is a parameter. We now write the KBE with respect to the Green's function of the classical system using the decoupling approximation in the non-interacting system. We also introduce the chain rule with the density. This is justified by the one-to-one relation between the density and the external potential given by time-dependent density functional theory. We use the decoupling of the matrix elements of the Green's function of the classical system $G^H_{cj} = \delta_{cj}G^H_{cc}$ taken with a core state c. For the matrix elements taken with the core state c, we get the equation

$$G_{cc}(t_1, t_2) = G^H_{cc}(t_1, t_2) + iG^H_{cd}(t_1, \bar{t}_3)\sum_{dklij} v_{cdkl}\frac{\delta G_{dc}(\bar{t}_3, t_2)}{\delta n_{ij}(\bar{t}_4)}\frac{\delta n_{ij}(\bar{t}_4)}{\delta U_{kl}(\bar{t}_3^+)}. \tag{7.6}$$

Then we apply the non-overlapping approximation on the matrix elements of the Coulomb interaction $v_{cdkl} = \delta_{cd}v_{cckl}$, and eq.7.6 becomes

$$G_{cc}(t_1, t_2) = G^H_{cc}(t_1, t_2) + iG^H_{cc}(t_1, \bar{t}_3)\sum_{klij} v_{cckl}\frac{\delta n_{ij}(\bar{t}_4)}{\delta U_{kl}(\bar{t}_3^+)}\frac{\delta G_{cc}(\bar{t}_3, t_2)}{\delta n_{ij}(\bar{t}_4)}. \tag{7.7}$$

Again the non-overlapping approximation applied to the matrix elements of the Coulomb interaction results in the decoupling of the matrix elements of the interacting Green's function. We also use the approximation that the Green's function takes contribution only from its lesser part ($G^>_{cc} = 0$) meaning that there is always a hole propagating to the level c of the interacting system $G_{cc}(t_1, t_2) = G^<_{cc}(t_1, t_2)\theta(t_2 - t_1)$. Finally eq.7.7 becomes

$$\begin{aligned} G^<_{cc}(t_1, t_2)\theta(t_2 - t_1) &= G^{H<}_{cc}(t_1, t_2)\theta(t_2 - t_1) \\ &+ iG^{H<}_{cc}(t_1, \bar{t}_3)\theta(\bar{t}_3 - t_1)\sum_{klij} v_{cckl}\frac{\delta n_{ij}(\bar{t}_4)}{\delta U_{kl}(\bar{t}_3^+)}\frac{\delta G^<_{cc}(\bar{t}_3, t_2)}{\delta n_{ij}(\bar{t}_4)}\theta(t_2 - \bar{t}_3). \end{aligned} \tag{7.8}$$

The last is the KBE written with the density as the variable. The effects of the applied potential appear through the response of the density to the applied potential $\frac{\delta n_{ij}(\bar{t}_4)}{\delta U_{kl}(\bar{t}_3^+)}$. Note that strictly speaking the KBE is a non-equilibrium equation, which would require solution on the Keldysh contour [88]. However, since we make the approximation that greater and lesser contributions decouple, we can avoid this complication.

7.1.1 The equation for the non-linear cumulant

The solution of eq.7.8 can be written as a general ansatz, where G is given as a product of two functions, namely the Green's function of the classical system and a still unknown function F,

$$G^<_{cc}(t_1, t_2)\theta(t_2 - t_1) = F(t_1, t_2)G^{H<}_{cc}(t_1, t_2)\theta(t_2 - t_1). \tag{7.9}$$

Due to the decoupling of the Green's function of the classical system the following property holds

$$\frac{\delta G^H_{cc}(t_1, t_2)}{\delta n_{ij}(t_4)} = v_{ccij}G^H_{cc}(t_1, t_4)G^H_{cc}(t_4, t_2) + G^H_{cc}(t_1, \bar{t}_2)\frac{\delta U_{cc}(\bar{t}_2)}{\delta n_{ij}(t_4)}G^H_{cc}(\bar{t}_2, t_2). \tag{7.10}$$

Inserting eq.7.9 into eq.7.8 and using eq.7.10 we obtain

$$
\begin{aligned}
&G^{<}_{cc}(t_1,t_2)\theta(t_2-t_1) = \theta(t_2-t_1)G^{H<}_{cc}(t_1,t_2) \\
&+ i\theta(t_2-t_1)\int_{t_1}^{t_2} dt_3 \int_{t_3}^{t_2} dt_4 G^{H<}_{cc}(t_1,t_3)\sum_{klij} v_{cckl}\frac{\delta n_{ij}(t_4)}{\delta U_{kl}(t_3^+)}G^{H<}_{cc}(t_3,t_4)G^{H<}_{cc}(t_4,t_2)v_{ccij}F(t_3,t_2) \\
&+ i\theta(t_2-t_1)\int_{t_1}^{t_2} dt_3 G^{H<}_{cc}(t_1,t_3)V^{x}_{cc}(t_3,t_2)F(t_3,t_2) \\
&+ i\theta(t_2-t_1)\int_{t_1}^{t_2} dt_3 \int dt_4 G^{H<}_{cc}(t_1,t_3)\sum_{klij} v_{cckl}\frac{\delta n_{ij}(t_4)}{\delta U_{kl}(t_3^+)}\frac{\delta F(t_3,t_2)}{\delta n_{ij}(t_4)}G^{H<}_{cc}(t_3,t_2),
\end{aligned}
\tag{7.11}
$$

where V^x_{cc} is an exchange contribution given by

$$
\begin{aligned}
V^{x}_{cc}(t_3,t_2) &= \int dt_4 \sum_{klij} v_{cckl}\frac{\delta n_{ij}(t_4)}{\delta U_{kl}(t_3^+)}\int dt_5 G^{H}_{cc}(t_3,t_5)\frac{\delta U_{cc}(t_5)}{\delta n_{ij}(t_4)}G^{H}_{cc}(t_5,t_2) \\
&= \sum_{kl} v_{cckl}\int dt_5 \frac{\delta U_{cc}(t_5)}{\delta U_{kl}(t_3^+)}G^{H}_{cc}(t_3,t_5)G^{H}_{cc}(t_5,t_2) \\
&= v_{cccc}G^{H}_{cc}(t_3,t_3^+)G^{H}_{cc}(t_3^+,t_2)
\end{aligned}
\tag{7.12}
$$

We insert the exchange of eq.7.12 in eq.7.11 and obtain

$$
\begin{aligned}
&G^{<}_{cc}(t_1,t_2)\theta(t_2-t_1) = \theta(t_2-t_1)G^{H<}_{cc}(t_1,t_2) \\
&+ i\theta(t_2-t_1)\int_{t_1}^{t_2} dt_3 \int_{t_3}^{t_2} dt_4 G^{H<}_{cc}(t_1,t_3)\sum_{klij} v_{cckl}\frac{\delta n_{ij}(t_4)}{\delta U_{kl}(t_3^+)}G^{H<}_{cc}(t_3,t_4)G^{H<}_{cc}(t_4,t_2)v_{ccij}F(t_3,t_2) \\
&+ i\theta(t_2-t_1)\int_{t_1}^{t_2} dt_3 G^{H<}_{cc}(t_1,t_3)v_{cccc}G^{H}_{cc}(t_3,t_3^+)G^{H}_{cc}(t_3^+,t_2)F(t_3,t_2) \\
&+ i\theta(t_2-t_1)\int_{t_1}^{t_2} dt_3 \int dt_4 G^{H<}_{cc}(t_1,t_3)\sum_{klij} v_{cckl}\frac{\delta n_{ij}(t_4)}{\delta U_{kl}(t_3^+)}\frac{\delta F(t_3,t_2)}{\delta n_{ij}(t_4)}G^{H<}_{cc}(t_3,t_2).
\end{aligned}
\tag{7.13}
$$

Now we substitute with

$$
G^{HX<-1}_{cc}(t_1,t_2) = G^{H<-1}_{cc}(t_1,t_2) - iv_{cccc}G^{H}_{cc}(t_2,t_2^+)\delta(t_1-t_2). \tag{7.14}
$$

G^{HX}_{cc} adds the exchange contribution to the classical potential of eq.7.3 and corrects for self-interaction. Setting in eq.7.3 $t_2 = t_1^+$ we see that the density of the classical system is equal to the non-interacting density. And it is also equal to the non-interacting density $G^{H}_{cc}(t_2,t_2^+) = n^0_0$ of the static system, because in the decoupling approximation a core level never mix with other particles under the effect of the external potential (see also later, eq.7.17 for $t_2 = t_1^+$). From eq.7.3 we see that once we neglect the coupling with the electron-propagator, the density always remains the same and equal to the non-interacting density. One can verify this fact by taking the limit $t_2 \to t_1^+$ in the limits of the integration, and the integral becomes equal to zero. Eq.7.13 then becomes

$$
G^{<}_{cc}(t_1,t_2)\theta(t_2-t_1) = \theta(t_2-t_1)G^{HX<}_{cc}(t_1,t_2)
$$

$$+ i\theta(t_2-t_1)\int_{t_1}^{t_2} dt_3 \int_{t_3}^{t_2} dt_4 G^{HX<}_{cc}(t_1,t_3)\sum_{klij} v_{cckl}\frac{\delta n_{ij}(t_4)}{\delta U_{kl}(t_3^+)} G^{H<}_{cc}(t_3,t_4)G^{H<}_{cc}(t_4,t_2)v_{ccij}F(t_3,t_2)$$

$$+ i\theta(t_2-t_1)\int_{t_1}^{t_2} dt_3 \int dt_4 G^{HX<}_{cc}(t_1,t_3)\sum_{klij} v_{cckl}\frac{\delta n_{ij}(t_4)}{\delta U_{kl}(t_3^+)}\frac{\delta F(t_3,t_2)}{\delta n_{ij}(t_4)} G^{H<}_{cc}(t_3,t_2), \tag{7.15}$$

where the time integrals of the $\theta-$ functions satisfy the relation

$$\int dt_3 \int dt_4 \theta(t_3-t_1)\theta(t_4-t_3)\theta(t_2-t_4) =$$
$$\theta(t_2-t_1)\int_{t_1}^{t_2} dt_4 \int_{t_1}^{t_4} dt_3 = \theta(t_2-t_1)\int_{t_1}^{t_2} dt_3 \int_{t_3}^{t_2} dt_4. \tag{7.16}$$

This commutative property of the time integrals also holds for the opposite time ordering.

In the decoupling approximation, the propagator of the non-interacting system satisfies the equation

$$G^{0<}_{cc}(t_1,t_2) = G^{0<}_{0cc}(t_1,t_2) + \int_{t_1}^{t_2} dt_3 G^{0<}_{0cc}(t_1,t_3)U_{cc}(t_3)G^{0<}_{cc}(t_3,t_2), \tag{7.17}$$

whose solution is, similar to eq.7.5, given by

$$G^{<}_{0cc}(t_1,t_2) = G^{0<}_{0cc}(t_1,t_2)e^{-i\int_{t_1}^{t_2} dtU_{cc}(t)}, \tag{7.18}$$

or by

$$G^{0<}_{cc}(t_1,t_2) = ie^{-i\int_{t_1}^{t_2} dtE^0_c(t)}, \tag{7.19}$$

where the energy is given by the sum of the energy in the static non-interacting system E^0_{c0} and the external potenital, $E^0_c(t) = E^0_{c0} + U_{cc}(t)$. The Green's function of the classical system taken from eq.7.19 and 7.5 has the following property,

$$G^{H<}_{cc}(t_1,t_2)G^{H<}_{cc}(t_2,t_3) = iG^{H<}_{cc}(t_1,t_3), \tag{7.20}$$

where

$$G^{H<}_{cc}(t_1,t_2) = ie^{-i\int_{t_1}^{t_2} dt(E^0_c(t)+\sum_{kl} v_{cckl}n_{kl}(t))}. \tag{7.21}$$

The property of eq.7.20 also holds for G^{HX}, which is given by

$$G^{HX<}_{cc}(t_1,t_2) = ie^{-i\int_{t_1}^{t_2} dt(E^0_c(t)+\sum_{kl\neq cc} v_{cckl}n_{kl}(t))} = G^{H<}_{cc}(t_1,t_2)e^{i\int_{t_1}^{t_2} dtv_{cccc}n_{cc}(t)}, \tag{7.22}$$

because $n_{cc}(t) = n^0_0$, the density of the core level is not affected from the dynamics of the system. Using eq.7.22, eq.7.15 becomes

$$F(t_1,t_2)e^{-i\int_{t_1}^{t_2} dtv_{cccc}n_{cc}(t)}G^{HX<}_{cc}(t_1,t_2) = G^{HX<}_{cc}(t_1,t_2) + i\int_{t_1}^{t_2} dt_3 \int_{t_3}^{t_2} dt_4 G^{HX<}_{cc}(t_1,t_3)$$
$$\sum_{klij} v_{cckl}\frac{\delta n_{ij}(t_4)}{\delta U_{kl}(t_3^+)}v_{ccij}G^{HX<}_{cc}(t_3,t_4)G^{HX<}_{cc}(t_4,t_2)e^{-i\int_{t_3}^{t_2} dtv_{cccc}n_{cc}(t)}F(t_3,t_2)$$
$$+ i\int_{t_1}^{t_2} dt_3 \int dt_4 G^{HX<}_{cc}(t_1,t_3)\sum_{klij} v_{cckl}\frac{\delta F(t_3,t_2)}{\delta U_{kl}(t_3^+)}e^{-i\int_{t_3}^{t_2} dtv_{cccc}n_{cc}(t)}G^{HX<}_{cc}(t_3,t_2). \tag{7.23}$$

Applying the analogue of eq.7.20 for G^{HX} on eq.7.23 we obtain the equation for F

$$F(t_1,t_2)e^{-i\int_{t_1}^{t_2}dtv_{cccc}n_{cc}(t)} = 1 - i\int_{t_1}^{t_2}dt_3\int_{t_3}^{t_2}dt_4\sum_{klij}v_{cckl}\frac{\delta n_{ij}(t_4)}{\delta U_{kl}(t_3^+)}v_{ccij}F(t_3,t_2)e^{-i\int_{t_3}^{t_2}dtv_{cccc}n_{cc}(t)}$$
$$-\int_{t_1}^{t_2}dt_3\sum_{kl}v_{cckl}\frac{\delta F(t_3,t_2)}{\delta U_{kl}(t_3^+)}e^{-i\int_{t_3}^{t_2}dtv_{cccc}n_{cc}(t)}. \quad (7.24)$$

In the last term we no longer need the density to appear explicitly but we can insert it at any time through the chain rule $\frac{\delta F(t_3,t_2)}{\delta U_{kl}(t_3^+)} = \sum_{ij}\frac{\delta F(t_3,t_2)}{\delta n_{ij}(\bar{t}_4)}\frac{\delta n_{ij}(\bar{t}_4)}{\delta U_{kl}(t_3^+)}$. We also renormalize

$$\tilde{F}(t_1,t_2) = F(t_1,t_2)e^{-i\int_{t_1}^{t_2}dtv_{cccc}n_{cc}(t)}. \quad (7.25)$$

This is equivalent to correcting the classical propagator in the ansatz of eq.7.9 for self-interaction as

$$G_{cc}^{<}(t_1,t_2)\theta(t_2-t_1) = F(t_1,t_2)G_{cc}^{H<}(t_1,t_2)\theta(t_2-t_1) = \tilde{F}(t_1,t_2)G_{cc}^{HX<}(t_1,t_2)\theta(t_2-t_1). \quad (7.26)$$

Using eq.7.25 we also rewrite the derivative of F as

$$\frac{\delta F(t_3,t_2)}{\delta U_{kl}(t_3^+)}e^{-i\int_{t_3}^{t_2}dtv_{cccc}n_{cc}(t)} = \frac{\delta\tilde{F}(t_3,t_2)}{\delta U_{kl}(t_3^+)} - (-i)\int_{t_3}^{t_2}dt_4\frac{\delta n_{cc}(t_4)}{\delta U_{kl}(t_3^+)}v_{cccc}\tilde{F}(t_3,t_2), \quad (7.27)$$

where $\frac{\delta n_{cc}(t)}{\delta U(t')} = 0$, because of the fact that the density of the core level is not affected from dynamical effects in the system. Eq.7.24 becomes an equation for $\tilde{F}$

$$\tilde{F}(t_1,t_2) = 1 - i\int_{t_1}^{t_2}dt_3\int_{t_3}^{t_2}dt_4\sum_{kl}\sum_{ij\neq cc}v_{cckl}\frac{\delta n_{ij}(t_4)}{\delta U_{kl}(t_3^+)}v_{ccij}\tilde{F}(t_3,t_2)$$
$$-\int_{t_1}^{t_2}dt_3\sum_{kl}v_{cckl}\frac{\delta\tilde{F}(t_3,t_2)}{\delta U_{kl}(t_3^+)}. \quad (7.28)$$

We have taken everywhere into account the fact that $\frac{\delta n_{cc}}{\delta U} = 0$. Eq.7.28 is the equation for the function $\tilde{F}$, where the self-interaction does no longer appear in the interaction with the density-response. As we will see, the solution is of the form $\tilde{F}(t_1,t_2) = e^{C(t_1,t_2)}$, where $C(t_1,t_2)$ is the cumulant.

7.1.2 The solution in the linear-response approximation

The task now is to determine the unknown function C. We start from eq.7.28 and write

$$\tilde{F}(t_1,t_2) = A(t_1,t_2)B(t_1,t_2) \quad (7.29)$$

or $C(t_1,t_2) = C_A(t_1,t_2) + C_B(t_1,t_2)$. Inserting this ansatz into eq.7.28 and using that

$$\frac{\delta\tilde{F}(t_3,t_2)}{\delta U_{kl}(t_3^+)} = A(t_3,t_2)\frac{\delta B(t_3,t_2)}{\delta U_{kl}(t_3^+)} + B(t_3,t_2)\frac{\delta A(t_3,t_2)}{\delta U_{kl}(t_3^+)}, \quad (7.30)$$

we obtain

$$A(t_1,t_2)B(t_1,t_2) = 1$$

$$
\begin{aligned}
&- i\int_{t_1}^{t_2} dt_3 \int_{t_3}^{t_2} dt_4 \sum_{kl}\sum_{ij\neq cc} v_{cckl}\frac{\delta n_{ij}(t_4)}{\delta U_{kl}(t_3^+)} v_{ccij} A(t_3,t_2)B(t_3,t_2) \\
&- \int_{t_1}^{t_2} dt_3 \sum_{kl} v_{cckl}(A(t_3,t_2)\frac{\delta B(t_3,t_2)}{\delta U_{kl}(t_3^+)} + B(t_3,t_2)\frac{\delta A(t_3,t_2)}{\delta U_{kl}(t_3^+)}).
\end{aligned} \tag{7.31}
$$

Deriving with respect to t_1, we obtain

$$
\begin{aligned}
&\frac{dA(t_1,t_2)}{dt_1}B(t_1,t_2) + \frac{dB(t_1,t_2)}{dt_1}A(t_1,t_2) \\
&= i\int_{t_1}^{t_2} dt_4 \sum_{kl}\sum_{ij\neq cc} v_{cckl}\frac{\delta n_{ij}(t_4)}{\delta U_{kl}(t_1^+)} v_{ccij} A(t_1,t_2)B(t_1,t_2) \\
&+ \sum_{kl} v_{cckl}(A(t_1,t_2)\frac{\delta B(t_1,t_2)}{\delta U_{kl}(t_1^+)} + B(t_1,t_2)\frac{\delta A(t_1,t_2)}{\delta U_{kl}(t_1^+)}).
\end{aligned} \tag{7.32}
$$

Concerning the time ordering, eq.7.11 is for $t_2 > t_1$. This gives one function $\tilde{F}$. We can write an analogous equation for $t_2 < t_1$. This would give another function $\tilde{F}$. We do not know whether the two are equal, probably they are not. So we get a different cumulant for $t_2 < t_1$ and $t_2 > t_1$. This is reasonable since the photoemission and inverse photoemission are different processes. Moreover, for the core-photoemission we are only interested in holes, where the decoupling from the equation for electrons is reasonable and safer than mixing components, which as pointed out earlier, is only rigorous on the Keldysh contour.

We can now choose any non-zero function A and then determine B. In our choice, the equation of motion of A for $t_1 < t_2$ is given by

$$
\frac{dA(t_1,t_2)}{dt_1} = i\theta(t_2-t_1)\int_{t_1}^{t_2} dt_4 \sum_{kl}\sum_{ij\neq cc} v_{cckl}\frac{\delta n_{ij}(t_4)}{\delta U_{kl}(t_1^+)} v_{ccij} A(t_1,t_2). \tag{7.33}
$$

Substituting with $A(t_1,t_2) = e^{C_A(t_1,t_2)}$ we obtain

$$
\frac{dC_A(t_1,t_2)}{dt_1} = i\theta(t_2-t_1)\int_{t_1}^{t_2} dt_4 \sum_{kl}\sum_{ij\neq cc} v_{cckl}\frac{\delta n_{ij}(t_4)}{\delta U_{kl}(t_1^+)} v_{ccij}. \tag{7.34}
$$

The last has the solution

$$
C_A(t_1,t_2) - C_A(t_2,t_2) = i\int_{t_2}^{t_1} d\tau\theta(t_2-\tau)\int_{\tau}^{t_2} dt_4 \sum_{kl}\sum_{ij\neq cc} v_{cckl}\frac{\delta n_{ij}(t_4)}{\delta U_{kl}(\tau)} v_{ccij}, \tag{7.35}
$$

where $C_A(t_2,t_2)$ is a pure function of t_2. This finally gives A as

$$
A(t_1,t_2) = e^{C_A(t_2,t_2)} e^{-i\int_{t_1}^{t_2} d\tau \int_{t_1}^{\tau} dt_4 \sum_{kl}\sum_{ij\neq cc} v_{cckl}\frac{\delta n_{ij}(\tau)}{\delta U_{kl}(t_4)} v_{ccij}}. \tag{7.36}
$$

For $\frac{\delta n}{\delta U} = 0$ we must obtain the Hartree-Fock solution G^{HX}. Therefore $C_A(t_2,t_2) = 0$. In the last equation we have also made use of the commutation property of the time integrals given in

eq.7.16. On the equilibrium limit $U \to 0$, $\frac{\delta n}{\delta U}$ is the linear response function χ^1 which depends on time differences since the system is static without the applied potential,

$$\lim_{U\to 0} \frac{\delta n_{ij}(\tau)}{\delta U_{kl}(t_4)} = \chi^1_{ijlk}(\tau - t_4). \tag{7.37}$$

With this approximation, A does no longer depend on U, and eq.7.32 has the solution $C_B = 0$ or $B = 1$. The final equilibrium solution is then given by

$$\begin{aligned} G_{cc}(t_1 - t_2) &= \theta(t_2 - t_1) G^{0H<}_{cc}(t_1 - t_2) e^{-i\int_{t_1}^{t_2} d\tau w_{cccc}(\tau;t_1)}, \\ w_{cccc}(\tau; t_1) &= -v_{cccc} n^0_0 + \sum_{ij\neq cc} v_{ccij}[\int dt_4 \sum_{ij} \chi^1_{ijlk}(\tau - t_4)\theta(\tau - t_4)\theta(t_4 - t_1) v_{cckl}]. \end{aligned} \tag{7.38}$$

The last is the cumulant solution in the linear-response approximation, also called second-order cumulant, since it is of second order in v. The cumulant is given by the matrix elements of the screened interaction w_{cccc} evaluated in the linear-response approximation. n^0 is the equilibrium density of the interacting system. Also the linear response in eq.7.38 takes only one contribution, namely $\tau > t_4$, while in the place of the perturbing potential the matrix elements of the Coulomb interaction appear. They play the role of an electrostatic potential from the core charge switched on at time t_1. The time t_1 appears as a parameter everywhere.

7.1.3 Discussion

Let us now summarize similar approaches concerning the response of a system with a localized state found in bibliography. In 1967 [89] Mahan had first introduced the approximation of an infinite hole mass in order to retrieve a perturbative expansion of the polarizability in all orders of a dynamical interaction. In 1969 Nozières et De Dominicis (ND) [82] have modeled the singularities near the threshold of x-ray absorption in metals through a model hamiltonian having introduced a scattering potential, the core-potential that we used, standing for the interaction between the deep state and the valence/conduction free states. Their scattering potential is also called transient potential since it starts acting on the system at the moment when the x-ray emission/absorption takes place. They study the valence spectrum of both x-ray absorption and emission while we have addressed only the absorption-case. They introduced a separable approximation for the scattering potential, which is something that we didn't have to do. They introduced the derivation of the cumulant solution using the linked cluster theorem. The cumulant includes the response function taken as a density-density correlation function, which is equivalent to the linear-response approximation once the equilibrium limit is taken. Their derivation is only valid in the steady state regime (arguments $t = t_1 - t_2$ large) where it is mentioned that the response must be slowly varying. In 1971 in [90] Combescot and Nozières made a different derivation of a cumulant based on Slater determinants again in the steady-state limit. They attributed a second peak of the absorption spectrum to electrons getting bound to the core-hole. This can be the role of the Auger phenomenon which allows for the relaxation of the valence electrons in the core-hole charge giving bound excitons. Then the outer electrons respond to a relaxed hole. There is the implication that non-linear effects in terms of an expansion in orders of the coupling constant, however they stop in the term which is equivalent to the linear-response approximation. They extract a low density limit of their final formula. In the same sense in 1982 Hänsch and Ekardt [91] pointed out the need to include electron-hole interaction in order to improve ND results.

In 1969 Langreth [83] modified the hamiltonian introduced by ND in order to include also coupling between the hole and a plasmon. He treated the single-particle scattering from the core-hole potential as a seperate process from the coupling to plasmon and showed that the coupling to a plasmon gives to the absorption spectrum the structure of multiple δ-peaks, while the effect of the interaction with individual electrons is to determine the position of the peaks. He got similar results in the framework of perturbation theory giving the cumulant in the lower order of the coupling constant, which is equivalent to the linear-response approximation in the equilibrium limit. In order to go beyond a plasmon model he derived the cumulant solution for a model accounting for the scattering from the core-hole potential in the homogeneous electron gas. It is mentioned that it is again not a necessary condition to remain in the lowest order of perturbation theory implying that non-linear effects might need to be taken into account. In 1970 Langreth [92] introduced the idea of the effect of two energy scales of electrons in the spectra, a fast and a slow-energy scale, in order to distinguish between the collective oscillations and single-particle scattering from a core-hole. The distinction between the two justifies the decoupling between those in model hamiltonians, as coupling might serve merely to renormalize the scattering potential. The distinction between fast and slow electrons provides interpretation of the different features attributed to particles and plasmons seen in different spectroscopy experiments. In 1972 Chang and Langreth [93] discussed interference effects from the coupling of fast electrons to slow plasmons and the implications of going to higher order in perturbation theory.

In 1970 Doniach and Sunjic [94] modeled the case where in XPS experiment a fast photoelectron is emitted while the initial core-hole has moved in a transient state followed by the readjustment of the valence electrons forming valence excitations. They used a model hamiltonian which includes two core-states in order to calculate the transition rate for a system with a transient hole state and reproduced the asymetry in the infrared peak of the spectrum which has been observed experimentally. In 1979 Bose, Kiehm and Lodge [95] modeled the energy dependence of the x-ray photoemission spectrum allowing for calculations for different photon momenta. In their model the bare interaction of ND is replaced by a screened interaction in the RPA which in principle includes also non-linear terms of the expansion to the bare interaction. They didn't make the approximation of a separable potential. They separated the screened interaction into a short-range and a long range part. The short range part of the interaction was treated in the linear-response approximation and is responsible for the infrared singularity. This part reflects the intrinsic part of the spectrum. The long-range part of the interaction gives contributions to the spectrum from multiple excitation processes of the valence electrons adding interference effects. They perform energy dependent calculations taking spectra of metallic systems for small and large value of the photon energy. Interference effects appear as cancellation between intrinsic and extrinsic effects for the low-energy photon, where the linear-response approximation should be valid. Instead, they vanish for the high-energy photon where the main plasmon satellite is enhanced.

Several efforts have been made over the past decades to describe the features of the spectra which correspond to several physical processes happening during the x-ray absorption and emission experiments. Such processes include valence electron response to the core-excitation, or looking deeper, the binding between the electrons and the core-hole leading to the relaxation of the hole through the formation of transient excitonic states. Another mechanism is the creation of plasmons as collective excitations of the valence electrons. All these mechanisms hide multiple par-

ticle excitations, which give rise to higher order correlation functions. However they have been usually treated in the linear-response approximation, using model hamiltonians to account for the non-linear effects. In this thesis we propose the direct treatment of non-linear effects introducing higher order correlation functions in the cumulant solution.

7.1.4 Cumulant solution beyond the linear-response approximation

Without the assumption $\frac{\delta A}{\delta U} = 0$ and therefore $C_B = 0$, the equation of motion for B is given by

$$A(t_1,t_2)\frac{dB(t_1,t_2)}{dt_1} = \sum_{kl} v_{cckl}(A(t_1,t_2)\frac{\delta B(t_1,t_2)}{\delta U_{kl}(t_1^+)} + B(t_1,t_2)\frac{\delta A(t_1,t_2)}{\delta U_{kl}(t_1^+)}), \tag{7.39}$$

where $t_2 > t_1$. The last equation still couples A and B. The second term of the equation requires the derivative of A with respect to the applied potential, which is evaluated from eq.7.36 as

$$\frac{\delta A(t_1,t_2)}{\delta U_{kl}(t_1^+)} = -A(t_1,t_2)i\int_{t_1}^{t_2} d\tau \int_{\tau}^{t_2} dt_4 \sum_{k'l'}\sum_{ij\neq cc} v_{cck'l'}\frac{\delta^2 n_{ij}(t_4)}{\delta U_{kl}(t_1^+)\delta U_{k'l'}(\tau)} v_{ccij}. \tag{7.40}$$

The last decouples A from B and gives the equation of motion for B

$$\begin{aligned}\frac{dB(t_1,t_2)}{dt_1} &= \sum_{kl} v_{cckl}\frac{\delta B(t_1,t_2)}{\delta U_{kl}(t_1^+)} \\ &- iB(t_1,t_2)\sum_{klk'l'}\sum_{ij\neq cc}\int_{t_1}^{t_2} d\tau\int_{\tau}^{t_2} dt_4 \frac{\delta^2 n_{ij}(t_4)}{\delta U_{kl}(t_1^+)\delta U_{k'l'}(\tau)} v_{cck'l'}v_{ccij}v_{cckl}.\end{aligned} \tag{7.41}$$

In order to proceed in the solution of eq.7.39 we again substitute with the product $B(t_1,t_2) = B'(t_1,t_2)C(t_1,t_2)$. Then we obtain again two equations, one for B' and one for C. B' now for $t_2 > t_1$ satisfies the equation

$$\frac{dB'(t_1,t_2)}{dt_1} = iB'(t_1,t_2)\sum_{klk'l'}\sum_{ij\neq cc}\int_{t_1}^{t_2} d\tau\int_{\tau}^{2} dt_4 \frac{\delta^2 n_{ij}(t_4)}{\delta U_{kl}(t_1^+)\delta U_{k'l'}(\tau)} v_{cck'l'}v_{ccij}v_{cckl}. \tag{7.42}$$

All the arguments that we used for the solution of the equation for A hold also for the case of B'. Following the same process as we did for A, we write $B'(t_1,t_2) = e^{C_{B'}(t_1,t_2)}$. For $t_2 > t_1$ we obtain $C_{B'}$ as

$$\begin{aligned}C_{B'}(t_1,t_2) &= C_{B'}(t_2,t_2) - i\int_{t_1}^{t_2} dt_4\int_{t_1}^{t_4} d\tau'\int_{t_1}^{\tau'} d\tau \\ &\sum_{klk'l'}\sum_{ij\neq cc}\frac{\delta^2 n_{ij}(t_4)}{\delta U_{kl}(\tau^+)\delta U_{k'l'}(\tau')} v_{cck'l'}v_{ccij}v_{cckl}.\end{aligned} \tag{7.43}$$

In the last equation we have again applied the commutation of the integration over times (eq.7.44) generalized to multiple time integrals as

$$\theta(t_2-t_1)\int_{t_1}^{t_2} d\tau\int_{\tau}^{t_2} d\tau'\int_{\tau'}^{t_2} dt_4 = \theta(t_2-t_1)\int_{t_1}^{t_2} dt_4\int_{t_1}^{t_4} d\tau'\int_{t_1}^{\tau'} d\tau. \tag{7.44}$$

The equation for C is given by

$$\frac{dC(t_1,t_2)}{dt_1}B'(t_1,t_2)=\sum_{kl}v_{cckl}(\frac{\delta C(t_1,t_2)}{\delta U_{kl}(t_1^+)}B'(t_1,t_2)+C(t_1,t_2)\frac{\delta B'(t_1,t_2)}{\delta U_{kl}(t_1^+)}), \tag{7.45}$$

for $t_2>t_1$, where again C is coupled to B'. We can decouple C from B' introducing the derivative of B' (eq.7.43) evaluated as

$$\frac{\delta B'(t_1,t_2)}{\delta U_{kl}(t_1^+)}=-iB'(t_1,t_2)$$
$$\sum_{k''l''k'l'}\sum_{ij\neq cc}\int_{t_1}^{t_2}d\tau\int_{\tau}^{t_2}d\tau'\int_{\tau'}^{t_2}dt_4\frac{\delta^3 n_{ij}(t_4)}{\delta U_{kl}(t_1^+)\delta U_{k'l'}(\tau')\delta U_{k''l''}(\tau)}v_{cck'l'}v_{ccij}v_{cck''l''}. \tag{7.46}$$

Using the last relation, we obtain the equation of motion for C for $t_2>t_1$

$$\frac{dC(t_1,t_2)}{dt_1}=\sum_{kl}v_{cckl}\frac{\delta C(t_1,t_2)}{\delta U_{kl}(t_1^+)}-iC(t_1,t_2)$$
$$\sum_{klk''l''k'l'}\sum_{ij\neq cc}\int_{t_1}^{t_2}d\tau\int_{\tau}^{t_2}d\tau'\int_{\tau'}^{t_2}dt_4\frac{\delta^3 n_{ij}(t_4)}{\delta U_{kl}(t_1^+)\delta U_{k'l'}(\tau')\delta U_{k''l''}(\tau)}v_{cck'l'}v_{ccij}v_{cck''l''}v_{cckl}. \tag{7.47}$$

We follow the same process assuming that $C(t_1,t_2)=C'(t_1,t_2)D(t_1,t_2)$, where $C'(t_1,t_2)=e^{C_{C'}(t_1,t_2)}$ and $C_{C'}(t_1,t_2)$ for $t_2>t_1$ is given by

$$C_{C'}(t_1,t_2)=C_{C'}(t_2,t_2)-i\theta(t_2-t_1)\int_{t_1}^{t_2}dt_4\int_{t_1}^{t_4}d\tau'\int_{t_1}^{\tau'}d\tau''\int_{t_1}^{\tau''}d\tau$$
$$\sum_{klk''l''k'l'}\sum_{ij\neq cc}\frac{\delta^3 n_{ij}(t_4)}{\delta U_{kl}(\tau^+)\delta U_{k'l'}(\tau')\delta U_{k''l''}(\tau'')}v_{cck'l'}v_{ccij}v_{cck''l''}v_{cckl}, \tag{7.48}$$

where we used the commutation property of the time integrals

$$\theta(t_2-t_1)\int_{t_1}^{t_2}d\tau\int_{\tau}^{t_2}d\tau''\int_{\tau''}^{t_2}d\tau'\int_{\tau'}^{t_2}dt_4=\theta(t_2-t_1)\int_{t_1}^{t_2}dt_4\int_{t_1}^{t_4}d\tau'\int_{t_1}^{\tau'}d\tau''\int_{t_1}^{\tau''}d\tau. \tag{7.49}$$

The contribution for $t_2<t_1$ is taken from a similar expression. The equation for D for $t_2>t_1$ becomes

$$\frac{dD(t_1,t_2)}{dt_1}=\sum_{kl}v_{cckl}\frac{\delta D(t_1,t_2)}{\delta U_{kl}(t_1^+)}-i\sum_{kl}v_{cckl}\int_{t_1}^{t_2}d\tau\int_{\tau}^{t_2}d\tau''\int_{\tau''}^{t_2}d\tau'\int_{\tau'}^{t_2}dt_4$$
$$\sum_{k'''l'''k''l''k'l'}\sum_{ij\neq cc}\frac{\delta^4 n_{ij}(t_4)}{\delta U_{k'''l'''}(\tau)\delta U_{k'l'}(\tau')\delta U_{k''l''}(\tau'')\delta U_{kl}(t_1^+)}v_{cck'l'}v_{ccij}v_{cck''l''}v_{cck'''l'''}D(t_1,t_2). \tag{7.50}$$

Grouping together the solutions from eq.7.36, 7.43, 7.43, one obtains the solution as a product

$$G_{cc}(t_1,t_2)=\theta(t_2-t_1)e^{C(t_2,t_2)}G_{cc}^{HX<}(t_1,t_2)A(t_1,t_2)B'(t_1,t_2)C'(t_1,t_2)... \tag{7.51}$$

The $\theta-$function allows only for $t_2 > t_1$. When the density desponse $\frac{\delta^i n}{\delta U^i}$ is zero, the Green's function must be equal to the propagator of the Hartree-Fock system. Therefore $C(t_2, t_2) = 0$. Finally the cumulant for $t_2 > t_1$ is given by

$$\begin{aligned} C(t_1, t_2) = -i \int_{t_1}^{t_2} dt \sum_{ij \neq cc} v_{ccij} \big[& n_{ij}(t) \\ & + \int d\tau \sum_{kl} \frac{\delta n_{ij}(t)}{\delta U_{kl}(\tau)} \theta(t-\tau)\theta(\tau - t_1) v_{cckl} \\ & + \int d\tau' \int d\tau \sum_{k'l'kl} \frac{\delta^2 n_{ij}(t)}{\delta U_{kl}(\tau)\delta U_{k'l'}(\tau')} \theta(t-\tau')\theta(\tau'-\tau) v_{cck'l'} v_{cckl} \theta(\tau - t_1) \\ & + \dots \big]. \end{aligned} \tag{7.52}$$

In the last expression we see that the matrix elements of the Coulomb interaction always appear together with $\theta-$functions saying that the times of the applied potential are always later than the time t_1. Moreover the variation of the density always happens at later times than the times of the applied potential. The matrix elements of the Coulomb interaction can be written as a classical potential from the core occupation number switched on at times t_1,

$$V^c_{kl}(\tau; t_1) = v_{cckl}\theta(\tau - t_1), \tag{7.53}$$

where t_1 appears as a parameter and can be interpreted for example as the time when a core-electron is ejected from the material in XPS experiment. Higher order derivatives are given by the response of the density to potentials varied at different times. However there is no reason to assume that the time ordering of the applied potential will affect the variation of the density. Making the assumption that $\frac{\delta^2 n_{ij}(t)}{\delta U_{kl}(\tau)\delta U_{k'l'}(\tau')}|_{\tau<\tau'} = \frac{\delta^2 n_{ij}(t)}{\delta U_{kl}(\tau)\delta U_{k'l'}(\tau')}|_{\tau>\tau'}$ the following property for the integration over times holds

$$\int_{t_1}^{t_2} dt \int_{t_1}^{t} d\tau \int_{t_1}^{\tau} d\tau' = \frac{1}{2} \int_{t_1}^{t_2} dt \int_{t_1}^{t} d\tau \int_{t_1}^{t} d\tau'. \tag{7.54}$$

The last equation can be generalized to higher order derivatives. The n^{th} order derivative allows for $(n-1)!$ permutations of the variations of the applied potential taken at $n-1$ different times. The times that appear in the derivative of the density with respect to the applied potential are always later than the time t_1 and this preserves the interpretation of the classical potential from the core charge switched on at time t_1 which can be complemented with the potential being switched off at time t when the variation of the density takes place,

$$V^c_{kl}(\tau; t_1, t) = v_{cckl}\theta(t-\tau)\theta(\tau - t_1). \tag{7.55}$$

Eq.7.52 can be written as

$$\begin{aligned} C(t_1, t_2) = -i \int_{t_1}^{t_2} dt \sum_{ij \neq cc} v_{ccij} \big[& n_{ij}(t) \\ & + \int_{t_1}^{t} d\tau \sum_{kl} \frac{\delta n_{ij}(t)}{\delta U_{kl}(\tau)} v_{cckl} \\ & + \frac{1}{2} \int_{t_1}^{t} d\tau' \int_{t_1}^{t} d\tau \sum_{k'l'kl} \frac{\delta^2 n_{ij}(t)}{\delta U_{kl}(\tau)\delta U_{k'l'}(\tau')} v_{cck'l'} v_{cckl} \end{aligned}$$

$$+ \dots \big]. \tag{7.56}$$

Taking the equilibrium limit we write the cumulant as

$$\begin{aligned} C(t_1,t_2) = -i \int_{t_1}^{t_2} dt \sum_{ij\neq cc} v_{ccij} \big[& n^0_{ij} \\ & + \int_{t_1}^{t} d\tau \sum_{kl} \chi^1_{ijlk}(t,\tau) v_{cckl} \\ & + \int_{t_1}^{t} d\tau' \int_{t_1}^{t} d\tau \sum_{k'l'kl} \chi^2_{ijlkl'k'}(t,\tau,\tau') v_{cck'l'} v_{cckl} \\ & + \dots \big]. \end{aligned} \tag{7.57}$$

The higher order response functions appearing in the last expression can be summed as

$$\begin{aligned} n_{ij}(t;t_1) = n^0_{ij} & + \int d\tau \sum_{kl} \chi^1_{ijlk}(t,\tau) V^c_{kl}(\tau;t_1,t) \\ & + \int d\tau' \int d\tau \sum_{k'l'kl} \chi^2_{ijlkl'k'}(t,\tau,\tau') V^c_{k'l'}(\tau;t_1,t) V^c_{kl}(\tau';t_1,t) + \dots . \end{aligned} \tag{7.58}$$

The fact that the response functions are causal is hidden in the core potential being switched off at the time of the variation of the density t. Eq.7.58 gives the induced density from the core potential switched on at time t_1 and switched off at time t. The core potential depends on the core density switched on and off at times t_1 and t respectively. Therefore the time-dependent core occupation can be taken to be the variable that determines the solution. This is in the sense of the parametrization of von Barth and Almbladh who introduced a fractional occupation number of the c core-orbitals[96]. We can finally write the solution in the form

$$G^<_c(t_1,t_2)\theta(t_2-t_1) = G^<_{0c}(t_1,t_2)\theta(t_2-t_1) e^{-i\int_{t_1}^{t_2} dt \sum_{ij\neq cc} v_{ccij} n_{ij}(t;t_1)}. \tag{7.59}$$

The last expression shows that the variation of the charge of a localized level switched on at some time t_1 and switched off at time t has the effect of a classical potential standing for the interaction with the induced time-dependent density. In comparison to the solution in the linear-response approximation (eq.7.38), in this case the screening of the interaction comes from the non-linear effects included in the time-dependent density

$$w^{nl}_{cccc}(t;t_1) = \sum_{ij\neq cc} v_{ccij}(n_{ij}(t;t_1)) - \sum_{ij} v_{ccij} n^0_{ij}. \tag{7.60}$$

7.1.5 Discussion

Looking back in the bibliography we found several efforts to introduce non-linear effects in x-ray absorption and emission experiments. In 1962 Kubo [97] was the first to formulate the expression of a cumulant with higher order correlation functions standing for multi-particle excitations. In 1971 Müller-Hartmann et al. [98] also addressed the problem of probing localized states in metallic systems. They proposed two approaches. The first is based on a ND hamiltonian for scattering from the electron gas, from which they propose cumulant getting contributions from all orders to

the scattering potential, which at the end they drop and they use the linear-response approximation. They proposed treating scattering from a boson, transforming electron-hole pairs into a boson. They discussed the time evolution of the scattering potential, specifically what are the implications of only switching-on at $t = -\infty$ or both switching-on and off beyond the adiabatic approximation compared to the adiabatic approximation where the ground-state of the hamiltonian is slightly affected from the transient behavior of the potential.

In 1975 Mahan [99] proposed a non-linear cumulant given by an expansion in the core-hole potential. In 1982 Mahan [100] used the ND hamiltonian aiming at the description of conduction electrons excitations due to the core-hole potential. He used a non-linear cumulant with an induced potential including all orders of polarization contributions, standing for higher order correlation functions contributions. He doesn't solve the equation of motion of the Green's function, but he follows an equivalent process based on the evaluation of the one-body Green's function passing from a final state hamiltonian with one electron less. His derivation is also based on the assumption of a separable potential. Based on Mahan's idea for introducing higher order excitations and on the von Barth and Ceberbaum's idea (1981) [101] to obtain the polarizability from the BSE, in 2009 Harbola and Mukamel [102] derived a set of equations for the two-body Green's function and the scattering matrix between two valence electrons in the presence of two core-holes as a way to introduce non-linear contributions to the x-ray spectra. In 2005 Mukamel [103] claimed that higher order response functions need to be taken into account in the theoretical calculation of the x-ray photoemission spectra. He performed calculations of higher order response functions both starting from an ND hamiltonian and a model hamiltonian standing for electron-boson coupling. Non-linear response on the Keldysh contour has been published in 2009 [104].

In 2015 [105] Silkin et al. used the cumulant in the linear-response approximation to discuss ultrafast phenomena in photoemission process. They studied metallic surfaces (Cu and Ag) and attributed the presence of density oscillations to the presence of preexistent states which form a transient regime preceding the steady state regime which appears at later times. Preexistent states are additional states formed at the moment of the creation of the hole-charge and they form transient states for the relaxation of the hole. The transient regime is material specific. In Ag they found that the transient regime is long, while in Cu it is almost non-existent. The underlying theory is explained in the review published by Gumhalter in 2012 [106]. In 2005 [107] Gumhalter published a cumulant expansion in all orders to the core-potential starting from a model hamiltonian which includes both scattering from the core-hole potential and the coupling to plasmons. In 2016 [108] Gumhalter et al. argued that for the case of a core-hole the sum of the first and the second order cumulant (equivalent to the linear-response approximation in the equilibrium limit) from the electron-plasmon model is the exact solution due to the fact that the hole has no dynamical behavior and therefore recoil of the photoelectron from the plasmon is neglected. They apply it on top of the G^0W^0 approximation to calculate the spectral function of Si and claim that the position of the plasmon satellites in silicon improves.

7.1.6 The evaluation of non-linear contributions to the density

The evaluation of the higher order response to the core hole perturbation can be done parametrizing the matrix elements of the Coulomb interaction with the core occupation number n_c as $v_{ccij} = n_c \bar{v}_{ccij}$. The non-linear contributions to the density can be taken summing the response functions with the matrix elements of the Coulomb interaction, keeping the core occupation number as a

parameter.

$$n^1_{ij}(t_1,t) = \int_{t_1}^{t} d\tau \sum_{kl} \chi^1_{ijlk}(t,\tau) n_c \bar{v}_{cckl} = \bar{\chi}^1_{ij}(t_1,t) n_c, \tag{7.61}$$

where $\bar{\chi}^1_{ij}(t_1,t) = \int_{t_1}^{t} d\tau \sum_{kl} \chi^1_{ijlk}(t,\tau)\bar{v}_{cckl}$

$$n^2_{ij}(t_1,t) = \int_{t_1}^{t} d\tau' \int_{t_1}^{t} d\tau \sum_{k'l'kl} \chi^2_{ijlkl'k'}(t,\tau,\tau') n_c^2 \bar{v}_{cck'l'} \bar{v}_{cckl} = \bar{\chi}^2_{ij}((t_1,t)) n_c^2, \tag{7.62}$$

and $\bar{\chi}^2_{ij}((t_1,t)) = \int_{t_1}^{t} d\tau' \int_{t_1}^{t} d\tau \sum_{k'l'kl} \chi^2_{ijlkl'k'}(t,\tau,\tau')\bar{v}_{cck'l'}\bar{v}_{cckl}$. Higher order of the response χ^n, integrated over time correspond to $\bar{\chi}^n$. This leads to the expansion of the density around zero values of the core occupation number

$$n_{ij}(t) = n^0_{ij}(t) + \bar{\chi}^1_{ij}(t,t_1) n_c + \bar{\chi}^2_{ij}(t,t_1) n_c^2 + \ldots. \tag{7.63}$$

The last equation shows that for a localized level c all non-linear effects are given from the expansion of the density in the occupation number of the level c. $\bar{\chi}^1_{ij}(t,t_1)$ is the linear response for $n_c = 0$,

$$\bar{\chi}^1_{ij}(t,t_1) = \frac{dn_{ij}(t,t_1)}{dn_c}|_{n_c=0}. \tag{7.64}$$

Then the $\bar{\chi}^2_{ij}(t,t_1)$ is evaluated from the derivative of the linear response in the presence of the core charge taken with respect to the core occupation,

$$\bar{\chi}^2_{ij}(\tau) = \frac{d^2 n_{ij}(\tau)}{dn_c^2}|_{n_c=0} = \frac{d\bar{\chi}^1(\tau,n_c)}{dn_c}|_{n_c=0}. \tag{7.65}$$

The last equation shows that once the linear response $\bar{\chi}^1(n_c)$ evaluated in the presence of the core charge $n_c \neq 0$ is different from the linear response evaluated in the absence of the core charge $n_c = 0$, it means that higher orders of the response are different from zero and therefore non-linear effects need to be taken into account.

In 1976 [96] C.O. Almbladh and U. von Barth introduced the idea to separate the density of the valence and the core electrons and vary the density of the core electrons in the system. They have used DFT to obtain a polarization potential as a correction to the classical potential standing for the interaction with the induced density. This allows them to parametrize the self-energy with the core-occupation number and interpolate it with a curve allowing for the calculation of second order self-energy contributions to metals, showing that it grows non-linearly with increasing core-hole charge by one. In the same sense Arnau [109] in 1997 suggested that DFT is powerful tool to obtain the induced valence density including also non-linear response to the core-hole charge of the valence electrons in metallic systems.

7.2 Spectral features from a core-hole charge

Creating a core-hole charge with x-rays can add features to the spectra of systems with localized electrons. Some work has been done in order to understand how the system reacts and suggest spectral features that emerge. Such additional features could be included in the non-linear cumulant of eq.7.59. In this section we will summarize previous works that go in this direction.

In 1977 Grebennikov, Babanov and Sokolov in [110], [111] studied the relaxation effects on the x-ray photoemission, x-ray emission and absorption spectra of systems with localized valence-conduction electrons (d-f) for different values of the hole occupation. The hole occupation is reflected in the conduction band filling and therefore to the position of the Fermi level appearing as a parameter in the calculation. They compare between the case of no correlation (no electron-hole interaction, Koopmans' theorem), an adiabatic approximation (relaxation to a static core-hole potential) and the effect of relaxation to the core-hole suddenly switched on at time $t = 0$. They treated the fully time-dependent phenomena in order to study relaxation effects in contrary to ND that only looked at the steady state regime. They treated the core level as a low-lying level and the outer electrons as localized Wannier orbitals standing for localized d-electrons. They introduced a Hubbard-like hamiltonian which accounts for the on-site screened Coulomb interaction between valence electrons and the deep core-level. The interaction is screened by the fast s-p electrons and appears as a parameter. They derived a phase-shift which accounts for the scattering of the localized valence electrons from the core-hole. They dropped indices that introduce scattering of conduction electrons between different lattice positions. From the phase shift, they calculate valence spectra of x-ray absorption, emission and core-photoemission spectra for different values of the interaction. In the uncorrelated case x-ray absorption and emission are symmetric with respect to the position of the valence-band. The adiabatic approximation for both absorption and emission shows a transfer of weight towards the lower edge of the band that can be attributed to the core-hole attraction which becomes a singularity for large values of the interaction. Lowering the values of the interaction the adiabatic spectrum tends towards the uncorrelated spectrum. The filling of the conduction band doesn't affect the shape and position of the adiabatic spectrum. In the case of the sudden creation of the core-hole, the combined spectra show a singularity at the position of the Fermi-level. Changing the filling of the band, the position of the singularity gets shifted accordingly. Only away from the Fermi level, spectra resemble to the uncorrelated spectrum. Increasing the value of the interaction there is a bigger transfer of weight from the uncorrelated spectrum towards the singularity at the Fermi level. They also introduce a third parameter which is the core-hole life-time standing for the fact that at later times the core-hole will be recombined with an electron from the outer shell. The effect of the core-hole life-time is to replace the singularity in the spectrum with a peak of finite height. In the photoemission spectrum there is a critical value of the interaction where an additional structure appears at higher energies in the spectrum. For such values of the interaction starting from an empty conduction band and increasing the band filling there is transfer of weight between the main peak and the additional local level. When the filling of the conduction band maximizes there is a total transfer of weight between the two peaks. This gives a clue about a transient spectrum depending on the portion of hole added in the system. The presence of the double peak in the photoemission spectrum is attributed to the transition of the electron to a local level which appears while increasing the values of the interaction, and the energy difference between the two peaks in the spectrum is equivalent to the energy of the removal from the local level.

In 2001 in [112] Privalov, Gel'mukhanov, and Ågren extend the model of Grebennikov, Babanov and Sokolov to study the dependence of relaxation effects on the size of the system. For this purpose they used atomic chains. They propose the calculation of the phase shift from the interaction with the core-hole potential solving a set of linear equations based on the expansion of the valence wavefunctions in atomic orbitals. The effect of the interaction in their spectra is to create a structure which consists of multiple discrete peaks that stand for the density of empty and occupied molecular states. In the x-ray absorption spectra, the relaxation effects are responsible for the transfer of weight to the egde of the absorption spectrum. When the valence band is empty the adiabatic approximation coincides with the relaxed calculation reflecting the density of unoccupied states in the system, giving the structure of a main peak and a series of satellites. Increasing the filling of the conduction band the edge of the absorption is shifted to higher energies and the effect of the relaxation is to create the main peak at the edge. The x-ray emission spectra of the relaxed calculation coincides with the adiabatic approximation only when the band is completely filled reflecting the density of occupied valence states. Decreasing the filling of the band, the edge of the spectrum is shifted to lower energies. The adiabatic approximation is responsible for the lower edge of the x-ray emission spectrum that can be attributed to the hole attraction. On the other hand the relaxation is responsible for the enhancement of the peak at the threshold of the x-ray emission spectra. The double peak structure (lower edge and threshold) is visible only for large number of atoms (> 30) while for small number of atoms the spectrum takes the structure of equal height discrete peaks with low intensity satellites at lower energies which are indicative of the presence of excitons due to transitions between highest occupied and lowest unoccupied levels (HOMO and LUMO). In the x-ray photoemission spectra for small number of atoms there is a main peak attributed to the transition from the deep core-level, while decreasing the filling of the valence band towards 0 there is the creation of a local (or excitonic) level at higher energies. Again the difference between the excitonic level and the main peak is attributed to the energy for the transition from the local level to the LUMO. Close to the main peak there are also shake-up satellites corresponding to transitions from the HOMO. The authors also study the time propagation of the phase shift and they extract three time scales. One is the small time scale when the formation of the molecular levels takes place. The second is the later time scale where the interaction affects the spectrum and the x-ray absorption intensity is redistributed towards the edge of the band. At larger times there is the singularity appearing at the edge of the x-ray emission spectra reflecting the screening of the core-hole field from valence electrons. In [113] they also study the relaxation effects of the Inelastic X-ray Scattering for systems with finite number of atoms. For this purpose they generalize their formalism to account for scattering of photons between different atoms passing from the creation and the scattering of a core-hole. This generalization requires the use of higher order correlation functions reflecting higher complexity of the scattering process. Such processes would give non-linear contributions in the equilibrium limit. They explain that the relaxation to the core-hole field becomes important for partial filling of the valence bands since relaxation happens through the formation of valence electron-hole pairs. They also discuss the effect of the finite lifetime of the core-hole and the effect of the detuning of the excitation frequency from the x-ray absorption edge being indicative of the duration of the interaction between the valence electrons and the core-hole.

7.3 Numerical evaluation of non-linear screening in real systems

The need to take the presence of the core hole into account has been realized in particular for molecules. In 2004 Brena et al. [114] used a combination of static $\Delta-$DFT and TDDFT in order to interpret the experimental 1s x-ray photoelectron spectroscopy (XPS) for the H_2Pc molecule. They applied the $\Delta-$DFT method on the calculation of the ionization potentials as the difference between the ground-state with and without a core hole for the different carbon atoms. Later (2005) [115] Brena, Carniato and Luo calculated H_2Pc and benzene explaining that they put the core-hole using the $Z+1$ approach. In this approach the excited state of an atom is taken from the ionized atom of higher-by-1 atomic number. The $\Delta-$DFT gave them the main peaks from the different species of carbon atoms in the molecule. Then they use TDDFT in order to obtain the shake-up (valence response) contributions for the two species of carbon atoms so that the intensities of the respective peaks give the correct molecular ratio. They have tried different functionals [115] and despite the qualitative differences, they found that they all succeed to interpret the experimental spectrum. They also compared with time-dependent Hartree-Fock approximation and found that it fails since it lacks in the description of correlation.

Here, we would like to build on these successes and on our general derivation in order to bring these ideas to ab initio calculations in solids using the framework of the GW +cumulant approach. In DFT the ground-state density is obtained solving the Kohn-Sham equations. There are two ways to obtain the time-dependent density. One is from the MBPT solving for the Green's function. The other way is propagating the Kohn-Sham equations in time. In both cases the linear response is usually obtained, since to go beyond involves usually complicated schemes and the evaluation of matrices of higher dimensions. However as eq.7.65 shows, a first indication of non-linear effects comes from the evaluation of the linear response in the presence of a core charge. In this section we briefly discuss the real-time TDDFT approach which solves the time-dependent Kohn-Sham equations in the presence of core charge. In the next section we will show some preliminary results to see the signatures of non-linear effects.

7.3.1 The time-dependent density from RTTDDFT

The discussion in this section is based on the real-time TDDFT approach (RTTDDFT) developed in the University of Washington by Joshua Kas and John Rehr on the SIESTA code [16]. In order to do RTTDDFT one solves the time-dependent Kohn-Sham Schrödinger equation for the time-dependent single-particle Kohn-Sham wavefunctions,

$$H^{KS}(x,t)\phi_i(x,t) = i\frac{\partial}{\partial t}\phi_i(x,t). \tag{7.66}$$

$H^{KS}(x,t)$ is the time-dependent Kohn-Sham hamiltonian,

$$H(x,t) = T(x) + V^{c-h}(x,t) + V^H(x,t) + V^{xc}(x,t), \tag{7.67}$$

where $V^H(x,t) = \int dx' \frac{\rho(x',t)}{|x-x'|}$ is the time-dependent Hartree potential and $V^{xc}(x,t;\rho(x,t))$ is the time-dependent exchange-correlation potential. This equation is propagated in time using discrete time steps. The potentials V^H and V^{xc} are evaluated from the density of the previous time-step.

$V^{c-h}(x,t)$ is the time-dependent core potential created by changing the core charge at time $t=0$ and therefore switching on a core potential for all later times,

$$V^{c-h}(x,t) = \int dx' \frac{n_c(x')}{|x-x'|}\theta(t). \tag{7.68}$$

$n_c(x)$ is the density of the core hole

$$n_c(x) = n_h \phi_c^{0\star}(x)\phi_c^0(x) \tag{7.69}$$

where n_h is a prefactor weighting the charge of the fractional core-hole. The time-dependent Kohn-Sham wavefunctions can be obtained from the time-dependent projection $A_i(t)$ on the static basis $\phi_i^0(x)$ obtained from a $\Delta-$SCF calculation carried out in the presence of the core-charge n_h,

$$\phi_i(x,t) = \sum_j A_i^j(t)\phi_j^0(x)e^{i\epsilon_j t}. \tag{7.70}$$

Using the time-dependent Kohn-Sham orbitals one obtains the time dependent density as

$$\rho(x,t) = \sum_i |\phi_i(x,t)|^2. \tag{7.71}$$

7.3.2 Preliminary calculations on real systems

In order to illustrate the effect of a core-hole, I have calculated the time-dependent density (eq.7.71) after the switch of a core-hole as a function of time for three different materials. From the density change, the induced potential is obtained as

$$\delta V(x,t;n_h) = \int dx' \frac{\delta\rho(x',t;n_h)}{|x-x'|}, \tag{7.72}$$

where $\delta\rho = \rho - n_0$ is obtained from eq.7.71 for a given core hole occupation n_h and shape $|\phi_c^0(x)|^2$. Then we evaluate the ratio

$$\frac{\delta V(x,t;n_h)}{n_h}. \tag{7.73}$$

In the linear-response approximation, the last is equal to the linear response coefficient evaluated in the absence of the core-charge

$$\delta V(x,t;n_h) = n_h \frac{dV^i(x,t;n_h)}{dn_h}|_{n_h=0}. \tag{7.74}$$

Variations of the response with respect to the core-occupation number indicate non-linear effects.

In fig.7.1 I show the induced potential in the steady state regime divided by the occupation number of the core-hole, as given by eq.7.73 calculated in frequency space for bulk silicon, sodium and cerium Oxide CeO_2. For small values of the core-hole n_h in all cases appears a dominant peak which we can attribute to the oscillations of delocalized valence electrons.

The spectrum of Si (fig.7.1a) has a main peak, around 18 eV. This is slightly higher than the plasmon frequency of 16.8 eV, because the response to the localized perturbation integrates over the plasmon dispersion. The spectrum remains very stable with respect to the core hole occupation. There is only a slight decrease of the main peak for large n_h (close to 2), a minor variation of the width, and the appearance of a small peak around 65 eV. The height and weight of the second peak increases, as we increase the portion of the hole in the system. This second peak might be a second mechanism of the response, since it appears increasing the strength of the perturbation and it seems that there is transfer of weight from the main peak to this satellite. However, we will have to investigate its origin further. Altogether, we observe that in silicon, where the cumulant in the linear-response approximation is already good [10], the change of the spectrum varying the hole charge is fortunately negligible, and the non-linear corrections from our expression will not worsen the agreement.

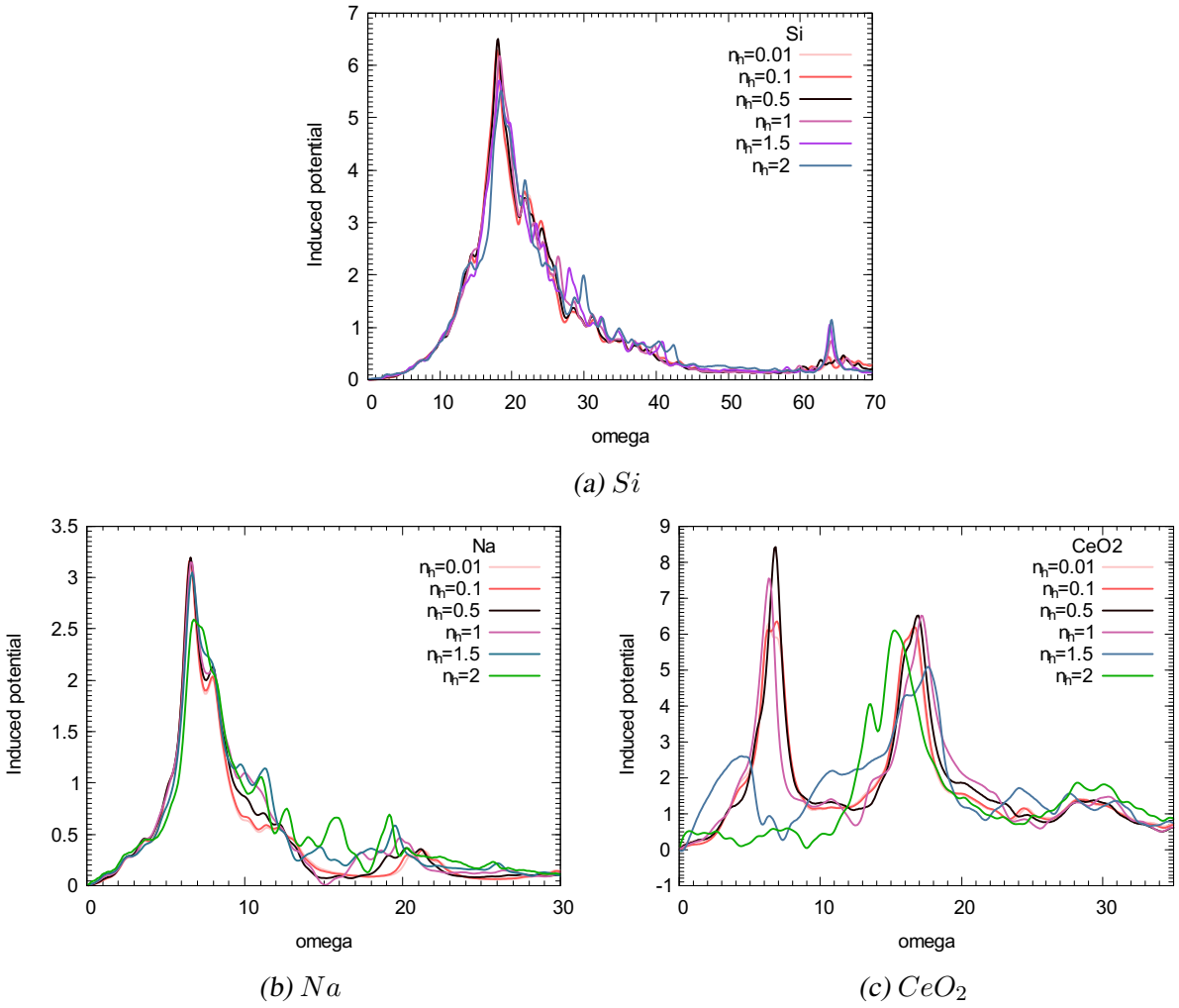

(a) Si *(b)* Na *(c)* CeO_2

Fig. 7.1: The induced potential in frequency space for different portions of a positive charge n_h introduced in the system.

In sodium the main plasmon peak above 6 eV remains stable with the core hole charge, but a structure develops on its high energy side (around 1 eV and above). Still the changes remain moderate even for $n_h = 2$.

In CeO_2 changes are more pronounced; already for $n_h = 0.5$ one can clearly distinguish an enhancement of the peak around 6 eV. For $n_h = 2$ the spectrum is completely modified. The 6 eV peak as well as the peak around 17 eV give rise to satellites in the XPS spectrum, which can be seen in the experiment. They are already explained by a linear response cumulant [116], but it might be worthwhile to check whether the non-linear effects will improve the positions, which do not come out perfectly in the linear response. Calculations have also been started by Stefano di Sabatino [117] for nickel, but they are based on the $Z + 1$ approach. One may expect that the presence of the hole, which translates into the non-linear effects, is crucial in spectra like the XPS of nickel, where the 6 eV satellite is explained as a hole-hole bound state.

Summary

In this chapter we have extended the cumulant solution to account also for non-linear screening of the core charge appearing in the core-electron photoemission. In order to evaluate the non-linear effects on the response to the core-hole charge we propose two different approaches for solids, namely the solution of the equation of motion of the linear response function using TDDFT for zero and finite core-hole charge and the RTTDDFT approach, which involves the solution of the Schrödinger equation within TDDFT for fractional core-hole occupation. Preliminary results suggest that non-linear effects are not important in simple metals and semiconductors, but might be important in more complex materials.

8

Vertex corrections from TDDFT and beyond

In the previous chapters we have used TDDFT to calculate the density response in the screened interaction w. One example is Chap.7. There we derived the non-linear cumulant, where the time-dependent density appears, which can be obtained from TDDFT. In the literature, TDDFT has also been introduced in the many-body perturbation theory framework to go beyond the GW approximation. For example Del Sole, Reining and Godby in [67] have used TDDFT to obtain an approximate vertex function Γ, which corrects the self-energy with respect to the GW approximation as $\Sigma = iGW\Gamma$. This vertex function Γ has only two arguments because V^{KS} is local. However, the true self-energy is non-local and therefore the true vertex Γ has three arguments. In this chapter we want to estimate the effect of this non-locality.

In this chapter we will introduce screening from the Kohn-Sham potential and the corresponding vertex function. We will evaluate vertex corrections from a model self-energy, which uses a non-local operator to shift the energies of the conduction states opening the Kohn-Sham band-gap of DFT. We will discuss the effects of non-locality on the photoemission of a localized state.

8.1 Vertex corrections from the Kohn-Sham system

We start from the equation of motion for the Green's function, which is equivalent to the Kadanoff-Baym equation (KBE)

$$[i\frac{\partial}{\partial t_1} - h(x_1) - V^H(1)]G(12) - iv(1\bar{3})\frac{\delta G(12)}{\delta U(\bar{3}^+)} = \delta(12). \tag{8.1}$$

We remind the fact that here U is an external potential. Then we screen the interaction with the Kohn-Sham potential, which contains also the external pontential U. Eq.8.1 becomes

$$[i\frac{d}{dt_1} - h(x_1) - V^H(1)]G(12) - i\frac{\delta G(12)}{\delta V^{KS}(\bar{4})}\tilde{w}(1^+\bar{4}) = \delta(12), \tag{8.2}$$

where the interaction, screened with the Kohn-Sham potential is given by

$$\tilde{w}(1^+4) = v(1\bar{3})\frac{\delta V^{KS}(4)}{\delta U(\bar{3}^+)}. \tag{8.3}$$

The KBE which corresponds to eq.8.2 is given by the differential equation

$$G(12) = G^H(12) + iG^H(1\bar{1})\tilde{w}(\bar{1}^+\bar{4})\frac{\delta G(\bar{1}2)}{\delta V^{KS}(\bar{4})}, \tag{8.4}$$

where G^H includes also the external potential. The derivative that appears in the KBE can be rewritten as

$$\frac{\delta G(12)}{\delta V^{KS}(4)} = G(1\bar{1})\Gamma^{KS}(\bar{1}\bar{2}4)G(\bar{2}2), \tag{8.5}$$

where

$$\Gamma^{KS}(\bar{1}\bar{2}4) = -\frac{\delta G^{-1}(\bar{1}\bar{2})}{\delta V^{KS}(4)} \tag{8.6}$$

is a vertex function accounting for self-energy corrections with respect to the Kohn-Sham system. Vertex corrections vanish ($\Gamma^{KS}(\bar{1}\bar{2}4) = \delta(\bar{1}\bar{2})\delta(\bar{1}4)$) when the interacting Green's function becomes equal to the Green's function of the Kohn-Sham system. The diagonal of the two Green's functions, which corresponds to the density, is equal by definition. This is the reason why the screened test-charge test-charge interaction W (eq.3.40) can be calculated in principle exactly within TDDFT. We may refer to W as test-charge test-charge interaction, because it adds correlation effects only from the the variation of the "total classical" potential, and therefore of the density which gives the classical charge. On the contrary, the full Green's function is a non-local in space and time object and contains much more information than the density. Therefore the two Green's functions are different and vertex corrections emerge with respect to the TDDFT screened interaction $\tilde{w}$. We may refer to $\tilde{w}$ (eq.8.3) or $\tilde{W}$ from eq.3.37 as the test-charge test-electron interaction, because it includes all exchange-correlation effects from the real interacting or the Kohn-Sham system (through the variation of the self-energy or the Kohn-Sham potential). The Dyson equation can be written as

$$G(12) = G^H(12) + iG^H(1\bar{1})\tilde{w}(\bar{1}^+\bar{4})G(\bar{1}\bar{1}')\Gamma^{KS}(\bar{1}'\bar{2}\bar{4})G(\bar{2}2). \tag{8.7}$$

Making approximations for Γ^{KS} accounting for effects of the interacting system with respect to the Kohn-Sham system, corresponds to the $G\tilde{w}\Gamma^{KS}$ approximation for the self-energy of the interacting system. Such effects are for example the non-locality in space and the non-locality in time of the self-energy.

8.2 Vertex corrections from the spatial non-locality of the self-energy

There are indications that $\Gamma^{KS} \approx 1$ is not always a sufficiently good approximation. For example, problems have been met by Godby [118] for atoms, or in [119] for the calculation of lifetimes in insulators. One property of the self-energy, which is not intrinsic to the Kohn-Sham potential is the non-locality. The non-locality of the self-energy has been linked to the band-gap opening with respect to Kohn-Sham DFT. It has been shown that the energy of the top of the valence states of the Kohn-Sham system remains unchanged under the effect of the self-energy [120, 121]. Therefore the self-energy effect is often taken into account by applying a rigid shift to the energies of the conduction states of the Kohn-Sham system, called "scissor shift". This can be used in calculations for real materials to simulate the correction of the Kohn-Sham band-structure by the GWA. The rigid shift to the conduction states can be simulated with a model self-energy [122],

$$\Sigma(12) \approx V^{KS}(1)\delta(12) + \Delta \sum_{s}^{unocc} \phi_s^{KS}(r_1)\phi_s^{KS\star}(r_2)\delta(t_1 - t_2) \tag{8.8}$$

$$= V^{KS}(1)\delta(12) + \Delta(\delta(12) + iG^{KS}(12)\delta(t_1^+ - t_2)), \tag{8.9}$$

where ϕ^{KS} are the Kohn-Sham orbitals. Δ is a parameter, whose value is equal to the gap opening with respect to Kohn-Sham. It multiplies the non-local projector operator to the conduction states of the Kohn-Sham system. The $\Delta-$model simulates only the effects of spatial non-locality, and temporal non-locality is neglected. Moreover, it does not change the wavefunctions.

From the $\Delta-$model of eq.8.9 vertex corrections (eq.8.6) are obtained as

$$\Gamma^{KS}(\bar{1}\bar{2}4) = \delta(\bar{1}\bar{2})\delta(\bar{1}4) + i\Delta\delta(\bar{t}_1^+ - \bar{t}_2)G^{KS}(\bar{1}4)G^{KS}(4\bar{2}). \tag{8.10}$$

Then the Dyson equation for the Green's function (eq.8.7) becomes

$$\begin{aligned} G(12) = {} & G^H(12) + iG^H(1\bar{1})\tilde{w}(\bar{1}^+\bar{4})G(\bar{1}\bar{4})G(\bar{4}2) \\ & - \Delta G^H(1\bar{1})\tilde{w}(\bar{1}^+\bar{4})G^{KS}(\bar{3}\bar{4})G^{KS}(\bar{4}\bar{5})G(\bar{1}\bar{3})\delta(\bar{t}_3^+ - \bar{t}_5)G(\bar{5}2), \end{aligned} \tag{8.11}$$

and the corresponding exchange-correlation contribution to the self-energy is given by

$$M(12) = iG(12)\tilde{w}(1^+2) - \Delta G(1\bar{1})\tilde{w}(1^+\bar{2})G^{KS}(\bar{1}\bar{2})G^{KS}(\bar{2}2)\delta(\bar{t}_1^+ - t_2). \tag{8.12}$$

Note that from the $\Delta-$model the interaction screened by the self-energy (eq.3.37), which includes the external potential, is given by

$$\tilde{W}(1^+2:\bar{1}) = v(1\bar{2})\frac{\delta\Sigma^{tot}(\bar{1}2)}{\delta U(\bar{2}^+)} = \tilde{w}(1^+2)\delta(\bar{1}2) + i\Delta\tilde{w}(1^+\bar{2})G^{KS}(\bar{1}\bar{2})G^{KS}(\bar{2}2)\delta(\bar{t}_1^+ - t_2). \tag{8.13}$$

This correction to the exact $\tilde{W}$ with respect to the $\tilde{w}$ is given by the $\Delta-$model. We can rewrite the first term applying a chain rule with the density, plus the second term as

$$\begin{aligned} \tilde{W}(1^+2:\bar{1}) = {} & v(12)\delta(\bar{2}^+2) + \delta(1\bar{1})v(\bar{1}^+\bar{2})f^{xc}(2\bar{2}')\frac{\delta\rho(\bar{2}')}{\delta U(\bar{2})} \\ & - \Delta v(1^+\bar{2})\frac{\delta\rho^{KS}(\bar{x}_1\bar{t}_1, x_2\bar{t}_1^+)}{\delta U(\bar{2})}\delta(\bar{t}_1^+ - t_2). \end{aligned} \tag{8.14}$$

From this expression we can distinguish between non-linear effects and the non-locality. With the $\Delta-$model the non-locality correction is taken into account through the derivative of the density matrix of the Kohn-Sham system, while non-linear effects are taken into account through the effective interaction f^{xc} with the density response. Since the density is a part of the density matrix, once this is non-linear, the non-locality correction adds a non-linear contribution. Therefore, for systems with localized electrons there might be an additional non-linear contribution to screening coming from the non-locality correction. Note, however, that here we are not discussing the measurable test-charge test-charge screening, but the test-charge test-electron screening, which is appropriate for fermions in the system.

8.3 The Dyson equation for non-varying Kohn-Sham orbitals

In this section we consider that the Kohn-Sham orbitals (KS) are identical to the Quasiparticle orbitals (QP), that diagonalize the interacting Green's function stemming from a static self-energy,

such as the one of a $\Delta-$model. Indeed, this model self-energy correction does not change the orbitals. Then, the two Green's functions in equilibrium differ only in the energy eigenvalues. Here we assume that the energy eigenvalues are frequency independent, which is a property of a frequency independent self-energy and Kohn-Sham potential. One may rewrite the Green's function of eq.2.23 in the following way,

$$G(12) = i\sum_s e^{-iE_s(t_1-t_2)}\phi_s(x_1)\phi_s^\star(x_2)(\theta(t_2-t_1)\theta(\mu-E_s)-\theta(t_1-t_2)\theta(E_s-\mu)), \quad (8.15)$$

where μ is the chemical potential separating empty and occupied states and E_s take different values for the Kohn-Sham and the Quasiparticle system. The correction from the $\Delta-$model in eq.8.11 takes two different contributions from two integrals between the interacting Green's function and the Green's function of the Kohn-Sham system. The first integral is

$$\int d\bar{5}G^{KS}(\bar{4},\bar{5})G(\bar{5},2)\delta(\bar{t}_3^+-\bar{t}_5) = -\sum_{s_1} e^{-iE_{s_1}^{KS}t_4}\phi_{s_1}(x_4)e^{iE_{s_1}^{QP}t_2}\phi_{s_1}^\star(x_2)e^{-i\Delta E_{s_1}t_3^+}\big(\theta(t_3^+-t_4)$$
$$\theta(\mu-E_{s_1}^{KS})\theta(t_2-t_3^+)\theta(\mu-E_{s_1}^{QP})+\theta(t_4-t_3^+)\theta(E_{s_1}^{KS}-\mu)\theta(t_3^+-t_2)\theta(E_{s_1}^{QP}-\mu)\big). \quad (8.16)$$

Here, we have used the orthogonality of the orbitals, and supposed that $\theta(E_{s_1}^{KS}-\mu)\theta(\mu-E_{s_1}^{QP})=0$ assuming that occupied and empty levels do not mix making the transition between the Kohn-Sham system and the interacting system. The energy difference $\Delta E_{s_1} = E_{s_1}^{QP}-E_{s_1}^{KS}$ is equal to the Quasiparticle shift of the Kohn-Sham level s_1 takes from the Quasiparticle. The second integral which appears in eq.8.12 is given by

$$\int dx_3 G(\bar{1}\bar{3})G^{KS}(\bar{3}\bar{4}) = -\sum_{s_3} e^{-iE_{s_3}^{QP}t_1}\phi_{s_3}(x_1)e^{iE_{s_3}^{KS}t_4}\phi_{s_3}^\star(x_4)e^{i\Delta E_{s_3}t_3}\big(\theta(t_3-t_1)$$
$$\theta(\mu-E_{s_3}^{QP})\theta(t_4-t_3)\theta(\mu-E_{s_3}^{KS})+\theta(t_1-t_3)\theta(E_{s_3}^{QP}-\mu)\theta(t_3-t_4)\theta(E_{s_3}^{KS}-\mu)\big), \quad (8.17)$$

where $\Delta E_{s_3} = E_{s_3}^{QP}-E_{s_3}^{KS}$. We combine the two integrals of eq.8.16, 8.17 in eq.8.12, to obtain

$$G(12) = G^H(12) + iG^H(1\bar{1})\tilde{w}(\bar{1}^+\bar{4})G(\bar{1}\bar{4})G(\bar{4}2) - \int d1'4\Delta G^H(11')\tilde{w}(1'^+4)$$
$$\sum_{s_1 s_3} e^{-i(E_{s_1}^{KS}-E_{s_3}^{KS})t_4}\phi_{s_1}(x_4)\phi_{s_3}^\star(x_4)e^{iE_{s_1}^{QP}t_2}\phi_{s_1}^\star(x_2)\int dt_3 e^{-i(\Delta E_{s_1}-\Delta E_{s_3})t_3}e^{-iE_{s_3}^{QP}t_1'}\phi_{s_3}(x_1')$$
$$\big(\theta(t_3-t_1')\theta(\mu-E_{s_3}^{QP})\theta(t_4-t_3)\theta(\mu-E_{s_3}^{KS})\theta(E_{s_1}^{KS}-\mu)\theta(t_3^+-t_2)\theta(E_{s_1}^{QP}-\mu)$$
$$+\theta(t_1'-t_3)\theta(E_{s_3}^{QP}-\mu)\theta(t_3-t_4)\theta(E_{s_3}^{KS}-\mu)\theta(\mu-E_{s_1}^{KS})\theta(t_2-t_3^+)\theta(\mu-E_{s_1}^{QP})\big). \quad (8.18)$$

A diagonal element in the Kohn-Sham basis of eq.8.18 becomes

$$G_{ii}(t_1-t_2) = G_{ii}^H(t_1-t_2) + i\int dt_1'\int dt_4\sum_{jk} G_{ij}^H(t_1-t_1')\tilde{w}_{jkik}(t_1'^+-t_4)G_{kk}(t_1'-t_4)G_{ii}(t_4-t_2)$$
$$-\int dt_1'\int dt_4\sum_{js_3}\Delta G_{ij}^H(t_1-t_1')\tilde{w}_{js_3is_3}(t_1'^+-t_4)e^{-i(E_i^{KS}-E_{s_3}^{KS})t_4}e^{iE_i^{QP}t_2}\int dt_3 e^{-i(\Delta E_i-\Delta E_{s_3})t_3}e^{-iE_{s_3}^{QP}t_1'}$$
$$\big(\theta(t_3-t_1')\theta(\mu-E_{s_3}^{QP})\theta(t_4-t_3)\theta(\mu-E_{s_3}^{KS})\theta(E_i^{KS}-\mu)\theta(t_3^+-t_2)\theta(E_i^{QP}-\mu)$$
$$+\theta(t_1'-t_3)\theta(E_{s_3}^{QP}-\mu)\theta(t_3-t_4)\theta(E_{s_3}^{KS}-\mu)\theta(\mu-E_i^{KS})\theta(t_2-t_3^+)\theta(\mu-E_i^{QP})\big). \quad (8.19)$$

In eq.8.19 the states i and s_3 belong to the different subsets: one must be a valence state and the other a conduction state. When there is no overlap between valence and conduction states the matrix elements of the screened interaction are zero. In this case the non-locality correction is zero, meaning that a localized level doesn't see the effect of the opening of the band gap shifting conduction levels. In this case the propagation of a localized electron is given in an exact way from the Dyson equation, where the interaction in a $G\tilde{w}$ self-energy is screened with the Kohn-Sham potential,

$$G_{ii}(t_1-t_2) = G^H_{ii}(t_1-t_2)+i\int dt'_1\int dt_4 G^H_{ii}(t_1-t'_1)\tilde{w}_{iiii}(t'^{+}_1-t_4)G_{ii}(t'_1-t_4)G_{ii}(t_4-t_2). \quad (8.20)$$

This implies that for example the photoemission of a core-level may be described to a good approximation by calculating screening from the variations of the Kohn-Sham potential, without the need of additional vertex corrections, which is a significant simplification.

8.4 Self-consistent calculation of the non-locality correction Δ.

In general, supposing that an occupied state has little overlap with all conduction states is a rough approximation. In this section, we go beyond. Since we suppose that all Green's functions are diagonal in the same basis, the Dyson eq.8.19 can be written as

$$G_{ii}(t_1-t_2) = G^H_{ii}(t_1-t_2) + \int dt_3\int dt_4 G^H_{ij}(t_1-t_3)M_{ji}(t_3-t_4)G_{ii}(t_4-t_2), \quad (8.21)$$

which, using eq.8.16, allows us to extract the exchange-correlation part of the self-energy of eq.8.12 and evaluate the non-locality correction

$$\begin{aligned}
&\Delta G(1\bar{1})\tilde{w}(1^+\bar{2})G^{KS}(\bar{1}\bar{2})G^{KS}(\bar{2}2)\delta(\bar{t}_1^+ - t_2)\\
&= -i\Delta\int d\tau\int dx\tilde{w}(1^+,x(\tau+t_2))\sum_{ss'}e^{-iE^{QP}_s(t_1-t_2+\delta)}\phi_s(x_1)e^{i(E^{KS}_s-E^{KS}_{s'})\tau}\phi^\star_s(x)\phi_{s'}(x)\phi^\star_{s'}(x_2)\\
&\big(-\theta(t_2-t_1)\theta(\mu-E^{QP}_s)\theta(\tau)\theta(\mu-E^{KS}_s)\theta(E^{KS}_{s'}-\mu)\\
&+\theta(t_1-t_2)\theta(E^{QP}_s-\mu)\theta(-\tau)\theta(E^{KS}_s-\mu)\theta(\mu-E^{KS}_{s'})\big), \quad (8.22)
\end{aligned}$$

where we set $\tau = \bar{t}_2 - t_2$. The $G\tilde{w}$ term becomes

$$\begin{aligned}
G(12)\tilde{w}(1^+2) &= i\sum_s e^{-iE^{QP}_s(t_1-t_2)}\phi_s(x_1)\phi^\star_s(x_2)(\theta(t_2-t_1)\theta(\mu-E^{QP}_s)\\
&-\theta(t_1-t_2)\theta(E^{QP}_s-\mu))\tilde{w}(1^+2). \quad (8.23)
\end{aligned}$$

The diagonal matrix elements of the exchange-correlation part of the self-energy is given by

$$\begin{aligned}
M_{ii}(t_1,t_2) &= -\sum_s e^{-iE^{QP}_s(t_1-t_2)}(\theta(t_2-t_1)\theta(\mu-E^{QP}_s)-\theta(t_1-t_2)\theta(E^{QP}_s-\mu))\tilde{w}_{isis}(t_1^+,t_2)\\
&+i\Delta\int d\tau\sum_s\tilde{w}_{isis}(t_1^+,\tau+t_2)e^{-iE^{QP}_s(t_1-t_2+\delta)}e^{iE^{KS}_s\delta}e^{i(E^{KS}_s-E^{KS}_i)\tau}
\end{aligned}$$

$$\big(-\theta(t_2-t_1)\theta(\mu-E_s^{QP})\theta(\tau)\theta(\mu-E_s^{KS})\theta(E_i^{KS}-\mu) \\ +\theta(t_1-t_2)\theta(E_s^{QP}-\mu)\theta(-\tau)\theta(E_s^{KS}-\mu)\theta(\mu-E_i^{KS})\big). \tag{8.24}$$

In equilibrium $\tilde{w}$ is a function of time-differences and can be given by its Fourier transform $\tilde{w}_{isis}(t_1^+-t_2)=\int\frac{d\omega}{2\pi}e^{-i\omega(t_1+\delta-t_2)}\tilde{w}_{isis}(\omega)$. The self-energy is also a function of time differences and is given by

$$M_{ii}(t)=-\sum_s(\theta(-t)\theta(\mu-E_s^{QP})-\theta(t)\theta(E_s^{QP}-\mu))e^{-iE_s^{QP}t}\int\frac{d\omega}{2\pi}e^{-i\omega(t+\delta)}\tilde{w}_{isis}(\omega) \\ +\Delta\int\frac{d\omega}{2\pi}e^{-i(E_s^{QP}+\omega)(t+\delta)}\sum_s e^{iE_s^{KS}\delta}\tilde{w}_{isis}(\omega)\big(\theta(-t)\frac{\theta(\mu-E_s^{QP})\theta(\mu-E_s^{KS})\theta(E_i^{KS}-\mu)}{\omega+E_s^{KS}-E_i^{KS}+i\delta} \\ +\theta(t)\frac{\theta(E_s^{QP}-\mu)\theta(E_s^{KS}-\mu)\theta(\mu-E_i^{KS})}{\omega+E_s^{KS}-E_i^{KS}-i\delta}\big), \tag{8.25}$$

where we have introduced $t=t_1-t_2$. The self-energy in frequency space $M_{ii}(\omega_1)=\int dte^{i\omega_1 t}M_{ii}(t)$ is given by

$$M_{ii}(\omega_1)=-i\int\frac{d\omega}{2\pi}e^{-i\omega\delta}\sum_s(\frac{\theta(E_s^{QP}-\mu)}{\omega-\omega_1+E_s^{QP}-i\delta}+\frac{\theta(\mu-E_s^{QP})}{\omega-\omega_1+E_s^{QP}+i\delta})\tilde{w}_{isis}(\omega) \\ +i\Delta\sum_s e^{i(E_s^{KS}-E_s^{QP})\delta}\int\frac{d\omega}{2\pi}e^{-i\omega\delta}\tilde{w}_{isis}(\omega)\big(\frac{\theta(\mu-E_s^{QP})}{\omega-\omega_1+E_s^{QP}+i\delta}\frac{\theta(\mu-E_s^{KS})\theta(E_i^{KS}-\mu)}{\omega+E_s^{KS}-E_i^{KS}+i\delta} \\ -\frac{\theta(E_s^{QP}-\mu)}{\omega-\omega_1+E_s^{QP}-i\delta}\frac{\theta(E_s^{KS}-\mu)\theta(\mu-E_i^{KS})}{\omega+E_s^{KS}-E_i^{KS}-i\delta}\big). \tag{8.26}$$

As in eq.8.19 we see that when there is no overlap between valence and conduction states, the non-locality correction gives zero contribution to the self-energy. In eq.8.26 the prefactor $e^{-i\omega\delta}$ enters in the integration over ω, where δ is a positive infinitesimal. This term tends to zero, in the limit of $\omega\to-i\infty$. Therefore the integral has to be carried out in the lower half complex plane. This practically means that only the poles with $+i\delta$ will be integrated using the residues' theorem.

Now considering that the conduction states might be delocalized (e.g.plane waves), they will have finite overlap with a localized core level. In this case the non-locality correction has to be calculated. To this aim, we need the parameter Δ. One might take it from a GW calculation or evaluate the non-locality correction self-consistently. In principle this gives a finite different shift for each level, including also the valence states, making the parameter Δ state dependent. In order to get an estimation of the non-locality correction, here we will make the shift self-consistent only for the bottom of the conduction states and then use it to correct for example a core level. In the following we will present the steps of a self-consistent calculation.

The Quasiparticle peak in the spectral function (eq.2.44) for a level i can be obtained from the self-energy as

$$E_i^{QP}=E_i^H+\Re M_{ii}(E_i^{QP}). \tag{8.27}$$

The matrix elements of the mass operator taken with the lowest conduction state c at the Quasiparticle energy are obtained using eq.8.26 as

$$M_{cc}(E_c^{QP})=M_{cc}^{(1)}(E_c^{QP})+\Delta M_{cc}^{(2)}(E_c^{QP}), \tag{8.28}$$

where

$$M_{cc}^{(1)}(E_c^{QP}) = -i\int \frac{d\omega}{2\pi} e^{-i\omega\delta} \sum_s \left(\frac{\theta(E_s^{QP}-\mu)}{\omega - E_c^{QP} + E_s^{QP} - i\delta} + \frac{\theta(\mu - E_s^{QP})}{\omega - E_c^{QP} + E_s^{QP} + i\delta}\right)\tilde{w}_{cscs}(\omega) \text{ and} \tag{8.29}$$

$$M_{cc}^{(2)}(E_c^{QP}) = i\sum_s e^{i(E_s^{KS}-E_s^{QP})\delta} \int \frac{d\omega}{2\pi} e^{-i\omega\delta}\tilde{w}_{cscs}(\omega)\frac{\theta(\mu - E_s^{QP})}{\omega - E_c^{QP} + E_s^{QP} + i\delta}$$
$$\frac{\theta(\mu - E_s^{KS})\theta(E_c^{KS}-\mu)}{\omega + E_s^{KS} - E_i^{KS} + i\delta}. \tag{8.30}$$

Then one can obtain a new non-locality correction Δ asking for self-consistency between eq.8.9 and eq.8.27

$$V_{cc}^{KS}(\omega_1 = 0) + \Delta = E_c^H + \Re M_{cc}^{(1)}(E_c^{QP}) + \Delta\Re M_{cc}^{(2)}(E_c^{QP}), \tag{8.31}$$

This equation can be solved with respect to Δ as

$$\Delta = \frac{E_c^H + \Re M_{cc}^{(1)}(E_c^{QP}) - V_{cc}^{KS}(\omega_1 = 0)}{1 - \Re M_{cc}^{(2)}(E_c^{QP})}. \tag{8.32}$$

When $M^{(2)} = 0$, eq.8.32 yields the original Quasiparticle shift. The presence of $M^{(2)}$ renormalizes the result. Eq.8.27 together with eq.8.28 yields the final Quasiparticle energy for the lowest conduction state c,

$$E_c^{QP} = E_c^H + \Re M_{cc}^{(1)}(E_c^{QP}) + \Delta\Re M_{cc}^{(2)}(E_c^{QP}) = E_c^{KS} + \Delta. \tag{8.33}$$

The new value of Δ in eq.8.32 together with the Quasiparticle energy can be plugged in eq.8.28 and eq.8.32 for the next iteration step of the self-consistent calculation of Δ. Once converged, the calculated value of Δ can now also be used in the estimation of the non-locality correction to the exchange and correlation part of the self-energy for a core level l,

$$M_{ll}(\omega_1) = M_{ll}^{(1)}(\omega_1) + i\Delta M_{ll}^{(2)}(\omega_1), \tag{8.34}$$

where

$$M_{ll}^{(1)}(\omega_1) = -i\int \frac{d\omega}{2\pi} e^{-i\omega\delta} \sum_s \left(\frac{\theta(E_s^{QP}-\mu)}{\omega - \omega_1 + E_s^{QP} - i\delta} + \frac{\theta(\mu - E_s^{QP})}{\omega - \omega_1 + E_s^{QP} + i\delta}\right)\tilde{w}_{lsls}(\omega) \tag{8.35}$$

$$M_{ll}^{(2)}(\omega_1) = -i\sum_s e^{i(E_s^{KS}-E_s^{QP})\delta} \int \frac{d\omega}{2\pi} e^{-i\omega\delta}\tilde{w}_{lsls}(\omega)\frac{\theta(E_s^{QP}-\mu)}{\omega - \omega_1 + E_s^{QP} - i\delta}$$
$$\frac{\theta(E_s^{KS} - \mu)\theta(\mu - E_l^{KS})}{\omega + E_s^{KS} - E_l^{KS} - i\delta}. \tag{8.36}$$

In order to evaluate the matrix elements of the exchange and correlation part of the self-energy, we need the expression of the screened interaction $\tilde{w}$. In the following section we will evaluate $\tilde{w}$ from a plasmon-pole model.

8.5 Estimation of the non-locality corrections from a plasmon-pole model

In order to be able to carry out the integration of eq.8.26 we need an expresion for $\tilde{w}$. We can take it from a plasmon-pole model,

$$\tilde{w}_{isis}(\omega) = v_{isis} + \sum_p a^p \Big(\frac{1}{\omega - \omega_p + i\delta} - \frac{1}{\omega + \omega_p - i\delta}\Big), \tag{8.37}$$

where $a^p = |v^p_{is}|^2$, with v^p_{is} to be the matrix elements of the Coulomb interaction between the i and s states and the two-particle states p, standing for all possible neutral excitations; these include interband transitions between valence and conduction states, excitons and plasmons. The poles ω_p are the transition energies, where exchange and correlation effects are taken into account in the model.

Using the plasmon-pole model, one may carry out the integration in eq.8.26. The first contribution, $M^{(1)}$ becomes

$$\begin{aligned}
M^{(1)}_{ii}(\omega_1) &= -i \int \frac{d\omega}{2\pi} e^{-i\omega\delta} \sum_s \Big(\frac{\theta(E^{QP}_s - \mu)}{\omega - \omega_1 + E^{QP}_s - i\delta} + \frac{\theta(\mu - E^{QP}_s)}{\omega - \omega_1 + E^{QP}_s + i\delta}\Big)\tilde{w}_{isis}(\omega) \\
&= -i \int \frac{d\omega}{2\pi} e^{-i\omega\delta} \sum_s \Big(\frac{\theta(E^{QP}_s - \mu)}{\omega - \omega_1 + E^{QP}_s - i\delta} + \frac{\theta(\mu - E^{QP}_s)}{\omega - \omega_1 + E^{QP}_s + i\delta}\Big) v_{isis} \\
&- i \int \frac{d\omega}{2\pi} e^{-i\omega\delta} \sum_s \Big(\frac{\theta(E^{QP}_s - \mu)}{\omega - \omega_1 + E^{QP}_s - i\delta} + \frac{\theta(\mu - E^{QP}_s)}{\omega - \omega_1 + E^{QP}_s + i\delta}\Big) \sum_p a^p \Big(\frac{1}{\omega - \omega_p + i\delta} - \frac{1}{\omega + \omega_p - i\delta}\Big) \\
&= \sum_s e^{i(-\omega_1 + E^{QP}_s)\delta} \theta(\mu - E^{QP}_s) v_{isis} - i \int \frac{d\omega}{2\pi} e^{-i\omega\delta} \sum_s \sum_p a^p \Bigg(\frac{1}{\omega - \omega_p + i\delta} \frac{\theta(E^{QP}_s - \mu)}{\omega - \omega_1 + E^{QP}_s - i\delta} \\
&+ \frac{1}{\omega - \omega_p + i\delta} \frac{\theta(\mu - E^{QP}_s)}{\omega - \omega_1 + E^{QP}_s + i\delta} - \frac{1}{\omega + \omega_p - i\delta} \frac{\theta(\mu - E^{QP}_s)}{\omega - \omega_1 + E^{QP}_s + i\delta}\Bigg) \\
&= -\sum_s e^{i(-\omega_1 + E^{QP}_s)\delta} \theta(\mu - E^{QP}_s) v_{isis} - \sum_s \sum_p a^p \Bigg(e^{-i\omega_p\delta} \frac{\theta(E^{QP}_s - \mu)}{\omega_p - \omega_1 + E^{QP}_s - 2i\delta} \\
&+ \theta(\mu - E^{QP}_s) \Big(\frac{e^{-i(\omega_1 - E^{QP}_s)\delta}}{\omega_1 - E^{QP}_s - \omega_p} + \frac{e^{-i\omega_p\delta}}{\omega_p - \omega_1 + E^{QP}_s} - \frac{e^{-i(\omega_1 - E^{QP}_s)\delta}}{\omega_1 - E^{QP}_s + \omega_p - 2i\delta}\Big)\Bigg),
\end{aligned} \tag{8.38}$$

where for the integration in the lower half-plane we have used the residue theorem $\int_{-\infty}^{+\infty} d\omega \frac{f(\omega)}{\omega - \omega_0 + i\delta} = -2\pi i f(\omega_0 - i\delta)$. For vanishing δ, we get

$$\begin{aligned}
M^{(1)}_{ii}(\omega_1) = &- \sum_s \theta(\mu - E^{QP}_s) v_{isis} \\
&+ \sum_s \sum_p a^p \Bigg(\frac{\theta(E^{QP}_s - \mu)}{\omega_1 - \omega_p - E^{QP}_s + i\delta} + \frac{\theta(\mu - E^{QP}_s)}{\omega_1 - E^{QP}_s + \omega_p - i\delta}\Bigg).
\end{aligned} \tag{8.39}$$

Eq.8.39 gives the $G\tilde{w}$ self-energy, where $\tilde{w}$ accounts for exchange and correlation effects within TDDFT and the plasmon, without non-locality correction. The first contribution is the exchange,

while the second stands for correlation within the plasmon-pole model. The exchange contribution is given by the the occupied levels in the system. In correlation, both occupied and empty levels contribute.

The second contribution to eq.8.26, $M^{(2)}$, which adds to the $G\tilde{w}$ the non-locality correction, is given by

$$
\begin{aligned}
&M^{(2)}_{ii}(\omega_1) = i\sum_s e^{i(E^{KS}_s - E^{QP}_s)\delta}\int \frac{d\omega}{2\pi} e^{-i\omega\delta}\tilde{w}_{isis}(\omega)\Big(\frac{\theta(\mu - E^{QP}_s)}{\omega - \omega_1 + E^{QP}_s + i\delta}\frac{\theta(\mu - E^{KS}_s)\theta(E^{KS}_i - \mu)}{\omega + E^{KS}_s - E^{KS}_i + i\delta} \\
&- \frac{\theta(E^{QP}_s - \mu)}{\omega - \omega_1 + E^{QP}_s - i\delta}\frac{\theta(E^{KS}_s - \mu)\theta(\mu - E^{KS}_i)}{\omega + E^{KS}_s - E^{KS}_i - i\delta}\Big) \\
&= i\sum_s e^{i(E^{KS}_s - E^{QP}_s)\delta}\int \frac{d\omega}{2\pi} e^{-i\omega\delta}\left(v_{isis} + \sum_p a^p\Big(\frac{1}{\omega - \omega_p + i\delta} - \frac{1}{\omega + \omega_p - i\delta}\Big)\right) \\
&\left(\frac{\theta(\mu - E^{QP}_s)}{\omega - \omega_1 + E^{QP}_s + i\delta}\frac{\theta(\mu - E^{KS}_s)\theta(E^{KS}_i - \mu)}{\omega + E^{KS}_s - E^{KS}_i + i\delta}\right. \\
&\left. - \frac{\theta(E^{QP}_s - \mu)}{\omega - \omega_1 + E^{QP}_s - i\delta}\frac{\theta(E^{KS}_s - \mu)\theta(\mu - E^{KS}_i)}{\omega + E^{KS}_s - E^{KS}_i - i\delta}\right).
\end{aligned}
\tag{8.40}
$$

We evaluate the terms in the integration one-by-one. The first term has two poles in the lower half plane,

$$
\begin{aligned}
&M^{(2)}_{ii1}(\omega_1) = i\sum_s e^{i(E^{KS}_s - E^{QP}_s)\delta}\int \frac{d\omega}{2\pi} e^{-i\omega\delta}\left(v_{isis} - \sum_p a^p\frac{1}{\omega + \omega_p - i\delta}\right) \\
&\left(\frac{\theta(\mu - E^{QP}_s)}{\omega - \omega_1 + E^{QP}_s + i\delta}\frac{\theta(\mu - E^{KS}_s)\theta(E^{KS}_i - \mu)}{\omega + E^{KS}_s - E^{KS}_i + i\delta}\right) \\
&= \sum_s e^{i(E^{KS}_s - E^{QP}_s)\delta}\theta(\mu - E^{QP}_s)\theta(\mu - E^{KS}_s)\theta(E^{KS}_i - \mu)\Bigg[\\
&e^{-i(\omega_1 - E^{QP}_s)\delta}\left(v_{isis} - \sum_p a^p\frac{1}{\omega_1 - E^{QP}_s - i\delta + \omega_p - i\delta}\right)\frac{1}{\omega_1 - E^{QP}_s - i\delta + E^{KS}_s - E^{KS}_i + i\delta} \\
&+ e^{i(E^{KS}_s - E^{KS}_i)\delta}\left(v_{isis} - \sum_p a^p\frac{1}{-E^{KS}_s + E^{KS}_i - i\delta + \omega_p - i\delta}\right) \\
&\frac{1}{-E^{KS}_s + E^{KS}_i - i\delta - \omega_1 + E^{QP}_s + i\delta}\Bigg)\Bigg].
\end{aligned}
\tag{8.41}
$$

For vanishing δ we get

$$
\begin{aligned}
&M^{(2)}_{ii1}(\omega_1) = -\sum_s \theta(\mu - E^{QP}_s)\theta(\mu - E^{KS}_s)\theta(E^{KS}_i - \mu)\sum_p a^p \\
&\left(\frac{1}{\omega_1 - E^{QP}_s + \omega_p - i\delta} - \frac{1}{-E^{KS}_s + E^{KS}_i + \omega_p - i\delta}\right)\frac{1}{\omega_1 - E^{QP}_s + E^{KS}_s - E^{KS}_i}.
\end{aligned}
\tag{8.42}
$$

This term is zero for an occupied state i. The second term has one pole in the lower half-plane,

$$
M^{(2)}_{ii2}(\omega_1) = -i\sum_s e^{i(E^{KS}_s - E^{QP}_s)\delta}\int \frac{d\omega}{2\pi} e^{-i\omega\delta}\sum_p a^p\frac{1}{\omega - \omega_p + i\delta}
$$

$$\frac{\theta(E_s^{QP}-\mu)}{\omega-\omega_1+E_s^{QP}-i\delta}\frac{\theta(E_s^{KS}-\mu)\theta(\mu-E_i^{KS})}{\omega+E_s^{KS}-E_i^{KS}-i\delta}$$
$$=-\sum_s e^{i(E_s^{KS}-E_s^{QP})\delta}e^{i\omega_p\delta}\sum_p a^p\frac{\theta(E_s^{QP}-\mu)}{\omega_p-\omega_1+E_s^{QP}-i\delta}\frac{\theta(E_s^{KS}-\mu)\theta(\mu-E_i^{KS})}{\omega_p+E_s^{KS}-E_i^{KS}-i\delta}. \quad (8.43)$$

For vanishing δ, $M_{ii2}^{(2)}$ becomes

$$M_{ii2}^{(2)}(\omega_1)=-\sum_s\sum_p a^p\frac{\theta(E_s^{QP}-\mu)}{\omega_p-\omega_1+E_s^{QP}-i\delta}\frac{\theta(E_s^{KS}-\mu)\theta(\mu-E_i^{KS})}{\omega_p+E_s^{KS}-E_i^{KS}-i\delta}. \quad (8.44)$$

This term is different from zero for an occupied state. We calculate the third contribution having three poles in the lower half plane,

$$M_{ii3}^{(2)}(\omega_1)=i\sum_s e^{i(E_s^{KS}-E_s^{QP})\delta}\int\frac{d\omega}{2\pi}e^{-i\omega\delta}\sum_p a^p\frac{1}{\omega-\omega_p+i\delta}$$
$$\frac{\theta(\mu-E_s^{QP})}{\omega-\omega_1+E_s^{QP}+i\delta}\frac{\theta(\mu-E_s^{KS})\theta(E_i^{KS}-\mu)}{\omega+E_s^{KS}-E_i^{KS}+i\delta}$$
$$=\sum_s e^{i(E_s^{KS}-E_s^{QP})\delta}\theta(\mu-E_s^{KS})\theta(E_i^{KS}-\mu)\theta(\mu-E_s^{QP})\sum_p a^p\Bigg($$
$$\frac{e^{-i\omega_p\delta}}{\omega_p-i\delta-\omega_1+E_s^{QP}+i\delta}\frac{1}{\omega_p-i\delta+E_s^{KS}-E_i^{KS}+i\delta}$$
$$+\frac{e^{-i(\omega_1-E_s^{QP})\delta}}{\omega_1-E_s^{QP}-i\delta-\omega_p+i\delta}\frac{1}{\omega_1-E_s^{QP}-i\delta+E_s^{KS}-E_i^{KS}+i\delta}$$
$$+\frac{e^{i(E_s^{KS}-E_i^{KS})\delta}}{-E_s^{KS}+E_i^{KS}-i\delta-\omega_p+i\delta}\frac{1}{-E_s^{KS}+E_i^{KS}-i\delta-\omega_1+E_s^{QP}+i\delta}\Bigg). \quad (8.45)$$

For vanishing δ we obtain

$$M_{ii3}^{(2)}(\omega_1)=\sum_s\theta(\mu-E_s^{KS})\theta(E_i^{KS}-\mu)\theta(\mu-E_s^{QP})\sum_p a^p\Bigg(\frac{1}{\omega_p-\omega_1+E_s^{QP}}\frac{1}{\omega_p+E_s^{KS}-E_i^{KS}}$$
$$+\Big(\frac{1}{\omega_1-E_s^{QP}-\omega_p}-\frac{1}{-E_s^{KS}+E_i^{KS}-\omega_p}\Big)\frac{1}{\omega_1-E_s^{QP}+E_s^{KS}-E_i^{KS}}\Bigg). \quad (8.46)$$

This term is zero for an occupied level i. Terms $M_{ii1}^{(2)}$ and $M_{ii3}^{(2)}$ will contribute only in the self-energy of an electron (unoccupied level i), while the term $M_{ii2}^{(2)}$ will only contribute to the self-energy of a hole (occupied level i). Therefore the exchange-correlation contribution to the self-energy of a localized hole l is given by

$$M_{ll}(\omega_1)=-\sum_s\theta(\mu-E_s^{QP})v_{lsls}+\sum_s\sum_p a^p\Bigg(\frac{\theta(E_s^{QP}-\mu)}{\omega_1-\omega_p-E_s^{QP}+i\delta}+\frac{\theta(\mu-E_s^{QP})}{\omega_1-E_s^{QP}+\omega_p-i\delta}\Bigg)$$
$$-\Delta\sum_s\sum_p a^p\frac{\theta(E_s^{QP}-\mu)}{\omega_p-\omega_1+E_s^{QP}-i\delta}\frac{\theta(E_s^{KS}-\mu)}{\omega_p+E_s^{KS}-E_l^{KS}-i\delta}. \quad (8.47)$$

Rewriting the last as

$$M_{ll}(\omega_1) = -\sum_s \theta(\mu - E_s^{QP}) v_{lsls} + \sum_s \sum_p a^p \Bigg(\Big[1 + \Delta \frac{\theta(E_s^{KS} - \mu)}{\omega_p + E_s^{KS} - E_l^{KS} - i\delta}\Big] \frac{\theta(E_s^{QP} - \mu)}{\omega_1 - \omega_p - E_s^{QP} + i\delta} + \frac{\theta(\mu - E_s^{QP})}{\omega_1 - E_s^{QP} + \omega_p - i\delta} \Bigg), \tag{8.48}$$

where I have highlighted the non-locality correction with respect to the $G\tilde{w}$, in red. As we can see, the non-locality correction renormalizes the empty-state contributions to the $G\tilde{w}$ self-energy. The change is proportional to $\frac{\Delta}{\omega_p + E_s^{KS} - E_l^{KS}}$. Since s is an empty state, $E_s^{KS} - E_l^{KS}$ is large for a core level, much larger than Δ, and the correction should be small. However, it might be important for states closer to the fermi level. One may calculate non-locality corrections to the $G\tilde{w}$ for an electron in a similar way. Δ can be evaluated self-consistently from the iterative scheme proposed in sec.8.4.

Summary

This chapter is based on a $GW\Gamma$ approximation of the self-energy similar to Hedin's equations, with the difference that the Coulomb interaction is screened from TDDFT and additional self-energy effects are taken into account introducing a vertex correction Γ. We have studied a particular case of vertex corrections, reflecting with a rigid shift of the energies of the conduction bands the bang-gap opening in DFT. This adds a non-locality correction to the exchange and correlation part of the self-energy, which will also contain non-linear effects once they contribute to the density. For localized electrons, once there is no overlap between valence and conduction states, the non-locality correction is zero, and therefore correlation can be given exactly by screening the Coulomb interaction within TDDFT and using the test-charge test-electron dielectric function. On the other hand, allowing for overlap with valence or conduction states, the non-locality correction appears also for a core-level and can be evaluated from a self-consistent scheme.

Conclusions

This thesis has explored new ways to describe spectroscopy of materials containing localized electrons. This is a many-body problem. One of the main challenges that one has to face in order to develop efficient approximations for systems with many electrons is the problem of correlation. The effects of correlation become stronger and more complicated when particles can occupy any position in space with the same probability. In many-body perturbation theory (MBPT) correlation is treated within approximations, which enter the inverse dielectric function, screening the bare Coulomb interaction, giving an effective interaction W. On the other hand, when electrons are localized in a small region, they can have small spatial overlap with other electrons in the system. In that case exchange effects are small, and therefore the description of correlation can be simplified. The potential from such electrons is similar to a classical potential. In this thesis we have settled the framework of this approximation and then applied it to theoretical approaches for the photoemission and absorption for systems with localized electrons. Our approaches are promising for spectroscopies of core electrons and insulating materials.

For the screening, we have taken advantage of the fact that time-dependent density functional theory (TDDFT) yields an in principle exact, yet relatively simple, description. In this framework it is important to properly account for the self-interaction and self-screening cancellations. In Chap.6 we studied the dielectric function of a simple solid with one electron per lattice position using localized Wannier functions and derived a Kohn-Sham potential. Using two different approaches, the Sham-Schlüter equation and the Schrödinger equation, we derived a periodic Kohn-Sham potential which is similar to the potential of a single atom in an environment in the following sense: each electron interacts with an external potential, reflecting the contributions from electrons outside the atom. The local form of this potential is based on absence of overlap between electrons and the self-interaction cancellation, which characterize an isolated electron. Using perturbation theory on a two level model we have shown that the effective interaction of this Kohn-Sham potential reproduces the cancellations between the self-energy and excitonic effects in the absorption energies. Such cancellations may explain the particular shape of inelastic x-ray diffraction spectra of some insulators, which motivated our TDDFT study.

Besides yielding absorption or IXS spectra, screening also enters the description of photoemission, through the self-energy, which is the kernel of a Dyson equation for the Green's function. Alternatively, one may overcome the need for drastic approximations of the self-energy, by solving a differential equation for the Green's function also called Kadanoff-Baym equation (KBE). In zero dimensions, this equation takes the form of a scalar differential equation which can be solved exactly. Therefore, we used a zero-dimensional model to study some fundamental open questions. In particular, we have introduced the screened interaction making a transformation between the non-interacting and the classical system (Chap.5). This is a good starting point to study and design TDDFT approximations for the screening and address the problem of multiple solutions, which appears in standard approximations used in ab initio calculations. One essential criterion to distinguish the physical solution is that it must tend to the exact non-interacting solution in the non-interacting limit. We have also found that multiple solutions arise from non-linear transfor-

mations, where one needs to specify the domain of validity for each solution. Moreover, one may extract expressions for effective interactions for TDDFT using perturbation theory. Also in this case one needs to be careful, because non-linear transformations give rise to multiple expressions, where again the domain of validity for each expression needs to be specified.

Improving the correlation in the screening is equivalent to accounting for non-linear effects. The zero dimensional model is a good starting point to study also the effects of non-linear screening. The model predicts that non-linear effects are important for cases where the cancellation between exchange effects and the classical Hartree potential is not complete, while when the exchange cancels the classical contribution, the linear response approximation suffices. In all cases the screened interaction needs to be treated beyond the RPA, for example within TDDFT. For localized electrons the model predicts that going only in one of the two directions, in the linear response approximation beyond the RPA or beyond the linear response approximation in the RPA, does not give significant improvement. One needs to overcome both approximations in order to get a systematic improvement.

In Chap.7 we went one step further by solving the full time-dependent KBE for one level in the decoupling approximation for localized electrons. This leads to a cumulant Green's function, where non-linear screening appears explicitly through the time-dependent density. This goes beyond the standard cumulant approximation where screening is usually taken in the linear response approximation and in the RPA. For the evaluation of non-linear effects we proposed two different schemes. The first relies on a static approximation, where the linear response is evaluated in presence of a full core-hole. The second is to obtain the time-dependent density solving the time-dependent Kohn-Sham equations (RTTDDFT), when a core-hole charge is switched on.

In Chap.8 we worked on Hedin's approach, where in order to go beyong the GW approximation in the self-energy, vertex corrections need to be taken into account. We combined Green's functions with TDDFT, screening with the Kohn-Sham potential. For the density, the Kohn-Sham potential contains in principle the exact correlation effects. This is not the case for the Green's function, which is a non-local object, where non-locality needs to be taken into account in the form of vertex corrections. We have introduced non-locality corrections using a Δ model, which opens the band gap of DFT for insulating materials. We found that Δ leads to a dynamical vertex correction, which can be calculated self-consistently. This correction vanishes for isolated electrons.

Usual approximations rely on low order correlation and this is true for systems where the strong exchange allows for the interaction to be treated perturbatively. For localized electrons, reduced exchange doesn't allow for the interaction to be treated perturbatively and therefore non-linear effects emerge. In this thesis, staying in the framework of Green's functions e.g. via the self-energy or the KBE, we have introduced screening from TDDFT. Therefore, our approach to correlation relies on a combination of Green's function and TDDFT in the framework of localized electrons, as shown schematically in fig.8.1. To sum up, in this thesis

- using a zero-dimensional model, it has been shown that non-linear effects enter in the screening of the excitation of electrons that have a reduced exchange with other electrons,
- work on the performance and optimization of approximations in TDDFT towards non-linear effects is presented,

- in the framework of localized electrons a Kohn-Sham potential for extended systems is derived,
- the cumulant Green's function is extended for systems with localized electrons and non-linear screening from TDDFT and
- a $GW\Gamma$ approximation is proposed, where screening is taken from the Kohn-Sham potential and the vertex Γ stands for non-locality-corrections evaluated within a model for insulating materials.

These findings open new ways to simplify the many-body problem for systems with localized electrons. The implementation of these approaches and their application on calculations for real systems are under way.

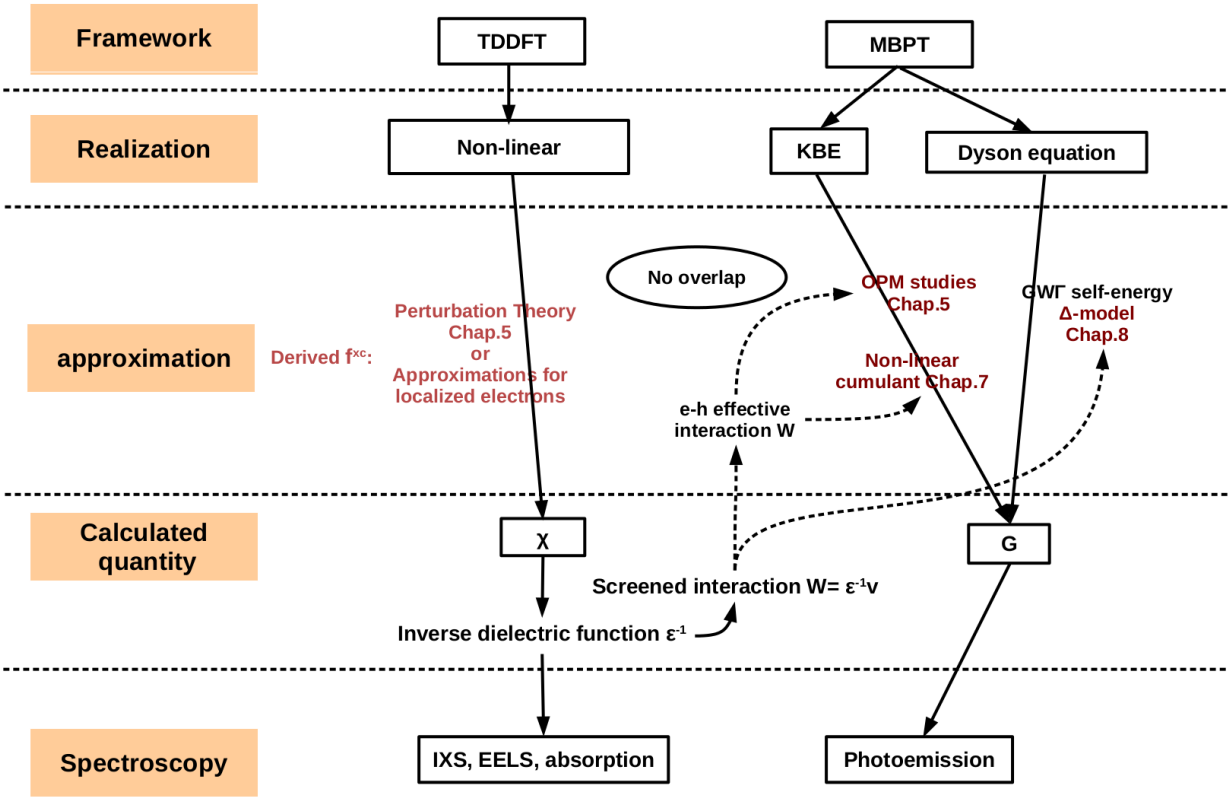

Fig. 8.1: Theoretical framework for the calculation of observables for systems with localized electrons.

APPENDIX

A

The Hedin equations in a basis

We can start from the five Hedin's equations eq.3.38,3.39,3.40,3.41,3.42, and define the matrix elements of the functions G, Σ, W, P, Γ with a discrete basis of orbital states as

$$
\begin{aligned}
G_{ab}(t_1 t_4) &= \int dx_1 \int dx_4 \phi_a^\star(x_1) G(x_1 t_1, x_4 t_4) \phi_b(x_4) \\
M_{ij}(t_1 t_2) &= \int dx_1 \int dx_2 \phi_i^\star(x_1) M(x_1 t_1, x_2 t_2) \phi_j(x_2) \\
W_{iadc}(t_1 t_3) &= \int dx_1 \int dx_3 \phi_i^\star(x_1) \phi_a(x_1) W(x_1 t_1, x_3 t_3^+) \phi_d(x_3) \phi_c^\star(x_3) \\
P_{efgh}(t_3 t_2) &= \int dx_3 \int dx_2 \phi_e^\star(x_3) \phi_f(x_3) P(x_3 t_3, x_2 t_2) \phi_g(x_2) \phi_h^\star(x_2) \\
\Gamma_{bjcd}(t_4 t_2 : t_3) &= \int dx_4 \int dx_2 \int dx_3 \phi_b^\star(x_4) \phi_j(x_2) \Gamma(x_4 t_4, x_2 t_2 : x_3 t_3) \phi_c(x_3) \phi_d^\star(x_3).
\end{aligned} \tag{A.1}
$$

We also define the independent particles polarization as

$$
P^0(2:34) = -iG(23)G(42) \tag{A.2}
$$

which is a three-point function. Its matrix elements are

$$
P^0_{hgbd}(t_2 : t_3 t_4) = \int dx_2 \int dx_3 \int dx_4 \phi_h^\star(x_2) \phi_g(x_2) P^0(x_2 t_2 : x_3 t_3 x_4 t_4) \phi_b(x_3) \phi_d^\star(x_4)
$$

As a consequence of the fact that the Γ function is a three point function we need to introduce the $4-$states overlap matrix elements I as

$$
I_{bjcd} = \int dx_1 \phi_b^\star(x_1) \phi_j(x_1) \phi_c(x_1) \phi_d^\star(x_1) \tag{A.3}
$$

We take the derivative of the self-energy with respect to the Green's function as

$$
\left. \frac{\delta M(12)}{\delta G(34)} \right|_{ijkl} = \int dx_3 \int dx_4 \phi_k(x_3) \phi_l^\star(x_4) \frac{\delta \Sigma_{ij}(t_1, t_2)}{\delta G(34)} \tag{A.4}
$$

We can then use the chain rule to pass to the derivative with respect to a discrete function.

$$
\left. \frac{\delta M(12)}{\delta G(34)} \right|_{ijkl} = \int dx_3 \int dx_4 \phi_k(x_3) \phi_l^\star(x_4) \int dt_5 \int dt_6 \sum_{lm} \frac{\delta M_{ij}(t_1, t_2)}{\delta G_{lm}(t_5, t_6)} \frac{\delta G_{lm}(t_5, t_6)}{\delta G(34)} \tag{A.5}
$$

Where

$$
\frac{\delta G_{lm}(t_5, t_6)}{\delta G(34)} = \phi_l^\star(x_3) \phi_m(x_4) \delta(t_5 - t_3) \delta(t_6 - t_4) \tag{A.6}
$$

So that we finally obtain that

$$\left.\frac{\delta M(12)}{\delta G(34)}\right|_{ijkl} = \frac{\delta M_{ij}(t_1,t_2)}{\delta G_{kl}(t_3,t_4)} \tag{A.7}$$

Using all the preceding definitions we obtain the set of five Hedin equations in a discrete basis of orbitals states

$$G_{ij}(t_1t_2) = G^0_{ij}(t_1t_2) + \sum_{ab} G^0_{ia}(t_1\bar{t}_3)\Sigma_{ab}(\bar{t}_3\bar{t}_4)G_{bj}(\bar{t}_4t_2) \tag{A.8}$$

$$M_{ij}(t_1t_2) = i\sum_{abcd} W_{iadc}(t_1\bar{t}_3)G_{ab}(t_1\bar{t}_4)\Gamma_{bjcd}(\bar{t}_4t_2:\bar{t}_3) \tag{A.9}$$

$$W_{iadc}(t_1t_2) = v_{iadc}\delta(t_1-t_2) + \sum_{efgh} W_{iaef}(t_1\bar{t}_3)P_{efgh}(\bar{t}_3t_2)v_{ghdc} \tag{A.10}$$

$$P_{efgh}(t_1t_2) = \sum_{bd} P^0_{hgbd}(t_1\bar{t}_3\bar{t}_4)\Gamma_{bdfe}(\bar{t}_3\bar{t}_4t_2) \tag{A.11}$$

$$\begin{aligned}\Gamma_{bjcd}(t_1t_2:t_3) &= I_{bjcd}\delta(t_1-t_2)\delta(t_1-t_3)\\ &+ \sum_{efgh}\left.\frac{\delta M(t_1t_2)}{\delta G(\bar{t}_4\bar{t}_5)}\right|_{bjef} P^0_{efgh}(\bar{t}_4\bar{t}_5:\bar{t}_6\bar{t}_7)\Gamma_{ghcd}(\bar{t}_6\bar{t}_7:t_3).\end{aligned} \tag{A.12}$$

We also give the Hedin equations obtained from a non-local in space and local in time applied potential(eq.3.56,3.57,3.58,3.59,3.60) and written in terms of the four-point interaction given by eq.3.48,

$$G_{ij}(t_1t_2) = G^0_{ij}(t_1t_2) + \sum_{ab} G^0_{ia}(t_1\bar{t}_3)\Sigma_{ab}(\bar{t}_3\bar{t}_4)G_{bj}(\bar{t}_4t_2) \tag{A.13}$$

$$M_{ij}(t_1t_2) = iW_{iadc}(t_1\bar{t}_1\bar{t}_4\bar{t}_5)G_{ab}(\bar{t}_1\bar{t}_3)\Gamma_{bjcd}(\bar{t}_3t_2\bar{t}_5\bar{t}_4) \tag{A.14}$$

$$W_{iadc}(t_1t_2t_4t_5) = v_{0iadc}(t_1t_2t_4t_5) + \sum_{efgh} W_{iaef}(t_1t_2\bar{t}_3\bar{t}_4)P_{efgh}(\bar{t}_3\bar{t}_4\bar{t}_5\bar{t}_6)v_{0ghdc}(\bar{t}_5\bar{t}_6t_4t_5) \tag{A.15}$$

$$P_{efgh}(t_3t_4t_5t_6) = -i\sum_{bd} G_{eb}(t_3\bar{t}_3)G_{df}(\bar{t}_4t_4)\Gamma_{bdgh}(\bar{t}_3\bar{t}_4\bar{t}_5\bar{t}_6) \tag{A.16}$$

$$\Gamma_{bjcd}(t_1t_2t_3t_4) = \delta_{bc}\delta_{jd}\delta(t_1-t_3)\delta(t_2-t_4) + i\frac{\delta M(t_1t_2)}{\delta G(\bar{t}_5\bar{t}_6)}|_{bjef}P_{efcd}(\bar{t}_5\bar{t}_6t_3t_4). \tag{A.17}$$

B

The solution of one electron problem from MBPT

Here we will use a system of two equations for the Green's function and the self-energy written in a discrete basis. We choose the basis of the non-interacting system, accounting also for the effects of the applied potential. The equations are written with respect to the Green's function of the non-interacting system g, which appears as a variable, while the difference between the matrix elements of the Coulomb interaction matrix elements Δv appears as a parameter,

$$\Delta v_{ijkl} = v_{ijkl} - v_{ikjl}. \tag{B.1}$$

We will use a system of two equations for the Green's function and the self-energy,

$$G_{ij}(t_1,t_2) = g_{ij}(t_1,t_2) + \int dt_3 t_4 \sum_{kl} g_{ik}(t_1,t_3)\Sigma_{kl}(t_3,t_4)G_{lj}(t_4,t_2) \tag{B.2}$$

$$\begin{aligned}\Sigma_{ij}(t_1,t_2) &= -i\delta(t_1-t_2)\sum_{kl}\Delta v_{ij:kl}G_{kl}(t_1,t_1^+) \\ &- \frac{1}{2}\int dt_3 \sum_{opklmn}\Delta v_{ik:ml}\int dt_5 t_6 \frac{\delta\Sigma_{nj}(t_3,t_2)}{\delta g_{op}(t_5,t_6)} g_{ol}(t_5,t_1)g_{mp}(t_1,t_6)G_{kn}(t_1,t_3).\end{aligned} \tag{B.3}$$

We will proceed in a perturbative solution to Δv for a system with only one electron, whose state is c and is decoupled from the rest of conduction states of the non-interacting system.

From eq.B.2 the zeroth order of the Green's function is given by

$$\begin{aligned}G^{(0)}_{ij}(t_1-t_2) = \delta_{ij}(&\delta_{ic}\delta_{jc}g_c^<(t_1-t_2)\theta(t_2-t_1) \\ &+[1-\delta_{ic}][1-\delta_{jc}]g_i^>(t_1-t_2)\theta(t_1-t_2)),\end{aligned} \tag{B.4}$$

which is equal to the Green's function of the non-interacting system. The zeroth order of the self-energy is zero.

$$\Sigma^{(0)}_{ij}(t_1-t_2) = 0. \tag{B.5}$$

We insert the density from the eq.B.4 to eq.B.3 and the 1st order of the self-energy is given by

$$\Sigma^{(1)}_{ij}(t_1-t_2) = -i\delta(t_1-t_2)\Delta v_{ijcc}g_c(t_1,t_1^+)[1-\delta_{ic}][1-\delta_{jc}] = \delta(t_1-t_2)\Sigma^{(1)}_{ij}(t_1). \tag{B.6}$$

This is static and different from zero only when its matrix elements are evaluated with conduction states. For $i=c$ or $j=c$ the self-energy is zero due to the *self-interaction cancellation*. The 1st order self-energy gives the Hartree-Fock self-energy, where the density is the density of the non-interacting system. Using eq.B.6 the 1st order correction to the lesser part of the Green's function is

$$G^{(1)<}_{ij}(t_1-t_2)\theta(t_2-t_1) = \theta(t_2-t_1)\int_{t_2}^{+\infty} dt_3 g_c^<(t_1-t_3)\Sigma^{(1)}_{cj}(t_3)g_j^>(t_3-t_2)\delta_{ic}[1-\delta_{jc}]$$

$$
\begin{aligned}
&+\theta(t_2-t_1)\int_{-\infty}^{t_1} dt_3 g_i^{>}(t_1-t_3)\Sigma_{ic}^{(1)}(t_3)g_c^{<}(t_3-t_2)\delta_{jc}[1-\delta_{ic}] \\
&+\theta(t_2-t_1)\int_{t_1}^{t_2} dt_3 g_c^{<}(t_1-t_3)\Sigma_{cc}^{(1)}(t_3)g_c^{<}(t_3-t_2)\delta_{ic}\delta_{jc} \\
=&0, \qquad \text{(B.7)}
\end{aligned}
$$

which is zero due to the fact that the matrix elements of $\Sigma^{(1)}$ with at least one state c are equal to zero. These elements appear due to the fact that they are coupled to the one-electron Green's function of the non-interacting system. Therefore the first order correction for the hole part of the Green's function is zero. The first order correction of the electron part of the Green's function is

$$
\begin{aligned}
&G_{ij}^{(1)>}(t_1-t_2)\theta(t_1-t_2) = \theta(t_1-t_2)\int_{t_1}^{+\infty} dt_3 g_c^{<}(t_1-t_3)\Sigma_{cj}^{(1)}(t_3)g_j^{>}(t_3-t_2)\delta_{ic}[1-\delta_{jc}] \\
&+\theta(t_1-t_2)\int_{-\infty}^{t_2} dt_3 g_i^{>}(t_1-t_3)\Sigma_{ic}^{(1)}(t_3)g_c^{<}(t_3-t_2)\delta_{jc}[1-\delta_{ic}] \\
&+\theta(t_1-t_2)\int_{t_2}^{t_1} dt_3 \sum_{kl} g_i^{>}(t_1-t_3)\Sigma_{ij}^{(1)}(t_3)g_j^{>}(t_3-t_2)[1-\delta_{jc}][1-\delta_{ic}] \qquad \text{(B.8)} \\
&=\theta(t_1-t_2)\int_{t_2}^{t_1} dt_3 \sum_{kl} g_i^{>}(t_1-t_3)\Sigma_{ij}^{(1)}(t_3)g_j^{>}(t_3-t_2)[1-\delta_{jc}][1-\delta_{ic}], \qquad \text{(B.9)}
\end{aligned}
$$

which is non-zero only when its matrix elements are evaluated with empty states of the non-interacting system. The energy to add a second electron to one of the empty levels of the non-interacting system takes a first order correction coming from the interaction with the Hartree-Fock field from the one-electron state. From eq.B.7,B.6 we obtain the 2nd order correction to the self-energy

$$
\begin{aligned}
\Sigma_{ij}^{(2)}(t_1-t_2) =& -i\delta(t_1-t_2)\sum_{kl}\Delta v_{ijkl}G_{kl}^{(1)}(t_1,t_1^{+}) \\
&-\frac{1}{2}\int dt_3 \sum_{opklmn}\Delta v_{ikml}\int dt_5 t_6 \frac{\delta\Sigma_{nj}^{(1)}(t_3-t_2)}{\delta g_{op}(t_5-t_6)} g_{ol}(t_5-t_1)g_{mp}(t_1-t_6)g_{kn}(t_1-t_3)] \\
=&\frac{i}{2}\sum_{opk}\Delta v_{ikpo}\Delta v_{kjop}g_o(t_2-t_1)g_p(t_1-t_2)g_k(t_1-t_2). \qquad \text{(B.10)}
\end{aligned}
$$

The second order self-energy takes two time ordered contributions

$$
\begin{aligned}
&\Sigma_{ij}^{(2)>}(t_1-t_2)\theta(t_1-t_2) = \\
&\frac{i}{2}\sum_{pk}\Delta v_{ikpd}\Delta v_{kjcp}g_c^{<}(t_2-t_1)g_p^{>}(t_1-t_2)g_k^{>}(t_1-t_2)[1-\delta_{ci}][1-\delta_{jc}]\theta(t_1-t_2) \qquad \text{(B.11)} \\
&\Sigma_{ij}^{(2)<}(t_1-t_2)\theta(t_2-t_1) = \frac{i}{2}\sum_{o}\Delta v_{icco}\Delta v_{cjoc}g_o^{>}(t_2-t_1)g_c^{<}(t_1-t_2)g_c^{<}(t_1-t_2)\theta(t_2-t_1) = 0 \\
&\qquad \text{(B.12)}
\end{aligned}
$$

The greater part of the self-energy (eq.B.11) is different from zero when its matrix elements are evaluated with empty states of the non-interacting system and stands for the screening of Δv

interaction with a hole from an electron-hole pair. The lesser part of the self-energy (eq.B.12) is always zero meaning that the screening of Δv interaction with the electron from an electron-hole pair is zero. This accounts for the *self-screening cancellation* meaning that an electron in an electron-hole pair cannot screen itself. From eq.B.11,B.6,B.9 the 2nd order Green's function becomes

$$G_{ij}^{(2)}(t_1-t_2) = \int dt_3 t_4 g_i(t_1-t_3)\Sigma_{ij}^{(2)>}(t_3-t_4)\theta(t_3-t_4)g_j(t_4-t_2) + \int dt_3 \sum_l g_i(t_1-t_3)\Sigma_{il}^{(1)}(t_3)G_{lj}^{(1)}(t_3-t_2). \tag{B.13}$$

The 2nd order correction of the Green's function gets two contributions,

$$G_{ij}^{(2)^>}(t_1-t_2)\theta(t_1-t_2) = [1-\delta_{ci}][1-\delta_{jc}]\theta(t_1-t_2) \Big[\int_{-\infty}^{t_1} dt_3 \int_{t_2}^{t_3} dt_4 g_i^>(t_1-t_3)\Sigma_{ij}^{(2)>}(t_3-t_4)g_j^>(t_4-t_2) + \int_{t_2}^{t_1} dt_3 \sum_l g_i^>(t_1-t_3)\Sigma_{il}^{(1)}(t_3)G_{lj}^{(1)>}(t_3-t_2)\Big] \tag{B.14}$$

$$G_{ij}^{(2)^<}(t_1-t_2) = 0 \tag{B.15}$$

The greater part is different from zero and only when its matrix elements are evaluated with empty states of the non-interacting system. The lesser part is zero due to the self-screening cancellation.

The lesser part of the Green's function terminates in the zeroth order due to the self-interaction and self-screening cancellations. On the other hand the addition of a second electron to the system is more complicated to be calculated exactly since it requires corrections of all orders to the Δv interaction accounting for screening from an electron-hole pair.

Application: two level model

We will apply the calculation to a model with only two levels, an occupied level c and an empty level k. The zeroth order of the Green's function is given by

$$G_{ij}^{(0)}(t_1-t_2) = \delta_{ij}(\delta_{ic}\delta_{jc}g_c^<(t_1-t_2)\theta(t_2-t_1) + \delta_{ik}\delta_{jk}g_k^>(t_1-t_2)\theta(t_1-t_2)) \tag{B.16}$$

The 0th order of the self-energy is zero, while the 1st order becomes

$$\Sigma_{ij}^{(1)}(t_1-t_2) = -i\delta(t_1-t_2)\Delta v_{kkcc}g_c(t_1,t_1^+)\delta_{ik}\delta_{jk}. \tag{B.17}$$

It stands for the Hartree-Fock interaction with the c state of the non-interacting system. The first order correction of the Green's function is zero for the lesser part due to the self-interaction cancellation. While the first order correction of the greater part

$$G_{ij}^{(1)>}(t_1-t_2) = \int_{t_2}^{t_1} dt_3 g_k^>(t_1-t_3)\Sigma_{kk}^{(1)}(t_3)g_k^>(t_3-t_2)\delta_{ik}\delta_{jk} \tag{B.18}$$

stands for the interaction with a Hartree-Fock field in the addition of a second electron. The 2nd order self-energy takes two contributions,

$$\Sigma_{ij}^{(2)>}(t_1-t_2)\theta(t_1-t_2) =$$

$$\frac{i}{2}\Delta v_{kkkc}\Delta v_{kkck} g_d^<(t_2-t_1) g_k^>(t_1-t_2) g_k^>(t_1-t_2)\delta_{ik}\delta_{jk}\theta(t_1-t_2) = 0 \tag{B.19}$$

$$\Sigma_{ij}^{(2)<}(t_1-t_2)\theta(t_2-t_1) = 0 \tag{B.20}$$

which are both zero, due to self-screening cancellation. An electron cannot screen itself, but also a hole cannot screen itself. In the absence of a second empty level the self-screening cancellation appears also for the hole. Then the 2nd order Green's function gets the two contributions,

$$G_{ij}^{(2)>}(t_1-t_2)\theta(t_1-t_2) = \int_{t_2}^{t_1} dt_3 g_k^>(t_1-t_3)\Sigma_{kk}^{(1)}(t_3)G_{kk}^{(1)>}(t_3-t_2)\delta_{ik}\delta_{jk}\theta(t_1-t_2) \tag{B.21}$$

$$G_{ij}^{(2)<}(t_1-t_2) = 0 \tag{B.22}$$

The lesser part is zero, while the greater part is different from zero including the effects of the Hartree-Fock self-energy. The Hartree-Fock self-energy is the exact self-energy for an electron in a two-level model.

C

Transformation to the dynamical variable of the classical system

C.1 Transformation $x \to w(x;v)x^2$

We multiply both parts of eq.5.20 with $\frac{1}{x}$ and we introduce the dynamical variable $Q(x;v) = w(x;v)x^2$ and the renormalized Green's function $\tilde{y}(x;v) = \frac{y(x;v)}{x}$ to obtain

$$\tilde{y}(x;v) = 1 + \lambda Q(x;v)x\frac{d\tilde{y}(x;v)}{dx} + \lambda Q(x;v)\tilde{y}(x;v). \tag{C.1}$$

We rewrite the derivative using a chain rule with Q,

$$\frac{d\tilde{y}(x;v)}{dx} = \frac{d\tilde{y}(x;v)}{dQ(x;v)}\frac{dQ(x;v)}{dx} \tag{C.2}$$

where the derivative $\frac{dQ}{dx}$ satisfies the relation

$$\frac{dQ(x;v)}{dx} = x^2\frac{dw(x;v)}{dx} + 2xw(x;v). \tag{C.3}$$

We will use the second eq.5.21 as $w^{-1}(x;v) = \frac{1}{v} + P(x;v)$ and we evaluate the derivative of the screening interaction which appears in eq.C.3

$$\frac{dw(x;v)}{dx} = -w^2(x;v)\frac{dP(x;v)}{dx} \tag{C.4}$$

to write eq.C.3 as

$$\frac{dQ(x;v)}{dx} = 2xw(x;v) - x^2w^2(x;v)\frac{dP(x;v)}{dx}. \tag{C.5}$$

Substituting the last equation to eq.C.1 we obtain

$$\tilde{y}(x;v) = 1 + \lambda Q^2(x;v)(2 - \frac{Q(x;v)}{x}\frac{dP(x;v)}{dx})\frac{d\tilde{y}(x;v)}{dQ(x;v)} + \lambda Q(x;v)\tilde{y}(x;v). \tag{C.6}$$

In order to complete the transformation we need to evaluate $\frac{dP(x;v)}{dx}$ as a function of $Q(x;v)$. This is a vertex correction introducing all orders of correlation. For the evaluation of the vertex corrections we will use TDDFT.

The equation of motion of an auxiliary system $y_s(z;v)$ interacting with an $f^{xc}(v)$ on top of the bare Coulomb interaction is

$$y_s(z;v) = y_0(z) - y_0(z)(v - f_s^{xc}(v))y_s(z;v)y_s(z;v). \tag{C.7}$$

$f_s^{xc}(x;v)$ will depend on the choice of $y_s(x;v)$. If $f_s^{xc}(v)$ is static, we include vy_s in the total classical potential and the polarization of the auxiliary system is given by

$$x^2\frac{dy_s(x;v)}{dx} = y_s^2(x;v) + y_s^2(x;v)f_s^{xc}(v)x^2\frac{dy_s(x;v)}{dx}. \tag{C.8}$$

If we ask for $x^2\frac{dy_s(x;v)}{dx} = P(x;v)$ to be equal to the polarization of the interacting system, we obtain the definition of the $f_s^{xc}(x;v)$ in terms of the independent-particle response function and the polarization,

$$f_s^{xc}(x;v) = \chi_s^{0-1}(x;v) - P^{-1}(x;v), \tag{C.9}$$

with the definition of $\chi_s^0(x;v) = y_s^2(x;v)$. In eq.C.9 f_s^{xc} must be static when y_s is the Kohn-Sham propagator. But we can also derive still exact $f_{s'}^{xc}$ from different choices of $y_{s'} \neq y_s$. We can use the definition of the f_s^{xc} (eq.C.9) and evaluate the derivative

$$\frac{dP(x;v)}{dx} = -P^2(x;v)\frac{dP^{-1}(x;v)}{dx} = \frac{2y_s(x;v)\frac{dy_s(x;v)}{dx} + y_s^4(x;v)\frac{df_s^{xc}(x;v)}{dx}}{(1 - y_s^2(x;v)f_s^{xc}(x;v))^2}. \tag{C.10}$$

Eq.C.10 gives vertex corrections in terms of the $f_s^{xc}(x;v)$ taken from TDDFT. It is often convenient for approximations that have physical meaning and perspective to be applied on realistic systems, to choose a simple $y_s(x;v)$, often the non-interacting one $y_0(z)$ or the classical x. The choice $y_s = y_0$ means neglecting all effects of the interaction in the independent particles response function, while the choice $y_s = x$ means neglecting only the exchange and correlation effects which would be a realistic approximation for systems with localized electrons.

C.1.1 The choice $y_s(x;v) = x$

With the choice of $y_s(x;v) = x$ eq.C.10 becomes

$$\frac{dP(x;v)}{dx} = \frac{2x + x^4\frac{df^{xc}(x;v)}{dx}}{(1 - x^2f^{xc}(x;v))^2}. \tag{C.11}$$

It is convenient at this point to renormalize $f^{xc}(x;v)$ with x^2

$$f^{xc}(x;v) = \frac{F^{xc}(x;v)}{x^2} \tag{C.12}$$

and substitute in eq.C.11. We obtain

$$\frac{dP(x;v)}{dx} = \frac{2x - 2xF^{xc}(x;v) + x^2\frac{dF^{xc}(x;v)}{dx}}{(1 - F^{xc}(x;v))^2}. \tag{C.13}$$

Assuming that we can write $F^{xc}(Q)$ as a function of Q, we introduce Q in eq.C.13 applying the chain rule with Q in the derivative

$$\frac{dF^{xc}(Q)}{dx} = \frac{dF^{xc}(Q)}{dQ}\frac{dQ}{dx} = \frac{dF^{xc}(Q)}{dQ}(2xw(x) - x^2w^2(x)\frac{dP(x;v)}{dx}) \tag{C.14}$$

where we used eq.C.5. Eq.C.13 becomes

$$\frac{1}{x}\frac{dP(x;v)}{dx} = 2\frac{1-F^{xc}(Q)+Q\frac{dF^{xc}(Q)}{dQ}}{(1-F^{xc}(Q))^2} - \frac{\frac{dF^{xc}(Q)}{dQ}Q^2(x)}{(1-F^{xc}(Q))^2}\frac{1}{x}\frac{dP(x;v)}{dx}. \tag{C.15}$$

The last equation has the structure of a Dyson equation for the vertex function $\frac{1}{x}\frac{dP(x;v)}{dx}$ and is complementary to eq.C.6. The solution of the last equation is

$$\frac{1}{x}\frac{dP(x;v)}{dx} = 2\frac{1-F^{xc}(Q)+Q\frac{dF^{xc}(Q)}{dQ}}{(1-F^{xc}(Q))^2+\frac{dF^{xc}(Q)}{dQ}Q^2(x)}. \tag{C.16}$$

Eq.C.16 requires that $F^{xc}(Q)$ is a pure function of Q. From eq.C.16, eq.C.6 becomes

$$\tilde{y}(Q) = 1+\lambda Q^2(2-2Q\frac{1-F^{xc}(Q)+Q\frac{dF^{xc}(Q)}{dQ}}{(1-F^{xc}(Q))^2+\frac{dF^{xc}(Q)}{dQ}Q^2})\frac{d\tilde{y}(Q)}{dQ}+\lambda Q\tilde{y}(Q). \tag{C.17}$$

This is a first order linear differential equation. The general form of the equation is

$$\frac{d\tilde{y}(Q)}{dQ}+f(Q)\tilde{y}(Q) = -g(Q) \tag{C.18}$$

Where $f(Q)$ and $g(Q)$ have the property,

$$f(Q) = -(Q-1)g(Q). \tag{C.19}$$

C.1.2 The general solution of the inhomogeneous differential eq.C.18

We multiply eq.C.18 with the unknown function $M(Q)$,

$$M(Q)\frac{d\tilde{y}}{dQ}+M(Q)f(Q)\tilde{y}(Q) = M(Q)g(Q). \tag{C.20}$$

The last equation has the general solution

$$\tilde{y}(Q) = \frac{1}{M(Q)}\int_c^Q dpM(p)g(p)+\frac{C(c)}{M(Q)} \tag{C.21}$$

$$M(Q) = e^{\int_b^Q dtf(t)dt+B(b)}. \tag{C.22}$$

The lower limit of the integration c is left open. The constant of the integration $C(c)$ will depend on c. $B(b)$ can be set equal to zero since it won't appear in the final result.

C.1.3 The general solution

Using the property given in eq.C.19 in eq.C.21 we get the general solution

$$\tilde{y}(Q) = -\frac{1}{M(Q)}\int_c^Q dp\frac{M(p)f(p)}{p-1}+\frac{C(c)}{M(Q)} \tag{C.23}$$

$$M(Q) = e^{\int_b^Q dtf(t)+B(b)} \tag{C.24}$$

The function $M(Q)$ satisfies the following relation:

$$M(Q) = \frac{1}{f(Q)} \frac{dM(Q)}{dQ} \tag{C.25}$$

We can substitute with eq.C.25 on eq.C.23 , integrate by parts and rewrite the general solution of the differential equation as

$$\tilde{y}(Q) = -\frac{1}{Q-1} - \frac{1}{M(Q)} \int_c^Q dp \frac{M(p)}{(p-1)^2} + \frac{C(c)}{M(Q)} \tag{C.26}$$

$$\text{with } C(c) = M(c)(\tilde{y}(c) + \frac{1}{c-1}) \tag{C.27}$$

We note here that the role of the constant of the integration in this case is to fix the lower limit of the eq.C.26. The constant of the integration $C(c)$ is given from the choice of c in eq.C.27.

D

F^{xc} as a function of the external potential

In this Appendix we discuss the $F^{xc}(y_0^{-1})$, given for the case of $\lambda = 1$ in eq.5.59, as a function of y_0^{-1}, which is linked to the external potential through the Dyson equation $y_0^{-1} = y_0^{0-1} - z$, including a static potential y_0^{0-1} and an applied potential z. In real systems the static potential also includes the nuclear potential which is material-dependent. In equilibrium $z = 0$ and $y_0^{-1} = y_0^{0-1}$, the external potential becomes equivalent to the static potential. In this case the large-y_0^{-1} regime can be seen as the regime of strong coupling to the nucleus, which is typical for localized electrons, while the small-y_0^{-1} regime can be seen as the regime of weak coupling to the nucleus, which is typical for free electrons in metallic systems. Here, we treat the interaction as a parameter. In

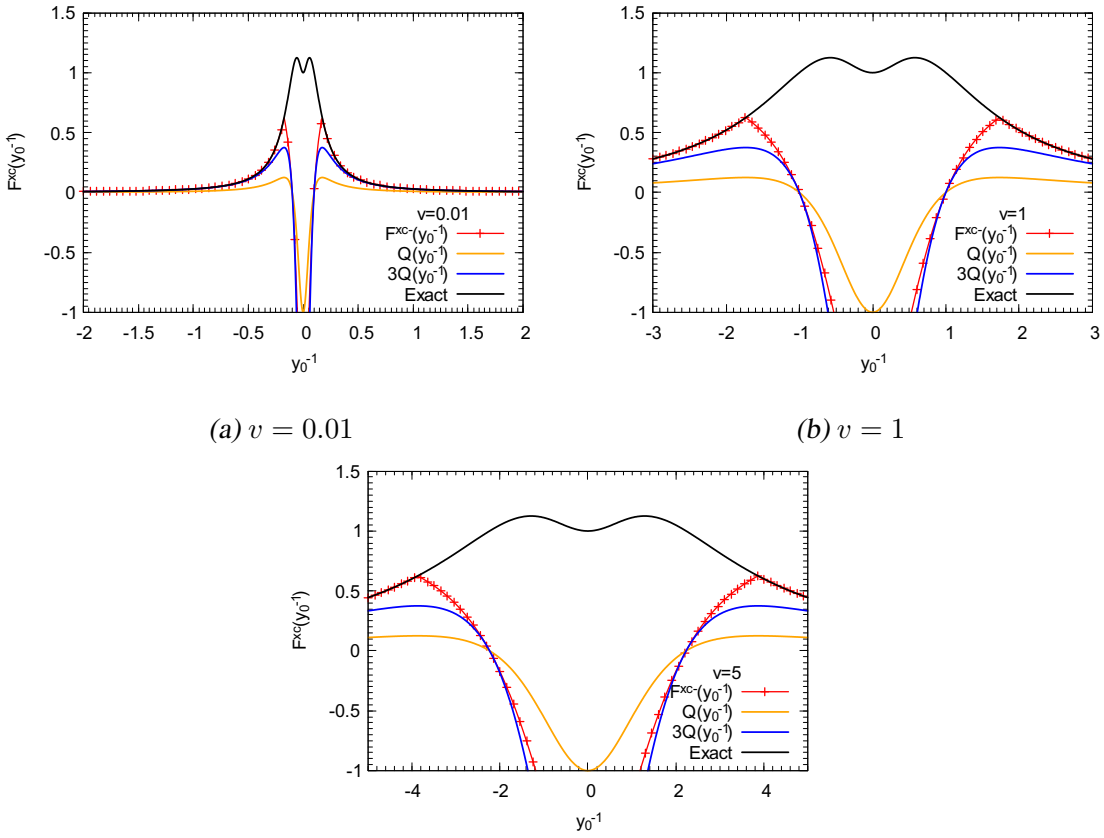

(a) $v = 0.01$ *(b)* $v = 1$

(c) $v = 5$

Fig. D.1: $F^{xc-}(y_0^{-1})$ for different values of the interaction v. Comparison with the exact $F^{xc}(y_0^{-1})$ (eq.5.58), the approximation from expansion for small Q (eq.5.60) and the $F^{xc}(y_0^{-1}) \approx Q(y_0^{-1})$ (eq.5.49).

fig.D.1,D.2 we see that $F^{xc+}(y_0^{-1})$ is always physical in the weak coupling regime $y_0^{-1} = 0$, while

$F^{xc-}(y_0^{-1})$ is always physical in the strong coupling regime $y_0^{-1} = \infty$.

In fig.D.1 the exact F^{xc} (eq.5.58) is equal to F^{xc-} (eq.5.59) for $y_0^{-1} > |\sqrt{3v}|$. For vanishing interaction, $v = 0.01$ (D.1a), the exact F^{xc} is given by F^{xc-} in the whole range of values of the nuclear potential. Increasing the value of the interaction (fig.D.1b,D.1c) the region of validity of F^{xc-} gets smaller. In the limit of strong interaction $v \to \infty$ F^{xc-} will be valid only in the strong coupling regime $y_0^{-1} \to \infty$. The approximation from the expansion to the interaction variable Q, $F^{xc-}(Q) \approx 3Q$, is valid in the non-interacting and strong coupling limits. On the other hand it fails at the points $y_0^{-1} = \pm\sqrt{3v}$, where F^{xc} changes branch. We can also observe that the approximation of $F^{xc} \approx Q$ in general deviates from the exact F^{xc}.

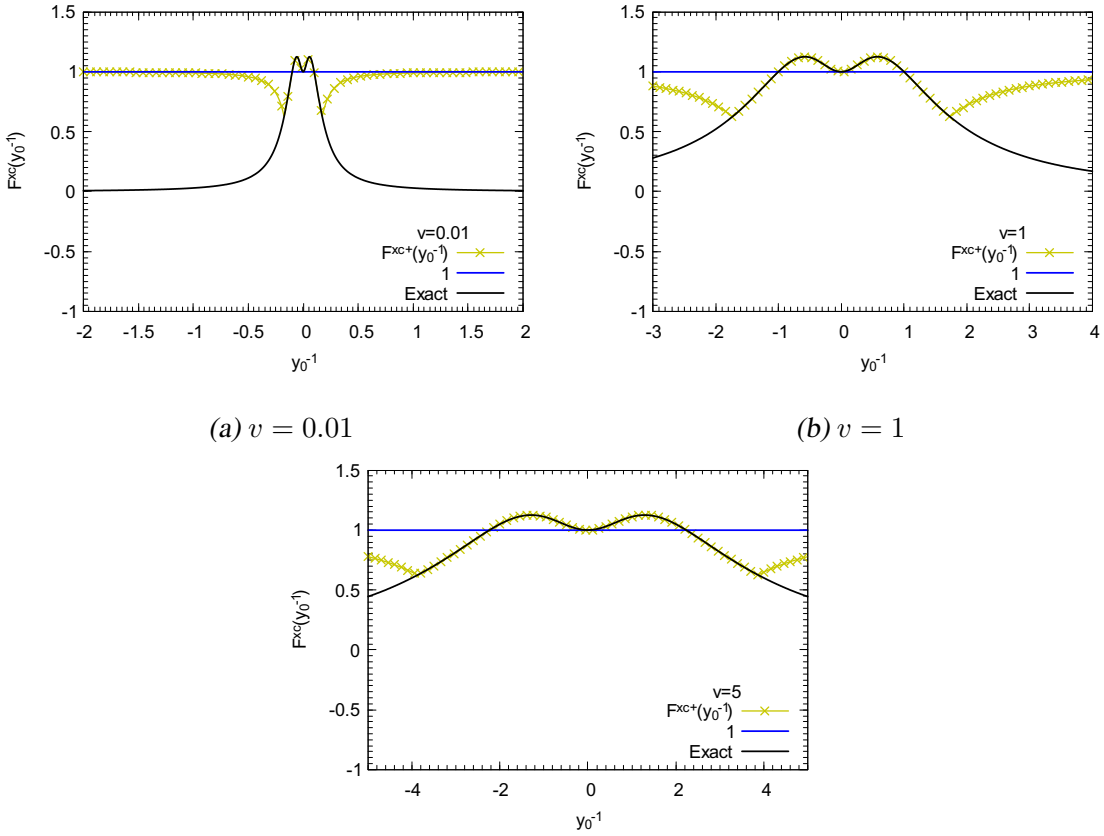

(a) $v = 0.01$ *(b)* $v = 1$

(c) $v = 5$

Fig. D.2: $F^{xc+}(y_0^{-1})$ (eq.5.59) for different values of the interaction v. Comparison with the exact $F^{xc}(y_0^{-1})$ (eq.5.58), the expansion for small values of Q (eq.5.61).

In fig.D.2 the exact F^{xc} (eq.5.58) is equal to F^{xc+} (eq.5.59) for $y_0^{-1} < |\sqrt{3v}|$. For vanishing interaction $v = 0.01$ (fig.D.2a) F^{xc+} is not valid. Increasing the value of the interaction (fig.D.2b,D.2c) the range of validity of $F^{xc+}(y_0^{-1})$ increases. The approximation $F^{xc+}(Q) \approx 1$ fails in the regime around $y_0^{-2} = \sqrt{3v}$. However in the limit of strong interaction $v \to \infty$, where the exact F^{xc} tend to a weakly varying function of y_0^{-1} $F^{xc+} \approx 1$ will be a good approximation.

E

Solutions from highly non-linear screening

In this appendix we will discuss the solutions from the F^{xc} of eq.5.59 for the case of $\lambda = 1$. We will also apply the transformation $o(Q)$ to the case of $\lambda = \frac{1}{2}$.

E.1 Solutions for the case of $\lambda = 1$ from $F^{xc}(Q) = aQ + b$

We have shown in sec.5.6.2 that the exact F^{xc} gives the exact solution which for the case of $\lambda = 1$ is equal to the non-interacting solution. In this section we give the solutions for the approximate $F^{xc}(Q) = aQ + b$. The last gives rise to a differential equation for $\tilde{y}$ when plugged in eq.C.17. Then the general solution of this equation is given by eq.C.26. For the choice of $F^{xc}(Q) = aQ + b$ the general solution is given by eq.C.26,C.27, where one needs to evaluate the integrating factor $M(Q)$. For the case of $F^{xc}(Q) = aQ + b$ the integrating factor is given by

$$M(Q) = Q^{-\frac{b}{2\lambda(1-b)}}((a+1)Q - (1-b))^{\frac{a+1+(b-1)\lambda}{2\lambda(1-b)}}(aQ - (1-b))^{\frac{(1-b)\lambda - a}{2\lambda(1-b)}}e^{\frac{1}{2Q\lambda}}. \tag{E.1}$$

This solution corresponds to the approximation for the response given by

$$\chi_{approx}(x) = \frac{x^2}{1 - (aw - v + \frac{b}{x^2})x^2} \tag{E.2}$$

The choice of $b = 0$ and $a = 0$ ($F^{xc}(Q) = 0$) gives the RPA with the Green's function of the classical system. The case of $a = 0$ gives the bootstrap approximation, which is equivalent to the screening of eq.5.29. The case of $b = 0$ gives the LRC approximation, where instead of the bare Coulomb interaction appears the screened interaction. The screened interaction in the bootstrap approximation is given by

$$w = v(1 + \frac{vx^2}{b - 1 - vx^2}). \tag{E.3}$$

For $b = 1$, $w = 0$ the screened interaction vanish. The zeros of the screened interaction do not only give the non-interacting limit, but they also give the classical limit. For the case of $b = 1$ the solution is equal to the Green's function of the classical system. We summarize the values of the integrating factor as taken from the different choices of screening in tab.E.1.

E.1.1 Solutions from non-linear screening in the RPA

We will first discuss the solutions from non-linear screening in the RPA, for $a = 0$ and $b = 0$. Starting from the general solution in eq.C.26 we will look for particular solutions that satisfy the non-interacting limit, fixing the solution to the branch of the solution which gives the exact solution. This is y^- for $o < \frac{1}{3}$ and y^+ for $o > \frac{1}{3}$.

In fig.E.1 we plot solutions in the RPA with the Green's function of the classical system. In fig.E.1a solutions are fixed to the exact solution $\tilde{y}^{-}(Q)$ in the interval $o \in [0, \frac{1}{3}]$. All solutions satisfy the non-interacting limit, but the choice of $c = 0.2$ remains close to the non-interacting solution for a

a	b	M(Q)	χ
a	0	$((a+1)Q-1)^{\frac{a}{2}}(aQ-1)^{\frac{1-a}{2}}e^{\frac{1}{2Q}}$	$\frac{x^2}{1-(aw-v)x^2}$
0	0	$e^{\frac{1}{2Q}}$	$\frac{x^2}{1+vx^2}$
0	b	$(\frac{Q-(1-b)}{Q})^{\frac{b}{2(1-b)}}(b-1)^{\frac{1}{2}}e^{\frac{1}{2Q}}$	$\frac{x^2}{1+(v-\frac{b}{x^2})x^2}$

Tab. E.1: The integrating factor and the response function for the different choices of screening.

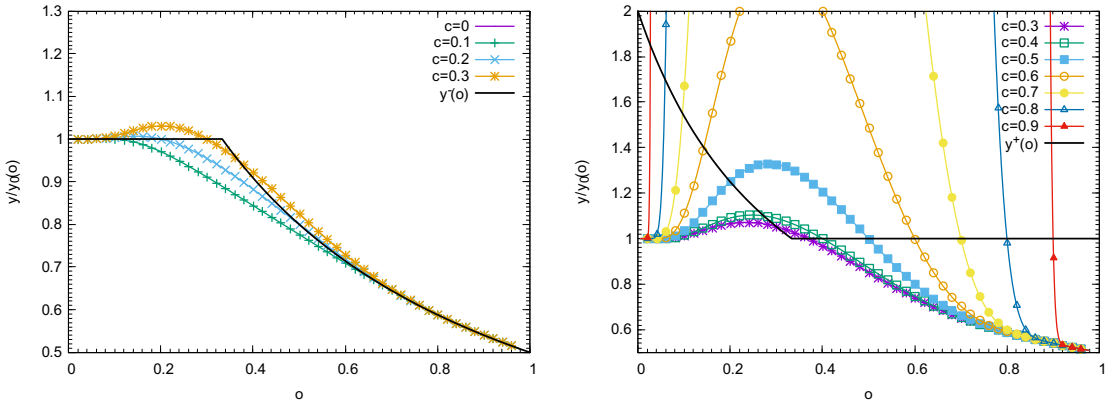

(a) Solutions fixed to the exact $\tilde{y}^{-}(Q(o))$ for $o \in [0, \frac{1}{3}]$.

(b) Solutions fixed to the exact $\tilde{y}^{+}(Q(o))$ for $o \in [\frac{1}{3}, 1]$.

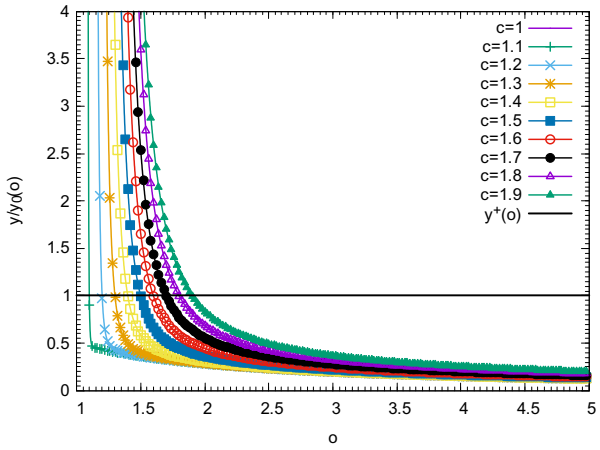

(c) Solutions fixed to the exact $\tilde{y}^{+}(Q(o))$ for $o \in [1, 2]$.

Fig. E.1: Particular solutions $\tilde{y}(o; c)$ for the RPA case of $a = 0, b = 0$ fixed to the exact solution for the case of $\lambda = 1$(eq.5.56) at different points c.

larger range of the interaction variable. In fig.E.1b we plot the solutions fixed to the exact solution $y^+(Q)$ in the interval $o \in [\frac{1}{3}, 1]$. Again all solutions satisfy the non-interacting limit. However they deviate from the exact solution and going towards $c = 1$ the solutions seem to worsen. In fig.E.1c we plot the solutions fixed to the exact solution $y^+(Q)$ in the interval $o \in [1, 2]$. These solutions are analytic in the interval $(1, +\infty]$, since they diverge at the point $o = 1$. In general they deviate from the exact solution.

E.1.2 Solutions from non-linear screening beyond the RPA

In this section we will discuss solutions from non-linear screening beyond the RPA, in the screened LRC and bootstrap approximations.

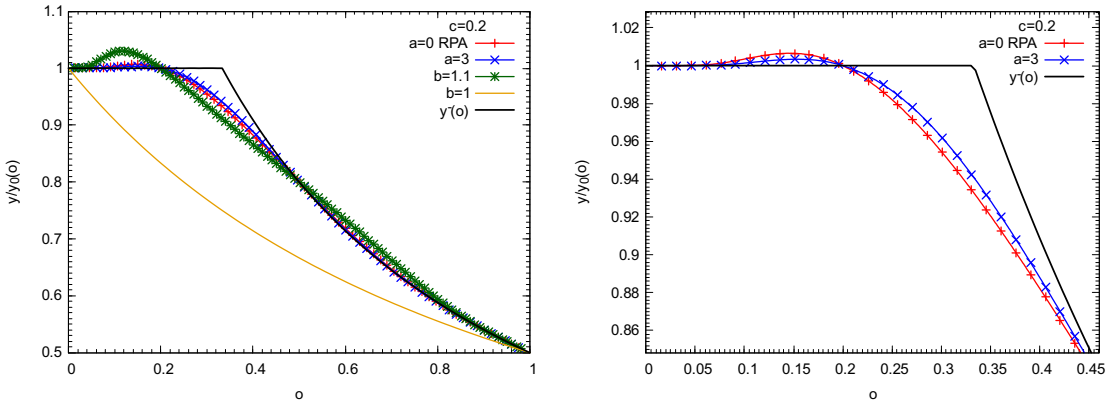

(a) Comparison in the interval $[0, 1]$. *(b)* Comparison between $a = 0$ and $a = 3$.

Fig. E.2: Comparison between the solutions for $a = 0$, $a = 3$, $b = 1$ and $b = 1.1$ fixed at $c = 0.2$ to the exact solution.

From fig.E.1 and E.2a we see that the RPA solution is close to the physical solution in the whole interval. In fig.E.2b *the solution from* $a = 3$, which is obtained from the expansion of $F^{xc-}(Q)$ for small values of Q *slightly improves the RPA solution*. In fig.E.2a the solution from the values of $b = 1$, which is the classical solution, and $b = 1.1$, obtained from the expansion of $F^{xc+}(Q)$ for small values of Q, deviate from the exact solution.

In fig.E.3 we compare between different solutions fixed to the exact solution in the interval $(1, +\infty]$. In fig.E.3a for the case of $b = 1.1$ and for $c \approx 2.9$ solutions are close to the exact solution. For the choice of $c = 2.9$ we compare between the cases of $a = 0$, $a = 3$, $b = 1$ and $b = 1.1$. The solutions for $a = 0$(RPA) and $a = 3$ deviate from the exact solution. The classical solution for $b = 1$ is close to the non-physical branch $y^-(o)$. *The solution for* $b = 1.1$ *seems to start from the non-physical branch* $y^-(o)$ *and due to the fact that we fix it at the exact solution, it deviates towards the physical solution and satisfies it for some values of* o.

In fig.E.4 we plot $y_0^{-1}\chi$ for the case of $\lambda = 1$. We see that the screened LRC approximation has different curvature than the bare one. The choice of $a = 3$ gives a curve, which is tangent to the exact screening for vanishing interaction. On the other hand the choice of $b = 1$ gives a behavior which is linear and again deviates from the exact screening.

From the transformation of the KBE to the interaction variable Q made of the screened Coulomb interaction and the Green's function of the classical system, the exact solution for the case of $\lambda = 1$ gets two branches, one which is valid in the non-interacting limit and one which is valid for large values of o. In the same sense the exact f^{xc} from TDDFT, written as a function of Q gets two branches, one that coincides with the exact f^{xc} for small values of the interaction and one that coincides with the exact f^{xc} for large values of the interaction variable. The F^{xc} for TDDFT obtained from the expansions for small Q suggest the aQ-approximation for small values of the interaction variable, and the b-approximation for large values of the interaction variable. This justifies the fact that the RPA($a = 0$) and the $a = 3$ are valid for small values of o, while the b is valid for large values of o. *Let us note that one needs to be careful in cases where we don't know the exact solution, and we rely on perturbative solutions in order to fix the physical solution. Because for example, in this case, the lowest order is the classical propagator, which is close to the non-physical branch for all values of the interaction variable.*

E.2 Application of the transformation $o(Q)$ for the case of $\lambda = \frac{1}{2}$

In this section we will apply the transformation $o(Q)$ of eq.5.50 for the case of $\lambda = \frac{1}{2}$. The exact solution of eq.3.69 for the case of $\lambda = \frac{1}{2}$ is

$$y_{\frac{1}{2}} = \frac{2y_0}{2 + vy_0^2} = \frac{2y_0}{2 + o}. \tag{E.4}$$

Using the transformation (eq.5.50) the exact solution for the case of $\lambda = \frac{1}{2}$ reads

$$\tilde{y}^{\pm}_{\frac{1}{2}}(Q) = \frac{8}{7 \mp \sqrt{1 - 8Q}}. \tag{E.5}$$

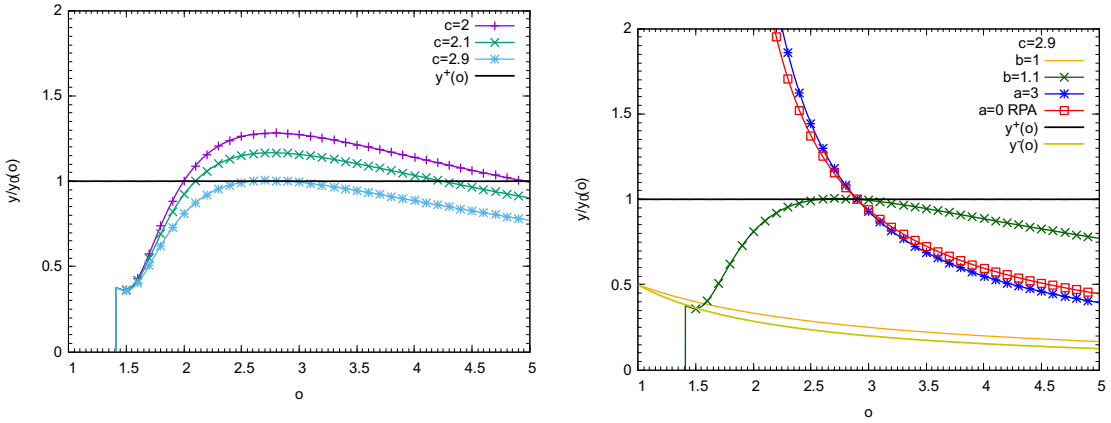

(a) Comparison between solutions for $b = 1.1$ fixed at values of c in $[2, 3]$.

(b) Comparison in the interval $[1 : 5]$.

Fig. E.3: Comparison between the solutions for $a = 0$, $a = 3$, $b = 1$ and $b = 1.1$ fixed at $c = 2.9$ to the exact solution.

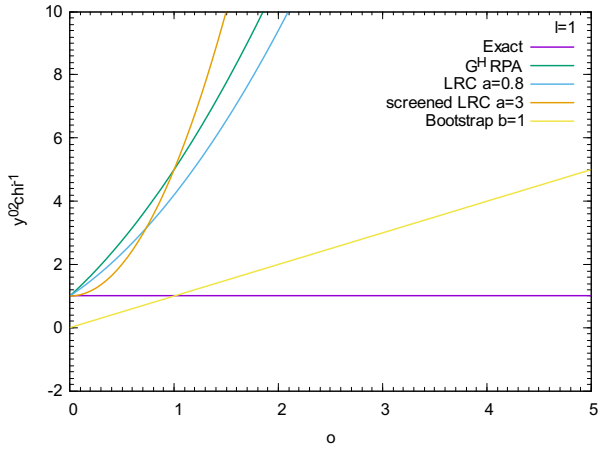

Fig. E.4: $y_0^{-1}\chi$ as a function of o for the case of $\lambda = 1$. Comparison between non-linear screening from the RPA with the Green's function of the classical system and for the choices of a and b estimated from perturbation theory in the interaction variable Q.

In fig.E.5 we plot the exact solution as a function of o and the two branches given in eq.E.5. As in the case of $\lambda = 1$ $\tilde{y}^+(o)$ gives the exact solution in the interval $o \in [0, \frac{1}{3}]$, while $\tilde{y}^-(o)$ gives the exact solution in the interval $o \in [\frac{1}{3}, +\infty]$.

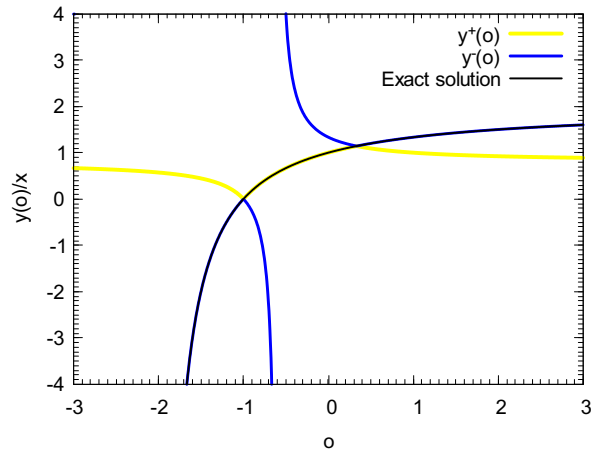

Fig. E.5: The exact solution $\tilde{y}(o) = \frac{2(1+o)}{2+o}$ for the case of $\lambda = \frac{1}{2}$ and the two branches $\tilde{y}^{\pm}_{\frac{1}{2}}(o)$ from eq.E.5.

E.2.1 $F^{xc}(Q)$ for the case of $\lambda = \frac{1}{2}$

For the case of $\lambda = \frac{1}{2}$ the exact $F^{xc}(Q)$ is obtained from the exact solution as

$$F^{xc}(o) = x^2\left(\frac{1}{x^2} - \frac{1}{\frac{dy_{\frac{1}{2}}}{dz}} + v\right) = 1 - \frac{-3o^2 - 4}{2(2-o)(1+o)^2}, \tag{E.6}$$

where o from eq.5.50 gives rise to two branches, the $F^{xc+}(Q)$ which is physical in the range $Q \in [-\infty, \frac{1}{8}]$ and $F^{xc-}(Q)$ which is physical in the range $Q \in [0, \frac{1}{8}]$. In fig.E.6 we plot the two branches as a function of Q. We see that $F^{xc+}(Q)$ (fig.E.6b) cannot be fitted directly with a linear

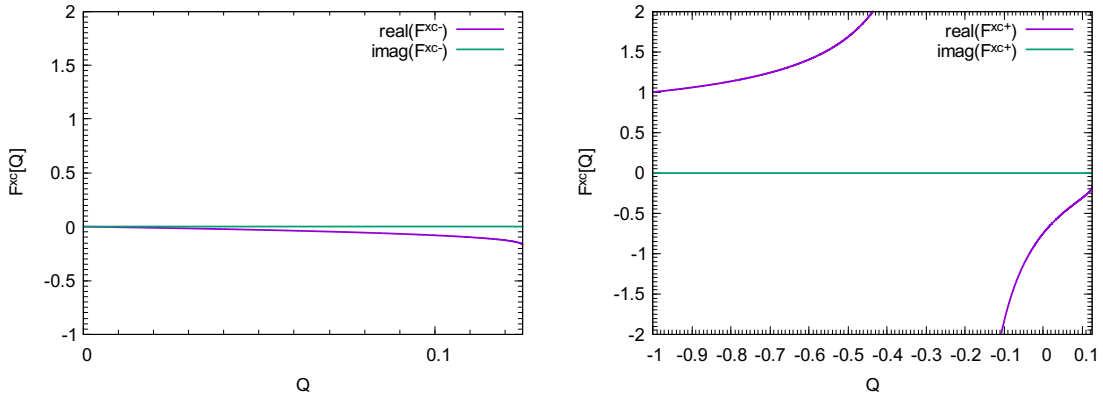

(a) $F^{xc-}(Q)$ for $Q \in [0, \frac{1}{8}]$. *(b)* $F^{xc+}(Q)$ for $Q < \frac{1}{8}$.

Fig. E.6: $F^{xc\pm}(Q)$ from eq.E.6 (real and imaginary parts).

curve. On the other hand $F^{xc-}(Q)$ *(fig.E.6a) can be fitted for vanishing* Q *with the* $a = 0$, $b = 0$, *which is the RPA*. The F^{xc} is non-analytic at $Q = \frac{1}{8}$ and therefore we cannot get an expansion around that point.

E.2.2 Solutions for the case of $\lambda = \frac{1}{2}$

In fig.E.7a we plot the solution for the case of $\lambda = \frac{1}{2}$ in the RPA, fixing the solution to the exact solution for $o \in [0, \frac{1}{3}]$. *The non-physical solution intersects the classical solution at the point of* $c = 1$ *and all solutions pass from this point.* In order to obtain the solutions in the branch $o \in [1, +\infty]$ we also fixed the solution to y^+ at values of $o > 1$. Similar to the case of $\lambda = 1$ the solutions that we have found follow the branch $y^-(o)$, which is the non-physical branch in the interval $o \in [\frac{1}{3}, \infty]$. For this reason we choose to fix the solution at $c = 0.3$ which is the highest value in the interval where the exact solution satisfies the non-interacting limit.

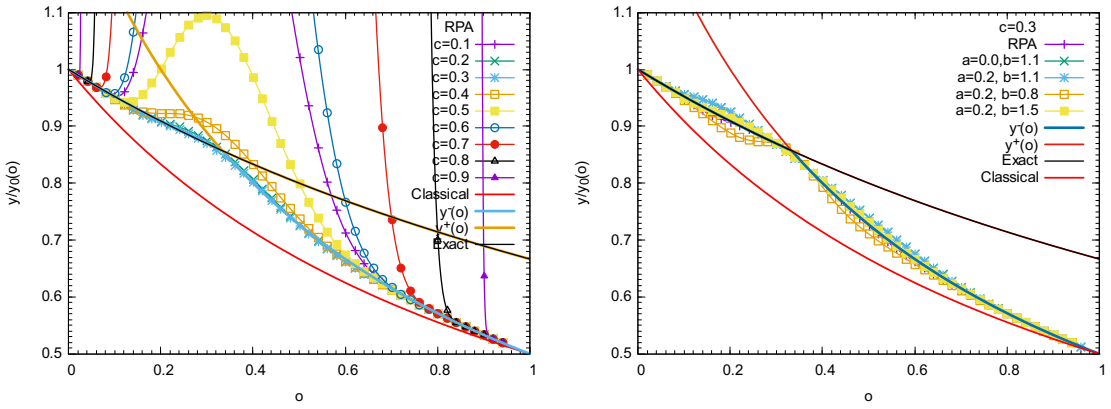

(a) Varying c *(b)* $c = 0.3$

Fig. E.7: The solution in the RPA and for different choices of the parameters a and b.

In fig.E.7b for the choice of $c = 0.3$, we plot the solutions from the choices of $b = 1.1$ and $b = 1.1, a = 0.2$ fitting in fig.E.6a,E.6b respectively at $Q = \frac{1}{8}$. We see that *the RPA gives the*

best solution, while the choice of $b = 1.1, a = 0.2$ deviates from the exact solution. We see that decreasing the value of $b < 1.1$ the deviation becomes larger, while increasing the value of $b > 1.5$ the deviation decreases. In all cases the quality of the RPA is the best.

In fig.E.8 we plot $y_0^{-2}\chi$ evaluated from the RPA with the Green's function of the classical system, and compare between the screened LRC fitted in fig.E.6b and the a and b as found from the fitting in fig.5.22. *The choice of* $F^{xc} = aQ$ *has a tendency to better reproduce the curvature of the exact screening for the case of* $\lambda = \frac{1}{2}$.

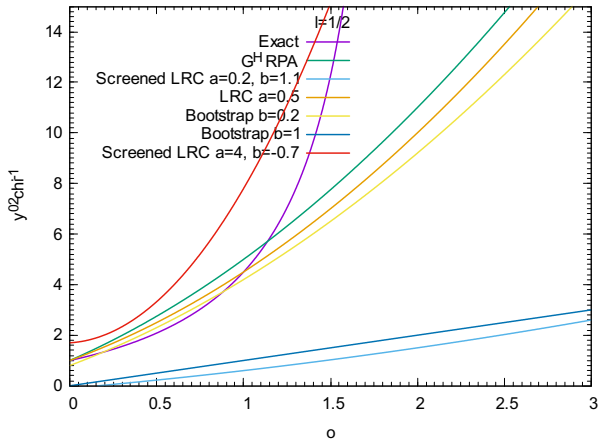

Fig. E.8: $y_0^{-2}\chi$ as a function of o for the case of $\lambda = \frac{1}{2}$. Comparison between non-linear screening for the choices of a and b as were found from the RPA with the Green's function of the classical system and the screened LRC approximation combined with the Bootstrap approximation $aQ+b$ as found from the fitting in fig.E.6b.

Index

Bibliography

[1] P. Hohenberg and W. Kohn. Inhomogeneous electron gas. *Phys. Rev.*, 136:B864–B871, Nov 1964.

[2] W. Kohn and L. J. Sham. Self-consistent equations including exchange and correlation effects. *Phys. Rev.*, 140:A1133–A1138, Nov 1965.

[3] E.N. Economou. *Green's Functions in Quantum Physics*. Springer Series in Solid-State Sciences. Springer, 2006.

[4] L. P. Kadanoff and G. A. Baym. *Quantum statistical mechanics: Green's function methods in equilibrium and nonequilibirum problems*. Frontiers in Physics. Benjamin, Menlo Park, CA, 1962.

[5] L. Hedin. New method for calculating the one-particle green's function with application to the electron-gas problem. *Phys. Rev.*, 139:A796–A823, Aug 1965.

[6] E. E. Salpeter and H. A. Bethe. A relativistic equation for bound-state problems. *Phys. Rev.*, 84:1232–1242, Dec 1951.

[7] P. Nozieres and D. Pines. *Theory Of Quantum Liquids*. Hachette UK, 1999.

[8] E. Runge and E. K. U. Gross. Density-functional theory for time-dependent systems. *Phys. Rev. Lett.*, 52:997–1000, Mar 1984.

[9] R. van Leeuwen, N. E. Dahlen, and A. Stan. Total energies from variational functionals of the green function and the renormalized four-point vertex. *Phys. Rev. B*, 74:195105, Nov 2006.

[10] M. Guzzo, G. Lani, F. Sottile, P. Romaniello, M. Gatti, J. J. Kas, J. J. Rehr, M. G. Silly, F. Sirotti, and L. Reining. Valence electron photoemission spectrum of semiconductors: Ab initio description of multiple satellites. *Phys. Rev. Lett.*, 107:166401, Oct 2011.

[11] G. Lani, P. Romaniello, and L. Reining. Approximations for many-body green's functions: insights from the fundamental equations. *New Journal of Physics*, 14(1):013056, 2012.

[12] J. A. Berger, P. Romaniello, F. Tandetzky, B. S. Mendoza, C. Brouder, and L. Reining. Solution to the many-body problem in one point. *New Journal of Physics*, 16(11):113025, 2014.

[13] S. Botti, F. Sottile, N. Vast, V. Olevano, L. Reining, H.C. Weissker, A. Rubio, G. Onida, R. Del Sole, and R. W. Godby. Long-range contribution to the exchange-correlation kernel of time-dependent density functional theory. *Phys. Rev. B*, 69:155112, Apr 2004.

[14] S. Sharma, J. K. Dewhurst, A. Sanna, and E. K. U. Gross. Bootstrap approximation for the exchange-correlation kernel of time-dependent density-functional theory. *Phys. Rev. Lett.*, 107:186401, Oct 2011.

[15] S. Rigamonti, S. Botti, V. Veniard, C. Draxl, L. Reining, and F. Sottile. Estimating excitonic effects in the absorption spectra of solids: Problems and insight from a guided iteration scheme. *Phys. Rev. Lett.*, 114:146402, Apr 2015.

[16] J. Kas, F. Vila, J. Rehr, and S. Chambers. Real-time cumulant approach for charge-transfer satellites in x-ray photoemission spectra. *Phys Rev B*, 91(12):121112, 2015.

[17] S. J. Portugal, T. Y. Hubel, J. Fritz, S. Heese, D. Trobe, B. Voelkl, S. Hailes, A. M. Wilson, and J. R. Usherwood. Upwash exploitation and downwash avoidance by flap phasing in ibis formation flight. *Nature*, 505(7483):399–402, 2014.

[18] P. A. M. Dirac. On the theory of quantum mechanics. *Proceedings of the Royal Society of London A: Mathematical, Physical and Engineering Sciences*, 112(762):661–677, 1926.

[19] A. L. Fetter and J. D. Walecka. *Quantum Theory of Many-Particle Systems*. Dover, 2003.

[20] E. Merzbacher. *Quantum Mechanics, 2nd Edition*. Wiley.

[21] L.D. Landau and E.M. Lifshitz. *Quantum Mechanics (Third Edition) Non-Relativistic Theor*. Pergamon, third edition, revised and enlarged edition, 1977.

[22] D. R. Hartree. The wave mechanics of an atom with a non-coulomb central field. part i. theory and methods. *Mathematical Proceedings of the Cambridge Philosophical Society*, 24(1):89–110, 1928.

[23] D. R. Hartree. The wave mechanics of an atom with a non-coulomb central field. part iii. term values and intensities in series in optical spectra. *Mathematical Proceedings of the Cambridge Philosophical Society*, 24(3):426–437, 1928.

[24] J. C. Slater. A simplification of the hartree-fock method. *Physical Review*, 81(3):385, 1951.

[25] D.R. Hartree. The calculation of atomic structures. *Reports on Progress in Physics*, 11(1):113, 1947.

[26] P. A. M. Dirac. Note on exchange phenomena in the thomas atom. *Mathematical Proceedings of the Cambridge Philosophical Society*, 26(3):376–385, 007 1930.

[27] R.M. Martin, L. Reining, and D.M. Ceperley. *Interacting Electrons*. Cambridge University Press, 2016.

[28] A. D. McLean, A. Weiss, and M. Yoshimine. Configuration interaction in the hydrogen molecule—the ground state. *Rev. Mod. Phys.*, 32:211–218, Apr 1960.

[29] *A Primer in Density Functional Theory*. Springer-Verlag, 2003.

[30] Carsten U. *Time-Dependent Density-Functional Theory: Concepts and Applications*. Oxford Graduate Texts.

[31] `https://sciencenotes.org/periodic-table-118-elements/`.

[32] `http://www.quasargroupconsulting.com/Encyclopedia/Physics/Light.php`.

[33] `https://en.wikipedia.org/wiki/X-ray_photoelectron_spectroscopy`.

[34] T. L. Gilbert. Hohenberg-kohn theorem for nonlocal external potentials. *Phys. Rev. B*, 12:2111–2120, Sep 1975.

[35] A. Georges, G. Kotliar, W. Krauth, and M. J. Rozenberg. Dynamical mean-field theory of strongly correlated fermion systems and the limit of infinite dimensions. *Rev. Mod. Phys.*, 68:13–125, Jan 1996.

[36] A.L. Fetter and J.D. Walecka. *Quantum Theory of Many-particle Systems*. Dover Books on Physics. Dover Publications, 2003.

[37] T. Koopmans. Über die zuordnung von wellenfunktionen und eigenwerten zu den einzelnen elektronen eines atoms. *Physica*, 1(1):104 – 113, 1934.

[38] C. C. J. Roothaan. New developments in molecular orbital theory. *Rev. Mod. Phys.*, 23:69–89, Apr 1951.

[39] C. C. J. Roothaan. Self-consistent field theory for open shells of electronic systems. *Rev. Mod. Phys.*, 32:179–185, Apr 1960.

[40] P. S. Bagus. Self-consistent-field wave functions for hole states of some ne-like and ar-like ions. *Phys. Rev.*, 139:A619–A634, Aug 1965.

[41] L. Hedin and A. Johansson. Polarization corrections to core levels. *Journal of Physics B: Atomic and Molecular Physics*, 2(12):1336, 1969.

[42] L. Hedin. On correlation effects in electron spectroscopies and the gw approximation. *Journal of Physics: Condensed Matter*, 11(42):R489, 1999.

[43] L. Hedin and J.D. Lee. Sudden approximation in photoemission and beyond. *Journal of Electron Spectroscopy and Related Phenomena*, 124(2–3):289 – 315, 2002.

[44] L. Hedin and S. Lundqvist. Effects of electron-electron and electron-phonon interactions on the one-electron states of solids. 23:1 – 181, 1970.

[45] T. Fujikawa. Theoretical studies of x-ray photoemission and exafs based on dyson orbitals. *Journal of the Physical Society of Japan*, 51(8):2619–2627, 1982.

[46] B. Lundqvist. Single-particle spectrum of the degenerate electron gas. *Physik Der Kondensierten Materie*, 6(3):193–205, 1967.

[47] J. J. Rehr and R. C. Albers. Theoretical approaches to x-ray absorption fine structure. *Rev. Mod. Phys.*, 72:621–654, Jul 2000.

[48] W. Bardyszewski and L. Hedin. A new approach to the theory of photoemission from solids. *Physica Scripta*, 32(4):439, 1985.

[49] J. J. Rehr. Lars hedin and the quest for a theory of excited states. *Physica Scripta*, 2005(T115):19, 2005.

[50] F. Sottile. Response functions of semiconductors and insulators: from the bethe-salpeter equation to time-dependent density functional theory, 2003.

[51] G. Strinati. Application of the green's functions method to the study of the optical properties of semiconductors. *RIVISTA DEL NUOVO CIMENTO*, 11, 1988.

[52] M. Gell-Mann and F. Low. Bound states in quantum field theory. *Phys. Rev.*, 84:350–354, Oct 1951.

[53] F. J. Dyson. The s matrix in quantum electrodynamics. *Phys. Rev.*, 75:1736–1755, Jun 1949.

[54] J. Schwinger. On the green's functions of quantized fields. i. *Proceedings of the National Academy of Sciences*, 37(7):452–455, 1951.

[55] G. Baym and L. P. Kadanoff. Conservation laws and correlation functions. *Phys. Rev.*, 124:287–299, Oct 1961.

[56] D. Pines and D. Bohm. A collective description of electron interactions: Ii. collective vs individual particle aspects of the interactions. *Phys. Rev.*, 85:338–353, Jan 1952.

[57] F. Aryasetiawan and O. Gunnarsson. The gw method. *Reports on Progress in Physics*, 61(3):237, 1998.

[58] N.M. Hugenholtz. Perturbation theory of large quantum systems. *Physica*, 23(1–5):481 – 532, 1957.

[59] W. Nelson, P. Bokes, P. Rinke, and R. W. Godby. Self-interaction in green's-function theory of the hydrogen atom. *Phys. Rev. A*, 75:032505, Mar 2007.

[60] P. Romaniello, S. Guyot, and L. Reining. The self-energy beyond gw: Local and nonlocal vertex corrections. *The Journal of Chemical Physics*, 131(15):154111, 2009.

[61] F. Aryasetiawan, R. Sakuma, and K. Karlsson. gw approximation with self-screening correction. *Phys. Rev. B*, 85:035106, Jan 2012.

[62] G.D. Mahan. *Many-Particle Physics*. Physics of Solids and Liquids. Springer, 2000.

[63] J. Sky Zhou, J.J. Kas, L. Sponza, I. Reshetnyak, M. Guzzo, C. Giorgetti, M. Gatti, F. Sottile, J.J. Rehr, and L. Reining. Dynamical effects in electron spectroscopy. *The Journal of Chemical Physics*, 143(4):109, 2015.

[64] J. J. Fernandez. gw calculations in an exactly solvable model system at different dilution regimes: The problem of the self-interaction in the correlation part. *Phys. Rev. A*, 79:052513, May 2009.

[65] L. G. Molinari. Hedin's equations and enumeration of feynman diagrams. *Phys. Rev. B*, 71:113102, Mar 2005.

[66] L. G. Molinari and N. Manini. Enumeration of many-body skeleton diagrams. *The European Physical Journal B - Condensed Matter and Complex Systems*, 51(3):331–336, 2006.

[67] R. Del Sole, L. Reining, and R. W. Godby. $GW\Gamma$ approximation for electron self-energies in semiconductors and insulators. *Phys. Rev. B*, 49:8024–8028, Mar 1994.

[68] `http://etsf.polytechnique.fr/People/Matteo`.

[69] G. Onida, L. Reining, and A. Rubio. Electronic excitations: density-functional versus many-body green's-function approaches. *Rev. Mod. Phys.*, 74:601–659, Jun 2002.

[70] L. J. Sham and M. Schlüter. Density-functional theory of the energy gap. *Phys. Rev. Lett.*, 51:1888–1891, Nov 1983.

[71] L. J. Sham. Exchange and correlation in density-functional theory. *Phys. Rev. B*, 32:3876–3882, Sep 1985.

[72] Y. Pavlyukh and W. H$'$ubner. Analytic solution of hedin's equations in zero dimensions. *Journal of Mathematical Physics*, 48(5):052109, 2007.

[73] W. Tarantino, P. Romaniello, J. A. Berger, and L. Reining. Self-consistent dyson equation and self-energy functionals: An analysis and illustration on the example of the hubbard atom. *Phys. Rev. B*, 96:045124, Jul 2017.

[74] A. Stan, P. Romaniello, S. Rigamonti, L. Reining, and J.A. Berger. Unphysical and physical solutions in many-body theories: from weak to strong correlation. *New Journal of Physics*, 17(9):093045, 2015.

[75] R. T. Sharp and G. K. Horton. A variational approach to the unipotential many-electron problem. *Phys. Rev.*, 90:317–317, Apr 1953.

[76] J. P. Perdew and A. Zunger. Self-interaction correction to density-functional approximations for many-electron systems. *Phys. Rev. B*, 23:5048–5079, May 1981.

[77] A. Görling. Orbital- and state-dependent functionals in density-functional theory. *The Journal of Chemical Physics*, 123(6):062203, 2005.

[78] Y.H. Kim and A. Görling. Exact kohn-sham exchange kernel for insulators and its long-wavelength behavior. *Phys. Rev. B*, 66:035114, Jul 2002.

[79] F. Bruneval, F. Sottile, V. Olevano, and L. Reining. Beyond time-dependent exact exchange: The need for long-range correlation. *The Journal of Chemical Physics*, 124(14):144113, 2006.

[80] M. E. Casida. Generalization of the optimized-effective-potential model to include electron correlation: A variational derivation of the sham-schlüter equation for the exact exchange-correlation potential. *Phys. Rev. A*, 51:2005–2013, Mar 1995.

[81] N. Marzari, A. A. Mostofi, J. R. Yates, I. Souza, and D. Vanderbilt. Maximally localized wannier functions: Theory and applications. *Rev. Mod. Phys.*, 84:1419–1475, Oct 2012.

[82] P. Nozières and C. T. De Dominicis. Singularities in the x-ray absorption and emission of metals. iii. one-body theory exact solution. *Phys. Rev.*, 178:1097–1107, Feb 1969.

[83] D. C. Langreth. Singularities in the x-ray spectra of metals. *Phys. Rev. B*, 1:471–477, Jan 1970.

[84] B.I. Lundqvist. Characteristic structure in core electron spectra of metals due to the electron-plasmon coupling. *Phys kondens Materie*, 9:236–248, 1969.

[85] L. Hedin, B.I. Lundqvist, and S. Lundqvist. New structure in the single-particle spectrum of an electron gas. *Solid State Communications*, 5(4):237 – 239, 1967.

[86] L. Hedin. Effects of recoil on shake-up spectra in metals. *Physica Scripta*, 21(3-4):477, 1980.

[87] F. Aryasetiawan, L. Hedin, and K. Karlsson. Multiple plasmon satellites in na and al spectral functions from ab initio cumulant expansion. *Phys. Rev. Lett.*, 77:2268–2271, Sep 1996.

[88] G. Stefanucci and R. van Leeuwen. *Nonequilibrium Many-Body Theory of Quantum Systems: A Modern Introduction*. Cambridge University Press, 2013.

[89] G. D. Mahan. Excitons in metals: Infinite hole mass. *Phys. Rev.*, 163:612–617, Nov 1967.

[90] Combescot, M. and Nozières, P. Infrared catastrophy and excitons in the x-ray spectra of metals. *J. Phys. France*, 32(11), 1971.

[91] W. Hänsch and W. Ekardt. Structure of the $L_{\frac{\text{ii}}{\text{iii}}}$-absorption-edge singularity of na metal. *Phys. Rev. B*, 25:7815–7817, Jun 1982.

[92] D. C. Langreth. Born-oppenheimer principle in reverse: Electrons, photons, and plasmons in solids—singularities in their spectra. *Phys. Rev. Lett.*, 26:1229–1233, May 1971.

[93] J.J. Chang and D. C. Langreth. Deep-hole excitations in solids. i. fast-electron-plasmon effects. *Phys. Rev. B*, 5:3512–3522, May 1972.

[94] S. Doniach and M. Sunjic. Many-electron singularity in x-ray photoemission and x-ray line spectra from metals. *Journal of Physics C: Solid State Physics*, 3(2):285, 1970.

[95] S. M. Bose, P. Kiehm, and P. Longe. Excitation energy dependence of the photoemission spectra of metals. *Phys. Rev. B*, 23:712–723, Jan 1981.

[96] C. O. Almbladh and U. von Barth. The spherical-solid model: An application to x-ray edges in li, na, and al. *Phys. Rev. B*, 13:3307–3319, Apr 1976.

[97] R. Kubo. Generalized cumulant expansion method. *Journal of the Physical Society of Japan*, 17(7):1100–1120, 1962.

[98] E. Müller-Hartmann, T. V. Ramakrishnan, and G. Toulouse. Localized dynamic perturbations in metals. *Phys. Rev. B*, 3:1102–1119, Feb 1971.

[99] G. D. Mahan. Collective excitations in x-ray spectra of metals. *Phys. Rev. B*, 11:4814–4824, Jun 1975.

[100] G. D. Mahan. Core-hole green's function: Dispersion theory. *Phys. Rev. B*, 25:5021–5031, Apr 1982.

[101] A. Barth and L. S. Cederbaum. Many-body theory of core-valence excitations. *Phys. Rev. A*, 23:1038–1061, Mar 1981.

[102] U. Harbola and S. Mukamel. Many-body green's function approach to attosecond nonlinear x-ray spectroscopy. *Phys. Rev. B*, 79:235129, Jun 2009.

[103] S. Mukamel. Multiple core-hole coherence in x-ray four-wave-mixing spectroscopies. *Phys. Rev. B*, 72:235110, Dec 2005.

[104] Thorsten Hansen and Tõnu Pullerits. Nonlinear response theory on the keldysh contour. *Journal of Physics B: Atomic, Molecular and Optical Physics*, 45(15):154014, 2012.

[105] V.M. Silkin, P. Lazić, Došli ć N., H. Petek, and B. Gumhalter. Ultrafast electronic response of ag(111) and cu(111) surfaces: From early excitonic transients to saturated image potential. *Phys. Rev. B*, 92:155405, Oct 2015.

[106] B. Gumhalter. Stages of hot electron dynamics in multiexcitation processes at surfaces: General properties and benchmark examples. *Progress in Surface Science*, 87(5–8):163 – 188, 2012.

[107] B. Gumhalter. Ultrafast dynamics and decoherence of quasiparticles in surface bands: Development of the formalism. *Phys. Rev. B*, 72:165406, Oct 2005.

[108] Gumhalter B., V. Kovač, F. Caruso, H. Lambert, and F. Giustino. On the combined use of GW approximation and cumulant expansion in the calculations of quasiparticle spectra: The paradigm of si valence bands. *Phys Rev B*, 94(3), 2016.

[109] A. Arnau. Nonlinear screening of highly charged ions in metals. *Physica Scripta*, 1997(T73):303, 1997.

[110] V. I. Grebennikov, Yu. A. Babanov, and O. B. Sokolov. Extra-atomic relaxation and x-ray spectra of narrow-band metals. i. formalism. *physica status solidi (b)*, 79(2):423–432, 1977.

[111] V. I. Grebennikov, Yu. A. Babanov, and O. B. Sokolov. Extra-atomic relaxation and x-ray spectra of narrow-band metals. ii. results. *physica status solidi (b)*, 80(1):73–82, 1977.

[112] T. Privalov, F. Gel'mukhanov, and H. Ågren. Role of relaxation and time-dependent formation of x-ray spectra. *Phys. Rev. B*, 64:165115, Oct 2001.

[113] T. Privalov, F. Gel'mukhanov, and H. Ågren. X-ray raman scattering from molecules and solids in the framework of the mahan-nozières-de dominicis model. *Phys. Rev. B*, 64:165116, Oct 2001.

[114] B. Brena, Y. Luo, M. Nyberg, S. Carniato, K. Nilson, Y. Alfredsson, J. Åhlund, N. Mårtensson, H. Siegbahn, and C. Puglia. Equivalent core-hole time-dependent density functional theory calculations of carbon 1s shake-up states of phthalocyanine. *Phys Rev B*, 70(19), 2004.

[115] B. Brena, S. Carniato, and Y. Luo. Functional and basis set dependence of k-edge shake-up spectra of molecules. *J Chem Phys*, 122(18):184316, 2005.

[116] J Kas, J Rehr, and J Curtis. Particle-hole cumulant approach for inelastic losses in x-ray spectra. *Phys Rev B*, 94(3), 2016.

[117] `https://etsf.polytechnique.fr/people/stefano`.

[118] A. J. Morris, M. Stankovski, K. T. Delaney, P. Rinke, P. García-González, and R. W. Godby. Vertex corrections in localized and extended systems. *Phys. Rev. B*, 76:155106, Oct 2007.

[119] A. Marini and A. Rubio. Electron linewidths of wide-gap insulators: Excitonic effects in LiF. *Phys. Rev. B*, 70:081103, Aug 2004.

[120] J. P. Perdew, R. G. Parr, M. Levy, and J. L. Balduz. Density-functional theory for fractional particle number: Derivative discontinuities of the energy. *Phys. Rev. Lett.*, 49:1691–1694, Dec 1982.

[121] C.-O. Almbladh and U. von Barth. Exact results for the charge and spin densities, exchange-correlation potentials, and density-functional eigenvalues. *Phys. Rev. B*, 31:3231–3244, Mar 1985.

[122] F. Iori, F. Rodolakis, M. Gatti, L. Reining, M. Upton, Y. Shvyd'ko, J. P. Rueff, and M. Marsi. Low-energy excitations in strongly correlated materials: A theoretical and experimental study of the dynamic structure factor in v_2o_3. *Phys. Rev. B*, 86:205132, Nov 2012.

université PARIS-SACLAY | ÉCOLE DOCTORALE Ondes et Matière (EDOM)

Titre : Vers une meilleure description de la spectroscopie des matériaux avec électrons localisés : potentiels et interactions effectives

Mots clés : spectroscopie, photoemission, rayon X, écrantage non-lineaire

Résumé : L'objectif de cette thèse est de développer des approximations pour décrire les effets à N-corps dans l'absorption et la photoémission des matériaux avec électrons localisés. Le traitement complet par la mécanique quantique de ce problème difficile repose sur la solution de l'équation de Schrödinger pour la fonction d'onde à N-corps, ce qui en pratique nécessite des approximations. Pour simplifier, la Théorie de le Fonctionnelle de la Densité (DFT) introduit le système de particules indépendantes de Kohn et Sham. Cependant, il s'avère difficile d' obtenir des propriétés autres que la densité et l'énergie totale. Dans cette thèse, nous travaillons avec des fonctions de Green. Le niveau de complexité de ce cadre, en principe exact, se situe entre la DFT et les méthodes des fonctions d'onde, et de nombreux problèmes restent à résoudre.

Quand l'électron localisé a peu de recouvrement avec les autres électrons, on peut penser que leur interaction est classique. Dans ce cas, l'effet principal à N-corps est la réaction des autres électrons : ils écrantent l'excitation. Dans les approximations habituelles telles que le GW ou la "cumulant expansion", l'écrantage est traité seulement en réponse linéaire. Cependant, l'excitation d'un électron localisé devrait représenter une forte perturbation. Par conséquent, il se pourrait que les contributions non-linéaires à l'écrantage soient importantes. Comment peut-on vérifier quand cela est vrai? Et comment peut-on inclure ces effets? D'autre part, même en réponse linéaire, on pourrait faire mieux que les approximations habituelles, parce que l'écrantage en réponse linéaire est souvent calculé dans l'approximation de la phase aléatoire (RPA). De combien peut-on améliorer les résultats, même en restant en réponse linéaire, si on va au-delà de RPA? Ces points seront adressés dans la thèse.

Title : Towards an improved description of spectroscopies for materials with localized electrons: Effective potentials and interactions

Keywords : spectroscopy, photoemission, x-rays, non-linear screening

Abstract : The aim of this thesis is to develop approximations to describe many-body effects in photoemission and optical properties of materials containing localized electrons. This is a tough problem. The full quantum-mechanical treatment is based on the solution of the Schrödinger equation for the many-body wavefunction, which is cumbersome and requires in practice some approximations. One simplified approach is given by Density Functional Theory (DFT) with the Kohn-Sham system of independent particles, but it is difficult to access properties other than the density and total energy. In this thesis we start from an in principle exact framework, the Green's functions. They are intermediate in complexity between DFT and the full wavefunction methods.

Supposing that the localized electron has little overlap with the others, we can think that their interaction is classical. Then the main many-body effect is the reaction of the other electrons to the removal or excitation of the localized electron: this is screening of the hole or electron-hole pair by the other electrons. However, in many standard approximations in the Green's functions framework, such as GW or the cumulant expansion, screening appears in the linear response approximation. Instead, we can expect that the removal or excitation of a localized electron is a strong perturbation to the other electrons. Therefore, it could be that non-linear contributions to screening are important. How can we verify when this is true? And how can we include these effects? On the other hand, even in linear response one could do better than standard approximations, because the linear response screening itself is often calculated in the Random Phase Approximation (RPA). How much do things improve when one goes beyond the RPA but stays in linear response? We address these points in the thesis.

Université Paris-Saclay
Espace Technologique / Immeuble Discovery
Route de l'Orme aux Merisiers RD 128 / 91190 Saint-Aubin, France